According to Sec. 17(8) of the University of Hohenheim's Doctoral Regulations for the Faculties of Agricultural Sciences

Dissertation to obtain the doctoral degree of Agricultural Sciences (Dr. sc. agr.)

Understanding the role of the Calcineurin B-like (CBL) proteins and the CBL-Interacting Protein Kinases (CIPK) of wheat (*Triticum aestivum*) in the regulation of its high affinity ammonium transporters

Faculty of Agricultural Sciences

Institute of Nutritional Crop Physiology

(340h)

University of Hohenheim

Under the Supervision of

Prof. Dr. Uwe Ludewig

submitted by

Toyosi Babatunde, IJATO

Born in Ikare-Akoko, Ondo state, Nigeria

2020

TABLE OF CONTENTS

LIST OF FIGURES

LIST OF TABLES

LIST OF ABBREVIATIONS

AA	Amino acid
AKT1	K^+ transporter 1
AMT	Ammonium transporter
AS	Asparagine synthetase
At	*Arabidopsis thaliana*
ATP	Adenosine triphosphate
BiFC	Bimolecular fluorescence complementation
CAM	Crassulacean acid metabolism
CBL	Calcineurin B-like protein
CIPK	Calcineurin B like (CBL)-interacting protein kinase
DNA	Deoxyribonucleic acid
DTT	Dithiothreitol
EDTA	Ethylenediaminetetraacetic acid
E. coli	*Escherichia coli*
G6PDH	Glucose-6-phosphate dehydrogenase
GDH	Glutamate dehydrogenase
GS	Glutamine synthetase
HAK5	High affinity K+transporter 5
HATS	High-affinity transport system
HL	Hoagland
KAT1	Potassium channel
l	Liter
LATS	Low-affinity transport system
LB	medium Lysogeny broth medium
MeA	Methylammonium
MEP	Methylammonium/ammonium permease

MES	2-(N-morpholino) ethanesulfonic acid
Mt	*Medicago truncatula*
N	Nitrogen
NO_3^-	Nitrate ion
NO_3	Nitrate
NH_4^+	Ammonium ion
NH_4	Ammonium
NRT1	Nitrate transporter 1
Os	*Oryza sativa*
PCR	Polymerase chain reaction
PEPc	Phosphoenolpyruvate carboxylase
PIP	Plasma membrane intrinsic proteins
PPP	Pentose phosphate pathway
Rh	Mammalian rhesus factor
RNA	Ribonucleic acid
Sc	*Saccharomyces cerevisiae*
SD	Synthetic Defined
Ta	*Triticum aestivum*
TIP	Tonoplast intrinsic proteins
qRT-PCR	quantitative Real-Time Polymerase Chain Reaction
YFP	Yellow fluorescent protein
YPD	Yeast Extract Peptone Dextrose

ABSTRACT

Ammonium is an important nitrogen source whose potential for toxicity (in plants) has been a limitation to its use as a fertilizer. In this work, the response of wheat to ammonium nutrition and the regulatory mechanism governing its high affinity ammonium transporters was investigated. Wheat was able to utilize sole ammonium in the 1 mM range just like sole nitrate. An elevated ammonium concentration of 10 mM caused ammonium induced toxicity effects. Unexpectedly, the wheat seedlings failed to downregulate TaAMT1;1 and TaAMT1;2 in response to elevated ammonium concentration. Nevertheless, TaAMT1;1 and TaAMT1;2 complement ammonium transport in the *ΔΔΔmep* yeast strain (lacking endogenous ammonium transporters). The Voltage dependent ammonium induced currents of the transporters saturated in a concentration dependent manner with $K_{m\ AMT1;1}$ = 76 µM and $K_{m\ AMT1;2}$ = 196 µM. The affinity of the transporters for ammonium was voltage dependent and indicated that ammonium passes around 35 % of the membrane electric field before rate limiting deprotonation in both transporters. Furthermore, phospho-proteomics study showed the differential phosphorylation of TaAMT1;1 and TaAMT1;2 specific proteotypic phosphopetides. Interestingly, a mutation that mimics phosphorylation at the conserved threonine T453 ($T_{453}D$) was able to inactivate the ammonium transport function of the transporters. Additionally TaCBL1, and TaCBL2 were able to independently regulate the activity of TaAMT1;1, while TaCBL1, TaCBL2 and TaCBL6 were able to independently impair the ammonium induced current of TaAMT1;2. Subsequently, TaCBL1, TaCBL2 and TaCBL6 interacted with TaCIPK9 to further reduce the ammonium induce current caused by the single TaCBLs proteins on TaAMT1s. TaCIPK23 and TaCIPK32 were only able to regulate TaAMT1;2 by interacting with both TaCBL2 and TaCBL6. Thus, the robust response of wheat to ammonium N was shown to include the phospho-regulation of its high affinity ammonium transporters in a manner that recruits the activity of its TaCBL and TaCIPK proteins.

ZUSAMMENFASSUNG

Ammonium ist ein wichtiger Stickstoff Nährstoff für Pflanzen, dessen Toxizität bei zu hohen Konzentrationen seinen Einsatz als Dünger limitiert. In dieser Arbeit wurde die Resonanz von Weizen gegenüber reiner Ammoniumernährung sowie die regulatorischen Mechanismen, der hochaffinen Ammoniumaufnahme untersucht. Während Weizen geringe Konzentrationen von Ammonium ebenso gut nutzen konnte wie geringe Konzentrationen von Nitrat, verursachten erhöhte Ammoniumkonzentrationen (10 mM) toxische Effekte. Bei diesen erhöhten Konzentrationen schafften es die Weizenkeimlinge unerwarteterweise nicht, die Expression ihre hochaffinen Ammoniumtransporter TaAMT1;1 und TaAMT1;2 zu reduzieren. Jedoch waren beide Transportproteine funktionell und konnten das Wachstum eines Hefestamms ohne eigene Ammoniumtransporter auf Ammonium komplementieren. Ammoniuminduzierte elektrische AMT Ströme in *Xenopus laevis* Oozyten waren spannungsabhängig und sättigten mit $K_{m\ AMT1;1}$ = 76 µM und $K_{m\ AMT1;2}$ = 196 µM. Diese Affinität der Transporter für Ammonium war ebenfalls spannungsabhängig was implizierte, dass der ratenlimitierende NH_4^+-Deprotonierung Schritt erst 35 % innerhalb des elektrischen Feldes der Plasmamembran stattfindet. Ein Phospho-Proteomics Ansatz zeigte TaAMT spezifische und ammoniumabhängige Phosphorylierung. Interessanterweise, konnte das Vortäuschen einer Phosphorylierung am konservierten AMT1 C-terminalen Proteinende ($T_{453}D$) die Aktivität der TaAMT1s in Hefe und Oozyten inaktivieren. Mehrere Calcium bindende TaCBL Proteine waren in der Lage die Aktivität der TaAMT1 direkt zu reduzieren. In Kombination mit der TaCIPK9 Kinase (bei TaAMT1;2 ebenso TaCIPK23/32) war dieser Effekt viel ausgeprägter und führte teilweise zu einer kompletten Inaktivierung der Transporter. Zusammenfassend konnte gezeigt werden, dass die Phosphoregulation der TaAMT1 Transporter durch TaCBL / TaCIPK Komplexe Teil einer schnellen und effektiven Ammoniumantwort in Weizen ist.

1. INTRODUCTION

1.1. WHEAT

Bread wheat (*Triticum aestivum*) is an important food crop that is cultivated all over the world due to its adaptability to numerous climates. It is cultivated in over 120 countries, where it accounts for about 19% of the world's calorie supplies (Aksoy and Beghin 2004). It is a prominent crop in temperate regions, (Zi et al. 2018) and serves as a primary source of starch, protein, dietary fibres and phytochemicals (Shewry and Hey 2015). Its ability to store for several years without deterioration (under proper conditions) makes it well suited for use as a buffer against food shortages (Aksoy and Beghin 2004). It is also the perfect raw material for the production of bake food products, due to its viscoelasticity properties, which is conferred by its high gluten content (Shewry 2009). In the drink production industry, it is the second most malted cereal, a feat conferred by the high starch contents of its endosperm (Svihus 2014).

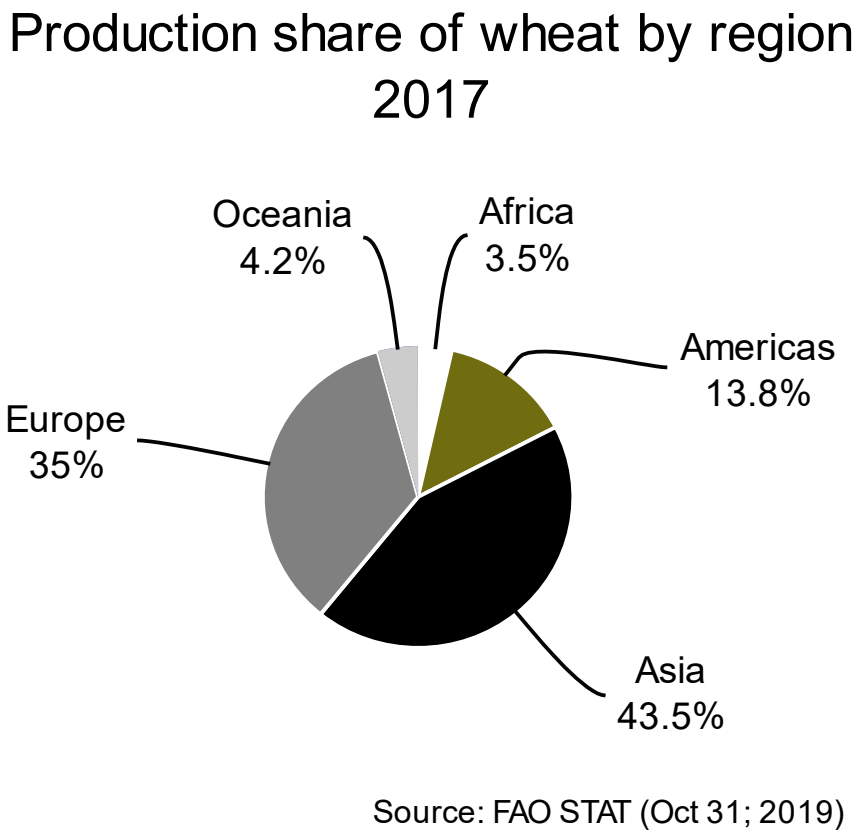

Figure 1. A pie chart showing the total distribution of wheat production across the world for the year 2017 (adapted from (FAO 2019), with slight modifications).

Over 218 million hectares of land was used in 2017 for the global production of over 771 million tonnes of wheat (Fig. 2), making it the commercial crop that is cultivated on the largest land area (FAO 2014). Economically, its global trade exceeds that of all other crops combined (Curtis et al. 2002). In fact, about 19 percent of the world's wheat production is traded internationally, primarily as exports from countries of the Organisation for Economic Co-operation and Development (OECD) (Aksoy and Beghin 2004).

All wild and cultivated wheat are classified into three groups based on their genome (Melinda Smale 1996). Diploid wheat (AA) known as the Eincorn (*Triticum monococcum* or *Triticum urartu*), tetraploid wheats (AABB) known as the durum and emmer wheat (*Triticum turgidum*), and hexaploid wheat (AABBDD) popularly known as bread wheat (*Triticum aestivum*) (Arnold and Austin 1989; Austin et al. 1980; Melinda Smale 1996).

The A genomes of tetraploid and hexaploid wheats are related to the A genomes of the red wild and the cultivated einkorn (*Triticum urartu*) (Dvorak et al. 1988). Its D genome is believed to be from *Triticum tauschii* (McFadden and Sears 1946). Despite the uncertainty surrounding the origin of the B genome (Melinda Smale 1996), it is believed to be derived from the S genome of *Aegilops speltoides* (Shewry 2009). Another classification that is based on chromosome number also exist (Bennici 1986a), where wheat crops with 14 choromosomes are regarded as the diploid wheat, those with 28 chromosomes as tetraploid wheat, and those with 42 chromosomes as hexaploid wheat. Simply put, each of the seven-chromosome set of hexaploid wheat consist of six homologous chromosomes, where two homologous pair belong to each genome (i.e., a pair from each of A, B, and D). Thus, hexaploid wheat is made up of 42 homologous chromosomes "(2n) = (6x)" (Bennici 1986b).

More than 90 percent of cultivated wheat is the allohexaploid bread wheat, which is believed to have been developed over thousands of years of improving domesticated landraces (Shewry 2009; Sun et al. 2015). The prominent consensus is that the bread wheat genome is formed long ago via the fusion of these ancestral genomes, especially from two wide hybridization events. The first event is believed to have occurred between 0.5–3.0 million years ago between two diploid ancestral species carrying, the A (*Triticum urartu*) and B (believed to be from *Aegilops speltoides*) genomes, resulting in the formation of wild tetraploid wheat (*Triticum turgidum* ssp. dicoccoides, AABB). Wild tetraploid wheat was then cultivated as the emmer (*Triticum turgidum* ssp. dicoccum, AABB) (Dubcovsky and Dvorak 2007; Shi and Ling 2018). The second event was estimated to have taken place about 9000 years ago between the cultivated emmer and diploid goat grass (Aegilops tauschii, DD), which resulted in the

formation of allohexaploid bread wheat (Peng et al. 2011; Shi and Ling 2018). Consequently, the genome of allohexaploid wheat is known to have an approximate genome size of 17 GB, making it one of the largest and most complex plant genomes (Sun et al. 2015).

1.2. NITROGEN FERTILIZATION AND WHEAT PRODUCTIVITY

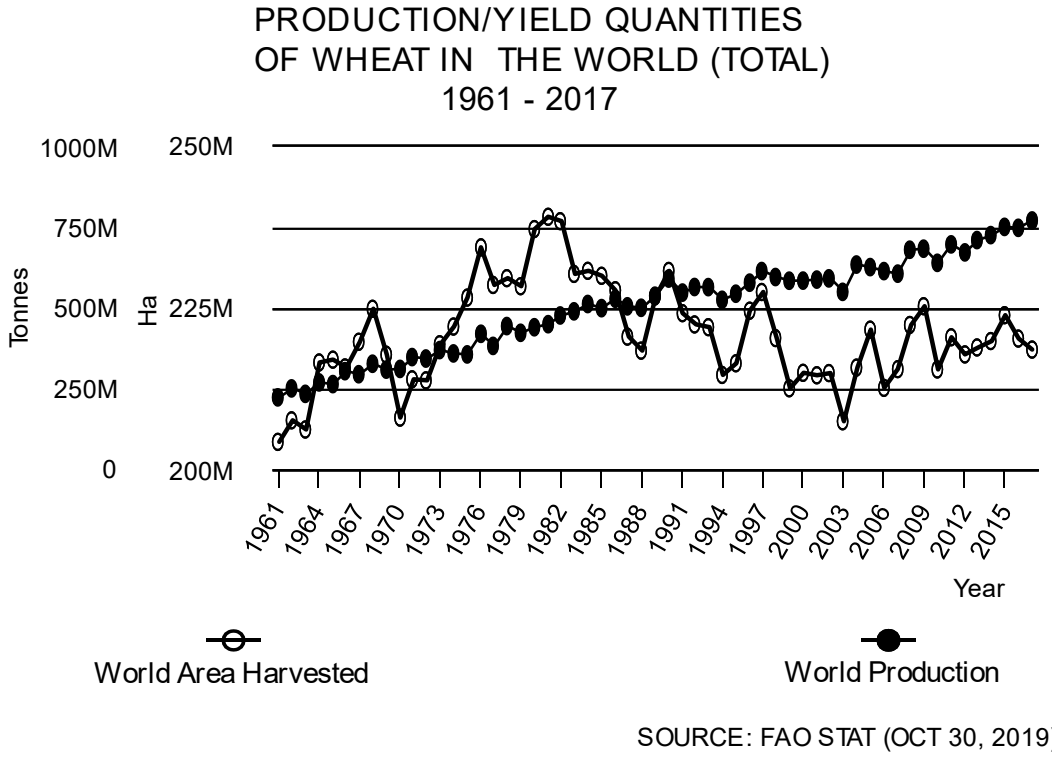

Figure 2. A chart showing the sum total of wheat production/yield all over the world, as well as the total area harvested for wheat from 1961 to 2017 (adapted from (FAO 2019), with slight modifications).

The increase in the utilization of farm inputs (such as fertilizer) and the introduction of high-yielding semi-dwarf seed varieties (which are easily adaptable to several climate conditions) increased worldwide wheat production (Aksoy and Beghin 2004; Dalrymple 1974). These semi-dwarf varieties displayed a higher yield, a better nitrogen use efficiency (Fischer and Maurer 1978; Ortiz-Monasterio et al. 1997), and a better resistance to lodging compared to the older tall varieties (Curtis et al. 2002). As a result, they have been adopted by developing economies that were not previously known for wheat production (Dalrymple 1974).

The ensuing reduction in plant loss of the new semi-dwarf varieties as well as improved fertilization and agricultural practices across the world, have all contributed to the increased

agricultural and economic return of allohexaploid wheat. This significant increase in wheat production has helped to meet the food need of the world, especially as the demand for cereals continue to increase worldwide (Fischer et al. 2014). Global wheat production has continued to increase by an average of 2.4 percent each year since the middle of the 20th century((Aksoy and Beghin 2004), increasing from just over 500 million tonnes in 1982 to more than 770 million tonnes in 2017 (FAO 2019). This is despite the decrease in the land area used for wheat production (Fig. 2). While the improvement in agriculture has continued to help in mitigating hunger poverty and malnutrition around the globe, the continuous growth in the world's population (estimated to rise over 9 billion by 2050 (Fig. 3)) implies that a multi-strategic approach for improving food production is needed. This is especially true if the growing world population is expected to be fed adequately in an environmentally conscious world (Vaarst et al. 2017).

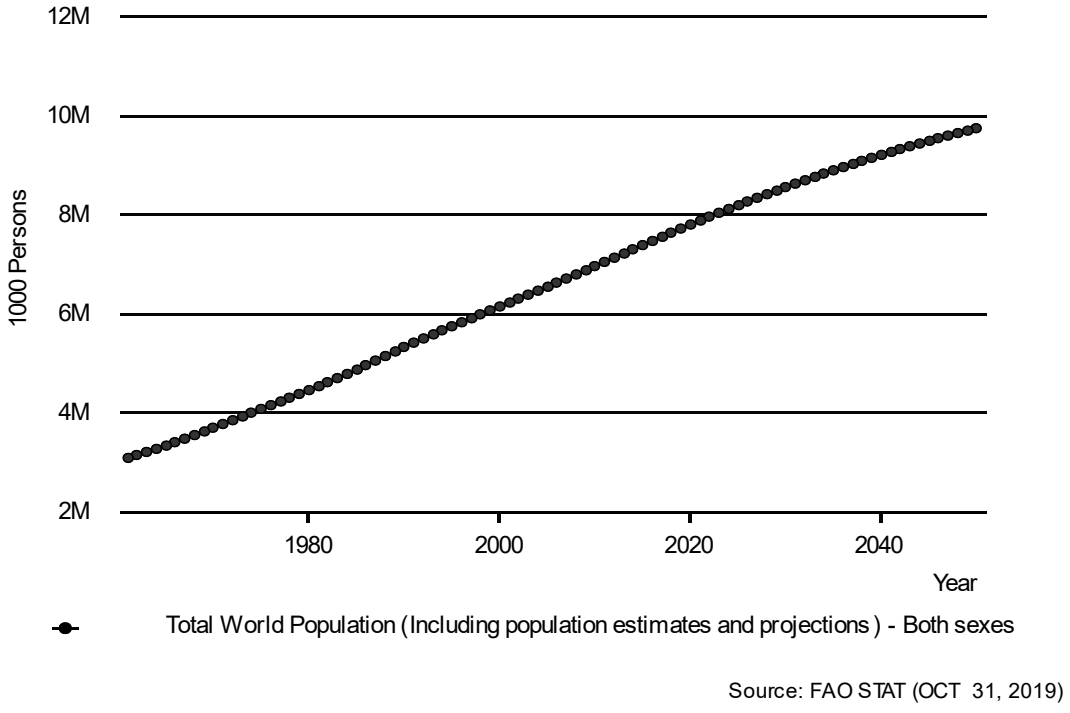

Figure 3. A chart showing the world population and population estimate up till the year 2050 (adapted from (FAO 2019), with slight modifications).

Nitrogen is a very important macronutrient in agroecosystems whose importance cannot be overemphasized (Albornoz 2016). It is involved in many plant physiological and metabolic processes, while also serving as the primary constituent of proteins, enzymes and nucleic acids (Maathuis 2009). It is for this reason that nitrogen-containing fertilizers are commonly used in modern agriculture, due to the limited nature of nitrogen in many natural ecosystems (Ludewig

et al. 2007). In fact, nitrogen fertilization has been repeatedly shown to improve growth, grain yield, grain quality, as well as the grain nutritional status of wheat (Belete et al. 2018; Hinzman et al. 1986; Khalil et al. 1987; Litke et al. 2018; Rekaby et al. 2016).

The wheat plant takes up nitrogen continuously throughout its 3 to 4 months life cycle (Hawkesford 2017; McGuire et al. 1998; Zörb et al. 2018); which allows for the accumulation of grain proteins that is necessary for baking and processing quality (Zörb et al. 2018). The high nitrogen demand of wheat has thus led to the investments of significant effort in the improvement of the nitrogen use efficiency of wheat (Laidig et al. 2014; Mackay et al. 2011). Yet, the grain yields of winter wheat (*Triticum aestivum* L.) have plummeted over the recent past (Fischer et al. 2014). Although most of the decline could be attributed to shifts in the acreage percentage, input extensification, climatic changes, as well as stricter environmental legislation limiting farmers in the allowed nitrogen and phosphorus fertilization rates (Laidig et al. 2014; Lassaletta et al. 2014; Lobell et al. 2011; van Grinsven et al. 2012), yet the improvement in the production of wheat is still important in the fight against global hunger and malnutrition.

1.3. AMMONIUM AND NITRATE IN NITROGEN FERTILIZATION

The ability of nitrogen to improve yield and grain quality has led to nitrogen over-fertilization in most fields, (Albornoz 2016). This is mostly due of its consideration by farmers as an insurance to maximize yield during growing seasons (Hendricks et al. 2019). In another twist, it is considered as the sustenance of an extended harvest when market conditions are favourable (Hendricks et al. 2019).

Soil N is mostly available as nitrate (NO_3^-) and ammonium (NH_4^+). Nitrate solubilizes easily in soil water, and could be easily leached as pollutant into underground water (Majumdar 2003; Ronald F. Follett 2001). It could also be washed off into water bodies, where excess nitrogen accumulation can cause overstimulation growth in aquatic plants and algae (USGS 2019). Lakes, reservoir and estuary eutrophication (one of the leading environmental problems) can also occur, leading to algal blooms and anoxic conditions (Carpenter 2005; Conley et al. 2009; Howarth and Marino 2006; Lewis et al. 2011; Yang et al. 2008). Disturbingly, excessive nitrate in drinking water can also be harmful to infants, causing the notorious "blue baby syndrome", by restricting oxygen transport in their blood stream (Majumdar 2003; USGS 2019).

Ammonium on the other hand is not as mobile as nitrate in the soil due to its tendencies to be sorbed to the cation exchange capacity (CEC) of the soil, fixed into clay and other complexes

within the soil, released by weathering back into the available mineral pool, or immobilized into organic form by microbial processes taking place in the soil (Ronald F. Follett 2001). Interestingly, ammonium concentration could also be as high as 20 mM in certain agricultural ecosystem (Britto and Kronzucker 2002). While most of the ammonium could still be subjected to active nitrification process going on in the soil, it still makes ammonium a major form of inorganic nitrogen (Liu and Wirén 2017). Although the high soil mobility of nitrate leads to a more rapid diffusion towards plant roots (Boudsocq et al. 2012), the less mobile ammonium is less prone to loss from agroecosystems, and as such less likely to contaminate underground water (Brady and Weil 2001; Marschner 2008). Incidentally, ammonium nutrition has been reported to trigger modifications in plant metabolism in a way that can be beneficial for crop quality and plant's cross-tolerance to biotic or abiotic stresses (Marino and Moran 2019).

Several plants species, including wheat, have displayed a preference for ammonium N over nitrate (Boudsocq et al. 2012; Brian Gordon Forde, and David T. Clarkson 1999; Britto and Kronzucker 2013; Fredeen and Field 1992; Gazzarrini et al. 1999; Kronzucker et al. 1995; Pantoja 2012; Sarasketa et al. 2016), despite the ability of sole ammonium N nutrition to cause toxic effects at elevated concentrations (Chaillou et al. 1986; Hachiya et al. 2012). This tendency is explained in part by the lesser amount of energy required to fix ammonium N compared to its nitrate counterpart (Fig. 4) (Bloom et al. 1992; Boudsocq et al. 2012; Britto and Kronzucker 2005, 2013; Howitt and Udvardi 2000; Kurimoto et al. 2004; Reisenauer 1978). Wheat in particular has displayed an increased grain yield, improved processing quality parameters, and an improved grain storage proteins (GSPs) with sole ammonium treatment, compared to sole nitrate (Fuertes-Mendizábal et al. 2013; Zheng et al. 2018). It is noteworthy that sole ammonium nutrition situation is an artificial phenomenon mostly created in the laboratory (Marino and Moran 2019), nonetheless, the use of nitrification inhibitors together with ammonium fertilizers (or organic fertilizers) makes ammonium more stable and available at high concentrations in the soil for a longer period of time; and has been proposed as a means to mitigate the negative impact of nitrogen fertilizers on the environment (Sanz-Cobena et al. 2017).

Also, the ability of ammonium nutrition to coordinates with soil microorganism in a way that improved plant acquisition of phosphorous from the soil has also been reported (Mpanga et al. 2019). While the preferential uptake of ammonium (over nitrate) by plants could be because of its obvious benefits, the preference of a particular form of nitrogen over the other (β) has also been reported in several plants species (Boudsocq et al. 2012; Britto and Kronzucker 2013),

and has been shown to be important for their ecosystem functioning and the establishment of plant community structure (Boudsocq et al. 2012). Yet, despite the long list of the reported benefit of ammonium nutrition, the potential toxic effect of sole ammonium nutrition has been a major limitation.

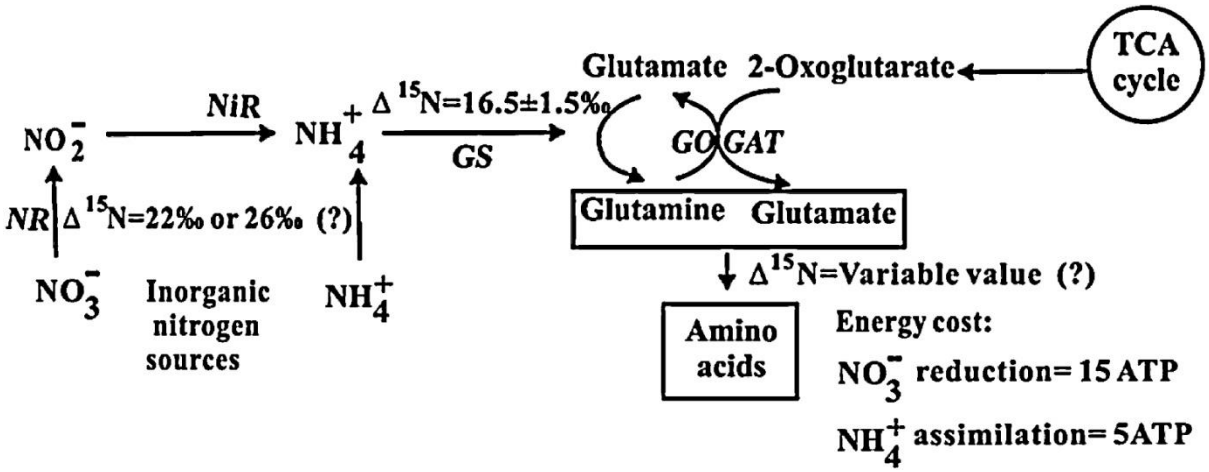

Figure 4. Schematic representation of the assimilation of inorganic nitrogen in plants. *NR* nitrate reductase; *NiR* nitrite reductase; *GS* glutamine synthetase; *GOGAT* glutamate synthase. Ammonium is incorporated into organic molecules in the form of glutamine and glutamate through the combined action of the two enzymes GS and GOGAT in the plastid or chloroplast (Zhang et al. 2019a).

1.4.EFFECT OF AMMONIUM TOXICITY ON PLANTS

The most common symptoms of ammonium toxicity are a reduced biomass, leaf chlorosis, apoptosis, root dieback, root discoloration, accelerated lateral rooting, necrosis, shrinking of the root axis root hairs, inhibition of tap root elongation, growth reduction, growth stimulation and increased frost sensitivity (Bittsánszky et al. 2015; Li et al. 2014; Marino and Moran 2019; Pan et al. 2016; Schortemeyer 1997; van der Eerden 1982). Leaf chlorosis in particular has been related to ionic imbalances, disturbance of pH gradients across plant membranes and oxidative stress (Bittsánszky et al. 2015; Britto and Kronzucker 2002; Esteban et al. 2016; Li et al. 2014). Growth inhibition on the other hand has been associated to the futile energy cost required to control the NH_3/NH_4^+ level in plant tissues (Britto et al. 2001; Marino and Moran 2019).

Furthermore, ammonium nutrition is known to induce rapid changes in cytosolic pH, leaf ATP, gene expression, post-translational modifications of proteins, apoplastic acidification, co-ordinated ammonium uptake, enhanced ammonium assimilation, altered oxidative status, and

the reshaping of the root system architecture (Liu and Wirén 2017; Matsumoto and Wakiuchi 1974).

It is noteworthy that every plant species appears to be susceptible (at least to different extent) to ammonium toxicity (Marino and Moran 2019; van der Eerden 1982). Thus, ammonium tolerance has been defined as "a situation where the plant is somehow sensing and responding towards ammonium stress prior to suffering a serious damage such as chlorosis or cell death" (Marino and Moran 2019).

Efforts to elucidate the mechanism behind the observed effects of excessive ammonium nutrition have produced several explanations: one of such, is the possibility of ammonium uptake to exceed the ammonium assimilation rate, thereby leading to the accumulation of toxic concentrations of free ammonium /ammonia in plant tissues (Findenegg 1987). A popular example has been the case of rice (an ammonium expert) and barley (a more ammonium sensitive plant), which both accumulated cytosolic ammonium in the range of hundreds of mM at an external ammonium concentration of 10 mM (Britto and Kronzucker 2002). Compare to rice, toxicity symptoms were more severe in barley. Barley it seems, exhibited an ammonium regulation breakdown at elevated external ammonium concentration, while rice seemed capable of managing elevated concentration of accumulated ammonium N (Britto et al. 2001). Even though rice is regarded as the cliché ammonium N specialist, varieties with a better nitrogen use efficiency have also displayed a better utilization of ammonium N in the seedling stage (Chen et al. 2013). Rice has also shown a substantial increase in the expression of ammonium assimilating enzymes, and a better growth rate at elevated ammonium supply compared to corn and tomato (Magalhäes and Huber 1989). Thus, despite the tendency of excessive accumulation of ammonium to cause toxicity, certain species have developed a more efficient ammonium N management strategy than others, which involves an efficient synchrony between cytosolic ammonium accumulation and an optimum ammonium N assimilation rate.

The tendency of ammonium fed plants to acidify the rhizosphere is known (Findenegg 1987). Deprotonation of ammonium (to ammonia) as ammonium is transported across the plasma membrane (Ganz et al. 2020; Ishikita and Knapp 2007) is believed to release a proton burden on the cytosol, thereby necessitating the need for proton extrusion. While this strategy allows the electrical potential gradient to provide the driving force for the downhill transport of net NH_4^+ across the plasma membrane (Dyhr-Jensen and Brix 1996), it also enables plants to maintain the proton gradients across the plasma while ammonium is being taken up (Britto and

Kronzucker 2002). Interestingly, while maximum net NH_4^+ influx occurred at pH 6.2 in wheat (Zhong et al. 2014), net proton efflux was observed from pH 5 to 8. The effort of plants to maintain the sensitive ionic balance across their plasma membrane may lead to the accumulation of protons in the rhizosphere, which could also result in toxicity, mainly due to the build-up of unhealthy acidic conditions. This possibility has hitherto been tipped as the reason why ammonium toxicity tends to be more severe at lower pH than at higher pH (Magalhäes and Huber 1989), even though ammonium uptake rate has been shown to be lower at acidic pH than at neutral pH (Dyhr-Jensen and Brix 1996).

The idea of the pH dependency of ammonium toxicity to plants seem to vary from one species to another. *Typha latifolia* for example demonstrated its highest growth rate at a relatively acidic pH compared to its growth rate at neutral and alkaline pH (Dyhr-Jensen and Brix 1996). Oat and maize on the other hand had a higher total biomass accumulation at pH 5 than at pH 6 (Findenegg 1987). Barley and sorghum performed worse at pH 5 than at pH 6, while Oat, Maize, Barley and Sorghum all had the lowest total biomass accumulation at pH 7. Although most plant species grew optimally at pH 6.0, the white and yellow lupines, accumulated their highest total biomass at pH 7 (Findenegg 1987).

Efforts of plants to maintain the delicate ionic balance across their cell membrane when supplied with ammonium are also known to cause an impaired cation uptake. For instance, ammonium fed plants exhibit a decreased uptake of important cations such as K, Ca and Mg, while increasing the uptake of anions such as Chloride, Sulphate and Phosphate (Britto and Kronzucker 2002). Notably, several cereals still maintained potassium uptake rates while also taking up ammonium, despite the possibility of an impaired electrical membrane characteristics (Findenegg 1987; Kong et al. 2014; Lee and Rudge 1986). This points to a high likelihood that an alternative strategy is being adopted by cereals to mitigate ammonium stress; which is further buttressed by the ability of potassium and calcium to alleviate ammonium toxicity in several plants (Britto and Kronzucker 2002; Guo et al. 2019; Hernández-Gómez et al. 2015). Interestingly, anions such as Nitrate, Carbon and Silicon have also shown the ability to ameliorate the effect of ammonium toxicity in Arabidopsis, Cucumber and Tomatoes respectively (Barreto et al. 2016; Hachiya et al. 2012; Roosta and Schjoerring 2008).

The problem of ammonium toxicity necessitates the effective regulation of ammonium uptake. Hence, faced with a dilemma to either shut down ammonium uptake and go into a period of nitrogen starvation, or come up with an effective regulatory mechanism to deal with the supplied ammonium N, it is therefore no surprising that different plant species show different

levels of tolerance and response to sole ammonium N application. Evolution becomes a key role player here, as the ability of a plant species to cope with ammonium nutrition then depends on how well it has evolved over evolutionary time to metabolise ammonium N.

Therefore, an effective strategy, from sensing, to uptake and metabolism of supplied ammonium N becomes imperative for ammonium N tolerance. Classical responses include the maintenance of the appropriate proton gradients across the plasma membrane, decrease in root length to limit the spatial accessibility to ammonium, down-regulation of ammonium transporters, vacuolar compartmentalization of accumulated ammonium, transcriptional up regulation of assimilation enzymes (GS, GDH, AS), as well the translational and the post-translational regulation of relevant genes (Bittsánszky et al. 2015; Dyhr-Jensen and Brix 1996; Gazzarrini et al. 1999; Howitt and Udvardi 2000; Li et al. 2014; LI et al. 2012).

The several effects of ammonium toxicity, as well as its inherent complexity, imply that plants need to respond appropriately, and effectively to ammonium N nutrition. Unfortunately, many plant species, aside from the more adapted species like Rice, and Larch (Guo et al. 2007; Li et al. 2009a; Malagoli et al. 2000) struggle at achieving this complex objective. Hence, inefficient coping mechanisms such as the futile cycling of ammonium (Britto et al. 2001) and the detoxification of radical oxygen species (Zhu et al. 2000) becomes inevitable, and if all fails, the manifestation of the observed toxicity effect.

1.5. AMMONIUM TRANSPORTERS

Ammonium exists as an equilibrium between two N forms with different membrane permeability (NH_4^+ and NH_3). Nevertheless, the pH-dependent equilibrium ($pK_a = 9.25$) between the uncharged NH_3 and the charged form NH_4^+ (Fig. 5) ensures that the ion form is predominant under all physiological conditions (Ludewig et al. 2007).

Plant ammonium uptake is mainly via membrane localised ammonium transporters (AMTs). Ammonium transporters (AMT) are members of the AMT/methylammonium permease/ Rhesus (AMT/Mep/Rh) family of integral membrane proteins (Ludewig et al. 2001) which transport ammonium across the plasma membrane in plant roots (Loqué and Wirén 2004; Ludewig et al. 2002; Marini et al. 1994; Ortiz-Ramirez et al. 2011; Wirén N., and Merrick M. 2004; Yuan et al. 2007). The typical properties of this family of transporters include affinities towards ammonium (K_m) within the micromolar range, as well as a high selectivity for ammonium and its methylated analog (Boeckstaens et al. 2008; Couturier et al. 2007; D'Apuzzo et al. 2004; Gazzarrini et al. 1999; Ludewig et al. 2002; Ortiz-Ramirez et al. 2011;

Pantoja 2012; Shelden et al. 2001; Wood et al. 2006). Plant AMT1 ammonium transporters defined the AMT subfamily, while the AMT2 group of plant AMT is more closely related to the AmtB of bacteria (Sohlenkamp et al. 2002), which are more related to the Mep2 subfamily.

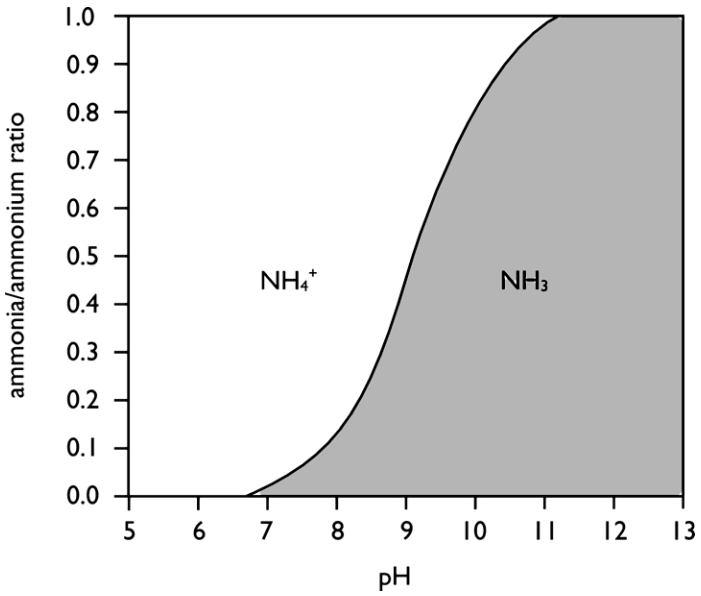

Figure 5. The pH dependence of NH_3/NH_4^+ ratio (Susan W. Gay and Katharine F. Knowlton 2009)

Available membrane topology depicts AMT proteins as trimers of subunits (Fig. 6). Each subunit is made up of mostly 11 trans-membrane helices, an extra-cytoplasmic N-terminus and a cytoplasmic C-terminus, with each subunit forming an ammonium transporting pore (Andrade and Einsle 2007; Bao et al. 2015; Khademi et al. 2004; Li et al. 2006; Li et al. 2007; Loqué and Wirén 2004; Wirén N., and Merrick M. 2004). The functionality of the ammonium transporting pore nevertheless depends on the successful crosstalk between the C-termini of the monomeric subunits that make up the trimeric complex (Marini et al. 2000; Neuhäuser et al. 2007).

After successful uptake, ammonium is assimilated in the root system via glutamine-syntethase (in the cytoplasm and plastids), before long distance transport to the shoot (Howitt and Udvardi 2000; Meeks et al. 1978; Stewart et al. 1980). It is also known that ammonium transporters help to deliver the ammonium generated de novo from molecular nitrogen (N_2) by nitrogen fixing bacteria living in the root of leguminous crops, into the plant cytoplasm (Howitt and Udvardi 2000).

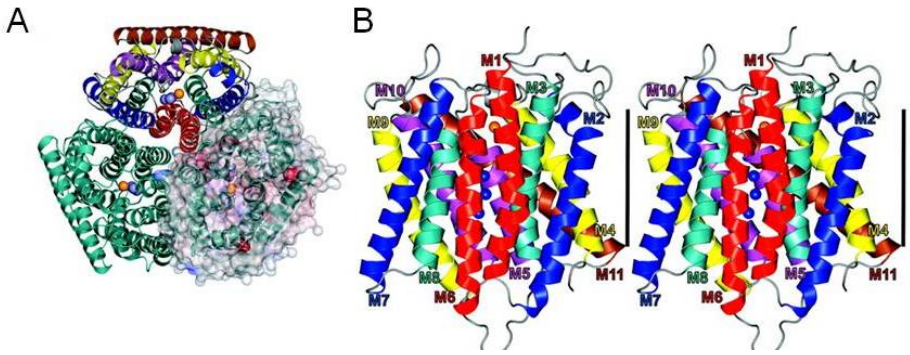

Figure 6. Three-dimensional fold of EcAmtB. (A) Ribbon representation of the AmtB trimer viewed from the extracellular side. (B) A stereo view of the monomeric ammonia channel viewed down the quasi-twofold axis. The vertical bar (35 Å) represents the inferred position of the hydrophobic portion of the bilayer (Khademi et al. 2004).

Ammonium uptake by plants is biphasic and can be separated into two components, the high affinity ammonium transport system (HATS) and the low affinity ammonium transporter system (LATS) (Kronzucker et al. 1996; Wang et al. 1993; Wang et al. 1994). The high affinity transport system (HATS) is a saturable system that is involved in the secondary active uptake of ammonium against chemical gradient, while the low-affinity transport system (LATS) is a non-saturable system that exhibits a linear increase in activity when the ammonium concentration increases (Kronzucker et al. 1996; Wang et al. 1993). High affinity ammonium transporters are responsible for plant ammonium uptake in the NH_4^+ form under conditions of little (lower than 1 mM) to no nitrogen (Gazzarrini et al. 1999; Sohlenkamp et al. 2000). The low affinity ammonium transporters on the other hand coordinate ammonium uptake at conditions of high concentration of ammonium availability. Notably, all members of the AMT/Mep/Rh family exhibit ammonium affinities in the micro molar range and therefore constitute the HATS of plants. Nonselective cation channels, potassium channels and members of the aquaporin family have also been shown to facilitate low affinity NH_3/NH_4^+ uptake at high concentrations. Yet, while these transporters might contribute to the LATS, a specific low affinity ammonium transporter has not yet been identified (Holm et al. 2005; Loqué et al. 2005; Loqué et al. 2009; Nakhoul et al. 2001; Schachtman et al. 1992; Szczerba et al. 2008).

The model plant *Arabidopsis thaliana* has six ammonium transporters (Yuan et al. 2007), five of which are known high affinity ammonium transporters (AtAMT1;1 AtAMT1;2 AtAMT1;3 AtAMT1;4 AtAMT1;5). AtAMT2;1 exhibits a lower affinity for ammonium, by exhibiting saturation at higher concentrations, but still in the micro molar range. In theory, ammonium is recruited to the transporter in a potential dependent way, before plant AMTs finally transport

the deprotonated ammonia (Guether et al. 2009; Neuhäuser et al. 2009; Sohlenkamp et al. 2002).

High affinity ammonium transporters are important for plant ammonium uptake. In *Arabidopsis thaliana*, two AMT1s (AtAMT1;1 and AtAMT1;3) have been shown to be additively responsible for up to 70% of the plant's ammonium uptake under conditions of nitrogen starvation (Loqué et al. 2006). Hence, the effective regulation of ammonium transporters is important in the response of plants to ammonium nutrition, especially at condition of nitrogen starvation, optimal ammonium supply and at ammonium concentrations that confer ammonium toxicity. Although mainly responsible for transporting ammonium, a "transceptor" model has also been postulated for ammonium transporters in plants and in yeast, where they have been described to act as a transporter and as a receptor that is actively involved in ammonium sensing and signalling (Lanquar et al. 2009; Thevelein et al. 2005).

1.6.TRANSCRIPTIONAL REGULATION OF AMMONIUM TRANSPORTERS

Since AMTs are mainly responsible for plant ammonium uptake, the problem of ammonium toxicity, especially at condition of elevated ammonium supply necessitate their effective regulation. In Arabidopsis, the downregulation of ammonium transporter expression at ammonium supply, and the up-regulation of ammonium transporters at conditions of nitrogen starvation have been observed (Gazzarrini et al. 1999; Loqué and Wirén 2004; Rawat et al. 1999; Shelden et al. 2001). Plants down regulate the expression of ammonium transporters, to reduce ammonium uptake, while the observed up regulation at condition of nitrogen starvation occur as an effort to increase nitrogen acquisition.

The expression of the plants ammonium transporters has been shown to be influenced significantly by diurnal changes, plant nitrogen status, plant nitrogen requirements, external nitrogen supply and plant glutamine levels in *Arabidopsis thaliana*, *Medicago truncatula* and *Oryza sativa* (Gazzarrini et al. 1999; Lejay et al. 2003; LI et al. 2012; Rawat et al. 1999; Straub et al. 2014). The effects of diurnal changes on the expression of plant ammonium transporters has been particularly attributed to the availability of photosynthetates during diurnal changes (Lejay et al. 2003). For instance, the expression of AtAMT1;1, AtAMT1;2 and AtAMT1;3 was induced by sucrose in a manner that showed correlation between induction by light and induction by sucrose, thereby indicating stimulation by the product of photosynthesis (Lejay et al. 2003).

1.7.POSTTRANSLATIONAL REGULATION OF PLANT AMMONIUM TRANSPORTERS

1.7.1. PII LIKE PROTEINS REGULATION OF AMTB

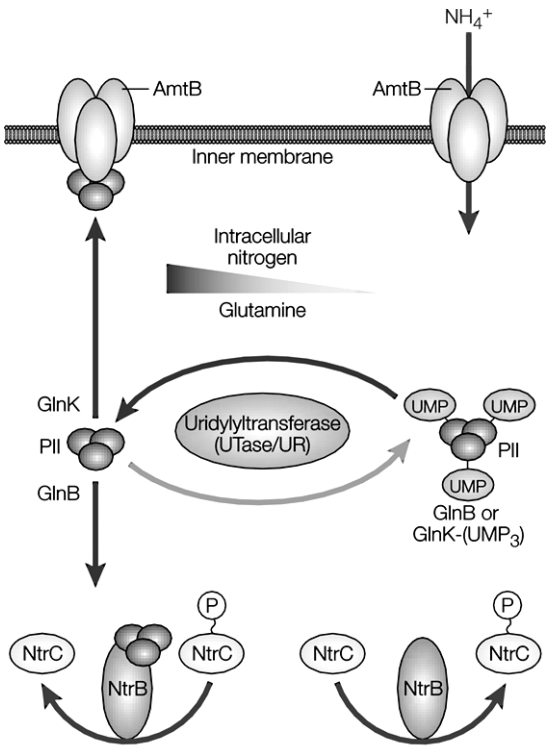

Figure 7. A schematic representation of the regulation of AMTB by PII signal proteins (Dixon and Kahn 2004). The regulation of ammonium uptake by GLnK is dependent on the nitrogen status of the organism, where the uridylation of GlnK by the Utase/UR protein (encoded by the glnD gene) under nitrogen-limiting condition prevents its interaction with its target proteins (Dixon and Kahn 2004). This process is reverse under conditions of nitrogen availability, where GlnK is de-uridylylated, and free to impair AmtB ammonium transport activity (Dixon and Kahn 2004).

The ability of the PII like signal transduction proteins, GlnK to regulate the ammonium transporter (AmtB) of *E. coli*, (Arcondeguy et al. 2001; Javelle et al. 2004) had broadened our understanding of the post translational regulation of ammonium transporters. The PII protein GlnK was shown to form a complex with AmtB via a long surface loop contain Y51, which eventually resulted in physiological conformation that allowed it to block the ammonium transport activity of the transporter (Conroy et al. 2007). The discovery opened the door to the understanding that even after translation, ammonium transporters could still be regulated.

1.7.2. PHOSPHORYLATION MEDIATED REGULATION OF AMMONIUM TRANSPORTERS

Protein phosphorylation is also a widespread type of post-translational modification that is involved in signal transduction (Yasuda et al. 2017). It plays an important role in cell signalling, gene expression and in the differentiation global control of DNA replication in eukaryotic organisms(Garcia-Garcia et al. 2016). It is also known to induce the reversible modulation of the activity of several proteins and enzymes (Ardito et al. 2017; Ohta et al. 2003; Poulsen et al. 2010). In fact, the activity of ion channels in particular are known to be modulated by the phosphorylation of important serine, threonine, and tyrosine residues (Ismailov and Benos 1995).

Ammonium transporters are not left behind in this regard, as the phosphorylation of ammonium transporters has been shown to effectively cause the allosteric inactivation of the AMT trimer, thereby preventing the accumulation of potentially toxic cytosolic ammonium concentrations (Boeckstaens et al. 2014; Lanquar et al. 2009). Interestingly, Six phosphorylation sites are located within the C-terminus of AtAMT1;1, namely; T460, S475, S488, S490, S492 and T496 (Gazzarrini et al. 1999; LI et al. 2009; Loqué and Wirén 2004; Wirén et al. 2000), all of which are believed to be relevant for the integration of multiple signaling pathways (Lanquar et al. 2009).

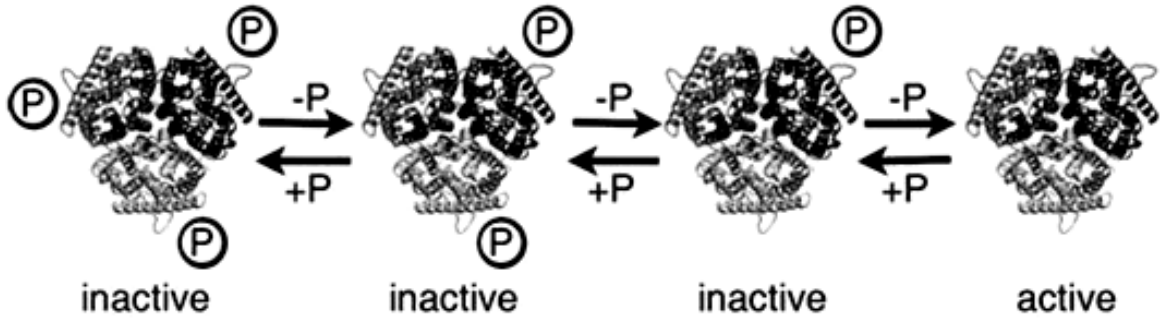

Figure 8. Phosphorylation of at least a monomer subunit of the Ammonium transporter's (AMT) trimeric complex inactivates ammonium transporters (Neuhäuser et al. 2007).

While earlier phospho-proteomics works have reported phosphorylated residues in the C-terminus of AtAMT1;1 (Nühse et al. 2004), experiments with phosphomimic mutants have also shown that an exchange of physiologically relevant threonine residue at the C-teminus (for aspartic acid) was able to impair ammonium transport in Arabidospsis (Loqué et al. 2007; Neuhäuser et al. 2007), and rice (Zhu et al. 2015) in a concentration and time dependent manner (Lanquar et al. 2009; Zhu et al. 2015). External ammonium concentration in particular

have also been shown to be the signal to the phosphoregulation of these ammonium transporters (Lanquar et al. 2009).

Furthermore, the formation of both functional hetero and homo oligomers (by the ammonium transporters of yeast and plants) with their respective homologs is known (Ludewig et al. 2003; Marini et al. 2000; Monahan et al. 2002; Yuan et al. 2013). This in addition to the existence of a crosstalk between the C termini of the monomeric subunits that make up the ammonium transporter's trimeric complex ensures that an inactivating modification on any single monomer subunit would inactivate or impair the transport activity of the whole trimer (Fig. 8) (Marini et al. 2000; Neuhäuser et al. 2007). Hence, the phosphorylation of an ammonium transporter has the capability to regulate both the homo oligomeric trimeric complexes, as well as the hetero oligomeric trimeric complexes. Interestingly earlier efforts have demonstrated that inactive mutated AMTs of yeast were also able to impair the activity of umutated ones (Marini et al. 2000). This was also shown in tomatoes, where the nonfunctional LeAMT1;1 impaired the activity of LeAMT1;2 (Ludewig et al. 2003). It has also been shown in *Arabidopsis thaliana* that the inactive phosphomimic mutants of Arabidopsis AtAMT1;1 were able to impair the transport activity of AtAMT1;3 (Yuan et al. 2013). Thus, while the phospho-regulation of ammonium transporters is a significant evolutionary feat, the formation of both homo and hetero oligomeric AMT trimeric complex further integrate the phospho-regulatory mechanism into the ammonium regulatory pathway, thereby creating a more efficient and effective regulation system for plant ammonium uptake.

1.8. THE CBL-CIPK COMPLEX REGULATION OF AMMONIUM TRANSPORTERS

1.8.1. THE CALCINEURIN B-LIKE PROTEIN (CBL)

Ca^{2+} is involved in various responses to abiotic and biotic stimuli. These stimuli elicit distinct calcium signals in the form of a spatio-temporal pattern of changes in free cytosolic Ca^{2+} concentration, which eventually form stimulus-specific signatures (Kudla et al. 2010; Sanders et al. 1999). The Calcium signals are thereafter decoded, transmitted and relayed by Ca^{2+} binding proteins into downstream responses (Kudla et al. 2010; Sanyal et al. 2015). Plants possess a number of these distinct Ca^{2+} sensor proteins, which contain EF-hand Ca^{2+}-binding motifs (Fig. 9) that are used for calcium binding and signaling (Cho et al. 2016).

Figure 9. General composition of calcineurin B-like (CBL) proteins and CBL-interacting protein kinases (CIPKs). The number 1,2,3, and 4 represent the EF-hand of CBL proteins. The CIPK proteins are typically made up of the regulatory domain part and the kinase domain part (Weinl and Kudla 2009)

Ca^{2+}-binding proteins are grouped into sensor responders and sensor relays according to their mode of decoding Ca^{2+} signals (Sanders et al. 2002). Sensor responders include proteins with enzymatic activity, which are also modulated by an intramolecular Ca^{2+}-binding domain (Cho et al. 2016). Sensor relays on the other hand lack enzyme activity but can associate with, and regulate other proteins in a Ca^{2+}-dependent manner (Cho et al. 2016).

Calcineurin B-like (CBL) proteins (Ca^{2+}-binding proteins) are sensor relay proteins due to their lack of enzymatic activity and their ability to bind to, and regulate target proteins (Cho et al. 2016; Kudla et al. 1999; Liu and Zhu 1998; Shi et al. 1999). They decode transient calcium signatures (elicited by a variety of abiotic stress) by interacting with and regulating the Calcineurin-B like (CBL)-interacting protein kinases (CIPK) (Batistic and Kudla 2009; Cho et al. 2016; Luan et al. 2002; Mohanta et al. 2015). They have also been shown to regulate the TOC (Translocon of the Outer membrane of the Chloroplasts) proteins of *Arabidopsis thaliana* (Cho et al. 2016). They are known to possess four EF-hand domains, made of a helix-loop-helix structure that is able to bind cytosolic calcium ions (Gifford et al. 2007; Sanyal et al. 2015), after which they undergo conformational changes that allow them to interact with downstream effector molecules or target proteins (Clapham 2007; DeFalco et al. 2009).

The canonical sequence of a Ca^{2+} binding EF-Hand motif contains twelve amino acid residues DKDGDGKIDFEE, that are conserved at positions 1(X), 3(Y), 5(Z), 7(-X), 9(-Y) and 12(-Z) (Li et al. 2009b). While the first EF-hand of all the 10 AtCBLs exhibits amino acid substitution at the critical Ca^{2+}-binding positions, the remaining three possess significant canonical amino acid sequences, thereby leading to suggestion that each plant CBL harbors three EF-hand motifs that could be canonical; where the first EF-hand motif sequence is regarded as non-

canonical (Gong et al. 2004; Li et al. 2009b; Luan et al. 2002; Mohanta et al. 2015). The variability in the number of classical canonical EF hand amino acid motifs possessed by the CBL proteins of *Arabidopsis thaliana* has been used to classify them into three groups, namely: group one (CBLs bearing two canonical EF-hand sequences; CBL1 and CBL9), group two (having only one canonical EF-hand sequence; CBL 6, 7, 10) and group three (has no canonical EF-hand CBL 2, 3, 4, 5, 8) (Batistic and Kudla 2009; Kolukisaoglu et al. 2004; Sanyal et al. 2015). Interestingly, the CBL4 of *Arabidopsis thaliana* was still able to bind Ca^{2+} in all its four EF-hands despite having no canonical EF-hand motif (Sánchez-Barrena et al. 2005; Sánchez-Barrena et al. 2007).

Table 1. Cellular/subcellular localization of the Calcineurin B-like proteins of *Arabidopsis thaliana* (Sanyal et al. 2015).

No.	Calcineurin B-like protein	Localization
1	AtCBL1	Plasma membrane
2	AtCBL 2	Tonoplast
3	AtCBL 3	Tonoplast
4	AtCBL 4	Whole cell
5	AtCBL 5	Whole cell
6	AtCBL 6	Tonoplast
7	AtCBL 7	Cytoplasm, Nucleus
8	AtCBL 8	Plasma membrane, Cytoplasm, Nucleus
9	AtCBL 9	Plasma membrane
10	AtCBL 10	Plasma membrane, Tonoplast

The 10 CBL proteins (Kolukisaoglu et al. 2004; Sanyal et al. 2015; Weinl and Kudla 2009) of *Arabidopsis thaliana* are localized at different or multiple cellular compartments (Table 1) (Sanyal et al. 2015). The conserved N myristolation motif MGXXXS/T(K) (Towler et al. 1988) at the N-terminal end of some CBL proteins is critical for the membrane localization of the CBL proteins (Ishitani et al. 2000). Myristoylation, followed by S-acylation of the myristolated Glycine (G) residue at the N-terminal end of CBLs effectively targets them to the plasma membrane (Sanyal et al. 2015). For CBL1, Myristoylation has been shown to first target CBL1 to the endoplasmic reticulum, after which, *S*-acylation facilitates its endoplasmic reticulum-to-plasma membrane trafficking (Batistic et al. 2008; Chaves-Sanjuan et al. 2014).

1.8.2. CBL-INTERACTING PROTEIN KINASES (CIPKS)

The discovery of the ability of the TORC1 effector kinase Npr1 and the upstream TORC1 regulator Npr2 of yeast (*S.cerevisiae*) to regulate the transport activity of Mep2 via the phospho-silencing of a C-terminal autoinhibitory domain (Boeckstaens et al. 2014) had drawn scientific attention to plant Calcineurin-B like (CBL)-interacting protein kinases (CIPK). CIPK proteins (Fig. 9) are a group of plant serine/threonine protein kinases that are related to the Npr1of yeast. They have been shown to be upregulated in response to both nitrate and ammonium N (Canales et al. 2014; Engelsberger and Schulze 2012). In total, 25 CIPK genes are present in the genome of *Arabidopsis thaliana*, while 30 CIPK genes are present in the genome of *Oryza sativa* (Kolukisaoglu et al. 2004). As members of the CaMK group of serine/threonin protein kinases, they have a N-terminal kinase catalytic domain and a C-terminal regulatory domain (Albrecht et al. 2001; Chaves-Sanjuan et al. 2014; Guo et al. 2001; Sanyal et al. 2015). The architecture of the classical catalytic domain of Ser/Thr-specific and Tyr-specific kinases shows that the 250 amino acids that makes up the catalytic domain are divided into (1.) β-sheets containing N-terminal lobe and (2.) a large α-helix containing C-terminal lobe (Sanyal et al. 2015).

While the N-terminal end of the kinase domain is similar to the SNF1 protein kinase (Sucrose Non-Fermenting 1) of yeast and the Ca^{2+} mammalian AMP-dependent protein kinase (Cho et al. 2016; Shi et al. 1999), their distinct regulatory domain, which is located at their C-terminal end is further divided into the NAF/FISL domain and the Protein–Phosphatase Interaction (PPI) domain (Batistic and Kudla 2009; Sanyal et al. 2015). The conserved nature of the amino acid residues, N311, A312, F313, I316, S319, and L322 of the CIPK protein's NAF/FISL motif has given the motif the name (NAF/FISL) (Sánchez-Barrena et al. 2007). The NAF domain is a 24 amino acid domain that is important for the binding of CBL to the CIPK proteins (Albrecht et al. 2001). Dimerized Ca^{2+}-bound CBL proteins (Albrecht et al. 2001; Sánchez-Barrena et al. 2005) bind to the conserved NAF (or FISL) motif in the auto-inhibitory C-terminal regulatory domain of the CIPK protein (Guo et al. 2001; Hrabak et al. 2003), causing a conformational change by the CIPKs that leads to the displacement of the auto-inhibitory domain, thereby making the kinase active (Chaves-Sanjuan et al. 2014; Sánchez-Barrena et al. 2007; Weinl and Kudla 2009).

The phosphatase-binding domain (PPI motif), which is present next to the NAF domain, enables the CIPKs proteins to interact with type 2C protein phosphatases (PP2C) (Lee et al.

2007; Ohta et al. 2003; Sánchez-Barrena et al. 2005, 2005). The mutually exclusive nature of the binding of the PP2C to the PPI domain and the binding of the CBLs to the NAF domain (Sánchez-Barrena et al. 2007), is believed to be important for the reversible regulation of the activity of the CIPK proteins. Thus, the replacement of the CBL protein (which binds to the NAF and partly to the PPI domain) by the PP2C phosphatase, dissociates the CBLs, and as such, releases the otherwise masked auto-inhibitory domain of the CIPKs, resulting in the inactivation of the kinase domain (Sánchez-Barrena et al. 2007). Nonetheless, the possibility of PP2C proteins binding to the N terminal kinase domain have also been postulated (Lan et al. 2011).

1.9. THE CBL-CIPK COMPLEX

CBL proteins interact with CIPK proteins forming the CBL-CIPK complex, which has been implicated in the regulation of several ion channels and transporters (Albrecht et al. 2001). The complex, which is also involved in the regulation of several abiotic and biotic stress responses in plants (Weinl and Kudla 2009), has been shown to modulate Carbon/Nitrogen Nutrient Response (Yasuda et al. 2017). It has also been shown to modulate the low-affinity phase of the primary response of plants to nitrate (Hu et al. 2009). Its role in the maintenance of ion homeostatis in plants has shown that the CBL1/9-CIPK23 is able to activate AKT1 (an important potassium transporter) (Cheong et al. 2007; Xu et al. 2006), while also acting as a cellular switch which transforms the low affinity non phosphorylated nitrate transporter (NRT1;1) of *Arabidopsis thaliana* to a high-affinity nitrate transporter (Ho et al. 2009). Additionally, the CBL1-CIPK23 complex has also been shown to be able to regulate the high affinity ammonium transporters of *Arabidopsis thaliana*, by inactivating the transport function of the transporters via a phosphorylation mediated mechanism (Fig. 10).

The lack of a distinct cellular localization signal (so far) in CIPK proteins has led to the conclusion that the subcellular localization of the CBL-CIPK complex is determined by the interacting CBLs. Several CBL proteins appear to be targeted to the plasma membrane and vacuolar membrane, while the CIPK proteins are targeted to the cytoplasm and the nucleus (Batistic et al. 2008; Batistic et al. 2010; Sanyal et al. 2015; Zhang et al. 2014). Nonetheless, CBL-CIPK complexes have also been found to be localized in other cellular compartments (Batistic and Kudla 2009). The NAF domain on the other hand is known to confer the specificity of a CIPK protein for a particular CBL protein (Sánchez-Barrena et al. 2007). Such preferential complex formation (of CBLs with defined CIPK proteins) is now known as one of

the mechanisms generating the temporal and spatial specificity of calcium signals in plant cells (Albrecht et al. 2001; Batistic and Kudla 2004; Guo et al. 2001; Kim et al. 2000).

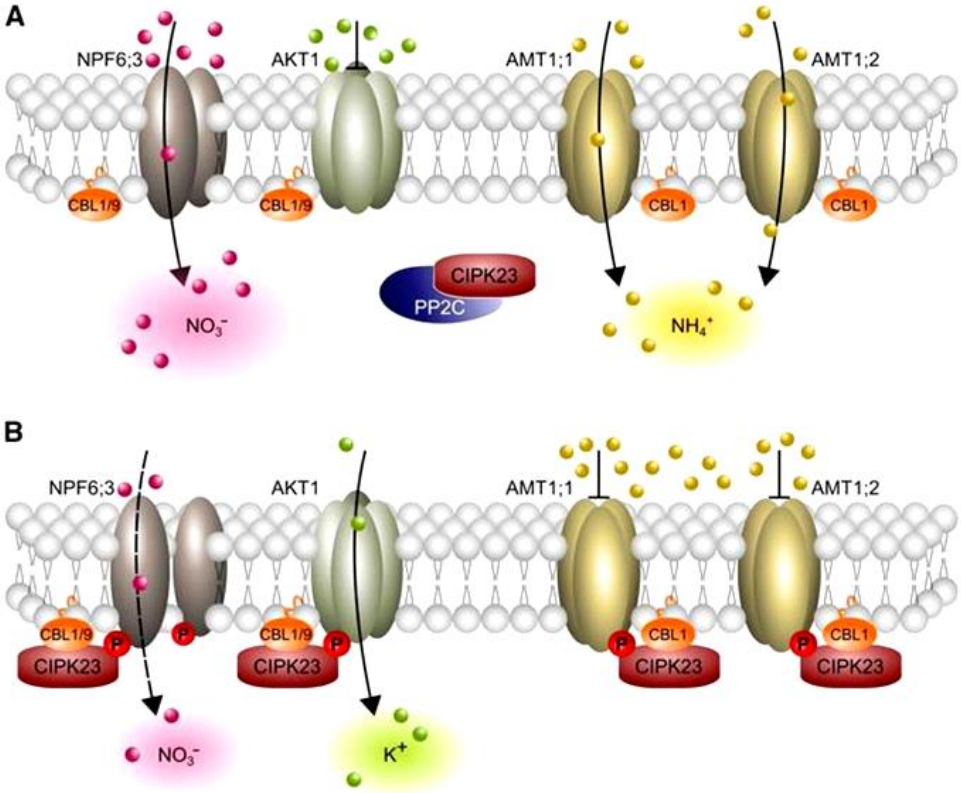

Figure 10. A model showing how CIPK23 regulates ion homeostasis (A) Under moderate ammonium conditions and/or high nitrogen demand. (B) Under toxic ammonium conditions (or possibly low nitrogen demand) (Straub et al. 2017).

However, while some CIPK proteins can only interact with one CBL protein, the ability of a CIPK protein to perform multiple functions by binding to multiple CBL proteins have also been demonstrated (Batistic and Kudla 2004, 2009; Gong et al. 2004; Guo et al. 2001; Sánchez-Barrena et al. 2007). A typical example is the CIPK24 of *Arabidopsis thaliana*, which is able to interact with multiple CBLs (CBL1, CBL4, and CBL10) to form a multifunctional kinase that is very important in the regulation of salt stress (Batistic and Kudla 2009). For instance, while the CBL4–CIPK24 modulate Na^+-extrusion via the Na^+/H^+ exchanger (SOS1) at the plasma membrane of roots, the CBL10–CIPK24 complexes, which are vacuole localized, facilitates the compartmentalization of Na^+ in the vacuole (Batistic and Kudla 2009).

1.10. HYPOTHESIS AND RESEARCH QUESTIONS

Despite the significant progress that has been made in understanding the regulation mechanism of ammonium uptake in plants, it is safe to say that most of the work done so far has been on plants other than wheat e.g., Arabidopsis, Rice, and Maize. However, the constant utilization of nitrogen fertilizer in agroecosystems and the soil properties of ammonium makes it a desired N source for fertilization. It is therefore expedient to understand the response of wheat (which is an important crop plants that is adaptable to numerous climates) to sole ammonium nutrition. This might aid the knowledge to further prepare the plant to take advantage of the high concentrations of soil bound ammonium in certain agroecosystems. Interestingly, the wheat genome contains numerous putative ammonium transporters, with two candidates showing to be potential high affinity ammonium transporters. Additionally, the high abundance of the CIPK and the CBL gene in the wheat genome also suggest that these groups of proteins might be involved in the regulation of high affinity ammonium transporters in wheat, especially since their role in the regulation of ion homeostasis in plants have been repeatedly shown.

It was therefore hypothesized that wheat will respond robustly to ammonium nutrition in a manner that involves the systematic regulation of its high affinity ammonium transporters. This implicit mechanism is anticipated to also involve the phosphorylation mediated regulation of wheat high affinity ammonium transporters, especially via a network that involves the participation of a regulating TaCBL-TaCIPK complex.

Thus, the following research question were asked:

1. What is/are the typical response of wheat to sole ammonium N?
2. Does wheat adopt phospho-regulation of its high affinity ammonium transporters as post-translational regulation mechanism?
3. What is the role of TaCBLs and TaCIPKs in the post-translational regulation of high affinity ammonium transporters from wheat?
4. By which mechanism of action do the candidate TaCBLs and TaCIPKs proteins of wheat regulate its high affinity ammonium transporters?

2. MATERIALS AND METHODS

2.1.MATERIALS

Table 2. A Table showing equipment used, their application and source.

Equipment	**Application**	**Source**
PCR machine (peqSTAR X cycler)	Gene amplification via Polymerase Chain Reaction	(PEQlab)
Biorad CFX 384	qRT-PCR performance	Bio-Rad, Munich, Germany
Laser Scanning Confocal Microscope (LSM700_ZEN_2010	Visualization of Yellow Fluorescent Proteins	Zeiss, Germany
Winrhizo (WinRHIZO pro)	Measurement of morphological parameters	Regent Instrument Inc., Canada
NanoDrop (ND-1000) spectrophotometer	Quality and concentration measurement of DNA, RNA, and miRNA	Thermo Scientific, Brunswick, Germany
Micro-dispenser	Oocyte injection	Drummond scientific Co.
Two electrode Voltage Clamp	Electrophysiology assay test with the Oocytes of *Xenopus laevis*	Group Ludewig Lab, Uni-Hohenheim, Stuttgart, Germany

2.1.1. SOFTWARE UTILISED

- Ugene sequence viewer V.35
- CLC sequence viewer 8.0.0
- Office 365
- pClamp
- Notepad 2019
- Visualization /analysis of the result of qRT-PCR procedure: BioRad CFX Manager™ Software Version 3.1
- Ensembl Plants for *Triticum aestivum* database queries: https://plants.ensembl.org/Triticum_aestivum/Tools/Blast

- BAR Classification SuperViewer Tool: http://bar.utoronto.ca/ntools/cgi-bin/ntools_classification_superviewer.cgi
- protein structure homology-modelling server: https://swissmodel.expasy.org/
- Alignment of modelled proteins structures with Pymol: The PyMOL Molecular Graphics System, Version 2.0 Schrödinger, LLC.
- Venn diagram: http://bioinformatics.psb.ugent.be/webtools/Venn/

2.1.2. MISCALLANEOUS ENZYMES/ ANTIBIOTICS

- Restriction Endonucleases, 10 U/µl (FastDigest) (Thermo Scientific)
- Shrimp Alkaline Phosphatase (SAP), 1 U/µl (Thermo Scientific)
- Ribonuclease A (RNase A) DNase free, 10 µg/µl (AppliChem)
- T4 DNA Ligase, 400 U/µl (New England Bio Labs)
- Kanamycin 50 µg/ml (final concentration)
- Ampicillin 50 µg/ml (final concentration)

2.1.3. ORGANISMS

- *Triticum aestivum* / Bob white
- *Escheriechia coli* / DH5α (Thermofischer Scientific).
- *Saccharomyces cerevisiae* /ΔΔΔ*mep* (Marini et al. 1997)
- *Xenopus laevis* / Oocyte (ordered from Ecocyte Bioscience; Germany)

2.1.4. PLASMID VECTOR BACKBONE

- pCR™-Blunt II-TOPO® Vector (Invitrogen, By Thermofischer Scientific)
- p002 Vector (Oocyte expression vector)
- pDR199 Vector (Yeast Expression vector)

2.1.5. PRIMERS

All primers were diluted on arrival with sterilized deionized water to achieve a 100 µM primer stock solution and stored in a -20^{o}C freezer.

Table 3. A table showing the primers used for the transcript quantification of the genes of interest (via the qRT-PCR).

GENE	Fw primers	Rv primers
TaAMT1;1	TGGACTCGACCTACCTGCTC	GTCCTTGAGGCCGAAGAAGT
TaAMT1;2	TGGAGTCCTCGTCGGTG	TCATCTGCGGGTTCGTGT
TaCBL1	GAACGGAAGGAGGTAAAGCA	GGAAGGATTCCTGGACACAA
TaCBL2	AAGACGTTTGAGGAGGCAGA	ATGGAAGACGAAGCTTGGAA
TaCBL3	CCCGTGCGCTATCAGTATTT	TGTCTGCCTCCTCGAAAGTC
TaCBL6	GAGGTGAAGCAAATGGTGGT	CAACAAAGATGGATGCCTCA

TaCIPK3	TGCAGACCTTTGGTCTTGTG	AATCCTGGGAATCAGCCTTT
TaCIPK9	TATGGCTGCTGATGTGTGGT	GGCGATTGTTATCCTCGTGT
TaCIPK23	ATGTCGCCATCAAGATCCTC	TCCTCTTTGAGCCTCCCA
TaCIPK31	AAGCCAACCTCAATGAATGC	GTTCTCCATCCGCATCTTGT
TaCIPK32	ATGTCAGCAGGCCTCAATCT	AGAAGGTCCGACTCGCAGTA
ACT	ACCTTCAGTTGCCCAGCAAT	TCGACCGCTGGCATACAAG
EF1α	CAGATCAGCAACGGCTATGC	TCTGGATCTCAGCAAACTTGACA

Table 4. A table listing the primers used for amplifying the candidate genes of interest from the cDNA of the wheat plants (prior to ligation into the topo-isomerase vectors).

GENE	Fw primers	Rv primers
TaAMT1;1	ATGTCGGCGACGTGCGCGGC	TTAGACCTGGCTGTTGGCCGCGGC
TaAMT1;2	ATGTCGACGTGCGCCGCGAG	TTAGACCGAGCTGCTCGGGGACG
TaCBL1	ATGGGGTGCATCCAGTCC	TCATGTAACGATATCATCAACCTCC
TaCBL2	ATGGTGCAGTGTCTCGACG	TCAGGTATCGTCGACCTGAGA
TaCBL6	ATGGTGGATTTCCCGGAAGG	TCAAGCATCCTCGACCTGAGA
TaCIPK9	CATTGATCCATTGATTTGATTAATTC	CTATTTCGCAATTGTGTTGGATTC
TaCIPK23	ATGGTTGATTCGAGCGCGGGA	TCATGGAGACCTCCGGTGGC
TaCIPK32	ATGAGTACAACCAAGGTGAA	CTAGGAAGGTTGGATCTGAAG

Table 5. A table listing the primers used for generating the mutation of the TaAMT1s.

Gene	Mutation	Fw primers	Rv primers
TaAMT1;1_T_{453}D	Site directed mutagenesis	TGGACCTGGATCGGCACGG	CCGTGCCGATCCAGGTCCA
TaAMT1;2_T_{453}D	Site directed mutagenesis	TGGACCAGGATCGGCACGG	CCGTGCCGATCCTGGTCCA
TaAMT1;1C	C-terminus deletion	GCACCAGGATCCATGTCGGCGACGTGCGCGGC	GCACCACTGCAGTTACTTGTCGTGCTCGTCGTCGTCGTGGT
TaAMT1;2C	C-terminus deletion	GCACCAGGATCCATGTCGACGTGCGCCGCGAGCCTGG	ATACCACTGCAGTTAGCCGCCGGCGCCGCGGC

Table 6. A Table listing the primers used for the amplification of the constructs used for the Bimolecular Florescence Complementation (BiFC) assay (The split YFP (yellow fluorescent protein)). All primers carry the appropriate restriction site in their adapter overhang.

Gene	Fw primers	Rv primers
TaAMT1;1-CYFP	GCACCAGGATCCATGTCGGCGACGTGCGC	GCACCATCTAGAGACCTGGCTGTTGGCCGC
TaAMT1;1C-CYFP	GCACCAGGATCCATGTCGGCGACGTGCGCGGC	GCGCGCTCTAGACTTGTCGTGCTCGTCGTCGTCGTGGT
TaAMT1;2-CYFP	GCACCAGGATCCATGTCGACGTGCGCCGC	GCACCATCTAGAGACCGAGCTGCTCGGGGAC
TaAMT1;2C-CYFP	GCACCAGGATCCATGTCGACGTGCGCCGCGAGCCTGG	CGCGCATCTAGAGCCGCCGGCGCCGCGGC

TaCBL1-NYFP	GCACCAGGATCCATGGGGT GCATCCAGTCCA	GCGAGCGCACCATCTAGAT GTAACGATATCATCAACCTC CGAG
TaCBL2-NYFP	GCACCAGGATCCATGGTGC AGTGTCTCGACGG	GCGCACCATCTAGAGGTATC GTCGACCTGAGAATGGAAG
TaCBL6-NYFP	CGCGCACCAACTAGTATGGT GGATTTCCCGGAAGG	ATACCAGGGCCCAGCATCCT CGACCTGAGAGTT
TaCIPK9-NYFP	ATCTATAGGATCC ATGGCGGCGGCGGGC	ATTATACCGCGGCTTTCGCA ATTGTGTTGGATTCAGTTTT CCACAC
TaCIPK23-NYFP	GCACCAGGATCC ATGGTTGATTCGAGCGCGG	ATTATACCGCGGCTGGAGAC CTCCGGTGGC
TaCIPK32-NYFP	GCACCAGGATCC ATGAGTACAACCAAGGTGA A	AcTTATACCGCGGGGAAGGT TGGATCTGAAG

2.1.6. KITS

Table 7. A table showing the kits utilised, the description of their application, and their supplier.

KIT	APPLICATION	SUPPLIER
Nucleospin Plasmid DNA purification Kit (MINI)	Plasmid DNA extraction from *E. coli*	MACHEREY-NAGEL GmbH & Co. KG
Nucleospin Plasmid DNA purification Kit (MIDI)	Plasmid DNA extraction from *E. coli*	MACHEREY-NAGEL GmbH & Co. KG
Nucleopsin PCR clean-up, gel extraction Kit	PCR clean-up, gel extraction	MACHEREY-NAGEL GmbH & Co. KG

innuPREP Plant RNA Kit	RNA extraction from plant materials	Analytikjena
Quantitect Reverse transcription kit (Qiagen)	cDNA synthesis	Qiagen
KAPA SYBR FAST qPCR Kit (2x) Universal	performance of qPCR	peqlab
mMESSAGE mMACHINE™ SP6 Transcription Kit	synthesis of capped RNAs for oocyte microinjection,	Thermo Scientific

2.1.7. NUTRIENT SOLUTION

Table 8. Composition of the nutrient solutions used for hydroponic plant growth. Concentrations are given in µM/mM. Final volume per pot was 3 l.

NUTRIENT	CONCENTRATION
K_2HPO_4	1 mM
$MnSO_4.H_2O$	9 µM
$ZnSO_4.7\ H_2O$	0.77 µM
$CuSO_4.5H_2O$	0.5 µM
$Na_2MoO_4.2\ H_2O$	0.0161 µM
H_3BO_3	46 µM
$CaCl_2$	5 mM
$MgSO_4$	1 mM
KCl	1 mM
Fe-EDTA	0.02 mM
**Nitrogen supply in HL medium was dependent on experiment requirement and described in the methods of the appropriate experiments. K_2HPO_4 was supplied a phosphate buffer (K_2HPO_4/KH_2PO_4) to achieve the desire pH.	

2.2.METHODS

2.2.1. IN SILICO ANALYSIS

The amino acid sequence of putative ammonium transporters, Calcineurine B- like proteins (CBLs) and the CBL-interacting protein kinase (CIPK) of wheat were obtained by BLAST using the plants.ensembl.org database (Table S 1, S 2, and S 3). A multiple sequence alignment was then performed with the ammonium transporters (AMTs) sequence of *Arabidopsis thaliana*, *Medicago truncatula*, *Oriza sativa*, and *Saccharomyces cerevisiae* using the MUSCLE algorithm of the UGENE sequence viewer. The amino acid sequence of candidate CBLs of wheat were aligned with AtCBL1 of *Arabidopsis thaliana*, while the sequence of the candidate CIPK proteins were aligned with the amino acid sequence of the AtCIPK23 of *Arabidopsis thaliana* respectively. A phylogenetic tree was then constructed from the alignment, using the CLC sequence viewer software.

2.2.2. SEED STERILIZATION AND GERMINATION

The Wheat seeds (bob white cultivar) were sterilized in 100 ml of 20 % (v/v) chlorox solution with continuous stirring for 30 min. the seed were then rinsed four times with sterile deionized water. Afterwards, they were sown on damp filter paper in square petri dishes. Sown seed were cold treated at 4 ^{o}C in the dark for 4 days, after which the petri dishes were transferred to a dark climate chamber (25 ^{o}C) for 4 days to induce germination. 3 ml of sterile distilled water was added to the plates to prevent water stress. The Plates were then transferred to a plant growth chamber with long day light conditions (161 µmol/m^2/s; 14 h day; 10 h night) at 25 ^{o}C for 4 days. The plants were transferred to nutrient solutions (as described in Table 8) for treatment on the fourth day.

2.2.3. PLANT GROWTH AND ANALYSIS

Germinated seedlings were transferred to nutrients solution with the different treatments as described in Table 8 & 9 (for one or two weeks) in 3 liters pots as indicated in the tables. The experiment was designed with for replicates (pots) and each pot was sown with four plants. The experimental set up was in a plant growth chamber with long day light conditions (161 µmol/m^2/s; 14 h day; 10 h night) at a temperature of 25^{o}C and a relative humidity of 65 %. A 4 X 4 Randomized Complete Block experimental design was utilized for the “Nitrogen source preference in winter wheat”, and “the Ammonium tolerance of winter wheat experiment”. However, A 4 X 8 Randomized Complete Block design was adopted for the “pH effects of

ammonium usage and toxicity" experiment. All experimental set up was in a Randomized Complete Block grid designs, which were generated with the "proc plan" procedure of the SAS statistical package. The nutrient solution was changed after 7 days. Whole plant root and shoot were harvested after two weeks for the "Nitrogen source preference in winter wheat", and "the Ammonium tolerance of winter wheat experiment". For the "pH effect of ammonium usage and toxicity" experiment, whole plant roots and shoot was harvested after 1week, due to the extreme toxic symptoms of the plants grown in the 10 mM treatment, at pH 8.

Table 9. The nitrogen treatment applicable in each of the wheat growth experiment performed.

EXPERIMENT	TREATMENT
Nitrogen source preference in winter wheat (2 weeks)	• -N (Nitrogen Starvation) • 1 mM NH_4Cl • 0.5 mM NH_4NO_3 • 1 mM KNO_3 • pH 6
Ammonium tolerance of winter wheat (2 weeks)	• -N (Nitrogen Starvation) • 0.1 mM NH_4Cl • 1 mM NH_4Cl • 10 mM NH_4Cl • pH 6
pH effect of ammonium usage and toxicity (1 week)	• 1 mM NH_4Cl (pH 5, 6, 7, 8) • 10 mM NH_4Cl (pH 5, 6, 7, 8)

The total root length obtained from the plants for each treatment were measured with WinRHIZO washed root measurement software, after being scanned. Total root and shoot samples collected were freeze-dried for 5days, after which the dry root and shoot biomass were measured. Total dry root and shoot sample were grounded to powder, and the carbon and nitrogen concentration measured with the Euro EA Elemental analyzer.

2.2.4. AMMONIUM SHOCK EXPERIMENTAL DESIGN FOR THE qRT-PCR

Germinated seedlings were transferred to hydroponic culture solutions (as described in Table 8) containing 1 mM ammonium nitrate (pH 6) in 3 Liters pots for seven days. The plants were then subjected to three days nitrogen starvation period, by transferring them to hydroponic

culture solutions without nitrogen (pH 6). Samples were collected on the third day of starvation (two plants), which served as the -N treatment. The remaining plants were transferred to a similar nutrient solution with sole NH_4^+ N in the form of 1 mM ammonium chloride for six hours. Afterwards, another two plant samples were collected, which served as the 1 mM (6 h) treatment. The remaining plants were then immediately transferred to nutrients solution containing 1 mM, 10 mM, and 50 mM of ammonium chloride (pH 6). This was done to investigate the shock effect of elevated ammonium chloride on the plants. The total root samples of two plants were collected after 30 min (6 h+30 min), and 2h (6h+120 min) for each treatment and were frozen in liquid nitrogen for RNA extraction and cDNA preparation. The experiment was successfully repeated twice.

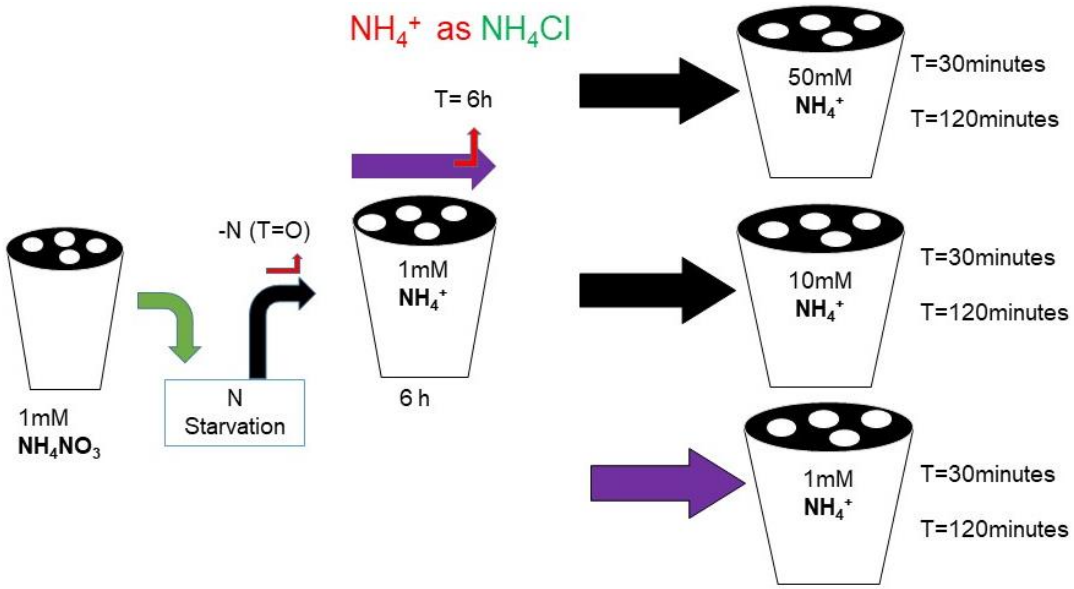

Figure 11. Schematic representation of the experimental design used for growing the plants utilised for the qRT-PCR.

2.2.5. RNA EXTRACTION AND cDNA PREPARATION

The frozen samples were grounded to powder in liquid nitrogen before total RNA extraction was performed. RNA was extracted using the Innuprep Plant RNA extraction of kit (Analytic Jena) according to the manufacture's protocol. cDNA was then prepared for each sample from 1 µg of the total extracted RNA with the Quantitect Reverse transcription kit (Qiagen) according to the supplier's protocol. 10 ng of cDNA per reaction was thereafter used with the GreenMasterMix (Genaxxon bioscience) for the qRT-PCR procedure, using a Bio-rad CFX 384 machine (also according to the manufactures protocol). The ACT (GenBank ID:

AB181991.1) and EF1α (GenBank ID: AF479046.1) genes of wheat were used as the reference genes (Dubcovsky et al. 2007; Jurczyk et al. 2014).

Primers specificity was checked by first performing a BLAST with the primer sequences against the wheat genomic sequence. Subsequently, the quality and specificity of the primers were also verified with the melting curves of the amplified products. This was done in addition to monitoring for amplification in a negative control with no cDNA template. It is noteworthy that all primers were designed to amplify all three homeologs of the genes of interest. Normalized expression was then estimated using the $\Delta\Delta C_q$ algorithm of the Bio-rad CFX 384 software.

2.2.6. QUANTITATIVE REAL TIME PCR (QRT-PCR)

For the qRT-PCR procedure, the reaction was pipetted according to the description recorded in Table 10. The CFX384 instrument was then programmed according to the parameters in Table 11. At completion, the results of the procedure were visualized and analyse with the BioRad CFX Manager™ Software Version 3.1. Using The melting curve, the amplicon were analysed to ensure the single product amplification of the primers.

Table 10. A table showing the components of the reaction mixture used for the qRT-PCR.

qRT-PCR COMPONENTS	VOLUME (µl)
dH_2O	1.9
KAPA	7.5
Forward primer (100uM)	0.3
Reverse primer (100uM)	0.3
Template cDNA (2ng/µl aliquot)	5
Total	20

Table 11. Parameters used for programming the c1000 with CFX384 instrument for the qRT-PCR procedure.

CYCLE STEP	TEMPERATURE	TIME	
Initial Denaturation	95 °C	20 min	1 cycle
Denaturation	95 °C	15 s	50 cycles
*Annealing temperature	60	30 s	
Extension	Plate read		
Melting Curve	65 - 95 °C		
	Plate read	0.05s	
End			

2.2.7. POLYMERASE CHAIN REACTION (PCR)

For the genes of interest, the combination listed in Table 12 was pipetted in a PCR tube and placed in the PCR machine to initiate the Polymerase Chain Reaction. The machine was then programmed according the parameters contained in the Table 13 for the single PCR procedure. In cases where the PCR procedure was performed with primer carrying adapter overhangs.

Table 12. Components of the reaction mixture used for the Polymerase Chain Reaction (PCR) procedure.

PCR COMPONENTS	VOLUME (µl)
dH_2O	Added up to 50
dNTPs	1
GC Buffer	10
Forward primer	2.5
Reverse primer	2.5
Template DNA	1
S7 DNA Phusion DNA polymerase	0.5

The double step PCR procedure (Table 14) was utilised in the amplification of the gene of interest. Nonetheless, all samples were electrophoresed by the Agarose Gel Electrophoresis procedure at the end of the PCR procedure to verify the successful amplification of the gene of interest.

Table 13. A table showing the parameters used for programming the PCR machine for the single PCR procedure. The single step PCR procedure was used for the reaction with primers carrying no adapter overhang.

Cycle Step	Temperature	Time	
Initial Denaturation	98 °C	2 min	1 cycle
Denaturation	98 °C	30 s	35 cycles
*Annealing	*	30 s	
Extension	72 °C	2 min 30 s	
Final Extension	72 °C	10 mins	
Store at 10 degrees			
*Annealing temperatures were optimized for each gene-specific primer pair			

Table 14. **A table showing the parameters used for programming the PCR machine for the double step PCR procedure. The double step PCR procedure was used for the reaction with primers carrying adapter overhangs.**

CYCLE STEP	TEMPERATURE	TIME	
Initial Denaturation	98 °C	2 min	1 cycle
Denaturation	98 °C	30 s	5 cycles
*Annealing temperature	*	30 s	
Extension	72 °C	2 min 30 s	
Denaturation	98 °C	30 s	35 cycles
*Annealing temperature	*	30 s	
Extension	72 °C	2 min 30 s	
Final Extension	72 °C	10 mins	
*Annealing temperatures were optimized for each gene-specific primer pair			

2.2.8. GENE AMPLIFICATION AND CLONING

The genes of interest were amplified from the cDNA (primer used are listed in Table 4) and electrophoresed. Amplicons were then extracted from the agarose gel, cleaned, and initially ligated into the pCR™-Blunt II-TOPO® Vector (Thermofischer Scientific). Construct amplification was done in MAX Efficiency™ DH5α competent *E. coli* (Thermofischer Scientific), which were grown on/in LB media. Afterwards, plasmid DNA extraction (Nucleospin Plamid DNA extraction kit MINI-Macherey Nagel) was done; and constructs control digested. The complete coding sequences were then Sanger sequenced (Eurofins Genomics Germany GmbH). Genes were thereafter subcloned into the appropriate vectors: pDR199 (yeast expression vector) and p002 vector (oocyte expression vector) using primers carrying the appropriate restriction sites in their adaptor overhangs.

2.2.9. PREPARATION OF THE LB MEDIA

LB media

- 1% (w/v) bacto-tryptone
- 0.5% (w/v) bacto-yeast extract
- 1% (w/v) NaCl

Agar plates: 1.5% (w/v) Bacto agar in LB medium

To prepare 1l of the solid LB media, 10g of Bacto-tryptone, 5g of Bacto-yeast extract, 5g of sodium chloride (NaCl) and 15g of Bacto-agar were all added into a 1l glass bottle with a tight cover. Sterilized deionized water was added to the mixture to make a final volume of 1l and shaken until complete dissolution. The media was then autoclaved at 140 ^{o}C for 25 minutes and stored at room temperature. To prepare the liquid LB media, Bacto-agar was simply omitted from the components of the solid LB media, autoclaved at 140 ^{o}C for 25 mins and stored at room temperature.

2.2.10. AGAROSE GEL ELECTROPHORESIS

- 0.75g of Agarose (basic)
- 1X TAE buffer
- Loading Dye
- Lambda-PstI
- PCR products

75ml of the agarose gel was prepared by adding 0.75g of basic agarose to 75ml of 1X TAE buffer in a beaker. The mixture was heated in a microwave until the agarose was completely dissolved. A comb was first placed in a cast tray (to create wells in the gel for sample loading). Afterwards, the dissolved agarose gel was poured into the gel casting tray and left to solidify. After solidification, the gel was placed in a 1X-TAE-buffer-filled electrophoresis chamber (containing a positive electrode and a negative electrode). The comb was removed from the gel to create pockets which could be viewed against a contrasting background. Loading dye was then added the samples (10% (v/v)) prior to loading. 10µl of Lambda-PstI was then pipetted into the first pockets to generate a standard reference for the PCR Products. The PCR products (already mixed with the loading dye) were then pipetted into the wells of the gel, and electrophoresed. The gel electrophoresis procedure was performed at 100 volts for approximately 45 minutes. At the end of the procedures, the gel was submerged in ethidium bromide solution for 15minutes, viewed under UV light, and pictures taken. Observed bands were compared against the standard band generated by the ladder (Lambda PstI) to ensure the

success of the PCR procedure. In appropriate cases, the band that correspond to the gene of interest in cut from the gel, and cleaned with the "Nucleopsin PCR clean-up, gel extraction kit" prior to further procedure (E.g., Ligation into the appropriate plasmid vector backbone).

2.2.11. CONTROL DIGESTION OF PLASMID DNA WITH RESTRICTION ENZYMES

To verify that plasmids carry the appropriate constructs, plasmids were first control digested with appropriate "Fast digest enzyme", prior to being sanger sequenced.

Reaction composition:

- 10X Fast Digest Green Buffer
- 2µl DNA
- 0.5 –1µgFast Digest restriction enzyme
- 0.5 µl H2O up to 20 µl

***The reaction was incubated for 90 min at 37°C and loaded on 1% (w/v) agarose gel for the electrophoresis procedure. The resulting bands were compared to expected band sizes.

2.2.12. TRANSPORT ASSAYS USING *Saccharomyces cerevisiae*

The *ΔΔΔmep* yeast (Marini et al. 1997) was grown in YPD media (Table 15) at 28^{o}C and transformed according to the LiAc/SS-DNA/PEG method (Gietz et al. 1995). The transformed yeast cells were then cultivated on a solid SD media (Table 15) containing arginine as the nitrogen source for 5days. Overnight cultures were thereafter prepared from each plate in 5 ml liquid SD media (Table 15).

Cells were harvested by centrifugation at 5000 rpm for 3 mins and washed four times in sterile deionized water and harvested (by centrifugation at 5000 rpm for 3 mins). The resulting yeast cell pellets were dissolved in 1 ml of sterile deionized water and their optical density at 595 nm was determined. Cells were then adjusted to an OD_{595} of 1 in 200 µl of sterile deionized water. 10 µl of OD_{595} = 1, and five 10X dilutions were spotted on selective SD media having 20 mg/ml arginine (control) or 1 mM of ammonium chloride (and in some experimental cases a combination of 1 mM ammonium chloride and 60 mM methylammonium chloride) as the sole nitrogen source (Table 15). Spotted plates were then incubated at 28 ^{o}C for 5 days after which the plates were scanned. The experiments were successfully repeated twice.

Table 15. Yeast media compositions.

Composition of 100 mL of Yeast Media					
CHEMICAL COMPONENTS	**YPD MEDIA**		**SD MEDIA**		
	****LIQUID**	****SOLID**	**LIQUID**	**SOLID**	
				CONTROL	**TREATMENTS**
**2% w/v Bacto Agar (20g/L)	-	-	-	80 ml	80 ml
Glucose	2g	2g	-		
**20% (Glucose) solution(200g/L)	-	-	-	10 ml	10 ml
**1.7% Yeast Nitrogen Base (17g/L)	-	-	-	10ml	10ml
Bacto-agar	2g	-	-		
Nitrogen source	Arginine (0.004 g)	Arginine (0.004 g)	Arginine (0.1g)	Arginine (0.1g)	• Ammonium chloride (0.00535g (1mM)) • Methylammonium Chloride (0.66g (60 mM)
Histidine	-	-	-	0.002g	0.002g
Adenine sulphate	-	-	-	0.002g	0.002g
Bacto Yeast Extract	1g	1g	-	-	-
Bacto peptone	2g	2g	-	-	-
** Autoclaved at 121 ^{o}C for 20 minutes					

2.2.13. FUNCTIONAL CHARACTERIZATION OF TaAMT1s VIA ELECTROPHYSIOLOGICAL STUDY USING *Xenopus laevis* OOCYTES

The pOO2 plasmid containing the gene of interests were first linearized with the Fast-Digest enzyme “MluI” and cleaned using a phenol-chloroform extraction/clean-up procedure

optimized/used in the Group ludewig laboratory (340h, University of Hohenheim, Stuttgart, Germany). cRNA synthesis was done *in vitro* for expression in the oocyte of *Xenopus laevis*, using the mMESSAGE mMACHINE™ SP6 Transcription kit (Thermofischer Scientific). Each oocyte was injected with approximately 25ng of cRNA with a micro-dispenser (Drummond scientific Co). 10 oocytes were injected for each construct. The oocytes were incubated in ND96 buffer (Table 17) for 4 days.

Table 16. Chemical composition of the Choline chloride buffer used for the electrophysiology measurements.

CHEMICAL COMPONENTS	5 L VOLUME	FINAL CONCENTRATION (MM)
Choline chloride	77 g	110
$CaCl_2$ x 2 H_2O	1.47 g	2
$MgCl_2$	2.03 g	2
500 mM MES-TRIS pH 5.5	50 ml	5

Choline chloride solutions with various ammonium chloride concentrations (30 µM, 100 µM, 300 µM, 1000 µM, and 3000 µM) were prepared. Electrophysiological test was then conducted with the injected oocytes using the two-electrode voltage clamp in the choline chloride buffer (Table S. 516) solutions (pH 5.5), where the choline chloride solution without ammonium chloride served as the wash buffer

Table 17. Chemical composition of the ND96 buffer used during oocyte injection and incubation.

CHEMICAL COMPONENTS	CONCENTRATION (MM)
NaCl	96
KCl	2
$MgCl_2$	1
$CaCl_2$ x 2 H_2O	1.8
Na-Pyruvate	2.5
HEPES pH 7	5
Adjust to pH 7.4 with NaOH	

The current in washing solution was measured before and after each ammonium measurements and the mean wash currents were subtracted from the ammonium induced currents. The concentration dependence of the current was fitted using the following equation: $I = I_{max} / (1 + K_m / c)$, with I_{max} being the maximal current at saturating concentration, K_m being the substrate concentration permitting half-maximal currents and c being the experimentally used

ammonium concentration. The voltage dependence δ of the K_m was calculated using the following equation: $K_{m\,(\delta)} = K_{m\,(0\ mV)}$ X exp (δ x e x V / k x T), with δ (fractional electrical distance), e (elementary charge), V (membrane potential), k (Boltzmann's constant), and T (absolute temperature).

2.2.14. PROTEOMICS STUDIES AND ITS AMMONIUM SHOCK EXPERIMENTAL DESIGN

The ammonium shock experiment (2.2.4) in this case was slightly modified to allow for the harvest of enough sample material. The experimental design was a 4 X 3 randomized completed block grid design, which was generated with the "proc plan" procedure of the SAS statistical package. Germinated seedlings were transferred to hydroponic culture solutions prepared (as described in Table 8) containing 1 mM ammonium nitrate (pH 6) in 3 Liters pots for seven days. Each pot served as a replicate and was sown with 4 seedlings.

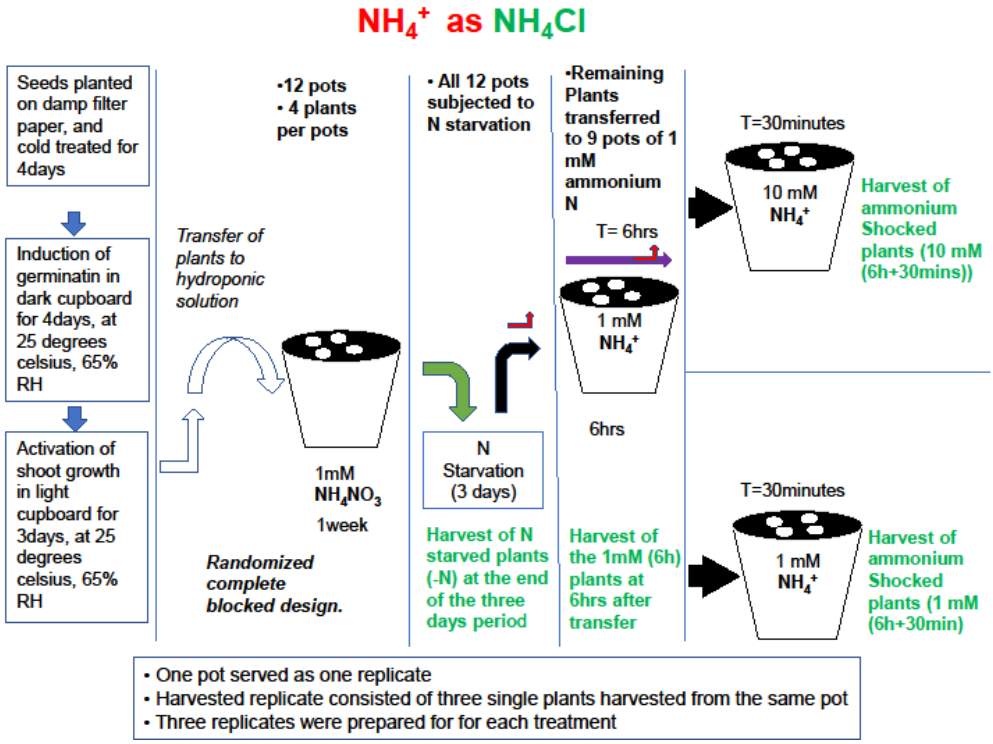

Figure 12. Schematic representation of the experimental design used for growing the plants samples used for the proteomics studies.

All plants were then subjected to a three days starvation period, by transferring them to hydroponic culture solutions without nitrogen (pH 6). Three pots were randomly selected and the total root sample of the three best plants in each pot were harvested on the third day of starvation. The root of the plants harvested from the same pot were combined and served as a

single replicate. The three pots therefore yielded three replicates (each replicate was made up of samples from the best three plants in the pot), which served as the -N treatment samples. The remaining plants were then transferred to a similar nutrient solution with sole NH_4^+ N in the form of 1 mM ammonium chloride for six hours (1mM (6 h)), after which samples were also collected (three pots). This samples served as the 1 mM (6 h) treatments. Plants were then transferred to nutrients solution containing 1 mM, and 10 mM of ammonium chloride. This was done to investigate the shock effect of a relatively optimum ammonium chloride concentration (1 mM) as well as an elevated concentration of ammonium chloride (10 mM) on the young wheat seedlings. A pH of 6 was maintained for all nutrient solutions. Total root samples (three pots) were then collected after 30 min (i.e., 6 h+30 min). The harvested total plant roots samples were frozen in liquid nitrogen for microsomal protein extraction.

2.2.15. MICROSOME PREPARATION FOR MASS SPECTROMETRY

Table 18. Homogenization buffer (HOB).

HOB Buffer (HOB)	
REAGENT	**AMOUNT**
Sucrose	22.592 g
Potassium chloride	1.491 g
EDTA	0.074 g
TRIS-BASE	1.211 g
FINAL VOLUME (made up with Deionized water)	200 mL

The microsomal protein fraction was obtained from approximately 0.5-1 g of frozen wheat root samples according to the method described elsewhere (Pertl et al., 2001) with minor modifications. Frozen roots were grounded in a potter with approximately 10.475 ml of Membrane Protein Extraction Buffer (MPEB) (Table 19).

Table 19. Membrane protein extraction buffer (MPEB).

MPEB	
REAGENT	**VOLUME**
HOB	10 mL
PIC	50 µl
DTT 1 M stock (200x)	50 µl
PMSF 0.2 M stock (200x)	50 µl
2 mM Leupeptin stock (666.67x)	15 µl
Natriumfluoride 1M (40x)	250 µl
Natriumvanadate 500 mM stock (500x)	20 µl
Benzamidine 250mM stock (250x)	40 µl
Final volume	10.475 mL

Homogenates were then centrifuged at 7500 g for 15 min, at 4°C; after which supernatants were collected and filtered through 4 layers of Miracloth (Cal-biochem). Filtrates were thereafter recentrifuged at 48,000 g for 75 min at 4°C. The pellets containing the extracted membrane protein were then dissolved in the appropriate volume of 6 M urea/2 M thiourea (pH 8 solution) and sonicated for 10 min to solubilize the protein pellet.

2.2.16. IN-SOLUTION TRYPSIN DIGESTION

1 µl of Reduction Buffer (1 µg/µl DTT in water) was added for every 50 µg of protein sample. Samples were then incubated for 30 min at room temperature. Afterwards, 1 µl of Alkylation Buffer (27 mM iodoacetamide in water) was added for every 50 µg sample protein and incubated (in darkness) at room temperature for 20 min. Samples were then digested with 1 µl Lys-C (0.5µg/µl Wako Chemicals, Neuss, Germany) for 3 h, at room temperature. Afterwards, samples were diluted by 4-fold in 10 mM Tris-HCl, pH 8, before overnight digestion with trypsin at room temperature. 1 µl of trypsin was utilised per 50 µg protein. Trifluoroacetic acid (TFA) was added until a pH of 2 was achieved (to stop digestion). Samples were later desalted with C18 tips (PepMan, ThermoScientific) before LC/Mass Spectrometry analysis.

2.2.17. C18-STAGE TIPS FOR PEPTIDE DESALTING

Samples were desalted with self-made stage tip made with a 200-µLpipette tip with a C18 disc plug (Rappsilber et al. 2003). The C18 stage tips were first conditioned with solution B (80% acetonitrile, 0.5% acetic acid). This was done by loading solution B into the tip, and using adapters to spin the stage tips in an eppendorf tube at 6,000g until the solution completely flow through the disc. The stage tip was thereafter equilibrated twice with solution A (0.5% acetic acid) at 5,000g. 150 µl of sample was transferred into the stage tip and centrifuged at 5,000g for 10 min (or until sample flows through completely). The Stage tips were then washed twice with solution A. Finally, stage tips were eluted twice with 20 µl of Solution B. The eluate were thereafter concentrated in the speed vacuum, after which samples were resuspended in 5-8 µl of resuspension solution (0.2% trifluoroacetic acid “TFA”, 5% acetonitrile in water) for the LC/Mass Spectrometry analysis. Desalted samples to be used for the preparation of the phospho-enriched samples were further dissolved in one equivalent volume of loading buffer (1M Glyconic acid in 80% acetonitrile and 0.1% TFA).

2.2.18. PHOSPHOPEPTIDE ENRICHMENT STEP

Phosphopeptides were enriched over TiO_2 as described elsewhere (Wu et al. 2017) with minor modifications. Approximately 1mg of the TiO_2 beads was first washed with 100 µl of Elution buffer (5% ammonium hydroxide solution) for 10 min and equilibrated with 50 µl of loading buffer (1M Glyconic acid in 80% acetonitrile and 0.1% TFA). Desalted samples adjusted in one equivalent of loading buffer were incubated at room temperature for about 30 min with the equilibrated TiO_2 beads. The reaction mixtures were thereafter centrifuged at 2,500g for 2 min and the supernatant discarded. TiO_2 beads were then washed with 100 µl of the loading buffer. This was followed by washing twice (centrifuged at 2500g for 2 min) with 100 µl of the wash buffer (80%ACN, 1%TFA). The TiO_2 beads were then eluted thrice with the 80 µl elution buffer (5% ammonium hydroxide solution) for a final eluate volume of 240µl. Finally, 60 µl of 10% Formic acid was added to the eluate to make a final volume of 300 µl. Eluate was then desalted with the C18 stage tip before the LC/Mass Spectrometry analysis.

2.2.19. LC-MASS SPECTROMETRY / ANALYSIS

Digested peptides of each samples were analysed by the LC-MS/MS in collaboration with the Institute of Plant Systems Biology. Peptide ion intensity values derived from the analysis and were utilized for further analysis. All the phospho-peptides and non phospho-peptides detected were used for quantification. Thus, ion intensity for a peptide or protein of interest was normalised separately for each sample and computed as the "fraction of total intensity" (peptide ion intensity/total sum of sample's ion intensities). Averages of ion intensities (as well as the corresponding standard errors) were calculated for each peptide, and/or protein of interest from the three replicates prepared for each treatment conditions and timepoints. All proteotypic peptide's ion intensities were utilized in the calculation of the protein-intensity for each sample. The log2 estimate of the fold-changes (Log_2FC) of the normalised ion intensities of the proteotypic phosphopeptides of interest were computed between the compared treatments for the phospho-enriched sample. A dataset that correspond to a cut off threshold of $Log_2FC \geq 1$ or $Log2FC \leq -1$ was computed and presented.

2.3.OVER REPRESENTATION ANALYSIS OF GENES/PROTEINS

The overrepresentation analysis of specific pathways was performed with the BAR for Plant-Biology Classification Super Viewer Tool (Provart and Zhu 2003) (http://bar.utoronto.ca/ntools/cgi-bin/ntools_classification_superviewer.cgi) using the corresponding Arabidopsis AGI codes from the LC-Mass Spectrometry analysis dataset.

2.4.ELECTROPHYSIOLOGY USING *Xenopus laevis* OOCYTES: COEXPRESION OF AMTS, CBLS, AND CIPKS.

The pOO2 plasmid containing the respective ORFs were first linearized with MluI, and thereafter cleaned using a phenol-chloroform extraction procedure. cRNA was sythensized *in vitro* for expression in the oocyte of *Xenopus laevis*, using the mMESSAGE mMACHINE™ SP6 Transcription Kit (Thermofischer Scientific). Each ooctyte was injected with approximately 25ng (except for the batch used for the TaCIPK23 experiment: approx. 50ng) of cRNA with a microsyringe. 10 oocytes were injected for each construct and incubated in ND96 buffer (Table 17) for 4 days. Electrophysiological tests were conducted with the injected oocytes using the two-electrode voltage clamp in a choline chloride buffer (Table 16) solution (pH 5.5). Ammonium chloride was added to make a final concentration of 30 µM, 100 µM, 300 µM, 1000 µM, and 3000 µM. The choline chloride solution without ammonium chloride served as the wash buffer. The current given in just the washing solution were measured before and after ammonium measurements and the mean washing solution currents were subtracted from the ammonium induced currents. For graphical visualization, the current injected at -100mV in 1mM ammonium chloride was plotted.

2.5.BIFC: PROTEIN PROTEIN INTERACTION ASSAY USING SPLIT YFP

The pOO2 plasmid containing the respective C-YFP and N-YFP tagged ORFs were first linearized with the appropriate restriction enzyme, and thereafter cleaned using a phenol-chloroform extraction procedure. cRNA was sythensized *in vitro* for expression in the oocyte of *Xenopus laevis*, using the mMESSAGE mMACHINE™ SP6 Transcription Kit (Thermofischer Scientific). Each ooctyte was injected with approximately 25ng of cRNA (or combination of cRNA as the case may be) with a microsyringe. 10 oocytes were also injected for each construct and incubated in ND96 buffer (Table 17) for 6 days, after which the oocytes were visualized under the laser scanning confocal microscope (LSM700_ZEN_2010, Zeiss, Germany) with the settings tabulated below.

Table 20. Settings utilised to visualise the split yellow fluorescent protein (YFP) under the laser scanning confocal microscope.

OBJECTIVE	PLAN-APOCHROMAT 10X
Master gain	Ch2 850
	ChD 230
Pinhole	70 µm
Filters	SP 555
Laser	488 nm: 2%

3. RESULTS

3.1.NITROGEN SOURCE PREFERENCES IN WINTER WHEAT

The response of wheat (Bobwhite cultivar) seedlings to the different nitrogen sources gave an insight into wheat's ammonium management strategy. The young seedlings, which were grown in hydroponic solutions without nitrogen (-N), 1 mM ammonium chloride (sole NH_4^+), 0.5 mM ammonium nitrate (NH_4NO_3), and 1 mM potassium nitrate (sole NO_3^-) responded to supplied nitrogen forms. Comparison between the different N sources showed no significant difference between the dry shoot biomass of the sole ammonium treatment and the sole nitrate treatment (Fig. 13A).

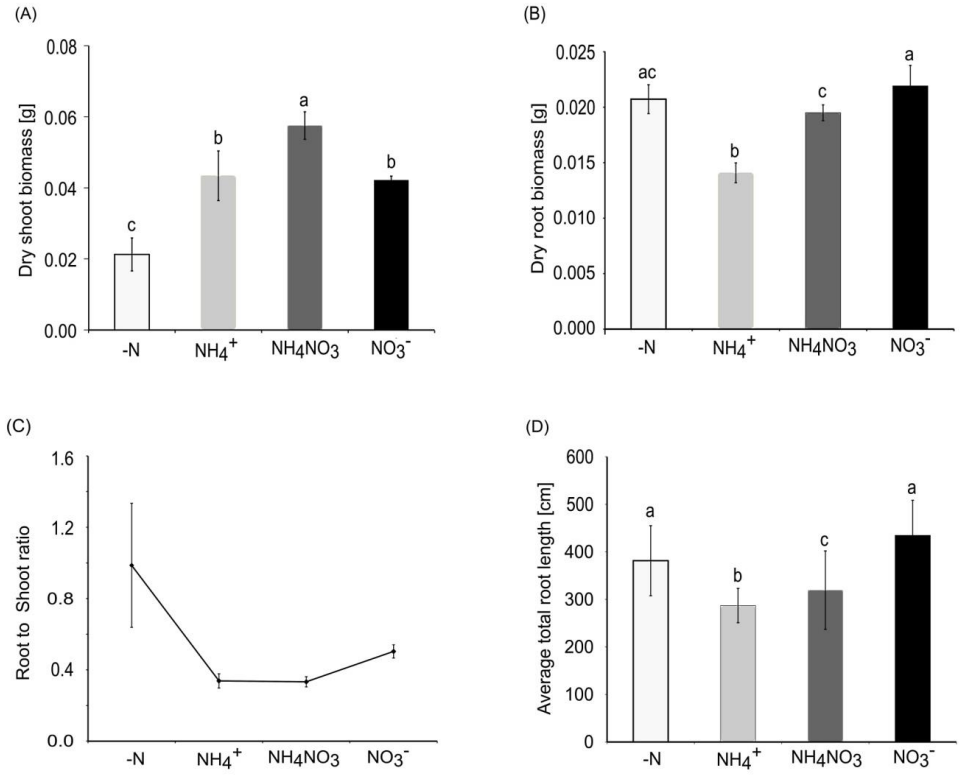

Figure 13. Response of wheat seedling to difference nitrogen sources. (A) Average total root length (B) Dry root biomass (C) Dry shoot biomass (D) Root to shoot ratio. Data is given as mean (n =4). Error bars show the standard deviation of the mean. Statistical significance at p≤0.05 is indicated by different letters.

The ammonium nitrate treatment expectedly produced the highest recorded shoot biomass. However, the absence of nitrogen, alongside the sole nitrate treatment, produced the highest root length and root biomass (Fig. 13D). Compared to the other nitrogen sources, a slight dip in average total root length was recorded for the wheat plants supplied with sole ammonium chloride (Fig. 13D. Although ammonium nitrate produced an average total root length that was higher than that of the sole ammonium chloride treatment, it was still lower than that of the

nitrogen starvation treatment and the sole nitrate treatment (Fig. 13D). A similar trend was produced by the total root biomass data. Nevertheless, there was no significance difference between the root biomass of the N starvation treatment and the ammonium nitrate treatment (Fig. 13B). The similarity in the average total shoot biomass yield of the sole nitrate treatment and the sole ammonium treatment (Fig. 13A) showed the ability of the wheat seedlings to manage the supplied ammonium N.

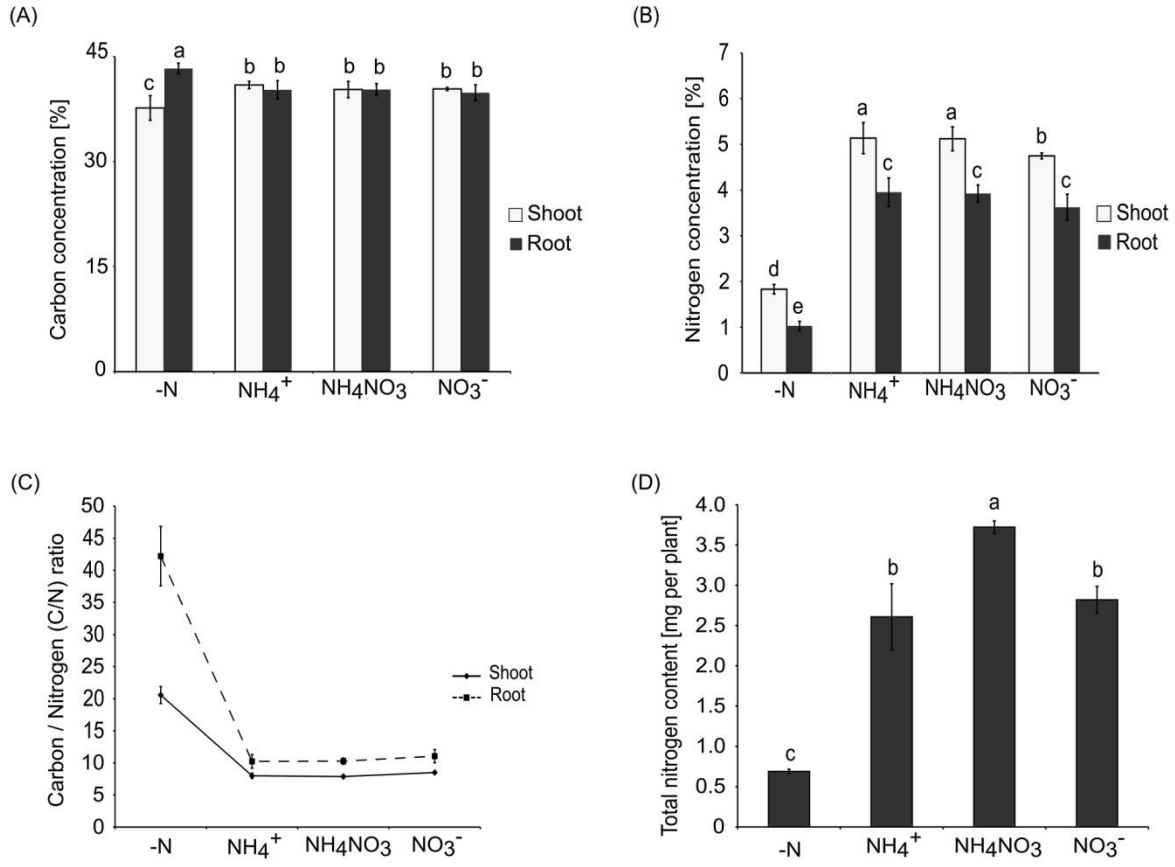

Figure 14. Carbon and nitrogen concentrations of wheat seedling respond to difference nitrogen sources. (A) Carbon concentrations (B) Nitrogen concentration (C) Carbon to Nitrogen ratio. Data is given as mean (n =4). Error bars show the standard deviation of the mean. Statistical significance at p≤0.05 is indicated by different letters.

Root biomass, average total root length, as well as the Root to Shoot ratio was higher in the sole nitrate treatment than in the sole ammonium treatment (Fig. 14), highlighting the ability of nitrate to trigger a higher investment in root development. Root and shoot carbon concentration and C/N ratio were also similar irrespective of the nitrogen source supplied (Fig. 14A, &C). Meanwhile, the lowest shoot nitrogen concentration was recorded in the sole nitrate treatment. Nitrogen concentration on the other hand was generally higher in the shoot than in

the roots irrespective of the N source. Although, the sole nitrate treatment had the lowest shoot N concentration, total nitrogen content in the sole nitrate treatment and the sole ammonium treatments were similar (Fig. 14D).

3.2.AMMONIUM TOLERANCE OF WINTER WHEAT

The ability of the seedling of the winter wheat (bobwhite cultivar) to tolerate 1 mM of sole ammonium (by producing shoot biomass that was similar to the sole nitrate treatment) was impressive. Thus, effort was made to investigate the response of the plants to an elevated concentration of sole ammonium N.

Interestingly, an elevated concentration of sole ammonium (10 mM) caused significant reduction in the average total root length, shoot biomass, and the root biomass of the wheat seedlings (Fig. 15A, B, & D). The shoot biomass recorded at the 1 mM treatment was higher than that of the N starvation (-N), N deficiency (0.1 mM) and the elevated ammonium concentration treatment (10 mM) (Fig. 15A). This showed the relatively better ability of the plants to manage sole ammonium N at 1mM than at an elevated concentration of 10 mM.

The lack of nitrogen or insufficient nitrogen (-N, 0.1 mM) produced an increased root development as expected (Fig. 15B, & D), highlighting the need of the plants to invest in root development. An elevated ammonium concentration (10 mM) also led to a decreased development of fine roots (Fig. 15E). The similarity in the root to shoot ratio of the 1 mM and the 10 mM treatments (Fig. 15C) showed no strategic change by the plants in terms of a preferential investment in shoot or root. However, the significant decrease in the root length, shoot biomass and root biomass at 10 mM (Compare to the 1 mM treatment) imply a general decrease in plant growth, which could be attributed to the higher concentration of the supplied ammonium N. Nevertheless, the elevated ammonium concentration still resulted in a higher nitrogen concentration, both in the shoots and in the roots (Fig. 16B).

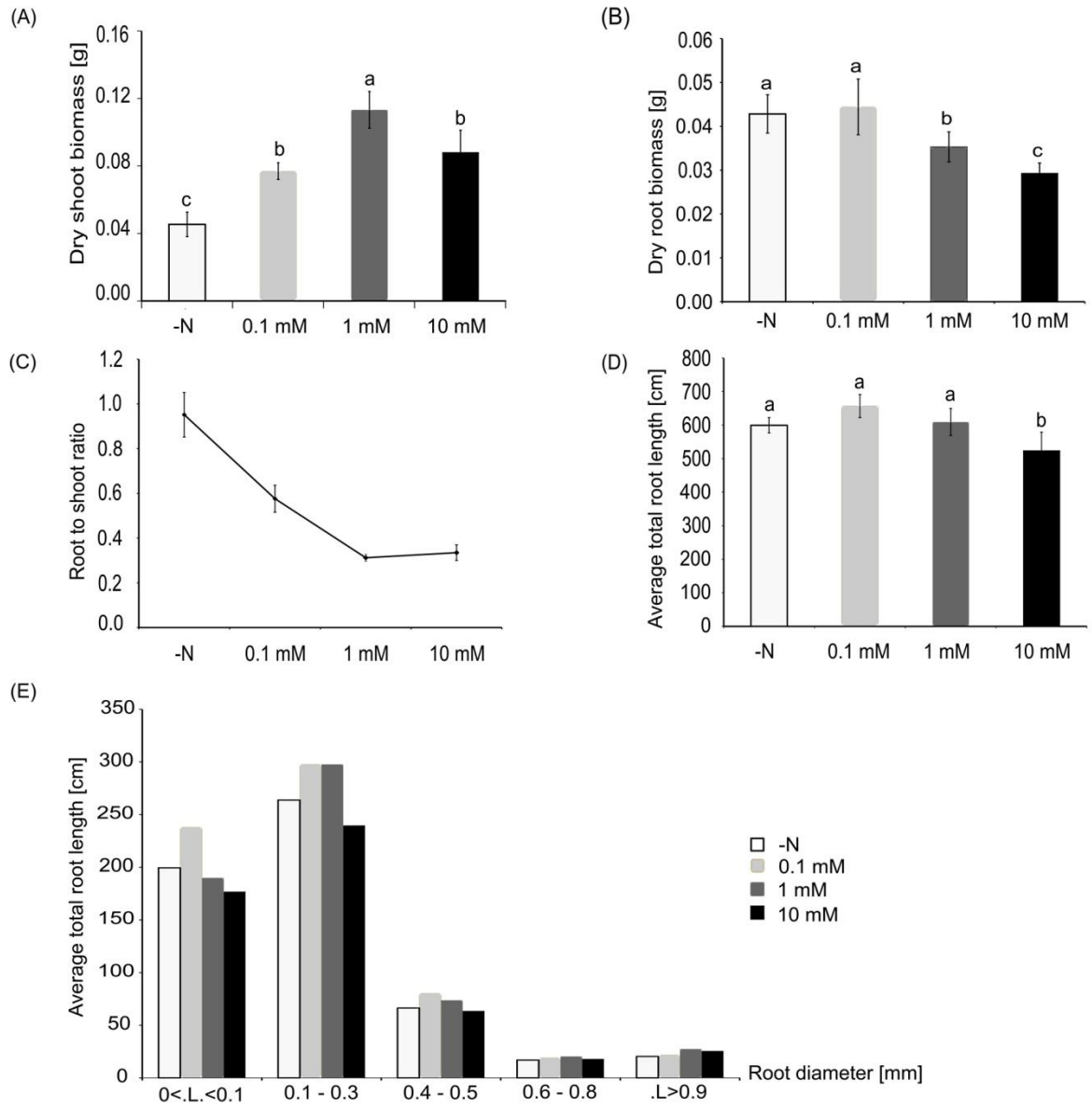

Figure 15. Response of wheat seedling to increasing ammonium concentrations. (A) Dry root biomass (B) Dry shoot biomass (C) Root to shoot ratio (D) Average total root length (E.) Average total root length per root diameter class. Data is given as mean (n = 4). Error bars show the standard deviation of the mean. Statistical significance at $p \leq 0.05$ is indicated by different letters.

Root carbon concentration was also lower as nitrogen was supplied (0.1 mM, 1 mM, 10 mM) (Fig. 16A). However, shoot carbon concentration was only slightly higher in the 1mM (and the 10 mM) treatment than in the 0.1 mM treatment and the -N treatments (Fig. 16A). Root and shoot nitrogen concentrations on the other hand increased with increasing ammonium concentrations in the media (Fig. 16B).

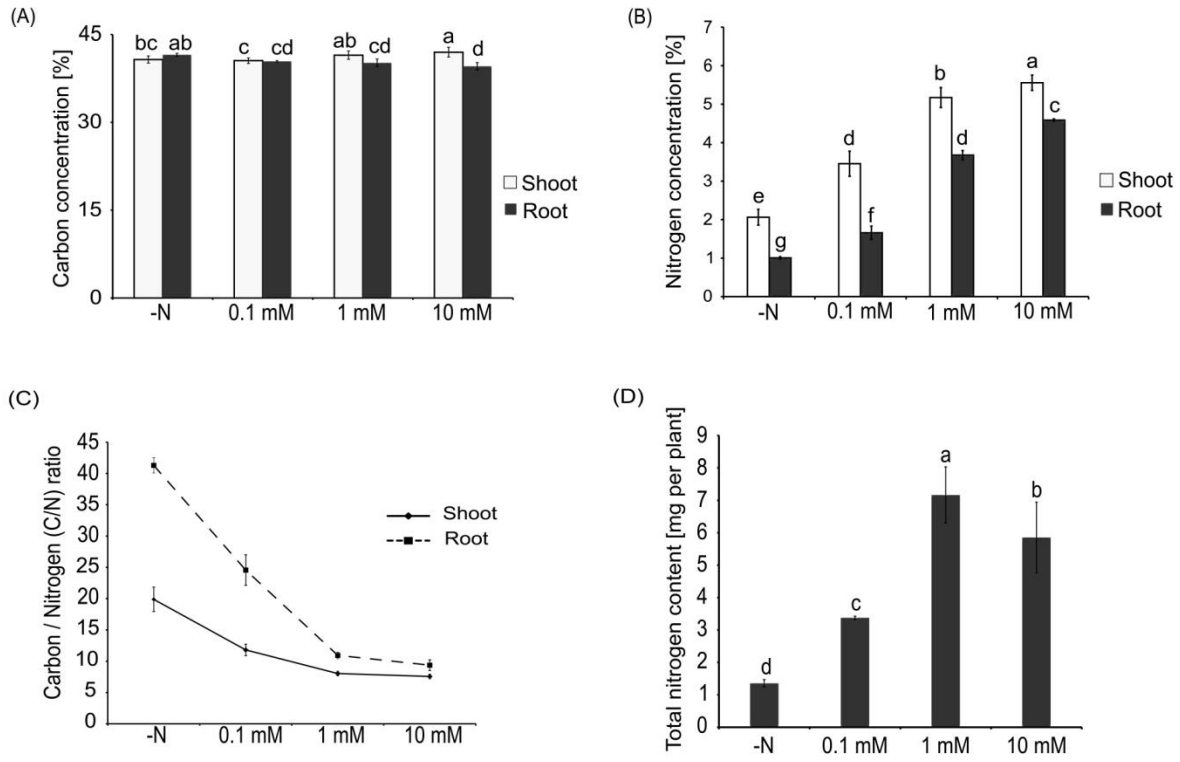

Figure 16. Carbon and nitrogen concentrations of wheat seedling respond to increasing ammonium concentration. (A) Carbon concentrations (B) Nitrogen concentration (C) Carbon to Nitrogen ratio. Data is given as mean (n = 4). Error bars show the standard deviation of the mean. Statistical significance at $p \leq 0.05$ is indicated by different letters.

Since the response of carbon concentration to the increasing concentration of the supplied sole ammonium was meager, the C/N ratio decreased with increasing NNH_4^+ supply (Fig. 16C). Even though, the increasing ammonium concentrations had led to an increased nitrogen concentration (Fig. 16B), the significant biomass decrease of the 10 mM treatment resulted in the reduction of the N-content of the 10 mM treatment (Fig. 16C).

3.3.pH EFFECT OF AMMONIUM USAGE AND TOXICITY

The response of the wheat seedlings to changes in the rhizospheric pH was ammonium concentration dependent. While shoot biomass accumulation remained unchanged in the 1mM treatment as pH tended towards alkalinity, an increased shoot biomass was observed for the 10 mM treatment (Fig. 17A). This trend was reversed in the root, as root biomass was unchanged in the 10 mM treatment as pH tends towards alkalinity (Fig. 17B). Instead, alkaline pH caused a higher root biomass yield at a pH of 8 for the 1 mM treatment (Fig. 17B). Interestingly though, average total root length, as well as the root to shoot ratio were highest for the 1mM treatment at a pH of 8, while decreasing towards pH 8 in the 10 mM treatment (Fig. 17D).

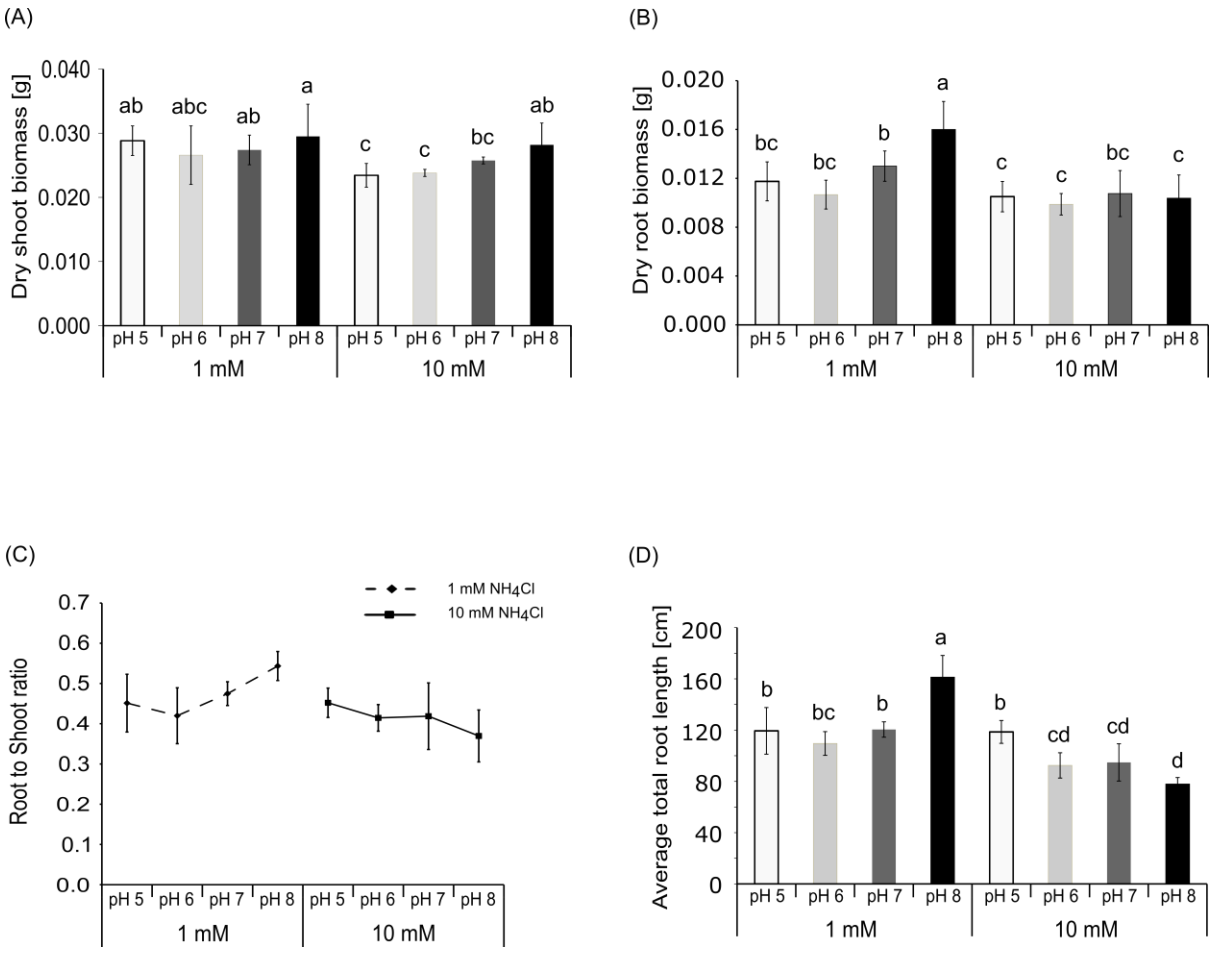

Figure 17. Response of wheat seedling to differences in pH at different ammonium concentrations. (A) Average total root length (B) Dry root biomass (C) Dry shoot biomass (D) Root to shoot ratio. Data is given as mean (n = 4). Error bars show standard deviation of the mean. Statistical significance at p≤0.05 is indicated by different letters.

The total nitrogen content for the 1mM treatment and the 10 mM treatment also increased, as the pH changed from 5 to 8 (Fig. 18D). Root nitrogen concentration was particularly higher for the 10 mM treatment at the of pH 7 and 8 (Fig. 18B). This observed phenomenon suggested the ability of an alkaline rhizospheric pH to foster an increased ammonium N accumulation in wheat seedlings, which appeared to be independent of the potential toxic effect of elevated ammonium N concentration.

Root and shoot carbon concentration seemed unperturbed by the change in pH for the 1mM treatment, as well as the 10 mM treatment. Notwithstanding, root carbon concentration was slightly lower for the 10 mM treatment at pH 7 and 8 (Fig. 18A). It could therefore be proposed that the effect of the pH change on the carbon to nitrogen (C/N) ratio was more prominent in the root than in the shoot; where it decreased as the pH tended towards alkalinity in the 1mM treatment and the 10 mM treatments (Fig. 18C).

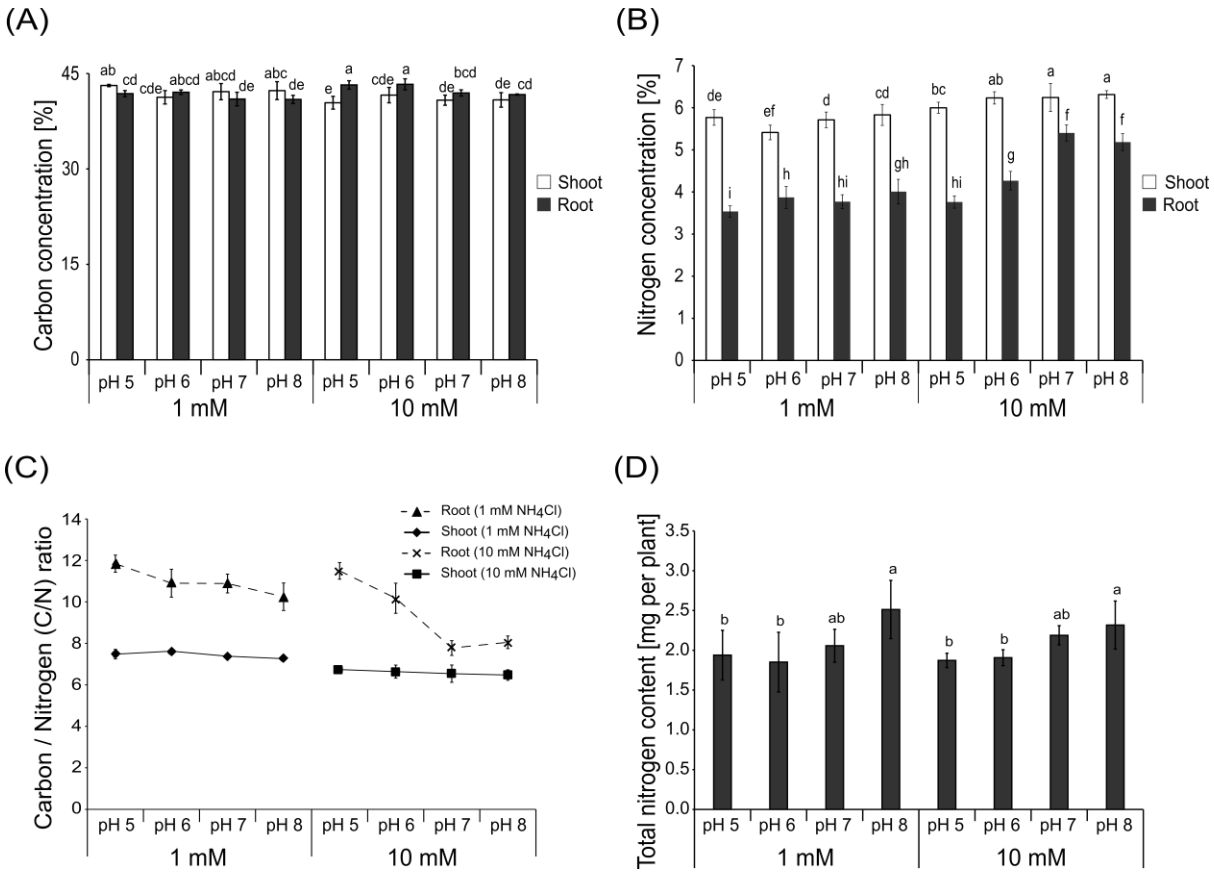

Figure 18. Carbon and nitrogen concentrations of wheat seedling in response to changing pH and ammonium concentrations. (A) Carbon concentrations (B) Nitrogen concentration (C) Carbon to Nitrogen ratio. Data is given as mean (n = 4). Error bars showing standard deviation of the mean. Statistical significance at p≤0.05 is indicated by different letters.

3.4.IN SILICO ANALYSIS / TRANSCRIPT QUANTIFICATION OF TaAMT1s IN AMMONIUM SHOCK CONDITIONS (qRT-PCR)

A blast search on the wheat (*Triticum aestivum*) genome (plant.ensemble.org), using the ammonium transporters of *Arabidopsis thaliana* as query revealed 22 putative ammonium transporters genes (Table S1). A phylogenetic tree (Fig. 19) of the genes (using the MUSCLE algorithm) with known ammonium transporters of Arabidopsis, Medicago, Rice and Yeast, showed two of the putative ammonium transporters of wheat (as well as their homeologs) grouped with known high affinity ammonium transporters from the other plant species, while the rest of the genes aligned with known AMT2s (Fig. 19). These two transporters were therefore regarded as TaAMT1;1 and TaAMT1;2.

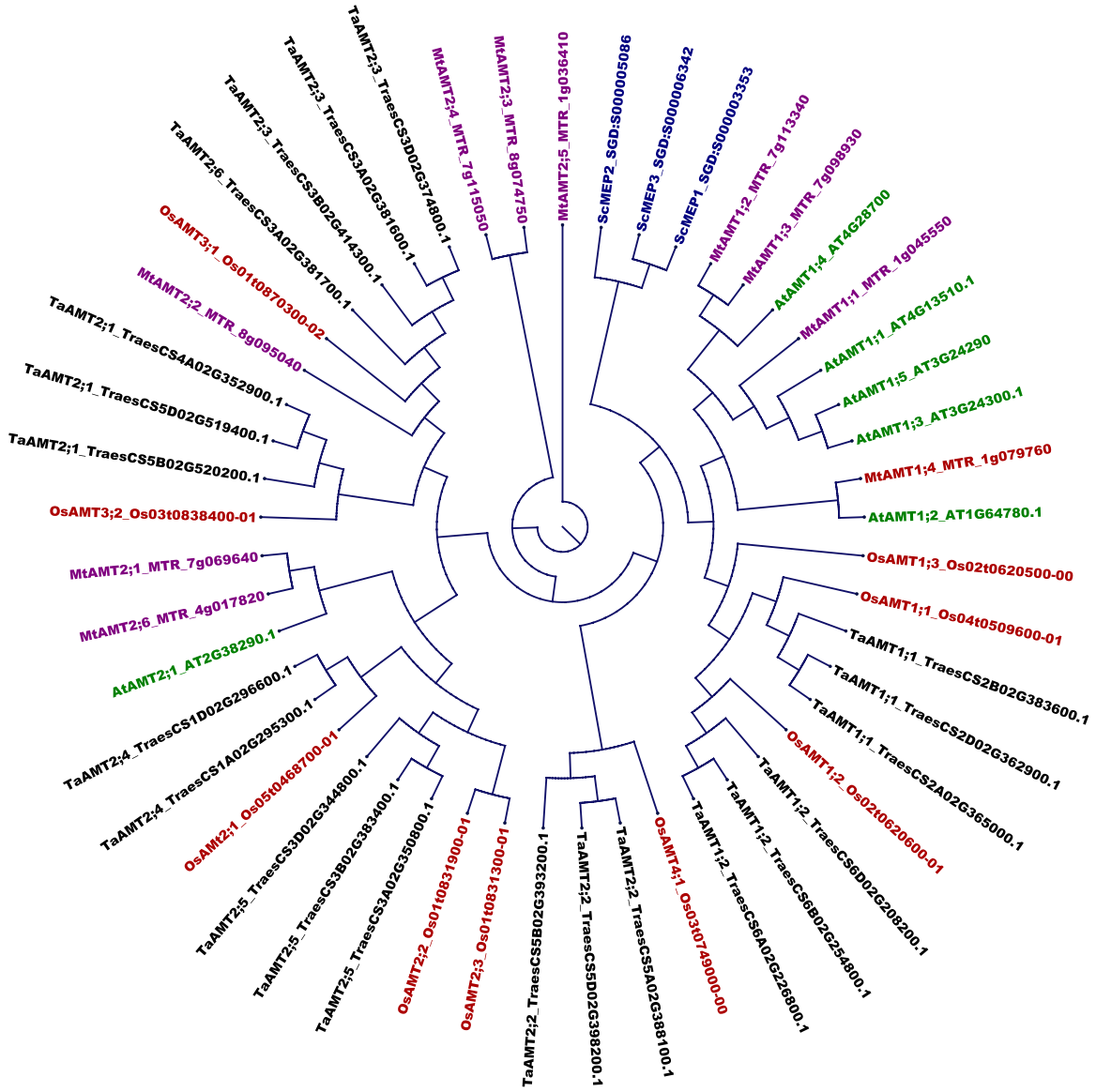

Figure 19. AMTs in the wheat genome. Phylogenetic tree showing the inter-relatedness between ammonium transporters of Wheat, Rice, Arabiodpsis, Medicago, and Yeast.

There was high homology in the amino acid sequence of the respective homeologs of TaAMT1;1, and TaAMT1;2. In order to validate their similarity, the protein structure of each of the homeologs was modelled with a protein structure homology-modeller (server at https://swissmodel.expasy.org/), and the protein structures aligned with Pymol (The PyMOL Molecular Graphics System, Version 2.0 Schrödinger, LLC.). The result showed similar protein structure by the homeologs of both TaAMT1;1 and TaAMT1;2 (Fig. 20).

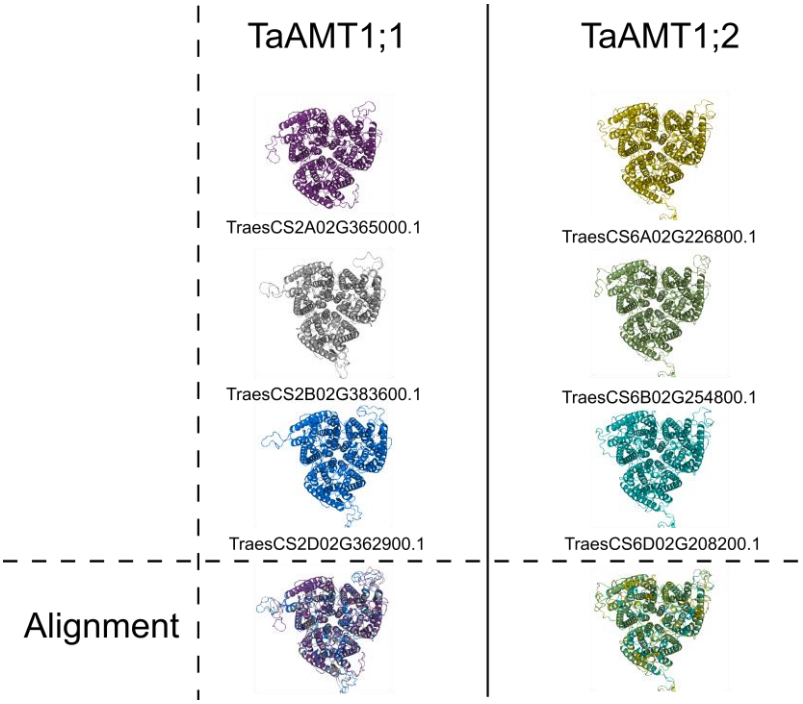

Figure 20. Protein structure homology-modelling (https://swissmodel.expasy.org/) of the homeologs of TaAMT1s and their alignment (Pymol).

Despite the high homology and similar proteins structures among the homeologs of the TaAMT1s, there were some amino acid exchanges between the homeologs (Fig. 21). The amino acid sequences of the homeologs of TaAMT1;1 showed five amino acid exchanges in TaAMT1;1 (Four in the B genome homeolog: $G_{10}A$, $A_{18}M$, $K_{384}Q$, $Q_{385}K$ and one in the A genome homolog: $F_{431}L$). TaAMT1;2 homeologs had only two amino acid exchanges, one ($V_{417}L$) in the A genome homeolog and the other ($A_{170}T$) in the D genome homeolog.

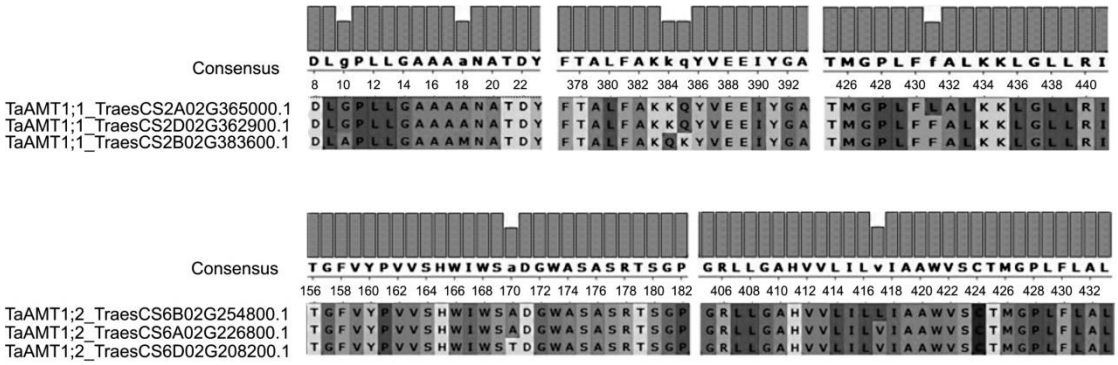

Figure 21. MUSCLE alignment with the Ugene sequence viewer showing five amino acid exchanges in TaAMT1;1 (Four in the B genome homeolog: $G_{10}A$, $A_{18}M$, $K_{384}Q$, $Q_{385}K$ and one in the A genome homolog: $F_{431}L$). TaAMT 1;2 homeologs only show two amino acid exchanges, one ($V_{417}L$) in the A genome homeolog and the other ($A_{170}T$) in the D genome homeolog.

Expression analysis using qRT-PCR showed an upregulation of the high affinity ammonium transporters of wheat (TaAMT1;1, and TaAMT1;2) in response to ammonium supply (Fig. 22A, & B). The increase was sustained in the 1 mM and 10 mM treatment after 30 minutes of ammonium shock. While the observed increase in TaAMT1s transcripts (observed at 1mM and 10 mM after 30 min) appeared to decrease after 2 h, it was only to the level of the starvation treatment. The extremely high ammonium concentration of 50 mM was able to reduce the transcript abundance of both TaAMT1s after 30 min of ammonium shock; however, there was an increase in transcript abundance after 2 hours (Fig. 22). Such upregulation of wheat's high affinity ammonium transporters in response to ammonium supply was contrasting to previously reported works in Arabidopsis, and Medicago (Straub et al. 2014; Straub et al. 2017; Yuan et al. 2007), where there was only an increase in high affinity AMT transcripts under conditions of nitrogen starvation. Nevertheless, it is highly noteworthy that a similar phenomenon had been reported in maize and rice's ammonium transporters, where ammonium supply had triggered the upregulation of their AMT1 transporters (Gu et al. 2013; Sonoda et al. 2003).

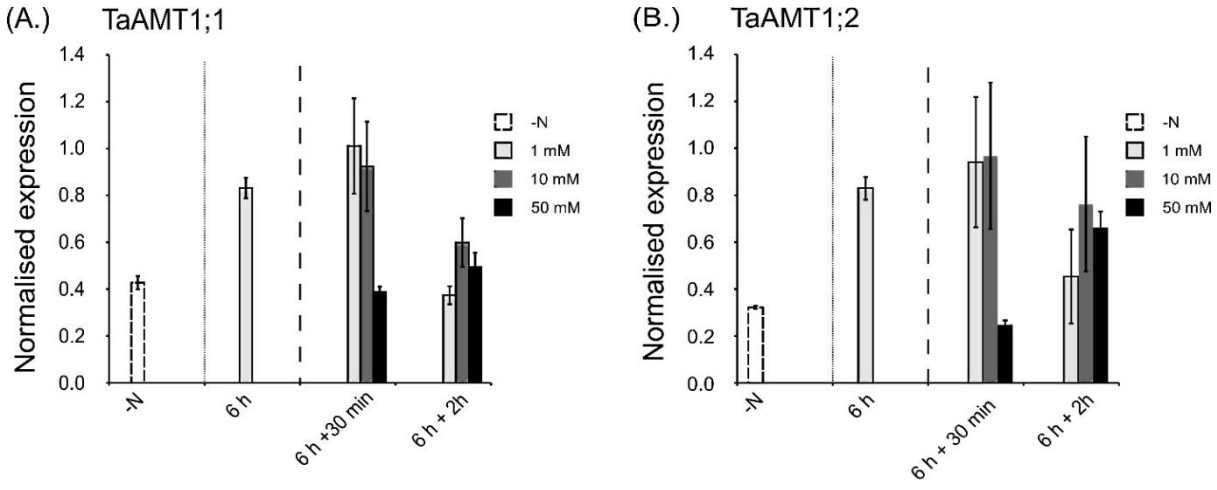

Figure 22. Concentration and time dependent normalised expression of (A.) TaAMT1;1. And (B.) TaAMT1;2; to sole ammonium N. Gene expression were normalised with the TaACT and TaEF1α genes of wheat. Error bars showing standard deviation of the mean.

3.5.FUNCTIONAL CHARACTERISATION OF THE AMT1s OF *Triticum aestivum*

The TraesCS2B02G383600.1 homeolog was amplified and cloned as the candidate TaAMT1;1 gene, while the TraesCS6A02G226800.1 homeolog of TaAMT1;2 was amplified and cloned as the TaAMT1;2 gene. Functional characterization of TaAMT1:1 and TaAMT1;2 in a yeast strain lacking endogenous ammonium transporters, as well as in the oocytes of *Xenopus laevis* showed that both transporters were able to transport ammonium in the positively charged (net

NH_4^+) form (Fig. 23A, & B). Further analysis showed that both TaAMT1;1 and TaMT1;2 had a Km in the µM range (a typical characteristics of high affinity ammonium transporters). TaAMT1;1 had a higher affinity for ammonium (Km=76 µM) of the two transporters (TaAMT1;2, Km=196 µM) (Fig. 23D). Interestingly, both transporters showed that ammonium passes around 35 % of the membrane electric field before the rate limiting deprotonation that occurs during ammonium uptake (Fig. 23C).

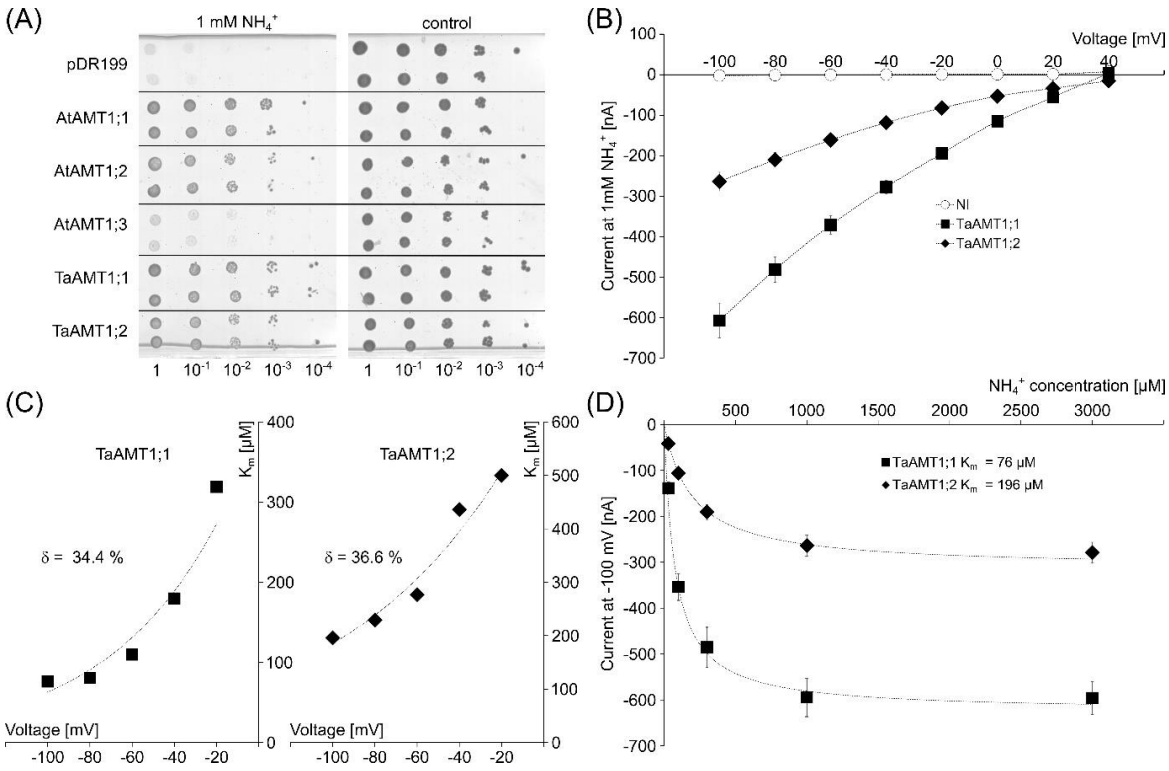

Figure 23. High affinity ammonium transport by TaAMT1;1 and TaAMT1;2. (A) TaAMT1;1 and TaAMT1;2 complement ammonium transport in the *ΔΔΔmep* yeast lacking endogenous ammonium transporters (left). Right plate shows comparable growth capacity of the transfected yeast strains in control conditions. (B) Voltage dependent ammonium induced (1 mM) currents of non-injected (NI) (n = 7) oocytes or oocytes expressing TaAMT1;1 (n = 20) or TaAMT1;2 (n = 19). Currents saturated in a concentration dependent manner with $K_{m\ AMT1;1}$ = 76 µM and $K_{m\ AMT1;2}$ = 196 µM (D). Ammonium affinity of the transporters was voltage dependent and indicated that in both transporters ammonium passes around 35 % of the membrane electric field before the rate limiting deprotonation (C).

3.6.PROTEOME RESPONSE OF WHEAT ROOTS TO AMMONIUM

The root proteome response of the wheat seedlings to ammonium exposure was distinctly dependent on ammonium concentration and time. While proteotypic peptides that represented 4616 proteins were detected in all treatments for the non-phosphoenriched samples, the numbers of proteins adapted to the individual treatments was less (Fig. 24). 79 proteins were adapted to the nitrogen starvation (-N) treatment, 107 proteins to the 1 mM treatment (6h), 101 proteins to the 1 mM treatments (6 h +30 min), and 98 proteins when transferred to the 10 mM treatment for a further 30 min (6h + 30 min). 324 proteins were particularly adapted to the presence of ammonium irrespective of the treatment conditions.

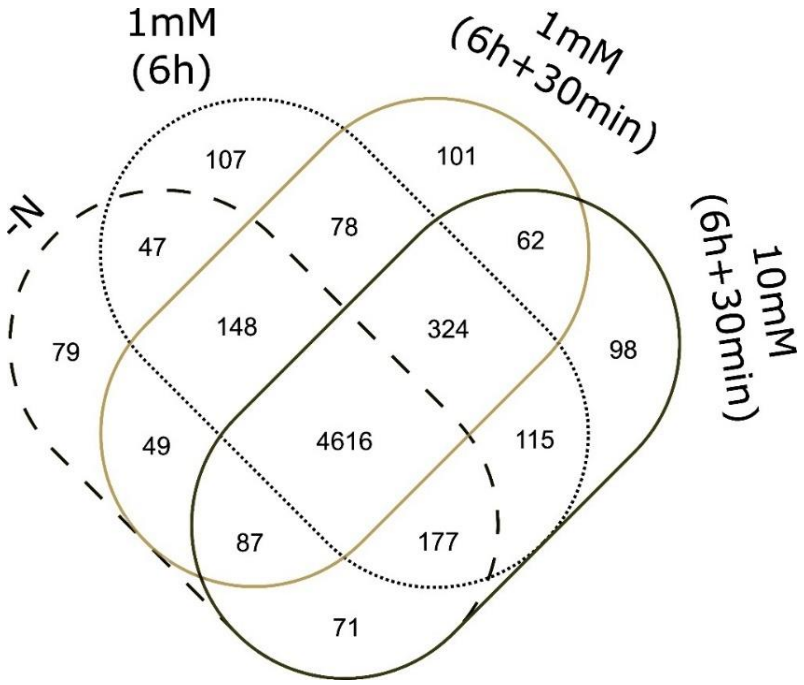

Figure 24. A Venn diagram showing the distribution of proteins between the four treatments, namely: nitrogen starvation (-N), 1 mM (6h), 1 mM (6h + 30min), and 10 mM (6h + 30min). Analysis was performed with the non-phosphoenriched sample's dataset at http://bioinformatics.psb.ugent.be/webtools/Venn/.

An over-representation assay (significance level of $p \leq 0.05$) was performed on the ammonium adapted proteins (324; Fig. 24). The presence of ammonium showed the overrepresentation of relevant pathways which include the transport pathways, and stress induction pathways (Fig. 25). Pathways indicative of an extensive "cellular process" as well as those involving "mitochondria electron transport/ATP synthesis" were also overrepresented. Lipid metabolism, amino acid metabolism, major CHO, and minor CHO pathways were all overrepresented in the ammonium adapted proteins.

Furthermore, an overrepresentation assay was performed with the proteins adapted to the individual treatments of the non phospho-enriched samples. This was done to determine the relevant pathways that were triggered by each treatment. Although, nitrogen starvation is a form of stress for plants, "stress" was not an overrepresented pathway by the N starvation adapted proteins (Fig. 26A).

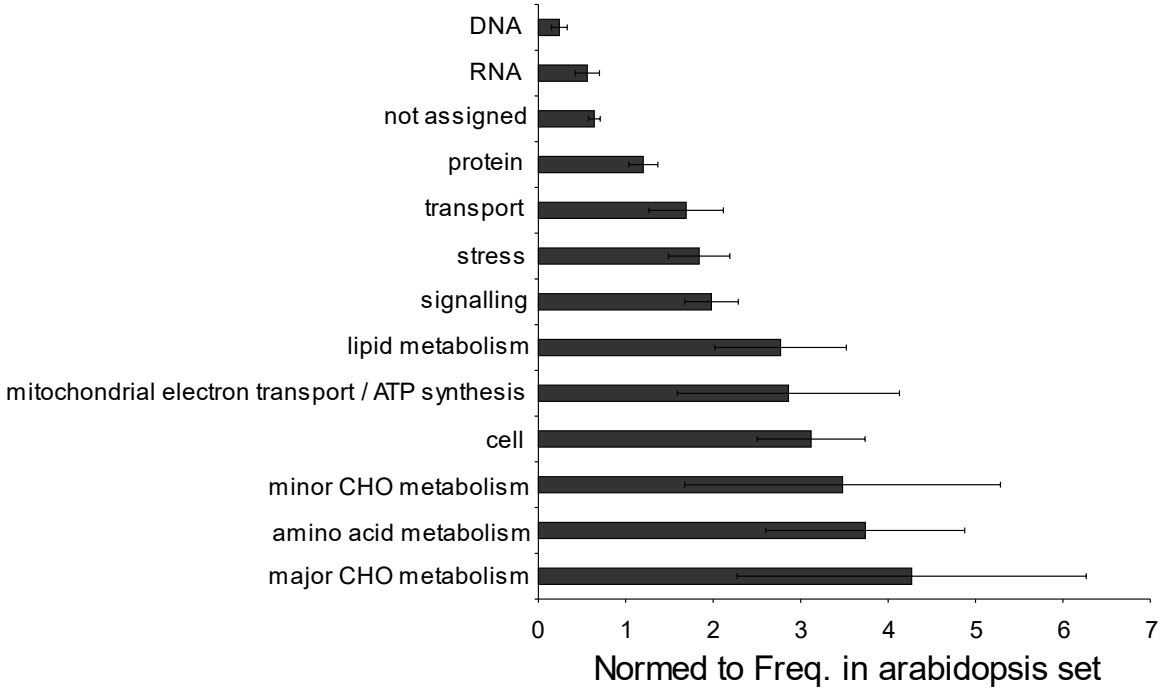

Figure 25. Significantly ($p<0.05$) overrepresented MapMan bins of 324 proteins identified in ammonium adapted roots (i.e 1 mM (6h), 1 mM (6h + 30min), and 10 mM (6h + 30min)). The chart was derived from BAR Classification Super Viewer Tool. Analysis performed with the non-phosphoenriched sample's dataset. Error bars shows Standard deviation.

However, elevated ammonium concentration of 10 mM (6h+30min) triggered amino acid metabolism, redox reactions, TCA/ organ transformation as well as gluconeogenesis / glycoxylate cycle (Fig. 26D). This suggests a change in amino acid metabolism, sugar synthesis and sugar metabolism. Even though redox reactions pathways were not particularly overrepresented in the 1 mM treatments (Fig. 26B & C), there was an extensive mitochondria electron transport/ATP synthesis (Fig. 26C). The overrepresentation of the transport pathways in all treatments also showed that the plants were actively involved in ion transport.

Ammonium supply was able to elicit stress responses in the wheat seedlings (Fig. 25C). An elevated ammonium concentration of 10 Mm also triggered redox reactions pathways (Fig. 26D), an indication of a cellular process responding to significant stress (Dangl and Jones 2001; Huang et al. 2019; Matika and Loake 2014). It is worthy of note that the ability of the wheat

seedlings to be able to manage 1 mM of sole ammonium had been previously highlighted (Fig. 13, & 14). The plant had also been shown to exhibit typical stress responses when 10 mM of sole ammonium was supplied (Fig. 15, & 16).

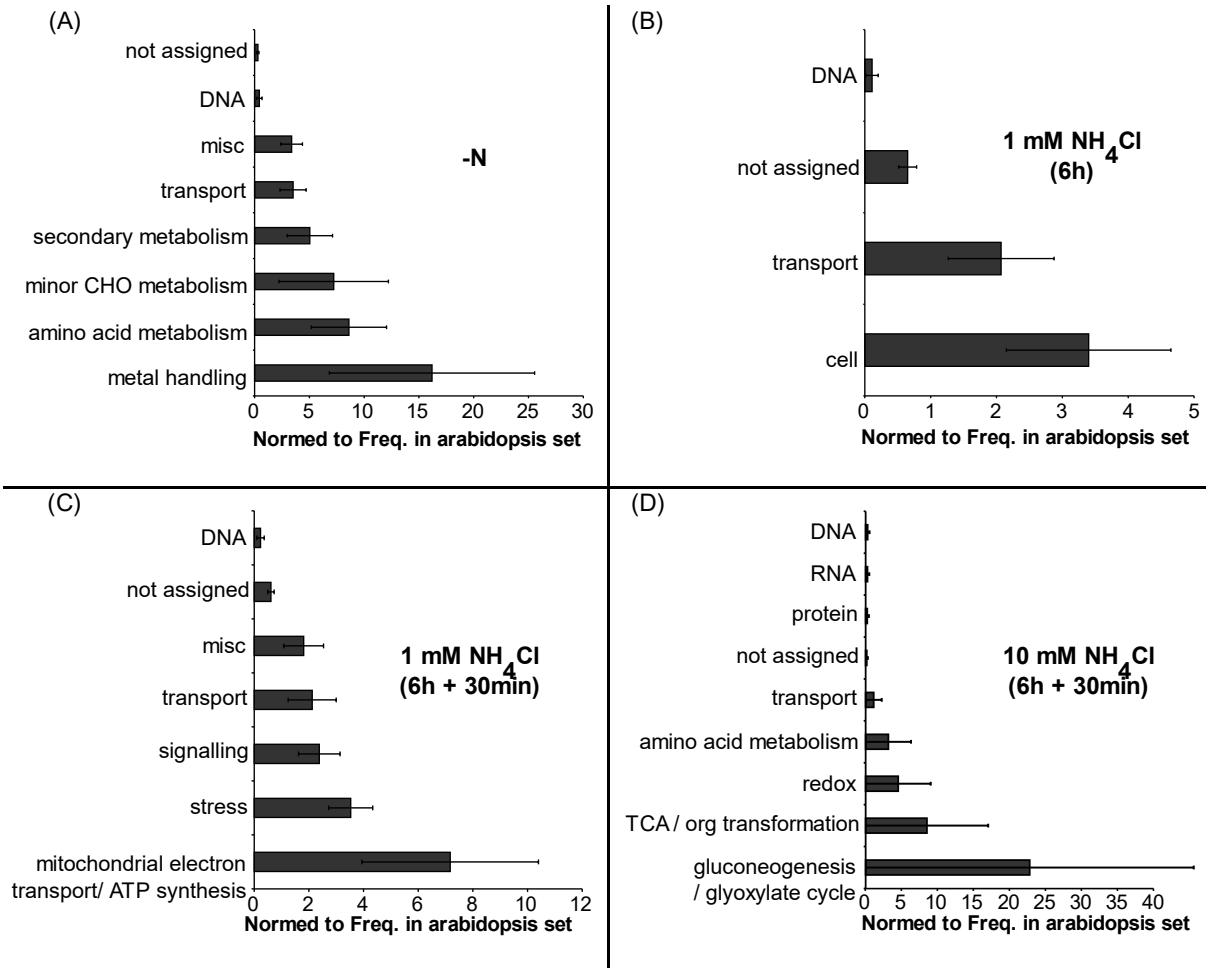

Figure 26. Significantly ($p<0.05$) over-represented MapMan bins of proteins identified in the treatment adapted roots. (A) -N. (B) 1 mM (6h). (C) 1 mM (6h + 30min). (D) 10 mM (6h + 30min)). The chart was derived from BAR Classification Super Viewer Tool. The analysis was performed with the non-phosphoenriched sample's dataset. Error bars show standard deviation.

3.7. PROTEOMIC RESPONSE OF WHEAT AMTS TO AMMONIUM

Interestingly, proteotypic peptide of the ammonium transporters proteins increased in the 10 mM treatment, which suggests the continuous accumulation of the supplied ammonium N by the wheat seedlings roots (Fig. 27). While the phenomenon was observed under a condition that could be regarded as transient (30 min), it was unexpected. Nevertheless, the result corroborated the results obtained from the qRT-PCR, where the upregulation of TaAMT1

transcripts was observed in response to elevated ammonium N (Fig. 22A, & B). Additionally, potassium transporters, and the potassium channel (AKT1), were also upregulated at the proteome level (Fig. 28). The ability of potassium to mitigate the adverse effect of elevated ammonium nutrition is well known (Britto and Kronzucker 2002; Guo et al. 2019; Hernández-Gómez et al. 2015). This is despite the possibility of the co-uptake of ammonium and potassium to affect the electrical properties of the plasma membrane (Findenegg 1987; Kong et al. 2014; Lee and Rudge 1986). Yet, the potassium transporters, as well as the potassium channel (AKT1) responded positively to elevated concentration of ammonium N (10 mM) just like the ammonium transporters (Fig. 28).

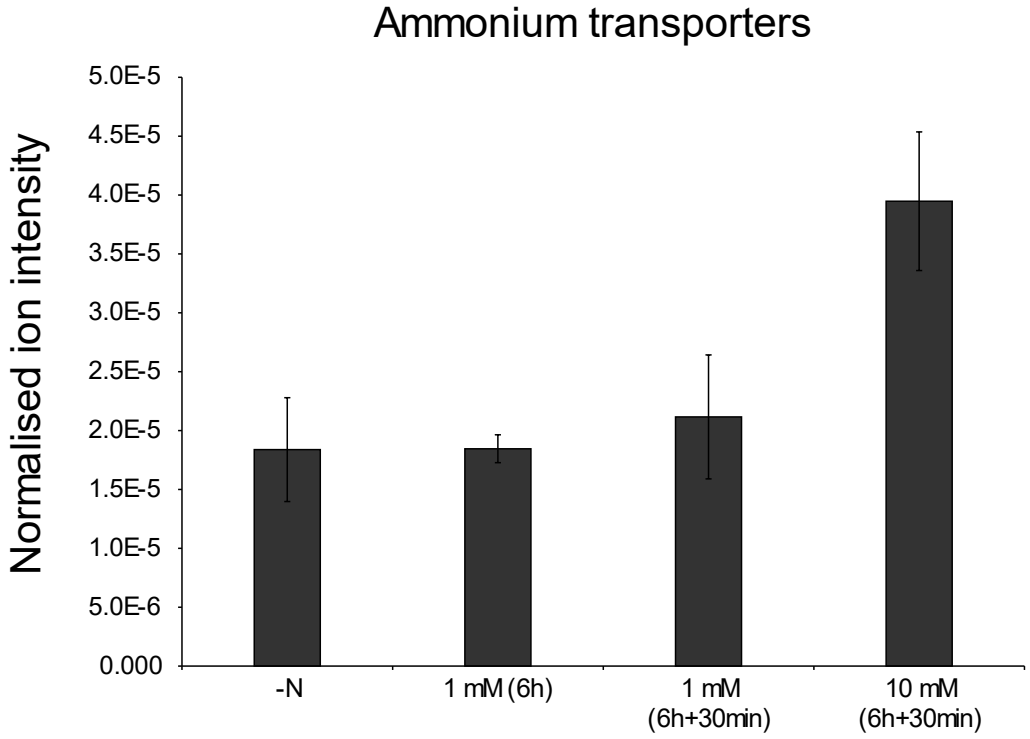

Figure 27. Response of ammonium transporters to ammonium treatment. Normalised ion intensity derived from all ammonium transporters proteotypic peptides. Normalised ion intensity ("fraction of total intensity" computed as "peptide ion intensity/total sum of sample's ion intensities"). The Analysis was performed with the non-phosphoenriched sample's dataset. Error bars show standard error of the mean.

MATE proteins were downregulated at elevated ammonium supply (Fig. 28). MATE proteins are proton-dependent efflux transporters (Eckardt 2001) which bind to a variety of potentially cytotoxic compounds and remove them from the cell in an ATP- or proton-dependent process (Zheleznova et al. 2000). It was therefore not expected that they would be downregulated as ammonium concentration transiently increased (Fig. 28), due to the potential toxic effect of elevated concentration of ammonium. Nonetheless, the downregulation of MATE proteins in

this case might be indicative of the change of organic acids, which might be necessary for stabilizing the internal pH, as well as for ammonium assimilation. Perhaps, the plant did not classify ammonium as toxic (irrespective of the concentration), even though it triggered stress responses.

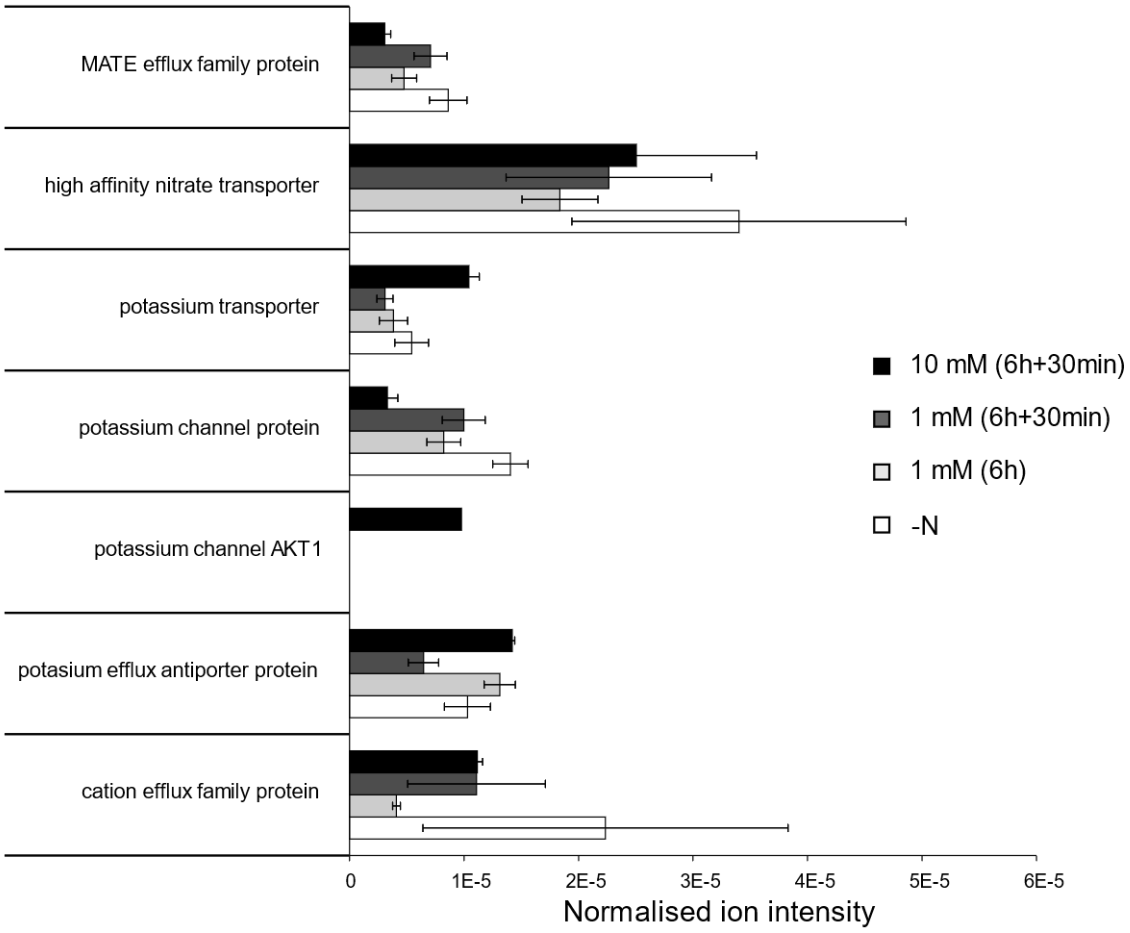

Figure 28. Graphical representation of the response of the MATE efflux family of proteins, high affinity nitrate transporters, potassium transporters/channels, and cation efflux family proteins to ammonium treatment. Normalised ion intensity derived from all proteotypic peptides. Normalised ion intensity ("fraction of total intensity" computed as "peptide ion intensity/total sum of sample's ion intensities"). Analysis performed with the non-phosphoenriched sample's dataset. Error bars show standard error of the mean.

Meanwhile, asparagine synthetase, 6-phosphofructokinase, phosphoenol pyruvate carboxylate as well as the nitrogen regulatory protein P-II increased at an elevated ammonium concentration of 10 mM (6h+30min) (Fig. S 1). There was also a decrease in glutamate decarboxylate level at 10 mM (6h+30min) of ammonium exposure (Fig. S 1). Although Fructose 1,6 bisphoshate appeared to decrease at elevated ammonium concentration, Calcineurin B protein, protein phosphatase 2-C, respiratory oxidase burst, ethylene-insensitive

proteins and the EF hand family proteins remained unchanged irrespective of the treatment (Fig. S 2).

It is therefore worthy to note that Calcineurin B-like proteins (CBLs) are important calcium sensors that have been repeatedly implicated in the regulation of ammonium transporters. They are known to form regulating complex with the CBLs-interacting protein kinases (CIPKs) (Straub et al. 2017). Since CIPK proteins are serine threonine protein kinases, it was therefore interesting that the proteotypic peptides specific to the Serine threonine protein kinases "family" were only detected in the 1 mM (6h) treatment in the non-phosphoenriched samples.

3.8.PHOSPHOPROTEOME RESPONSE OF WHEAT'S TaAMT1s TO ELEVATED AMMONIUM CONCENTRATIONS

Analysis of the phosphoproteome response of wheat roots showed similar phosphopepetide abundance trend for the phospho-enriched samples and the non phospho-enriched samples (Fig. 29). However, more phosphopeptides were detected in the phosphoenriched samples (Fig. 29).

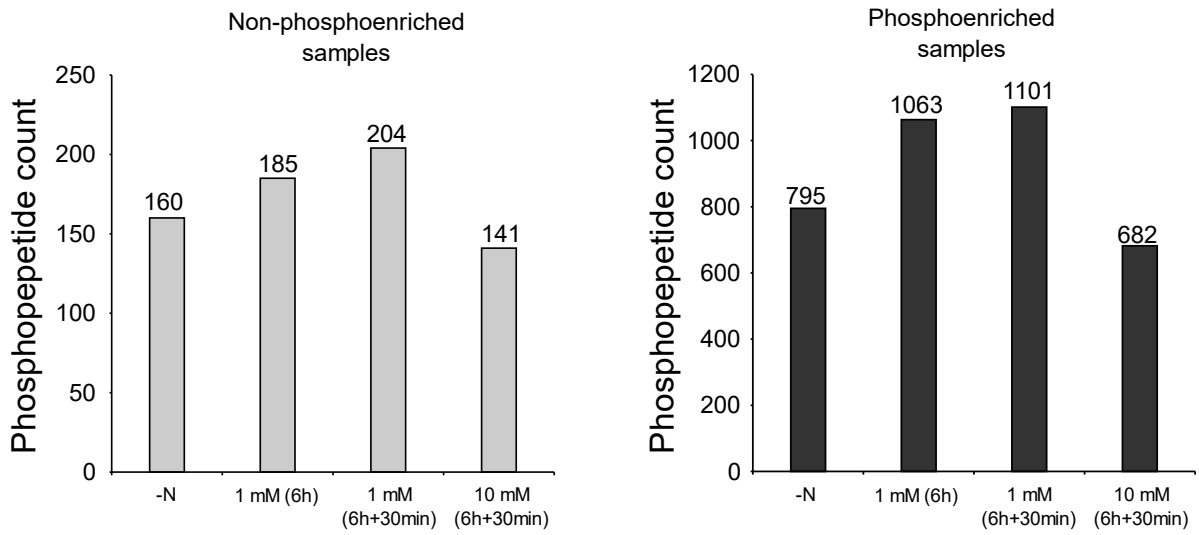

Figure 29. Phosphopeptide count of treatments for the Non-phosphoenriched and the Phosphoenriched samples. The analysis was performed with the non-phosphoenriched, and phospho-enriched sample's dataset.

The phospho-modification of high affinity ammonium transporters at relevant phosphorylation sites is one of the regulatory mechanisms adopted by plants in the regulation of high affinity ammonium transporters (Lanquar et al. 2009; Neuhäuser et al. 2007). Since the activity of high affinity ammonium transporters has been associated with up to 95% of ammonium uptake in

Arabidopsis thaliana under conditions of nitrogen starvation (Loqué et al. 2006; Yuan et al. 2007); the phosphorylated proteotypic phosphopetides of TaAMT1s were of primary interest.

Consequently, phosphorylated proteotypic phosphopeptides of TaAMT1s, which were phosphosphrylated at the conserved threonine located at position 453 of their amino acid sequence were detected. The peptide ISAEDEMAGMDLT(ph)R_, was specific to TaAMT1;1, while ISAEDEMAGMDQT(ph)R_ was TaAMT1;2 specific. Both peptide sequences were 100% conserved on the homeologs of their respective genes (Fig. 30). While the response of the peptides in the phosphoenriched samples and the nonphospho-enriched sample differ slightly, certain deduction could still be made.

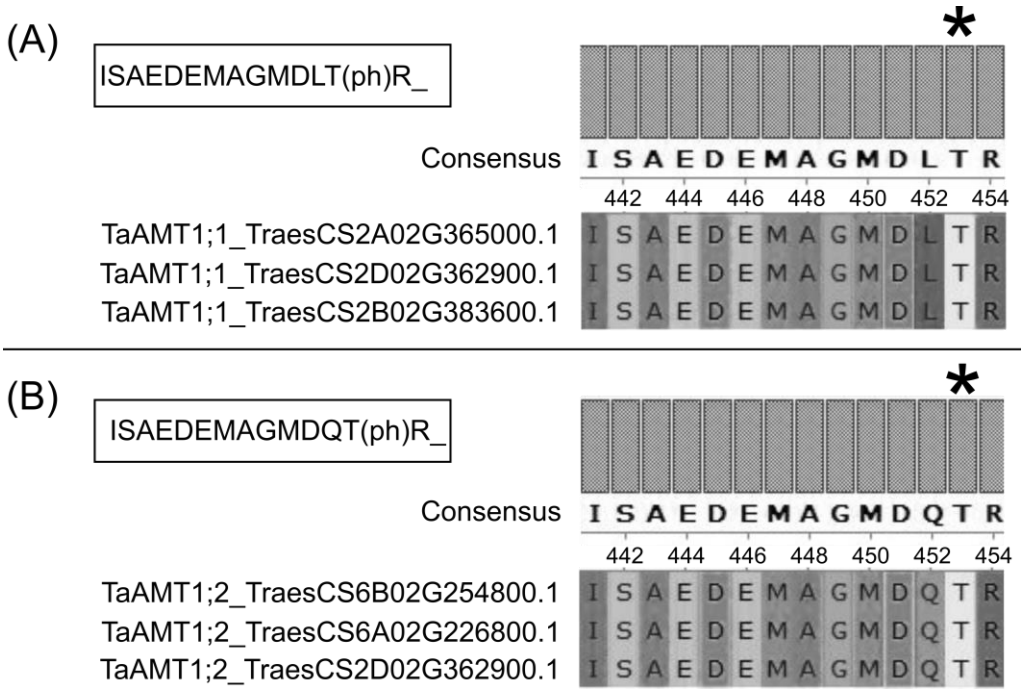

Figure 30. Phosphopeptides harbouring the conserved threonine T453 ((A) TaAMT1;1, and (B) TaAMT1;2) are conserved between the homeologs of TaAMT1s. Multiple sequence alignment was performed with the MUSCLE algorithm of the Ugene sequence viewer (Okonechnikov et al. 2012).

The normalized ion intensity of ISAEDEMAGMDLT(ph)R_ (TaAMT1;1) increased at elevated ammonium concentration in both the phosphoenriched and the non-phosphoenriched samples (Fig. 31A). Although the ion intensity of ISAEDEMAGMDQT(ph)R_(TaAMT1;2) appear to increase in the non-phosphoenriched sample, this was not seen in the phosphenriched samples, as the peptide was not detected at all in the 1 mM (6 h) and the 10 mM (6 h + 30 min) treatment (Fig. 31B). Yet, it is clear that the wheat plant phosphorylated both transporters (TaAMT1;1 “ISAEDEMAGMDLT(ph)R_” and TaAMT1;2 “ISAEDEMAGMDQT(ph)R_”)

at the conserved threonine 453T. Notably, this conserved Threonine (T) is widely conserved across the plant kingdom, where its phosphorylation has been shown to be able to impair ammonium uptake (Loqué et al. 2007; Neuhäuser et al. 2007; Zhu et al. 2015).

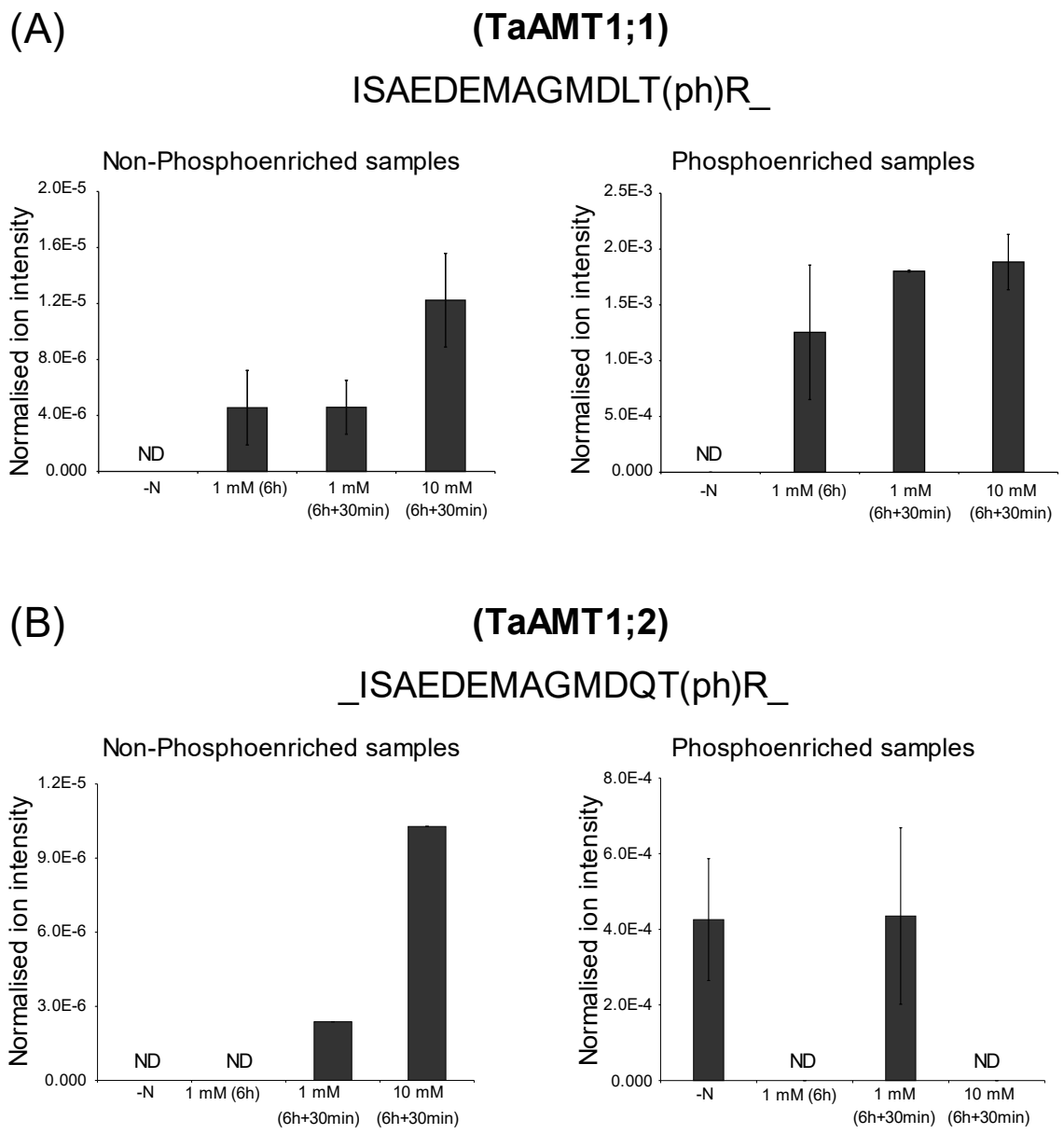

Figure 31. Response of (A) TaAMT1;1 "ISAEDEMAGMDLT(ph)R_, and (B)TaAMT1;2 ISAEDEMAGMDQT(ph)R_ to sole ammonium N. Data was computed from the non-phosphoenriched samples as well as the phosphoenriched samples. Error bars show standard error of the mean.

3.9.PHOSPHOMIMIC MUTANTS OF WHEAT'S AMT1S EXHIBIT LOSS OF AMMONIUM TRANSPORT FUNCTION

The response of the TaAMT1s phosphopeptides carrying phosphomodification of the conserved Threonine (T453) to elevated ammonium concentration led to the investigation of the effect of such modification on wild type transporters. Thus, a mutation that mimics phosphorylation was introduced via a site directed mutation of the transporters. The conserved threonine (T453) was exchanged for Aspartate (D) to make the $T_{453}D$ mutant. Heterologous expression of the mutants TaAMT1;1($T_{453}D$) and TaAMT1;2($T_{453}D$) in a yeast strain lacking endogenous ammonium transporters showed that the mutation caused the inactivation of the ammonium transport function of the TaAMT1;1 and TaAMT1;2 transporters (Fig. 32). The mutant also prevented the uptake of methylammonium chloride (the more toxic analogue of ammonium). Meanwhile, the wild type transporters were able to successfully transport ammonium. Nevertheless, a yeast spot growth in a media having "methylammonium chloride and Arginine" (as N sources) showed TaAMT1;1 to be a poorer transporter of methylammonium compared to TaAMT1;2 (Fig. 32).

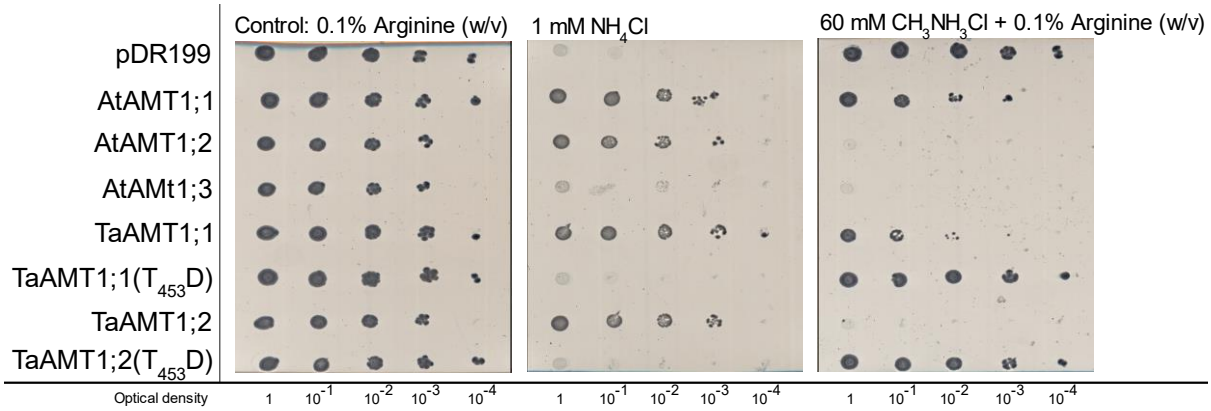

Figure 32. Mutation mimicking phosphorylation (exchange of threonine (T453) for Aspartate (D) to make the $T_{453}D$ mutant) impair the ammonium transport activity of TaAMT1s in a yeast strain lacking endogeneous ammonium transporters (*ΔΔΔmep* yeast). The TaAMT1;1 mutant is denoted as TaAMT1;1($T_{453}D$). The TaAMT1;2 mutant is denoted as TaAMT1;2($T_{453}D$).

It could thus be inferred that phosphorylation of the conserved Threonine T453, was able to inactivate the ammonium transport activity of the high affinity ammonium transporters (TaAMT1;1 and TaAMT1;2) of wheat. This observation strongly suggests that wheat also adopt the phosphorylation of its ammonium transporters in its mitigative effort against ammonium toxicity.

Furthermore, four additional proteotypic phosphopeptide of TaAMT1;2, all of which were located at the distal C-terminal end of TaAMT1;2 were detected (Fig. 33). HGGFAYAYTDEDS(ph)SSRPGR, and GAGGS(ph)VGGFLMK were detected in the phospho-enriched and the non phospho-enriched samples, while SAQTSQVAADATS(ph)PSSSV, and SAQTSQVAADATS(ph)PSS(ph)SV were only detected in the phosphoenriched samples.

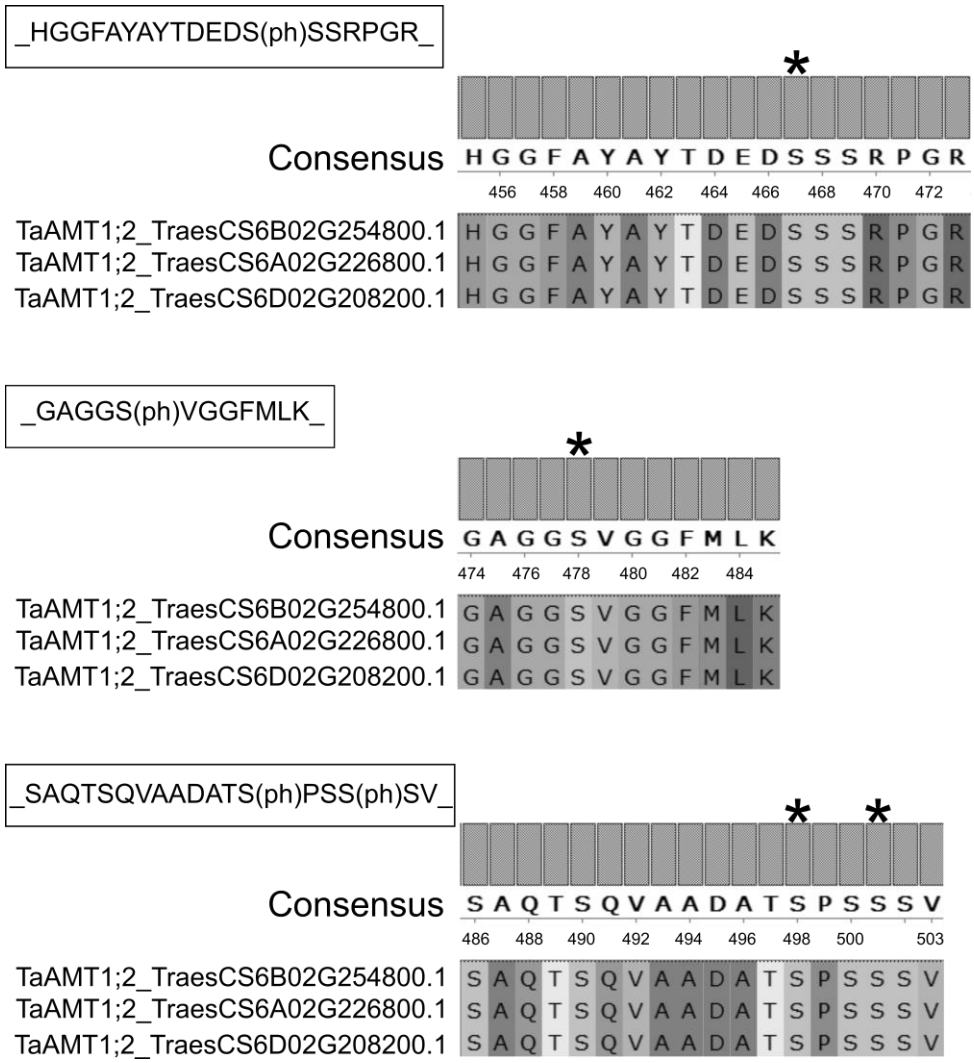

Figure 33. Multiple sequence alignment of three additional TaAMT1;2 proteotypic phosphopeptides (HGGFAYAYTDEDS(ph)SSRPGR, GAGGS(ph)VGGFLMK, and SAQTSQVAADATS(ph)PSS(ph)SV). Multiple Sequence alignment was performed with the MUSCLE algorithm of the Ugene sequence viewer (Okonechnikov et al. 2012).

GAGGS(ph)VGGFLMK showed a decreasing ion intensity in the 1 mM (6 h+ 30 min) and the 10 mM (6 h+ 30 min) treatment (Fig. 34A). However, there was no significant change in the ion intensity of HGGFAYAYTDEDS(ph)SSRPGR in the non-phosphoenriched samples (Fig. 34B). It is worthy to note that HGGFAYAYTDEDS(ph)SSRPGR was not detected in the N starvation treatment (-N) and the 10 mM (6 h+ 30 min) treatment for the phosphoenriched

samples (Fig. 34B). Nevertheless, the ion intensity of SAQTSQVAADATS(ph)PSSSV, and SAQTSQVAADATS(ph)PSS(ph)SV decreased in the 1 mM (6 h+ 30 min) and the 10 mM (6 h+ 30 min) compared to the nitrogen starvation (-N) and the 1 mM (6 h) treatments (Fig. 35A, & B) respectively.

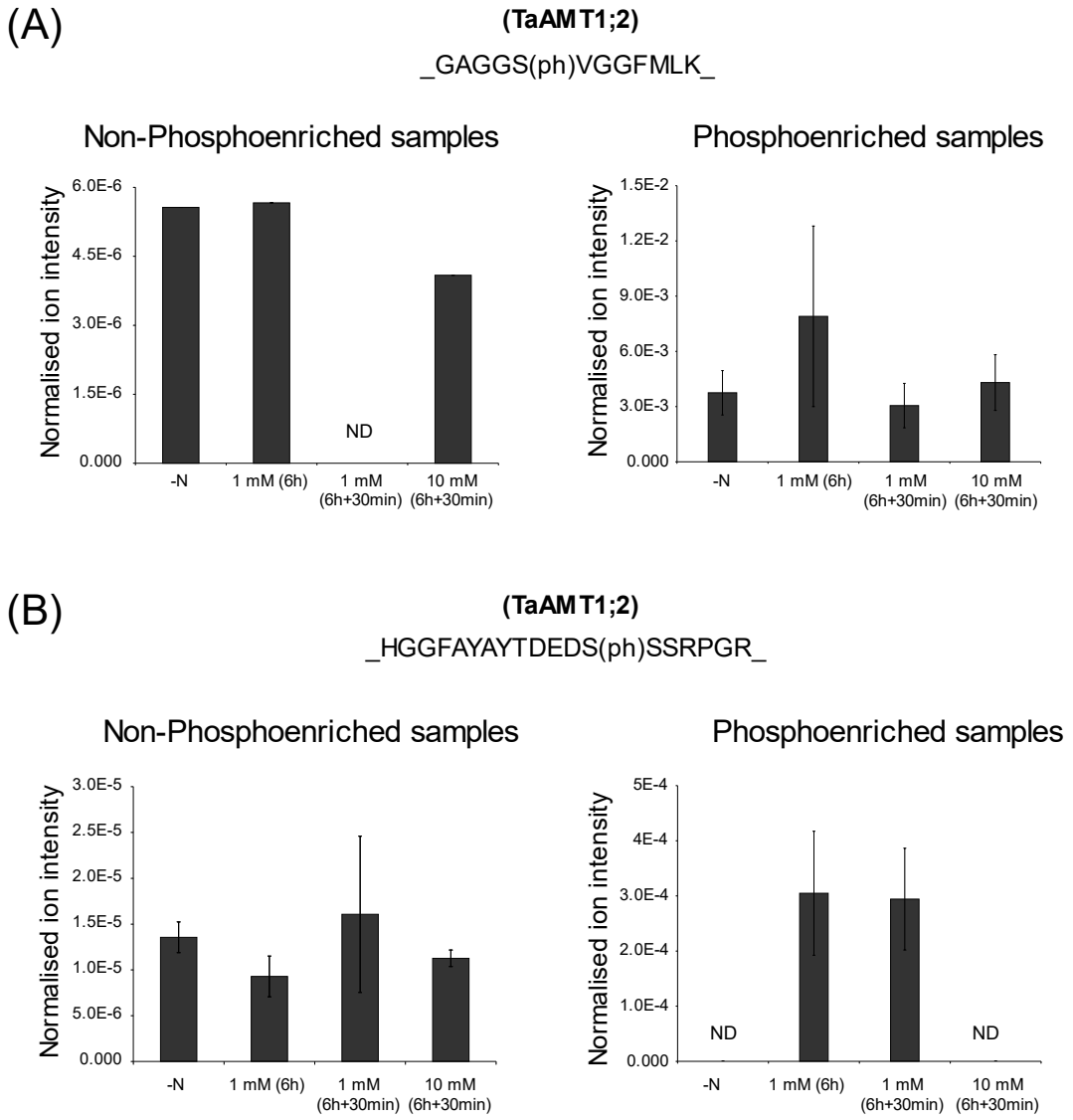

Figure 34. Concentration and time dependent response of (A) GAGGS(ph)VGGFLMK , and (B) HGGFAYAYTDEDS(ph)SSRPGR, to sole ammonium N. The Data from the non phosphoenriched samples as well as the phosphoenriched samples are presented. Error bars show standard error of the mean.

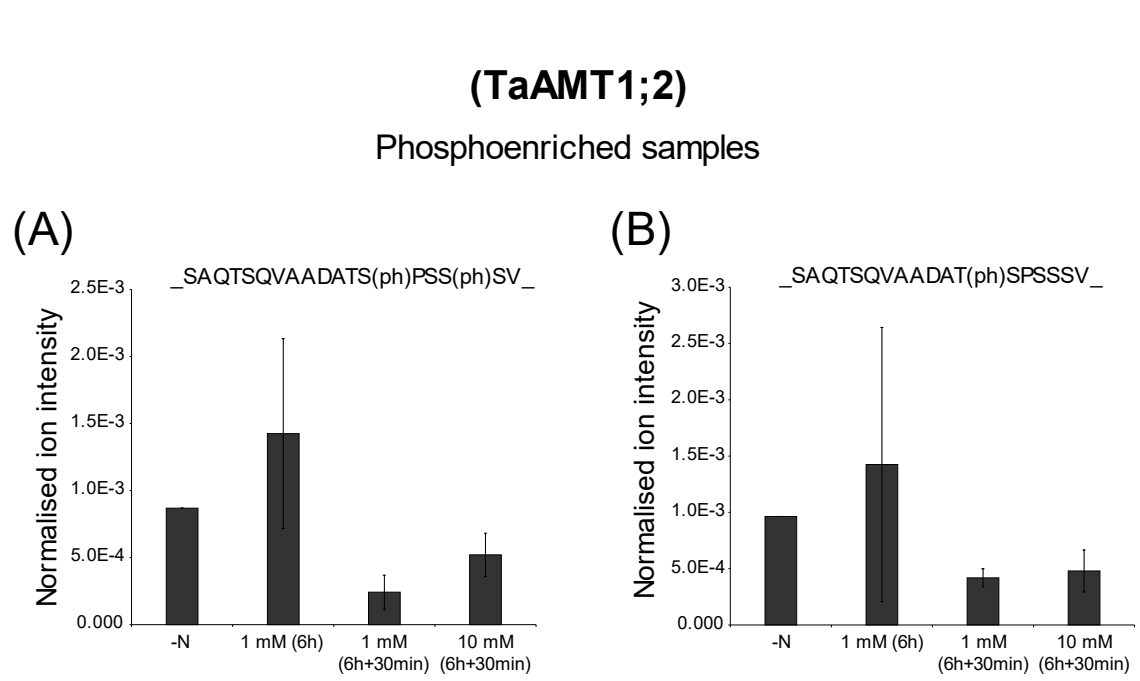

Figure 35. Concentration and time dependent response of (A.) SAQTSQVAADATS(ph)PSSSV, and (B.) SAQTSQVAADATS(ph)PSS(ph)SV to sole ammonium N. Phosphopeptides were only detected in the phosphoenriched samples. Error bars show standard error of the mean.

Although the effect of the phosphomodification of these Serine residues (HGGFAYAYTDEDS (ph)SSRPGR_, GAGGS(ph)VGGFLMK, SAQTSQVAADATS(ph)PSSSV, and SAQTSQVAADATS(ph)PSS(ph)SV) remain elusive, their localization in the functionally important C-terminal end of TaAMT1;2 suggest crucial roles. Especially since the C-terminus of Arabidopsis AtAMT1s is also know to contain multiple phosphorylation sites, all of which are believed to coordinate the integration of relevant regulatory signals (Lanquar et al. 2009; Wu et al. 2019).

Further analysis of the proteotypic phosphopeptide obtained from the phosphoenriched samples dataset was performed to gain more insight of the processes peculiar to each treatment condition. There was significant phosphopeptide response from the aquaporins (Table S 4 - S 9). While there was an increase in the phosphorylation of some phosphopeptides, the decrease in the phosphorylation of others were recorded. In fact, while the phosphorylation of a peptide (on a serine) could be upregulated for a particular treatment, the phosphorylation of the same peptide (phosphorylated on another serine residue) could still be downregulated in the same treatment. Such was the case of the phosphopeptide FGSS(ph)ASFGSR_ (Log_2FC 2.8) and FGSSAS(ph)FGS(ph)R_ (Log_2FC -2.2) of Traes_2AL_DD284DEA9 (Table S 4). Additionally, the phosphorylation of a putative plasma membrane ATPase (_GLDIDTINQNYT(ph)V_) decreased in the 1 mM (6h) treatment (relative to the N

starvation treatment "-N" (Table S 4)), suggesting an increased activity (Falhof et al. 2016) on ammonium exposure. Also, there was a decreased phosphorylation of glucose-6-phosphate-1-dehydrogenase (_(ac)AGTDSSASSRQSS(ph)FNS(ph)LAK_) at an elevated ammonium concentration of 10 mM (Table S 8).

3.10. CANDIDATE TaCBLs AND TaCIPKs RESPONDED SIGNIFICANTLY TO ELEVATED AMMONIUM CONCENTRATION

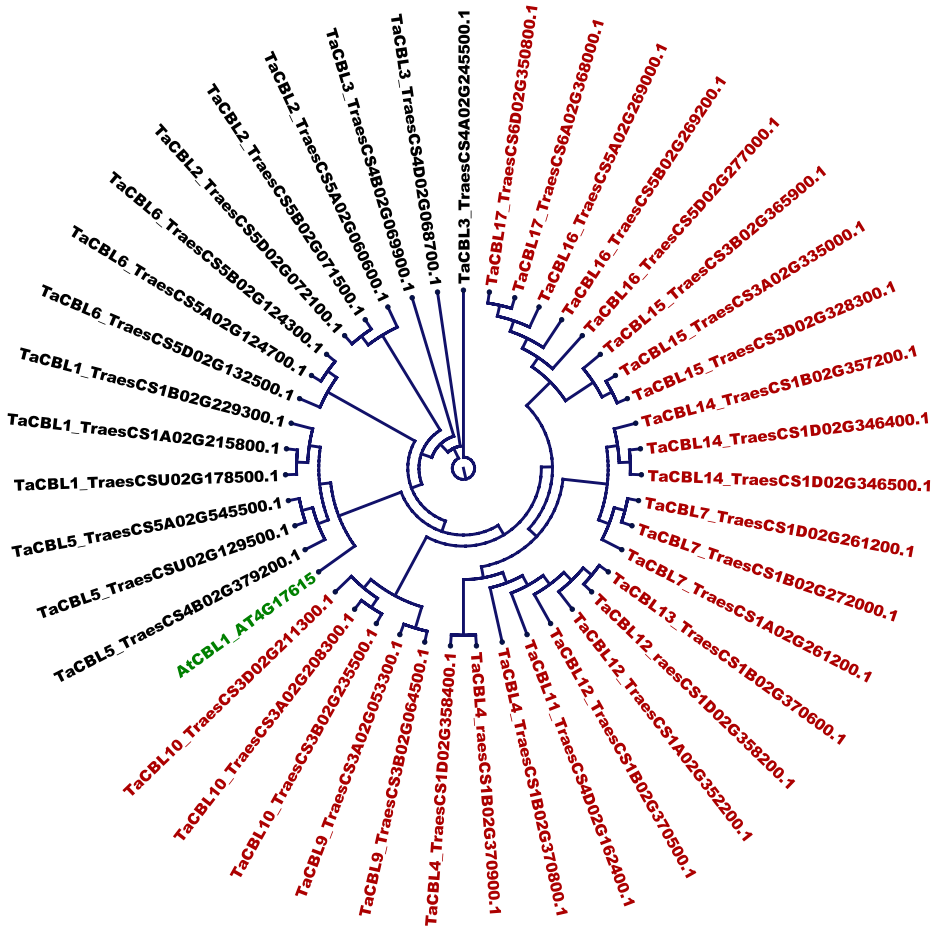

Figure 36. CBLs in the wheat genome. Phylogenetic tree showing the inter-relatedness between the Calcineurin B-like (CBL) proteins of wheat and the Arabidopsis AtCBL1 (green). Candidates (including homeologs) selected for the qRT-PCR highlighted in black letters.

The specificity of the interaction of Calcineurin B-like proteins (CBL) and CBL-interacting protein kinases (CIPKs), allows for several mechanism-generated specificity in plant calcium signaling (Batistic and Kudla 2009). An earlier work had analyzed the wheat genome for CBL and CIPK genes, reporting multiple candidates (Sun et al. 2015). Thus, using the work as a

guide, a blast search was performed on the genome of wheat using the CBLs and CIPKs of Arabidopsis as query (plants.ensemble.org). 84 coding sequences of CIPK proteins (Table S 2) as well as 42 CBL proteins (Table S 1) were found. A multiple sequence alignment, followed by a phylogenetic tree revealed the presence 16 putative CBL proteins (Fig. 36), and 30 putative CIPK proteins (Fig. 37), with homeologs of the same genes grouped together.

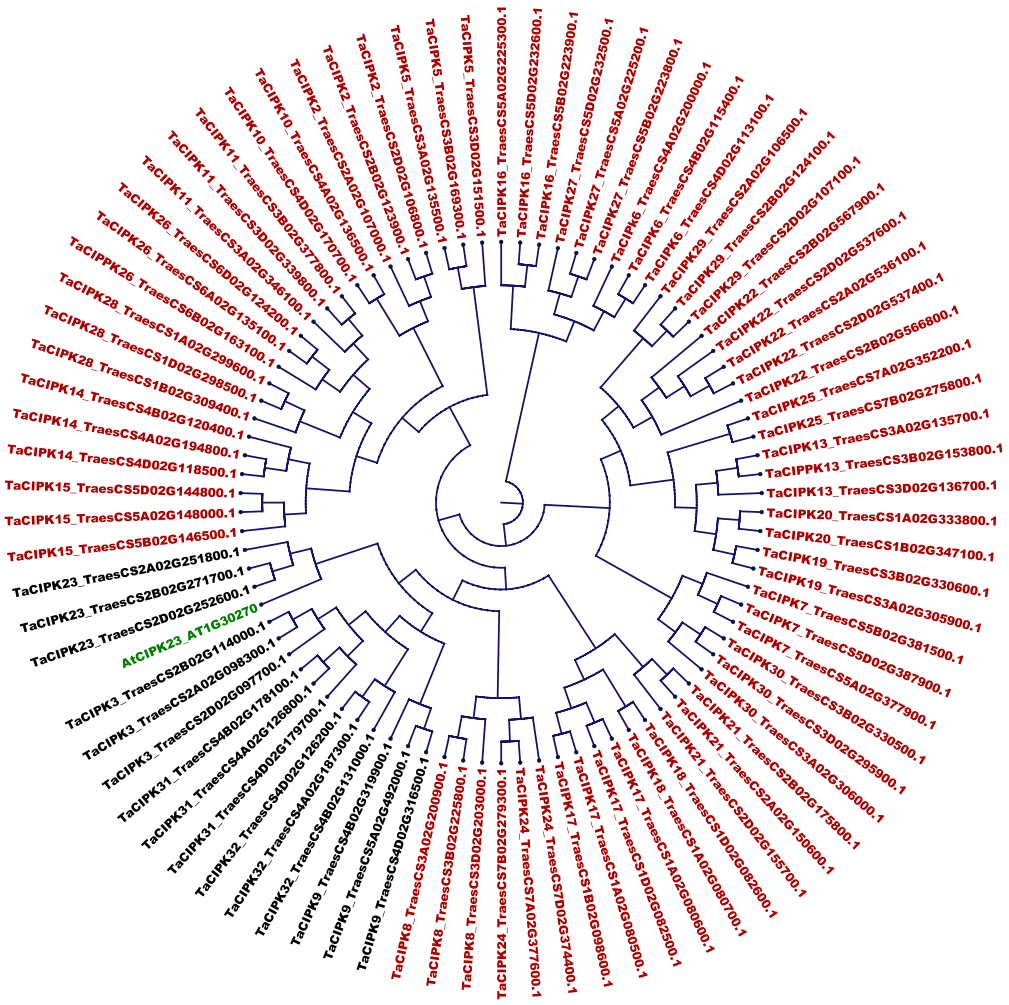

Figure 37. CIPKs in the wheat genome. Phylogenetic tree showing the inter-relatedness between the Calcineurin B-like (CBL)-Interacting protein kinases (CIPKs) of wheat and the Arabidopsis AtCIPK23 (green). Candidates (including homeologs) selected for the qRT-PCR procedures are highlighted in black letters.

Interestingly, certain TaCBL proteins grouped closely with the CBL1 of Arabidopsis (AtCBL1), which have been shown repeatedly to be involved in the regulation of abiotic and biotic response in plant (Cheong et al. 2003). AtCBL1 has also been shown to be involved in the regulation of plant ammonium transporters (Straub et al. 2017). These candidate TaCBL proteins (TaCBL1, TaCBL2, TaCBL3, and TaCBL6) were thus selected for further

investigation with the qRT-PCR procedure. It was therefore postulated that their relatedness to AtCBL1 suggests a potential involvement in the regulation of the high affinity ammonium transporters of wheat. Also, the possibility of the formation of a functional phosphorylating pair with appropriate candidate TaCIPK proteins was anticipated.

Five TaCIPK proteins (including their respective homeologs) on the other hand notably grouped with the CIPK23 (Fig. 37) of *Arabidopsis thaliana* (AtCIPK23). The candidate TaCIPK proteins include TaCIPK3, TaCIPK9, TaCIPK23 TaCIPK31, and TaCIPK32 (Fig. 37). AtCIPK23 has been shown to regulate the high affinity ammonium transporters of Arabidopsis via complex formation with AtCBL1 (Straub et al. 2017). Thus, the related genes were selected for further investigation with the qRT-PCR procedure.

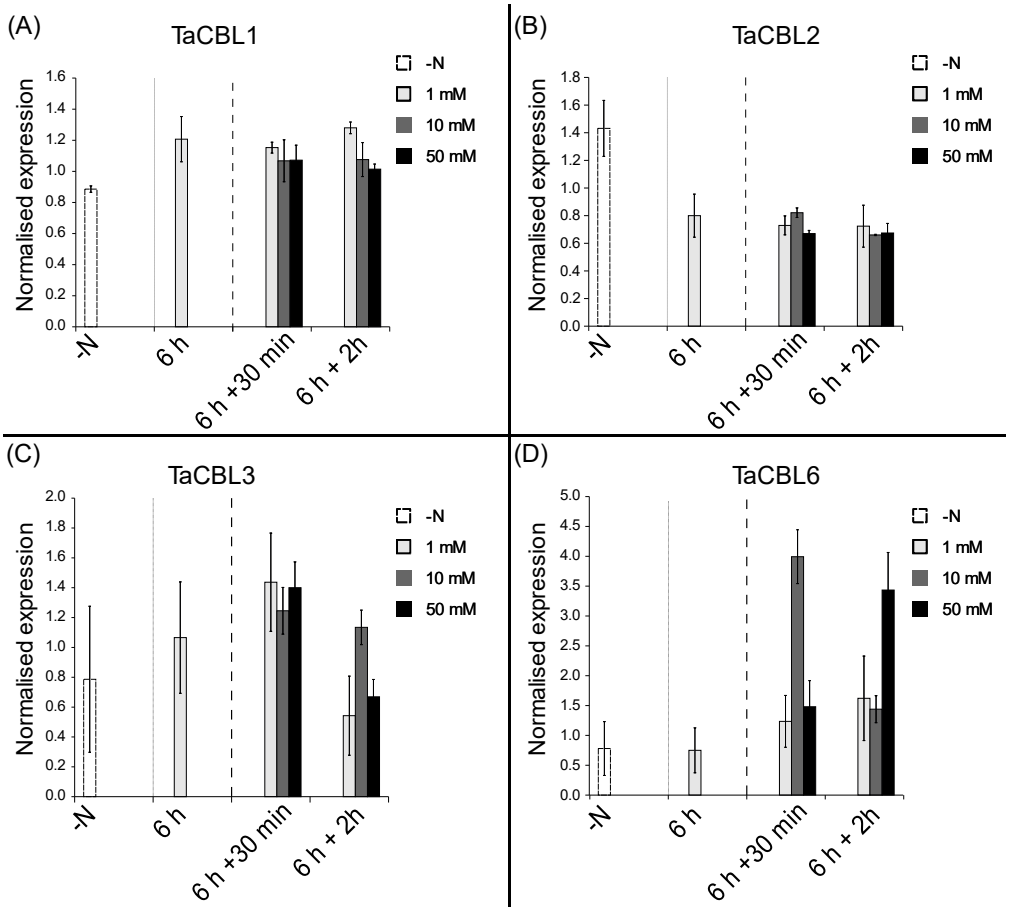

Figure 38. Ammonium concentration and time dependent normalised expression of (A) TaCBL1, (B) TaCBL2, (C) TaCBL3, (D) TaCBL6, to sole ammonium N. Gene expression were normalised using TaACT and TaEF1α as reference genes. Error bars show standard deviation of the mean.

Increased TaCBL1 transcripts was triggered by the presence of ammonium, irrespective of the supplied concentration and time (Fig. 38A). TaCBL2, on the other hand showed a decrease in transcripts abundance as ammonium N was supplied (Fig. 38B). TaCBL6 transcripts increased in response to 10 mM ammonium shock after 30 minutes as well as to 50 mM of ammonium shock after 2 hours (Fig. 38D). Although TaCBL3 appeared to show some responsive tendencies to elevated concentration of ammonium N, the large error bars observed in all the repetitions rendered this inconclusive (Fig. 38C). Thus, only TaCBL1, TaCBL2 and TaCBL6 were selected as the candidate genes for further investigation.

To further prove the homeolog similarities of the newly selected candidate genes, the protein structure of each of the homeologs was modelled with the protein structure homology-modelling (server at: https://swissmodel.expasy.org/). The respective models were aligned with Pymol (The PyMOL Molecular Graphics System, Version 2.0 Schrödinger, LLC.). The result demonstrated similar protein structure by the homeologs of the same gene (Fig. 39).

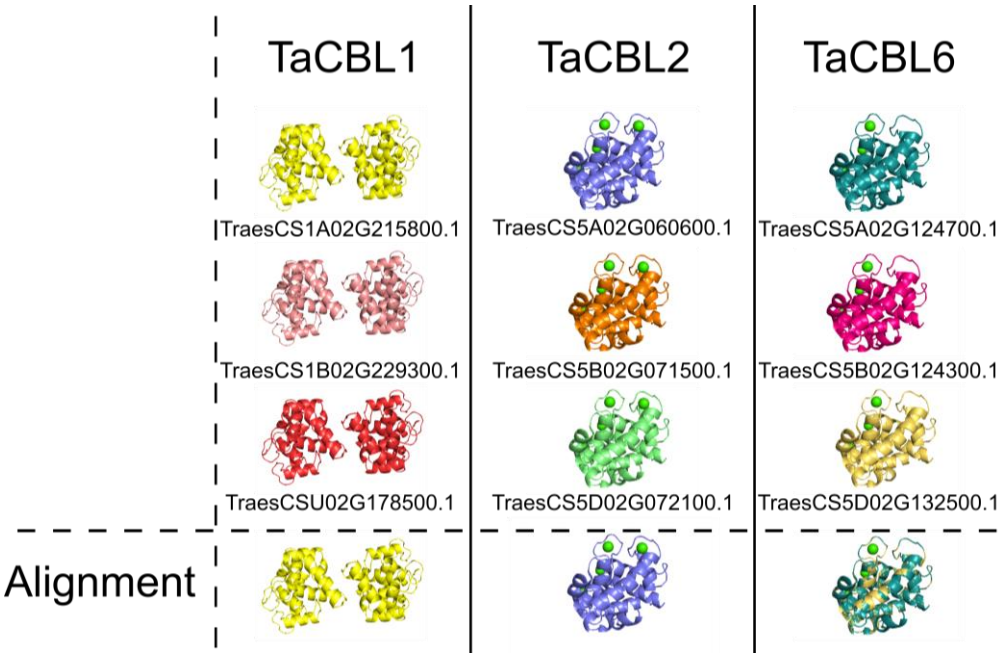

Figure 39. Protein structure homology-modelling (https://swissmodel.expasy.org/) of the homeologs of candidate TaCBL proteins and their alignment (with Pymol).

TaCIPK9, TaCIPK23, and TaCIPK32, showed significant increase in transcripts in response to elevated concentration of ammonium concentration (Fig. 40). TaCIK9 transcripts increased in response to 10 mM and 50 mM after 30 minutes of ammonium shock (6h +30min) (Fig. 40B). There was also an increase in the transcript abundance of TaCIPK23 in the 50 mM

treatment after 30 minutes, which was slightly reduced after 2 hours. However, the 10 mM treatment was only able to trigger an increase in the transcript abundance of TaCIPK23 after 2hours (Fig. 40C). TaCIPK32 was only upregulated by elevated ammonium concentration (10 mM and 50 mM) after 2 hours (6h + 2h) (Fig. 40E).

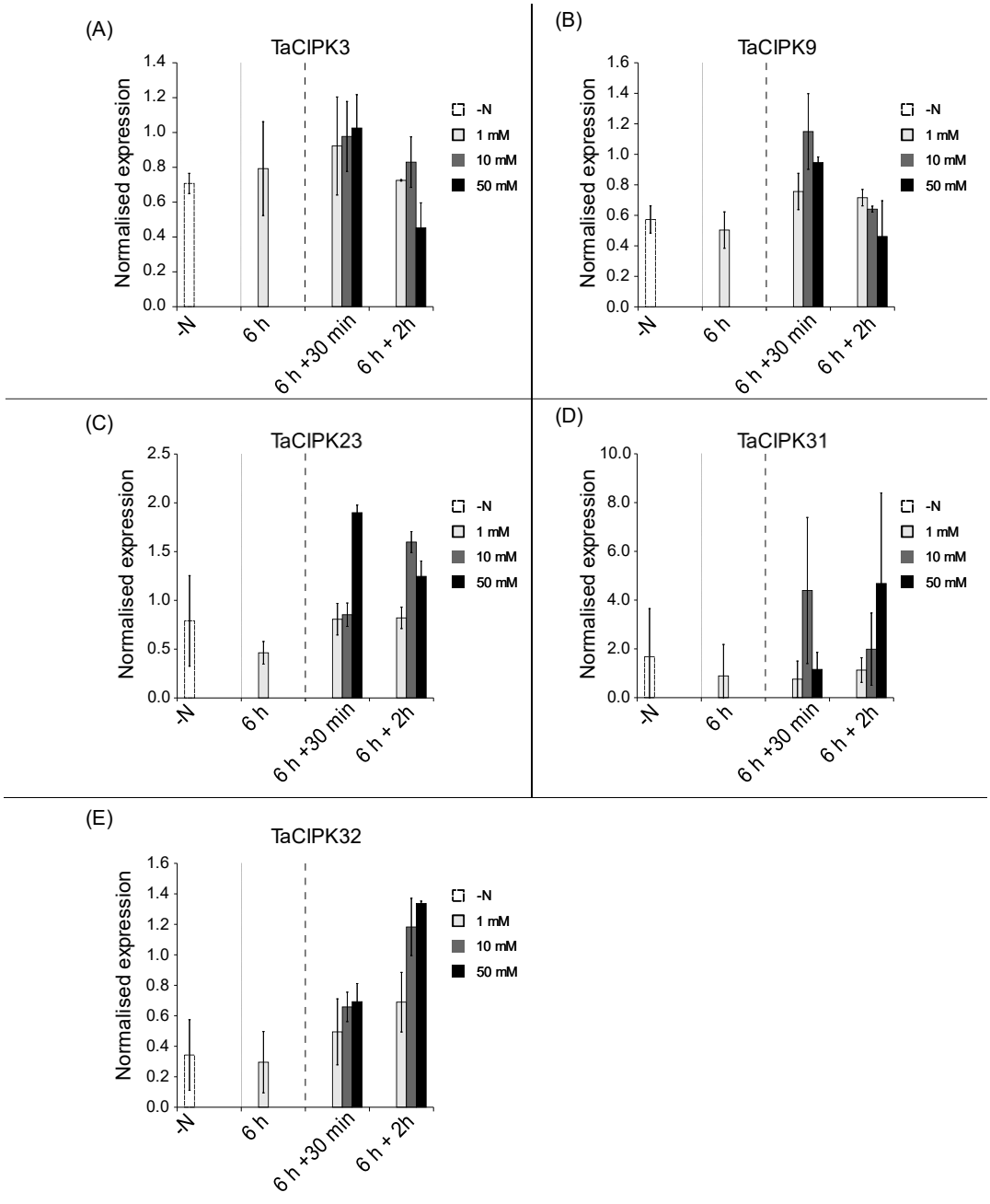

Figure 40. Concentration and time dependent normalised expression of the of (A) TaCIPK3, (B) TaCIPK9, (C) TaCIPK23, (D) TaCIPK31, (E) TaCIPK32, to sole ammonium N. Gene expression was normalised with the TaACT and TaEF1α genes. Error bars showing standard deviation of the mean.

Even though, the transcript of TaCIPK3 was reduced slightly in the 50 mM ammonium shock treatment after 2 hours (6h + 120 min), the large error bars displayed at other time points rendered any suspected trend unreliable (Fig. 40A). Such was also the case of TaCIK31, which appeared to be unresponsive to ammonium supply, irrespective of concentration and/or time of exposure (Fig. 40D). Thus, TaCIPK9, TaCIPK23, and TaCIPK32 were selected as the candidate genes for further investigation. The protein structure modelling of the homeologs (https://swissmodel.expasy.org/), and alignment (PyMOL Molecular Graphics System, Version 2.0 Schrödinger, LLC.) of the homeologs of the newly selected candidates (TaCIPK9, TaCIPK23, and TaCIPK32) demonstrated similar proteins structure by homeologs of the same gene (Fig. 42).

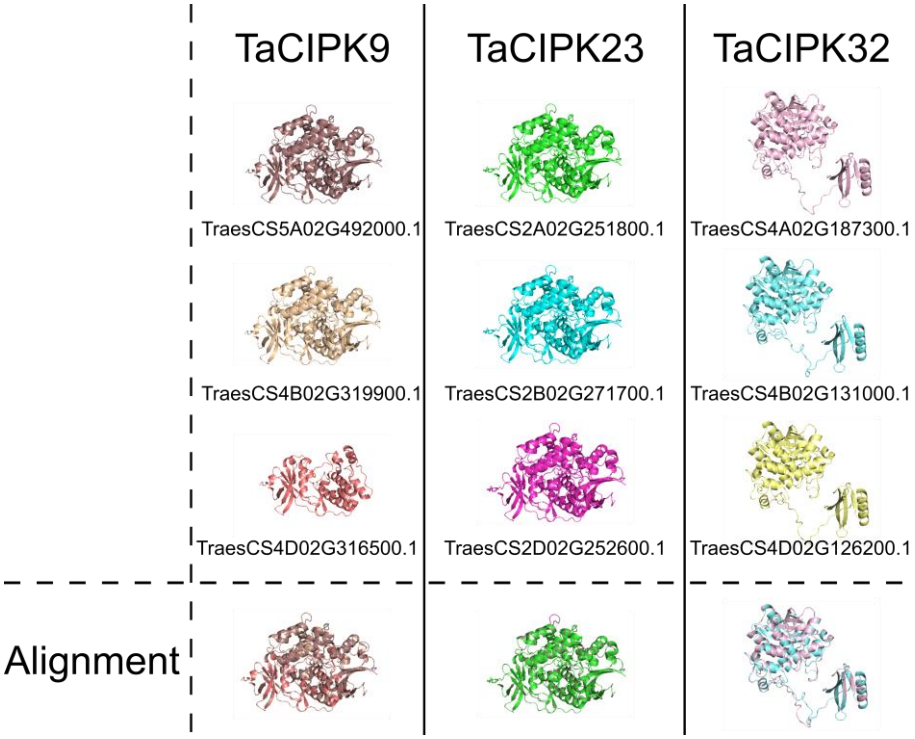

Figure 41. Protein structure homology-modelling (https://swissmodel.expasy.org/) of the homeologs of the TaCIPK proteins and their alignment with Pymol.

Even though protein structure modeling had shown similarities between the homeologs of the candidate TaCBL and TaCIPK proteins (TaCBL1, TaCBL2, TaCBL6, TaCIPK9, TaCIPK23, and TaCIPK32), a few amino acid exchanges existed between the homeologs of some genes. The homeologs of TaCBL1 and TaCBL2 showed an 100% amino acid sequence conservation on all homeologs. TaCBL6 also had an A and B genome homeolog that were 100% similar. However, amino acid exchanges existed on the D genome homeolog of TaCBL6 (TraesCS5D02G132500.1). There was an exchange of Methionine (M) for Leucine (L) at

position 15 ($L_{15}M$), a Tyrosine (T) for Aspartate (D) at position 209 ($D_{209}T$), as well as the lack of the C-terminus portion which extended from the Leucin (L) at position 210 to the Alanine (A) at position 226 (Fig. 42).

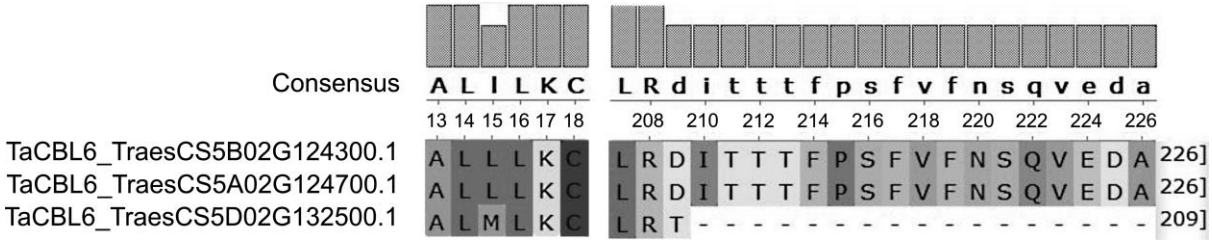

Figure 42. Alignment of TaCBL6 homeologs showing amino acid exchange ($L_{15}M$) and a missing portion of the C-terminus on the D genome homeolog. Multiple sequence alignment was performed with the MUSCLE algorithm of the Ugene sequence viewer (Okonechnikov et al. 2012)

Although all the candidate TaCBLs had four EF-hands, their number of canonical EF-hands varied (Fig. 44). The canonical sequence of the EF- hand motif (DKDGDGKIDFEE) is highly conserved at positions 1(X), 3(Y), 5(Z), 7(-X), 9(-Y) and 12(-Z) (Li et al. 2009b). Interestingly, all changes in EF-hand motifs were conserved in the three homeologs of the genes. Thus, all the homeologs had similar EF-hands motifs (Fig. 43).

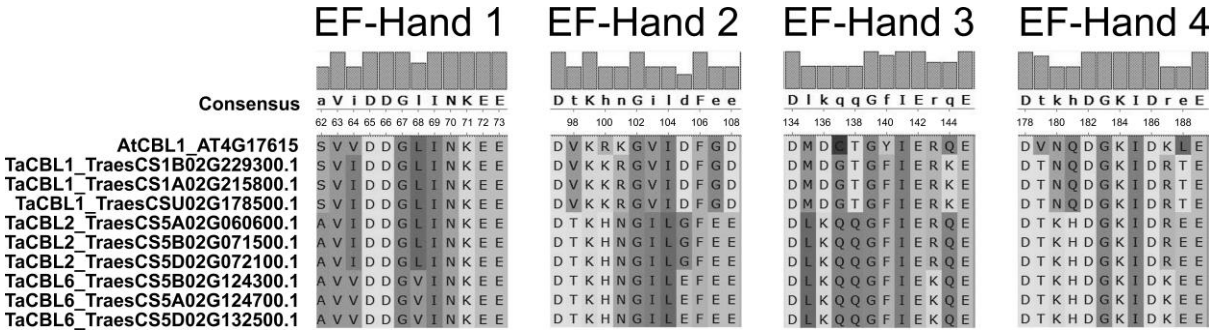

Figure 43. A multiple sequence alignment showing the alignment the EF-hand motif of AtCBL1 (Li et al. 2009b) with putative EF-hand motifs of candidate TaCBL proteins. Multiple sequence alignment was performed with the MUSCLE algorithm of the Ugene sequence viewer (Okonechnikov et al. 2012)

Meanwhile, there were 7 non-conserved amino acid residues among the homeologs of TaCIPK9. There is an exchange of Glycine (G) for Alanine (A) at position 5 (G_5A), a non-conserved amino acid residues at position 7, 9 and 234, a lack of the Glycine (G) at position 8 on the B genome homeolog, an exchange of the Alanine (A) at position 267 for Serine (S) on

the D genome homeolog ($A_{267}S$), and the exchange of Histidine (H) at position 283 for Glutamine (Q) on the B genome homeolog ($H_{283}Q$) (Fig. 44).

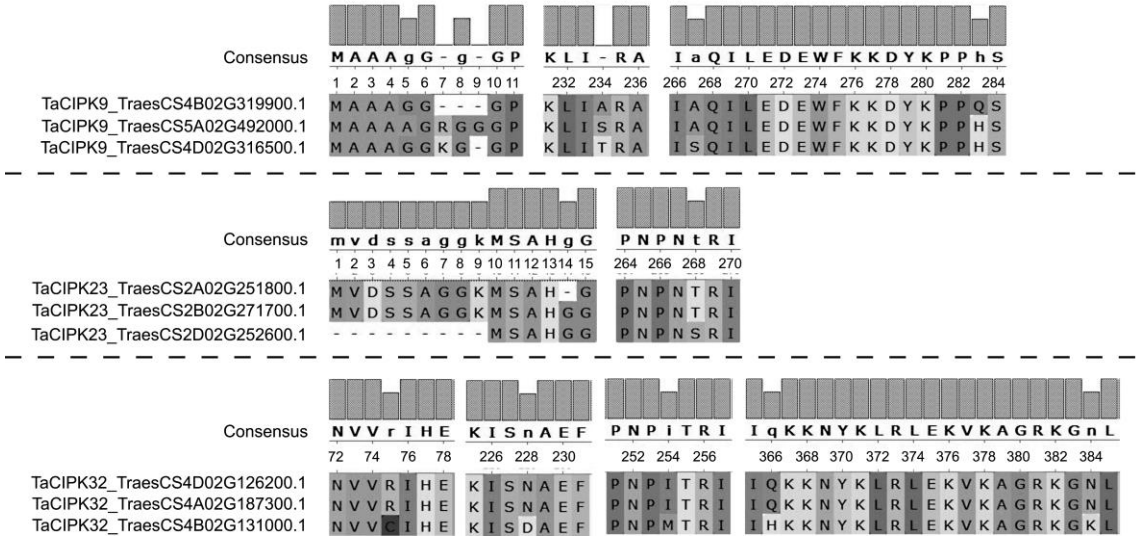

Figure 44. Multiple sequence alignments showing the amino acid exchanges that existed between the homeologs of TaCIPK9, TaCIPK23 and TaCIPK32. Multiple sequence alignment was performed with the MUSCLE algorithm of the Ugene sequence viewer (Okonechnikov et al. 2012)

TaCIPK23 had only three major differences among its homeologs. There was an extra N terminus motif (from the Methionine (M) at position 1 till the Lysin (K) at position 9) that was absent in the D genome homeolog. There was also a Glycine (G) at position 14, which was missing on the A genome homeolog. Additionally, the Threonine (T) at position 268 was exchanged for Serine (S) on the D genome homeolog ($T_{268}S$) (Fig. 44). All the five amino acid exchanges of the TaCIPK32 homeologs were carried on the B genome homeolog. There is an exchange of Arginine (R) for cysteine (C) at position 75 ($R_{75}C$), an exchange of the Asparagine (N) at position 228 for Aspartate (D) ($N_{228}D$), Isoleucine (I) for Methionine (M) at position 254 ($I_{254}M$), Glutamine (Q) for Histidine (H) at position 366 ($Q_{366}H$) as well as the exchange of Asparagine (N) for Lysine (K) at position 384 ($N_{384}K$) (Fig. 44).

A multiple sequence alignment of the candidate TaCIPKs with the AtCIPK23 of *Arabidopsis thaliana* showed the presence of regulatory domain that contains a highly conserved NAF/FISL and PPI domains (Fig. 45). The kinase domain also carried a highly conserved activation loop motif (Fig. 46). The high homology in the amino acid sequence, as well as similar protein structure of the homeologs of the candidate genes of interest suggested similar functions by the respective homeologs.

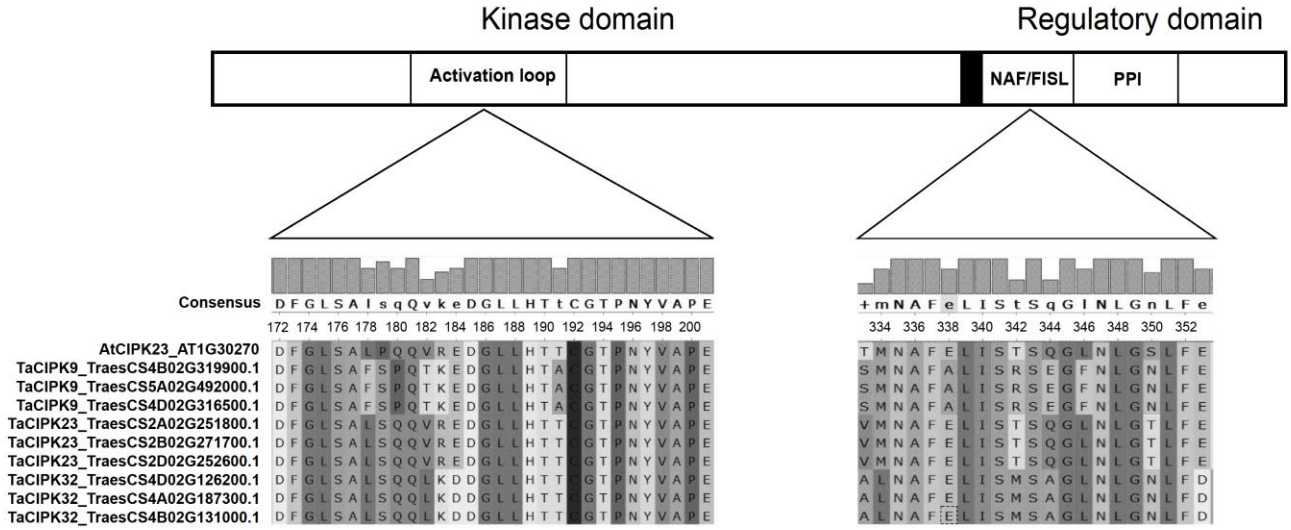

Figure 45. Candidate TaCIPK proteins show high homology to the activation loop and the NAF/FISL domain of the AtCIPK23 of Arabidopsis thaliana (Li et al. 2009b). Multiple sequence alignment was performed with the MUSCLE algorithm of the Ugene sequence viewer (Okonechnikov et al. 2012).

Sanger sequenced result of the cloned amplicons of the respective genes confirmed the identity of the cloned constructs. For the TaCBL1 gene, the TraesCS1A02G215800.1 was amplified and cloned. The homeolog TraesCS5D02G072100.1 was cloned for TaCBL2, while TraesCS5D02G132500.1 was amplified and cloned gene for TaCBL6. Furthermore, the TraesCS4B02G319900.1 homeolog of TaCIPK9 was cloned as TaCIPK9, the TraesCS2D02G252600.1 homeolog of TaCIPK23 as TaCIPK23, while the TraesCS4D02G126200.1 homeolog of TaCIPK32 was Cloned as TaCIPK32 (Table 15).

Table 21. Amplified homeologs for the candidate TaCBL and TaCIPK proteins

Gene	Cloned Homeolog ID (www.plants.ensembl.org)
TaCBL1	TraesCS1A02G215800.1
TaCBL2	TraesCS5D02G072100.1
TaCBL6	TraesCS5D02G132500.1
TaCIPK9	TraesCS4B02G319900.1
TaCIPK23	TraesCS2D02G252600.1
TaCIPK32	TraesCS4D02G126200.1

3.11. CANDIDATE TaCBLs REGULATE THE TaAMT1s OF WHEAT

The observed upregulation of TaCBL1, TaCBL2, TaCBL6 in response to elevated ammonium concentration suggested a possible role in the regulation of wheat's high affinity ammonium transporters. This was hypothesized to be via an interaction partnership with the candidate TaCIPK proteins (TaCIPK9, TaCIPK23 and TaCIPPK32).

Prior to investigating the effect of the co-expression of candidate TaCBL and TaCIPK proteins on TaAMT1s, the effect of the TaCBLs on the ammonium transporters was checked as a control. Unexpectedly, TaCBL1, and TaCBL2 were able to independently impair the ammonium transport activity of TaAMT1;1 in oocytes (Fig. 46A). Also, the ammonium transporting activity of TaMT1;2 was also impaired by TaCBL1, TaCBL2 and TaCBL6 (Fig. 47B).

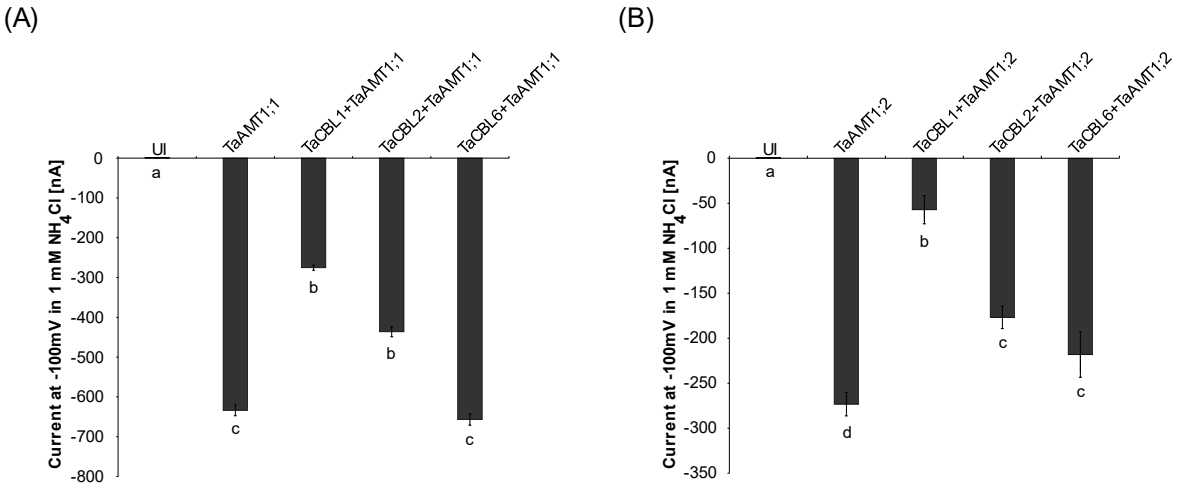

Figure 46. Regulation of TaAMT1s by TaCBLs. UI represent the uninjected oocytes used as the Control. (A) TaCBL1, and TaCBL2 impair the ammonium transport activity of TaAMT1;1 (n= 5 to 9). (B) TaCBL1, TaCBl2, and TaCBL6 impair the ammonium transport activity of TaAMT1;2 (n= 6 to 9). Injected current at -100 mV shown. Error bars shows standard error of the mean.

The unexpected ability of the TaCBL1, and TaCBL2 to independently regulate the activity of TaAMT1;1, as well as the ability of TaCBL1, TaCBl2, and TaCBL6 to independently regulate the activity of TaAMT1;2 begged for an explanation. One hypothesis was that the candidate TaCBLs had the capability to bind to the C-terminus of the transporters in a way that affects the conformation of the AMT trimeric complex: thereby impairing the transport function of the ammonium transporters. Since the CBLs of *Arabidopsis thaliana* were not able to directly regulate the activity of the high affinity ammonium transporters of the Arabidopsis plant

(Straub et al. 2017), it was hypothesised that the answer might lie in the differences harboured in the C-terminus of the transporters.

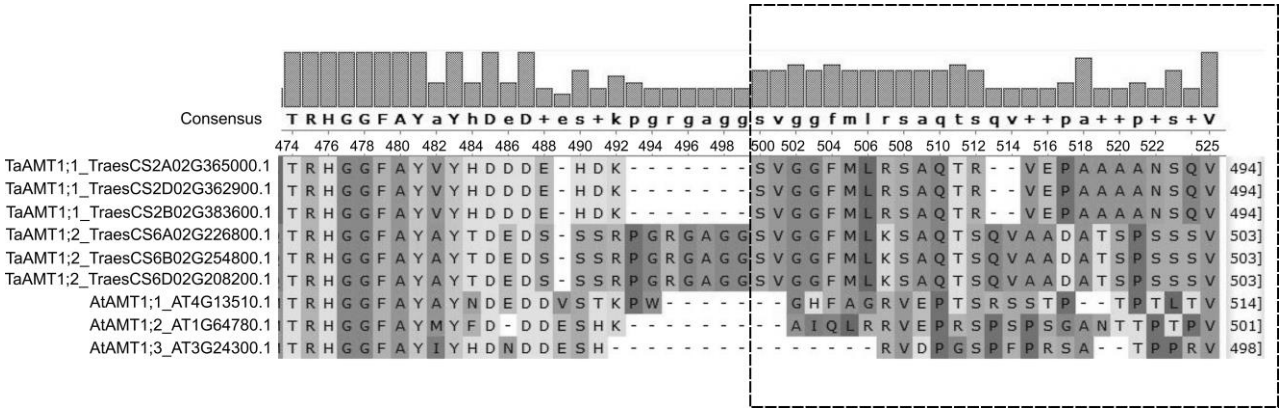

Figure 47. The high affinity ammonium transporters of wheat (TaAMT1;1 & TaAMT1;2) showed differences in the C-terminus amino acid sequence compared to that of the AtAMT1;1, AtAMT1;2, and AtAMT1;3 of Arabidopsis. Region with the broken rectangle was deleted in TaAMT1;1 and TaAMT1;2 to generate the TaAMT1;1C and TaAMT1;2C mutants. Amino acid differences are conserved among homeologs. Multiple sequence alignment was performed with the MUSCLE algorithm of the Ugene sequence viewer (Okonechnikov et al. 2012)

A multiple sequence alignment of the amino acid sequence of the high affinity ammonium transporters of Wheat and Arabidopsis revealed differences between the C-terminus of the transporters and Arabidopsis (Fig. 47). Although there were differences between the C-terminus of TaAMT1;1 and TaAMT1;2, such differences were conserved in their respective homeologs. Hence, C-terminus deletion mutants (TaAMT1;1C and TaAMT1;2C) were generated for TaAMT1;1 and TaAMT1;2 respectively, where the region from the Serine S500 to the Valine V525 (Fig. 47) was deleted. This was done with the expectation that such deletion will prevent the ability of the candidate TaCBLs to regulate the ammonium transporters (Fig. 46).

The mutants showed the ability to transport ammonium in a yeast strain lacking endogeneous ammonium transporters just like the wild type transporters (Fig. 48). Albeit the mutation affected methylammonium chloride transport characteristics, thereby highlighting the importance of the deleted C-terminus part in ammonium uptake (Fig. 48). Investigation of the ammonium transport function of the mutants in the oocyte of *Xenopus laevis* showed a complete inactivation of TaAMT1;1C, as the mutant failed to induce any ammonium triggered current in oocytes. Thus, the effect of the candidate TaCBLs on the TaAMT1;1C mutant could not be investigated in oocytes.

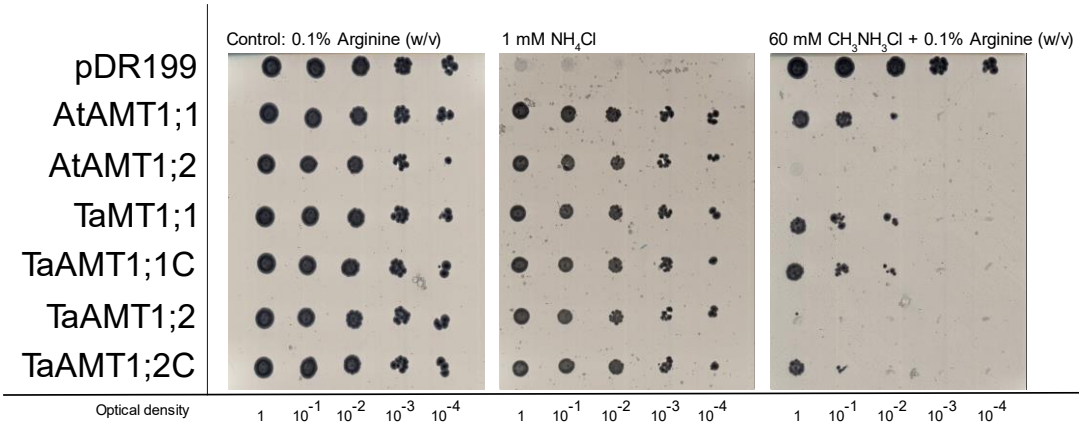

Figure 48. A yeast strain lacking endogeneous ammonium transporters (*ΔΔΔmep* yeast) was able to transport ammonium while expressing mutant TaAMT1s (TaAMT1;1C & TaAMT1;2C).

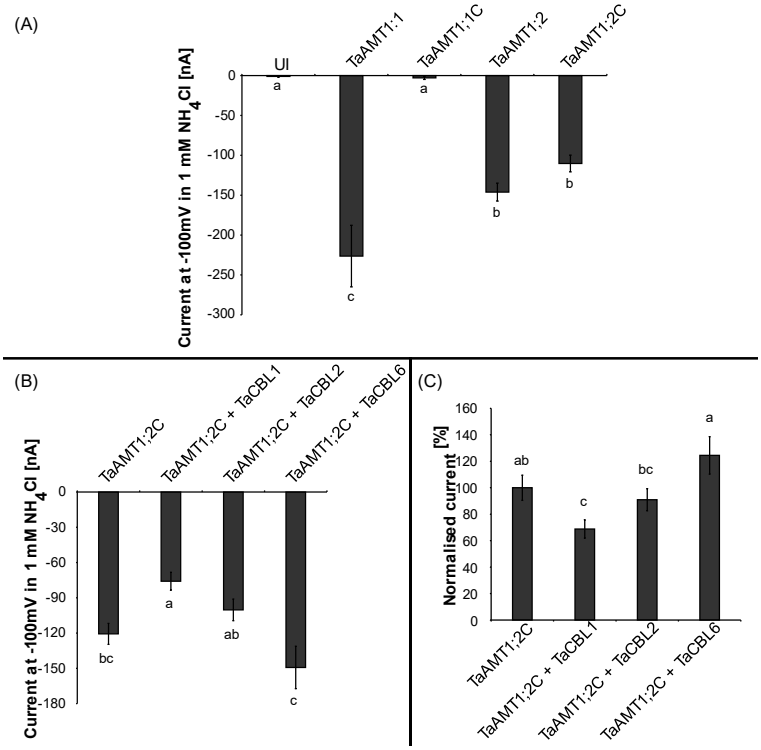

Figure 49. Ammonium transport activity of mutant TaAMT1s in Oocytes. (A) Ammonium induced current of wild type TaAMT1s and their mutants (TaAMT1;1C & TaAMT1;2C). (B) Regulatory action of candidate TaCBLs on TaAMT1;2C. (C) Normalized ammonium induced current of the Regulatory action of candidate TaCBLs on TaAMT1;2C. Error bars showing standard error of the mean (n = 8 to 14). Letters indicated statistical significance at p≤0.05.

Nonetheless, TaCBL1 was still able to cause a reduction in the ammonium induced current of the TaAMT1;2C in a manner similar to the effect of TaCBL1 on the TaAMT1;2. However, the regulatory action of TaCBL2 and TaCBL6 on TaAMT1;2 was lost, as both TaCBLs could not

reduce the ammonium induced current of TaAMT1;2C (Fig. 49). It is possible that the deletion of the C-terminus of TaAMT1;2 had remove the binding site and/or the ability of TaCBL2 and TaCBL6 to successfully bind to the C-terminus of TaAMT1;2C. Since CBLs are known to lack kinase activity (as they as typical calcium sensors), this unexpected discovery raised the question as to whether the presence of a phosphorylating candidate TaCIPK protein would result in a further decrease in the ammonium uptake activity of the two high affinity ammonium transporters.

3.12. EFFECTS OF THE CO-EXPRESSION OF CANDIDATE TaCBL AND TaCIPK PROTEINS ON TaAMT1s IN OOCYTES

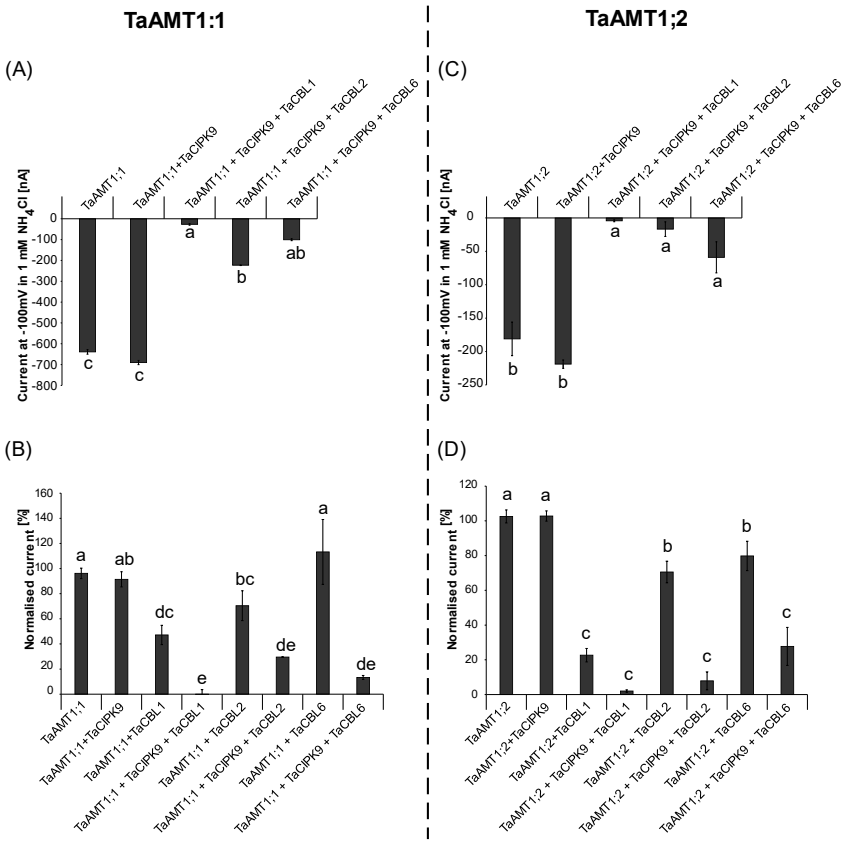

Figure 50. Co-expression of candidate TaCBL, TaCIPK, and TaAMT1s in Oocytes. (A.) Ammonium induced current of the effect of co-expressing TaCIPK9 and the candidate TaCBLs (TaCBL1, TaCBL2, and TaCBL6) on TaAMT1;1 (B.) Normalised ammonium induced current of the effect of co-expressing TaCIPK9 and the candidate TaCBLs (TaCBL1, TaCBL2, and TaCBL6) on TaAMT1;1 (C.) Ammonium induced current of the effect of co-expressing TaCIPK9 and the candidate TaCBLs (TaCBL1, TaCBL2, and TaCBL6) on TaAMT1;2 (D.) Normalised ammonium induced current of the effect of co-expressing TaCIPK9 and the candidate TaCBLs (TaCBL1, TaCBL2, and TaCBL6) on TaAMT1;2. Error bars showing standard error of the mean (n= 4 to 6). Letters indicated statistical significance at p≤0.05.

TaCIPK9 could not independently regulate the activity of TaAMT1;1 and TaAMT1;2 (Fig. 50A), however, it interacted with TaCBL1, TaCBL2 and TaCBL6 to cause a further reduction in the ammonium uptake induced current in TaAMT1;1 (Fig. 50B) in a way that was more than the effects of the individual candidate TaCBLs on the transporter. It is worthy to note that TaCBL6 on its own also does not affect the ammonium transport activity of TaAMT1;1(Fig. 46A), yet the presence of TaCBl6 and TaCIPK9 reduced the activity of TaAMT1;1 by up to 80%; thereby suggesting the formation of a highly functional CBL-CIPK complex (Fig. 50B).

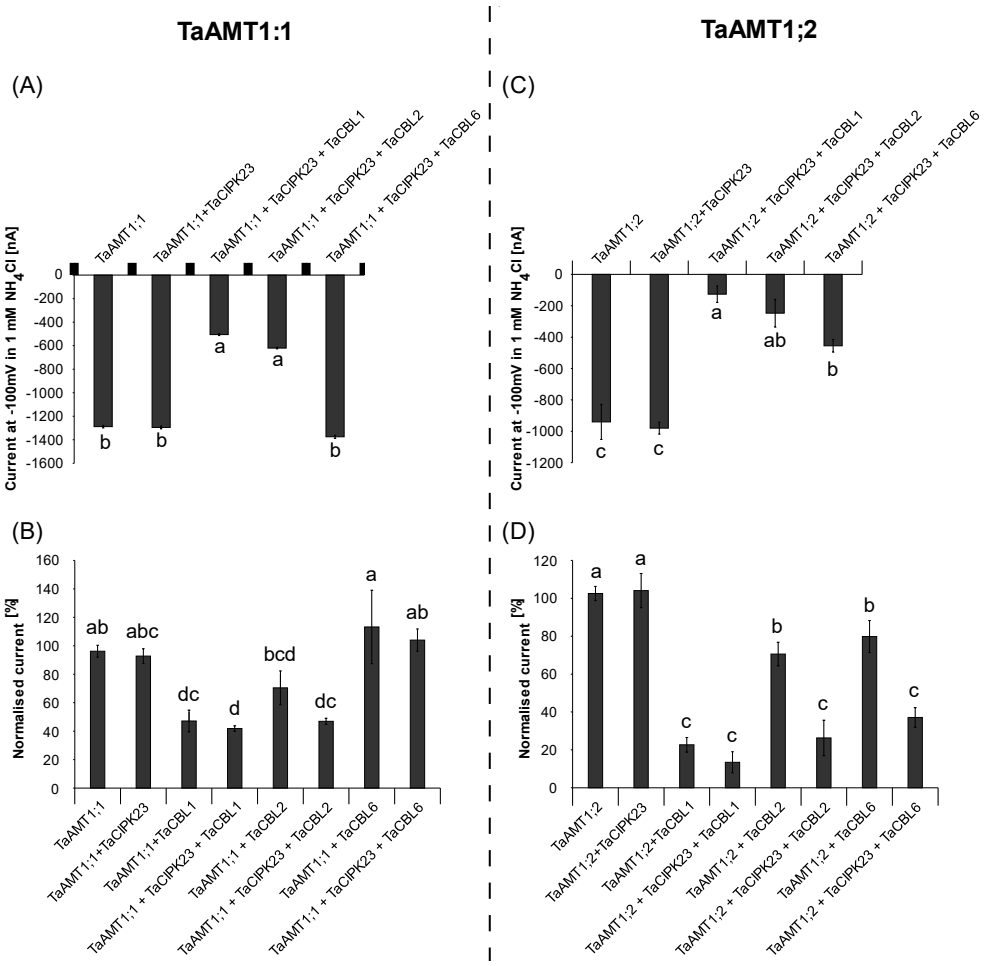

Figure 51. Co-expression of candidate TaCBL, TaCIPK, and TaAMT1s in Oocytes. (A.) Ammonium induced current of the effect of co-expressing TaCIPK23 and the candidate TaCBLs (TaCBL1, TaCBL2, and TaCBL6) on TaAMT1;1 (B.) Normalised ammonium induced current of the effect of co-expressing TaCIPK23 and the candidate TaCBLs (TaCBL1, TaCBL2, and TaCBL6) on TaAMT1;1 (C.) Ammonium induced current of the effect of co-expressing TaCIPK23 and the candidate TaCBLs (TaCBL1, TaCBL2, and TaCBL6) on TaAMT1;2 (D.) Normalised ammonium induced current of the effect of co-expressing TaCIPK23 and the candidate TaCBLs (TaCBL1, TaCBL2, and TaCBL6) on TaAMT1;2. Error bars showing standard error of the mean (n = 4 to 5). Letters indicated statistical significance at p≤0.05.

The co-expression of TaCIPK23 with TaAMT1;1, as well as with TaAMT1;2 did not affect the activity of both transporters (Fig. 51A). Unlike for TaCIPK9, TaCIPK23 appeared incapable of regulating TaAMT1;1, as the presence of TaCBL1, TaCBL2, and TaCBL6 did not cause any further reduction in the activity of the TaAMT1;1 transporter (compared to the reduction already conferred by the single TaCBLs) (Fig. 51B).

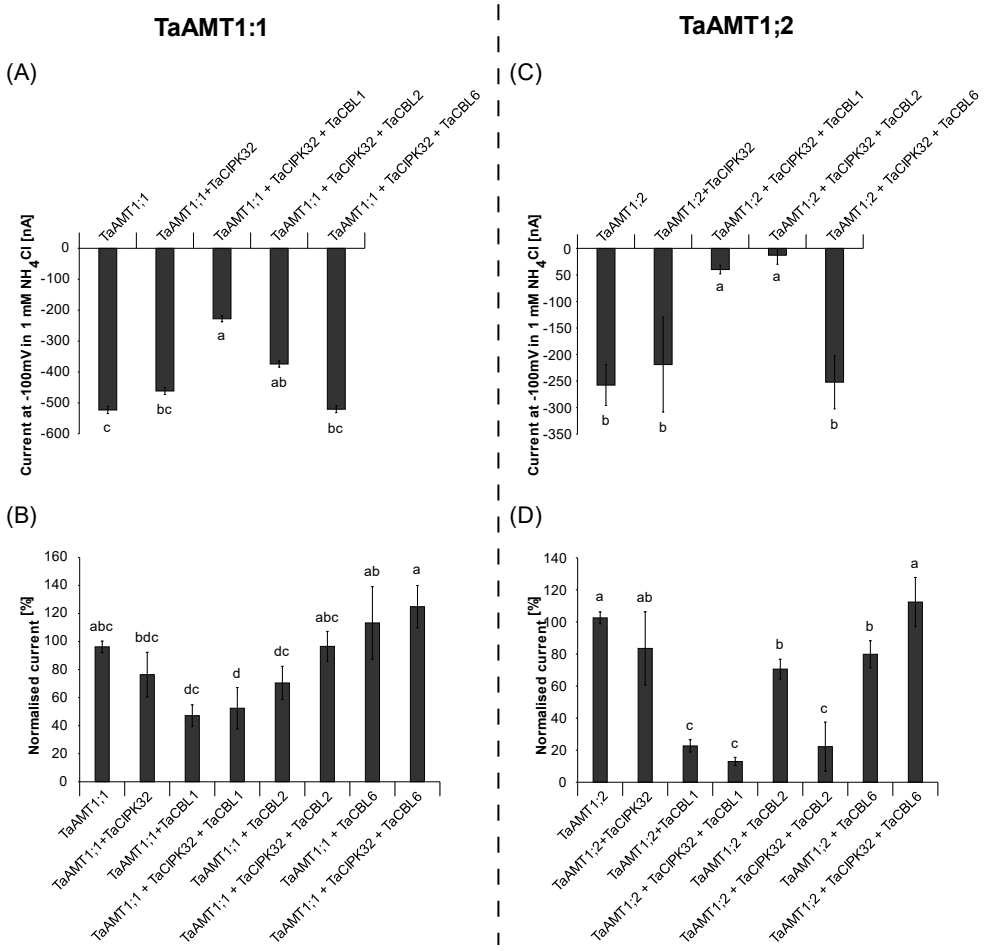

Figure 52. Co-expression of candidate TaCBL, TaCIPK, and TaAMT1s in Oocytes. (A.) Ammonium induced current of the effect of co-expressing TaCIPK32 and the candidate TaCBLs (TaCBL1, TaCBL2, and TaCBL6) on TaAMT1;1 (B.) Normalised ammonium induced current of the effect of co-expressing TaCIPK32 and the candidate TaCBLs (TaCBL1, TaCBL2, and TaCBL6) on TaAMT1;1 (C.) Ammonium induced current of the effect of co-expression TaCIPK32 and the candidate TaCBLs (TaCBL1, TaCBL2, and TaCBL6 on TaAMT1;2 (D.) Normalised ammonium induced current of the effect of co-expressing TaCIPK32 and the candidate TaCBLs (TaCBL1, TaCBL2, and TaCBL6) on TaAMT1;2. Error bars showing standard error of the mean (n= 4 to 14). Letters indicated statistical significance at p≤0.05

Albeit TaCIPK23 was able to cause a further reduction in the activity of TaAMT1;2 in the presence of TaCBL2 (compared to the effects of only TaCBl2), and TaCBL6 (compared to the effects of only TaCBL6) (Fig. 51D). Also, there was no further reduction of the activity of

TaAMT1;2 in the presence of TaCBL1 and TaCIPK23 (compared to the effects of only TaCBL1), which might also be due to the huge significant decrease in ammonium transport activity of TaAMT1;2 already caused by the TaCBL1 alone.

The co-expression of TaCIPK32 with the TaAMT1s of wheat also failed to produce any effect (Fig. 52A & C), as the ammonium induced current triggered in the oocytes was like that of the wild type transporters. TaCIPK32 also showed no significant effect on TaAMT1;1 in the presence of the candidate TaCBLs (TaCBL1, TaCBL2, and TaCBL6), when compared to the effects already conferred by the TaCBLs on their own (Fig. 52B). Nevertheless, TaCIPK32 appear to form a complex with TaCBL2, which was capable of further reducing the activity of TaAMT1;2 (compared to the effect of only TaCBL2). In the presence of TaCBL6 however, TaCIPK32 was able to reverse the observed regulatory effect of (just) TaCBL6 (Fig. 46B) on TaMT1;2 (Fig. 52D).

3.13. INVESTIGATION OF POSSIBLE PROTEIN-PROTEIN INTERACTIONS USING THE SPLIT YELLOW FLUORESCENCE PROTEINS (YFP)

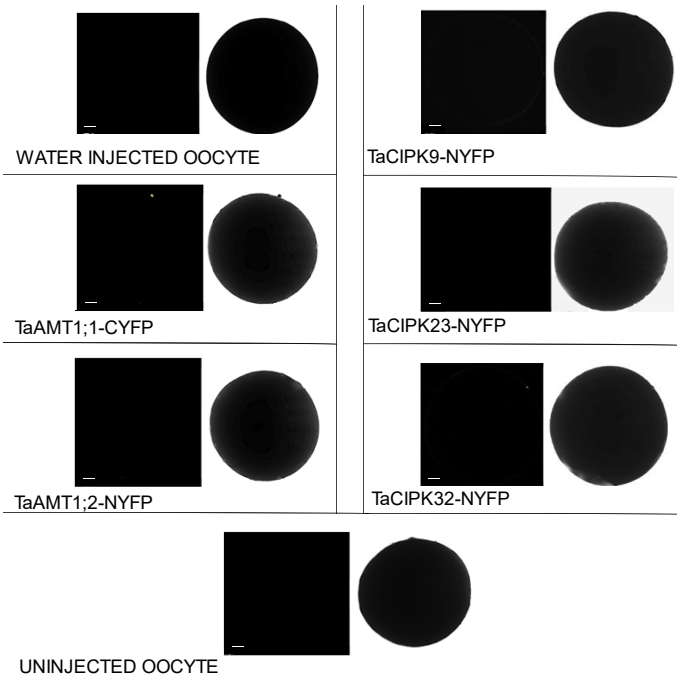

Figure 53. Split fragments of the yellow fluoresce (YFP) proteins showed no fluorescence (in Oocyte) with the Bimolecular Fluorescence complementation assay. Oocytes were viewed under the laser scanning confocal microscope. White line represents 100 µm.

To further gain insight into the role of the candidate TaCBLs on the candidate TaCIPKs in the regulation of TaAMT1;1 and TaAMT1;2, the split YFP (yellow fluorescent protein) assay was

utilized. The N terminal part of the YFP protein was fused to the candidate TaCIPKs, while the C-terminal end of the YFP protein was fused to the C-terminal end of the ammonium transporters (TaAMT1;1 and TaAMT1;2). Since the ammonium transporters are plasma membrane localized, it was expected that the successful binding of the TaCBLs to the TaCIPK (during activation) will activate and TaCIPKs, therefore allowing for the interaction of the candidate TaCIPK proteins and the TaAMTs, which should lead to the reconstitution of the YFP molecule.

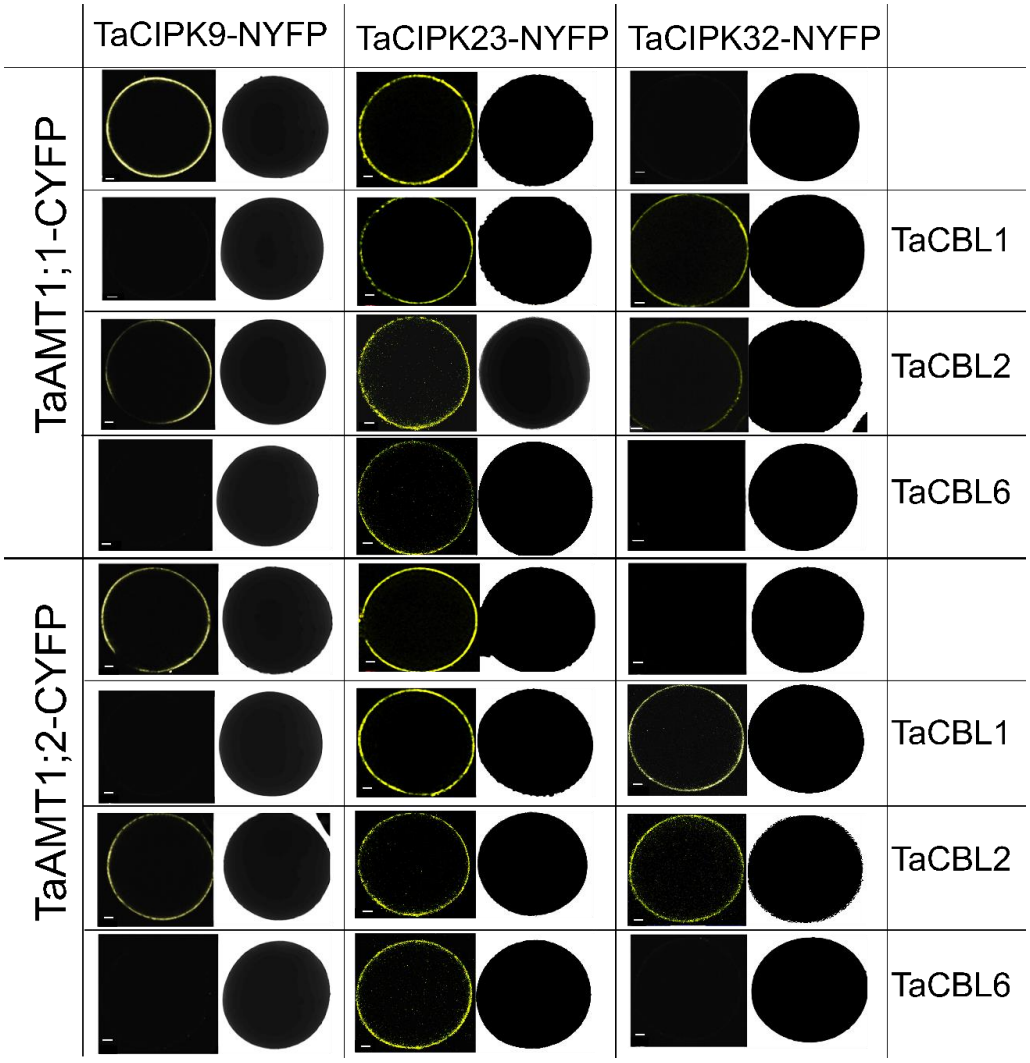

Figure 54. Investigation of the potential role of candidate TaCBLs (TaCBL1, TaCBL2, and TaCBL6) in the interaction of candidate TaCIPKs (TaCIPK9, TaCIPK23, and TaCIPK32) and TaAMT1s in oocytes. White line represents 100 µm.

The individual splitted fragments of the yellow fluoresce (YFP) proteins showed no fluorescence (in oocyte) with the Bimolecular Fluorescence complementation assay (Fig. 53). Nonetheless, the results showed that TaCIPK9 can independently interact with TaAMT1;1 and TaAMT1;2 (Fig. 54). Albeit this interaction was inhibited by the TaCBL2 and TaCBL6 (Fig.

54). TaCIPK23 was also able to interact independently with TaAMT1;1 and TaAMT1;2, while also maintaining the interaction in the presence of the candidate TaCBLs (TaCBL1, TaCBL2, and TaCBL6) (Fig. 54). Although TaCIPK32 was not able to independently form an observable interaction with the TaAMT1s of wheat, the presence of TaCBL1 and TaCBL2 was able to trigger the interaction of TaCIPK32 with both TaAMT1;1 and TAMT1;2 respectively. (Fig. 54)

Further investigation with the TaAMT1 mutants with a deleted C-terminus (bimolecular fluorescence complementation assay: with the Split YFP) showed no interaction between the wild type TaAMT1s and the candidate TaCBls. Also, there was no interaction between TaCBLs and the mutant TaAMT1s (TaAMT1;1C and TaAMT1;2C) (Fig. 55).

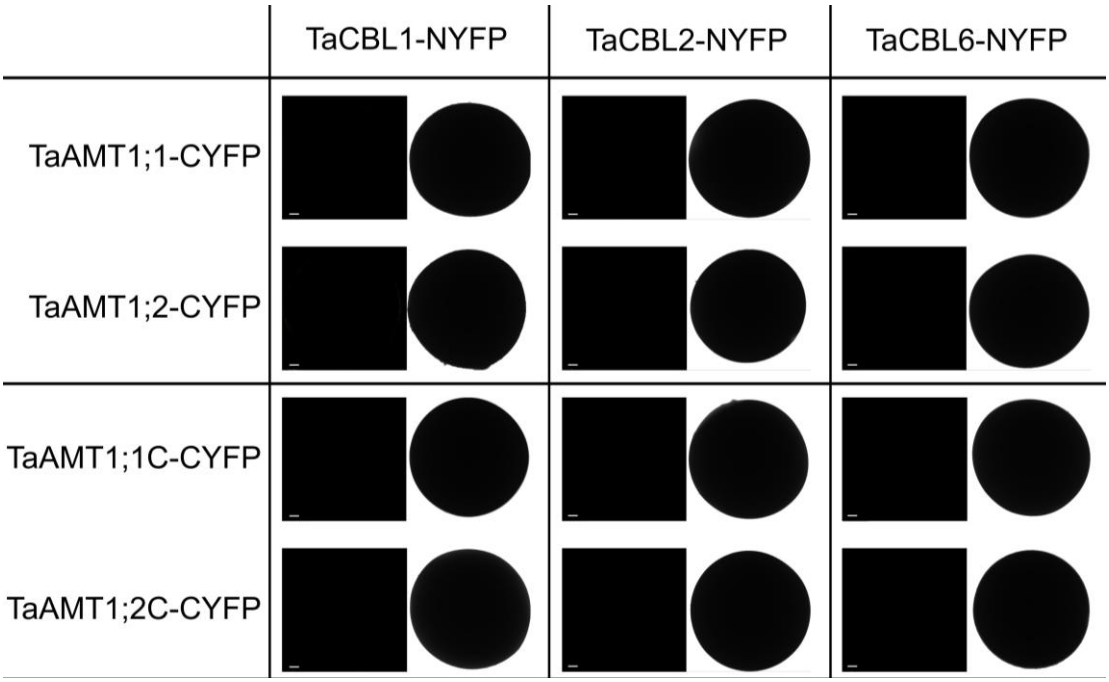

Figure 55. Investigation of the possible interaction between TaAMT1s (TaAMT1;1 & TaAMT1;2), mutant TaAMT1s (TaAMT1;1C-CYFP & TaAMT1;2C-CYP) and candidates TaCBL proteins. There was no visible yellow fluorescence indicative of a possible interaction between TaAMT1s, and Candidate TaCBLs. There was also no visible yellow fluorescence indicative of a possible interaction between mutant TaAMT1s, and Candidate TaCBLs. White line represents 100 µm.

4. DISCUSSION

4.1.NITROGEN SOURCE PREFERENCE IN WINTER WHEAT

Climatic and edaphic factors highly influence the variability in the nitrogen concentration of soil solution (Glass et al. 2002). Since these factors are well beyond the control of plants, the need to effectively respond to the constant changes in soil nitrogen concentration becomes imperative. Despite the potential for ammonium toxicity, the preference of several plants for ammonium over nitrate is widely documented (Boudsocq et al. 2012; Brian Gordon Forde, and David T. Clarkson 1999; Britto and Kronzucker 2013; Sarasketa et al. 2016). Toxicity is the major limitation in the consideration of ammonium as a reliable nitrogen fertilizer, as a concentration of just 1 mM is enough trigger toxicity in some species (Hachiya et al. 2012). Interestingly, the increase in N fertilization of several agricultural field has resulted in a situation where ammonium concentration could be up to 20 mM in highly fertilised agroecosystems (Britto and Kronzucker 2002). While most of the ammonium could be easily nitrified, the temporal effect of the high ammonium concentration could still be a problem to ammonium sensitive plants. Therefore, effort was made to investigate the performance of wheat seedlings under different nitrogen sources.

The ability of the wheat seedlings to produce a similar dry shoot biomass in the sole ammonium and the sole nitrate treatment showed that the young seedlings were able to manage the supplied 1 mM ammonium N in a way that at least minimises toxicity effects (Fig. 13A). The lack of difference (between the shoot biomass of the sole nitrate treatment and the sole ammonium treatment) was impressive, and was opposed to previous observation in Cucumber, where an exposure to 1 mM of sole ammonium caused a decreased in biomass compared to the sole nitrate treatment (Roosta and Schjoerring 2007). The decreased average root length of the sole ammonium treated plants (compare to the sole nitrate treatment) on the other hand pointed to a strategy aimed at reducing the spatial accessibility of the young plants to the supplied ammonium N (Fig. 13D), thereby reducing excessive ammonium N acquisition. Meanwhile, the supply of 1 mM ammonium have also been shown to reduce primary root growth, by decreasing both elemental expansion and cell production in *Arabidopsis thaliana* (Liu et al. 2013). It is noteworthy that while the accumulation of toxic concentrations of free ammonium /ammonia in plant tissues has also been tipped as a contributing factor to such decrease in root development (Findenegg 1987), the futile energy cost required to mitigate/manage the extreme NH_3/NH_4^+ levels in plant tissues (at elevated ammonium concentration) also

contribute significantly to the observed root growth inhibition associated with ammonium nutrition (Britto et al. 2001; Marino and Moran 2019).

Interestingly, total nitrogen content was similar in the sole ammonium treatment and the sole nitrate treatment (Fig. 14D). Albeit the shoot nitrogen concentration of the sole ammonium treatment was higher than in the sole nitrate treatment, despite both having similar shoot biomass yield (Fig. 14B). This shows a higher N assimilation and a higher root to shoot mobilization of ammonium N in the sole ammonium treatment compared to the sole nitrate treatment. The sole ammonium treatment however had a lower root length and a lower root biomass compare to the sole nitrate treatment (Fig. 13B&D). Nitrate is a known stimulator of lateral root development and a mitigator of ammonium toxicity (Hachiya et al. 2012; Sun et al. 2017). It is therefore not surprising that the presence of nitrate in both the ammonium nitrate treatment as well as the sole nitrate treatment resulted in a higher root length as well as a higher dry root biomass yield (Fig. 13B, &D).

The importance of carbon for the long-distance transport of assimilated ammonium from the root to the shoot cannot be overemphasized (Coleto et al. 2019). This was reflected in the root and shoot carbon concentrations, which were similar for the sole ammonium and the sole nitrate treatment (Fig. 14A). Shoot biomass yield was also similar in the sole ammonium treatment and the sole nitrate treatment. Thus, even though 1 mM of sole ammonium decreased root growth rate (Fig. 13), it appeared to have no effect on the photosynthetic rate of the plants, due to the similarity in the shoot carbon concentration of the sole nitrate and the sole ammonium treatment (Fig. 14A). Also, the wheat seedlings were able to effectively mobilise more N to the shoot in the sole ammonium treatment than in the sole nitrate treatment (Fig. 14B). This could be partly explained by the lesser amount of energy required to assimilate ammonium N in plant roots compared to its nitrate counterpart (Bloom et al. 1992; Boudsocq et al. 2012; Britto and Kronzucker 2005, 2013; Howitt and Udvardi 2000; Kurimoto et al. 2004; Reisenauer 1978; Zhang et al. 2019a). Although, this phenomenon suggested that the wheat seedlings showed an increased ammonium uptake, increased assimilation rate, as well as an increased root to shoot N mobilization in the sole ammonium treatment (compared to the sole nitrate treatment), it also highlighted an N form preference by the plants. An earlier study had reported a higher net influx of ammonium, compared to nitrate in wheat roots supplied with ammonium nitrate (Zhong et al. 2014). Furthermore, sole ammonium treatment has also been associated with an increase in grain yield, improved processing quality parameters as well as an increase in grain storage proteins (GSPs), compared to sole nitrate treatments in wheat (Fuertes-Mendizábal et

al. 2013; Zheng et al. 2018). While the observed preference of ammonium over nitrate by plants have been associated with the lesser amount of energy required by plant in the assimilation of ammonium (compared to nitrate) (Bloom et al. 1992; Boudsocq et al. 2012; Britto and Kronzucker 2005, 2013; Howitt and Udvardi 2000; Kurimoto et al. 2004; Reisenauer 1978; Zhang et al. 2019a), it is interesting that the N form preferential tendencies of plants have also been found to be important for the establishment of a functional ecosystem (Boudsocq et al. 2012; Britto and Kronzucker 2013). Nevertheless, the supply of ammonium nitrate to the wheat seedlings still produced the highest shoot biomass, as well as the highest nitrogen content, of the N sources compared. Wheat therefore seem to have evolved over evolutionary time to uniquely manage ammonium N (compared to *Arabidopsis thaliana*). Hence, the possibility of an ammonium toxicity response that is different from that of *Arabidopsis thaliana* was anticipated in wheat.

4.2.AMMONIUM TOLERANCE OF WINTER WHEAT

Although the response of wheat to an elevated concentration of ammonium (10 mM) was robust, it was still reminiscent of the symptoms associated with ammonium toxicity (Britto and Kronzucker 2002; Esteban et al. 2016; Liu et al. 2013). Compared to the 1 mM treatment, an elevated concentration of ammonium (10 mM) caused a drastic decrease in dry shoot biomass, dry root biomass and average total root length (Fig. 15A, B, & D). It also caused a decrease in fine root development, as well as a slightly higher development of roots with higher diameter (Fig. 15E). Even though the detailed understanding of the physiological and molecular mechanisms behind ammonium toxicity still remain elusive, it is believed that ammonium inhibits root growth and gravitropism via a largely distinct pathways (Liu et al. 2013). Thus, the need for an appropriate ammonium sensing system, that takes place at multiple steps along its transport, storage, and assimilation pathways is necessary for an effective ammonium N utilization (Liu and Wirén 2017). Plants typically respond to ammonium N by altering their root system developmental plan via the interpretation of systemic signals that are generated by changes in their nutritional status (Rogato et al. 2010). It was therefore interesting to see the wheat seedlings increase their root development at conditions of little to no nitrogen (-N, 0.1 mM), while also significantly decreasing root proliferation as ammonium increase to 1mM (Fig. 15B, &D). Albeit there was a further decrease in root system development as ammonium concentration becomes extremely elevated (10 mM) (Fig. 15B, &D).

The external application of ammonium is known to rapidly increase cellular $NH4^+$ concentration (Kronzucker et al. 1998; Li et al. 2017). Consequently, the total nitrogen concentration of the wheat plants expectedly increased in the root and shoot as the concentration of supplied ammonium increased from starvation (-N) to 10 mM (Fig. 16B). Total nitrogen content also increased significantly as ammonium concentration increased, but decreased slightly at the 10 mM treatment, due to the lower total biomass yield of the plants treated with 10 mM of ammonium (Fig. 16D).

Meanwhile, shoot carbon concentration was also slightly higher for the 1mM treatment and the 10 mM treatment, than for the nitrogen starvation treatment (-N) and the nitrogen deficiency treatment (0.1 mM) (Fig. 16A). This suggests a slightly higher photosynthetic rate. This would be expected if the wheat plants responded effectively to the supplied ammonium N. It therefore implies that the wheat plants demonstrated the presence of an ammonium sensing system that is ready to provide the carbon skeleton required for the shoot mobilization of the assimilated ammonium N. This was not an isolated observation, as an experiment comparing different nitrogen sources in this work (3.1, & 4.1) showed an increased shoot N concentration for the sole ammonium treatment, compared to the sole nitrate treatment, despite both having similar shoot biomass (Fig. 14B).

Exogenous NH_4^+ (in the root medium) only reaches plant leaves after saturating the storage capacity of the plant root system (Esteban et al. 2016). Thus, the energy cost of the long distance transport of ammonium as well the energy cost of the futile ammonium cycling process (already associated conditions of elevated ammonium concentration in plants) (Britto et al. 2001) is expected to exert significant energy demand on the plant roots cells, especially at extreme concentration of ammonium N exposure. 30% of the absorbed N is known to be translocated to the shoots within minutes of plants exposure to 0.1 mM ammonium (Kronzucker et al. 1998). Since carbon metabolism remained a prerequisite for the supply of the energy needed for long distance ammonium transport (Coleto et al. 2019), it was therefore not surprising that root carbon concentration declined (from the -N treatment) as ammonium was supplied to the plants (Fig. 16A).

The decrease in the root and shoot biomass of the 10 mM treatment (compared to the 1mM treatment) (Fig 15A, &B), but not the shoot and root nitrogen concentration (Fig. 16B), showed that the wheat seedlings continued to take up ammonium despite the decreased biomass. The failure of the plants to avoid ammonium uptake at elevated ammonium concentration (10 mM) was reminiscent of an ammonium sensitive plant like barley, which accumulated cytosolic ammonium beyond its ammonium management capabilities (Britto and Kronzucker 2002).

Rice by contrast, seemed to have evolved a cellular defence strategy that is able to withstand the accumulation of extreme ammonium concentrations in its cytosol (Britto and Kronzucker 2002), while also being able to reduce energy wastage when $NH4^+$ is supplied (Britto et al. 2001). Less adapted species (like wheat) seems susceptible to enhanced lipid peroxidation and higher activity of scavenging enzymes under ammonium N nutrition, which is an indication of a metabolic pathways with stronger radical formation (Zhu et al. 2000). Nevertheless, the major cause of N form-dependent stress sensitivity is still believed to be in the coupling between photosynthesis and respiration (Zhu et al. 2000). Hence, despite the ability of the wheat seedlings to effectively manage 1 mM of ammonium N, its ammonium coping mechanism seemed overpowered by the 10 mM ammonium exposure, resulting in typical ammonium toxicity symptoms in the form of a reduced shoot and root biomass, reduced root elongation, and a reduced formation of fine roots.

4.3.pH EFFECT ON AMMONIUM USAGE AND TOXICITY

Ammonium fed plants are known to actively release protons into the rhizosphere as ammonium is taken up. The deprotonation of ammonium as it is being taken up across the plasma membrane (Ganz et al. 2020; Ishikita and Knapp 2007) imposes a proton burden on the plants cellular machinery, thereby necessitating the extrusion of excess proton out of the cytosol. Continuous unchecked proton extrusion into the rhizosphere could lead to the creation of an unhealthy acidic condition. Rhizospheric (soil) pH is important for nutrient acquisition, nutrient availability, crop growth, crop development, establishment of important microbial communities, and the establishment of alien plants (Gentili et al. 2018; Yan et al. 2019; Zhang et al. 2019b; Zhao et al. 2018).

Thus, the effects of different rhizosphere pH on the response of wheat seedlings to a relatively tolerable concentration of ammonium of 1 mM, and an elevated concentration of 10 mM was investigated. Toxicity was particularly more severe for the 10 mM treatment at a pH of 8, as the root elongation (average root length) was significantly repressed (Fig. 17D). The formation of free ammonia at elevated pH (Findenegg 1987) would have suggested the influx of free ammonia (closer to the pKa value of ammonium: 9.25), which could have resulted in the accumulation of toxic ammonia in plants tissues. However, the high ratio between net ammonium extrusion and net ammonium uptake observed at pH 8 (Dyhr-Jensen and Brix 1996) suggested that this might not be the case (Britto and Kronzucker 2002). In fact, barley, a relative of wheat, displayed an increased efflux of ammonia against concentration gradients, with

NH_3/NH_4^+ efflux consisting of about 80% of the primary influx (Britto et al. 2001). Hence, the resultant toxic effect of ammonium supply seem to be from ammonium accumulation rather than ammonia influx (Britto and Kronzucker 2002).

The wheat seedlings responded to the pH effects in a concentration dependent manner. The dry root biomass of the 1 mM treatment increased as the pH tended towards alkalinity, while the dry shoot biomass of the 10 mM treatment increased as pH become more alkaline (Fig. 17A & B). The plants therefore favoured root development in the 1 mM treatment as pH tends towards alkalinity; an effort that is bound to facilitate more ammonium N acquisition. The strategy however shifted to shoot development in the 10 mM treatment as pH tends towards alkalinity, showing that the plants favoured the development of more shoot sink for the assimilated ammonium N in this regard (Fig. 17A).

Interestingly, total nitrogen content increased for the 1mM and the 10mM as the pH become more alkaline (Fig. 18D). However, the root nitrogen concentration of the 10 mM treatments, was highest at pH 7 and 8, while that of the 1 mM treatment was relatively unchanged (Fig. 18B). Alkaline pH therefore seems to have triggered an increased ammonium uptake rate in the plants. Yet, despite the dynamic nature of plants response to pH differences, the ammonium taken up at the pH of 5, 6, 7 and 8 appeared to be effectively mobilized to the shoot in the 1 mM treatment (Fig. 17B). This was not the case for the 10 mM treatment as the nitrogen saturation of the shoot seemed to have been attained as pH became more alkaline. Hence, shoot N mobilization was impeded/reduced at pH 7 and 8 for the 10mM treatment, leading to the accumulation of nitrogen in the root (Fig. 18B). Since ammonium accumulation is a known trigger of ammonium toxicity (Britto and Kronzucker 2002; Findenegg 1987), the increased toxicity effects of the 10 mM treatment at pH 8 (in the form of root elongation repression (Fig. 17D)) is attributed to excessive ammonium N accumulation in the root of the wheat plants.

Nevertheless, the highest shoot biomass was still recorded for the 10 mM treatment at a pH of 8 (Fig. 17A), showing that the plants exhibited a higher growth rate and development under this condition before the onset of toxicity. It is noteworthy that the highest total nitrogen content was recorded for both the 1mM and the 10 mM at an alkaline pH of 8 (Fig. 18D). It was therefore fascinating that to cope with the increase in the ammonium uptake rate caused by an alkaline rhizospheric pH of 8, the wheat plants opted for a strategy that involved a decreased root length at elevated ammonium concentration (10 mM) and an increased root elongation at a more favorable concentration of 1 mM (Fig. 17D). In fact, the plants also increased shoot biomass at elevated concentration (10 mM) at pH 8 (Fig. 17A). It is noteworthy that the highest

total nitrogen content was recorded for both the 1mM and the 10mM treatment at pH 8. Thus, an increase in ammonium uptake rate at an alkaline pH, which existed regardless of the concentration of ammonium supplied is postulated.

4.4.QUANTIFICATION OF TaAMT1 TRANSCRIPTS WITH qRT-PCR

Plant ammonium uptake is via membrane localized ammonium transporters. Additively, two high affinity ammonium transporters of *Arabidopsis thaliana* have been shown to be responsible for up to 70% of the plants ammonium uptake under condition of limited N supply (Loqué et al. 2006). This highlights the important position occupied by the high affinity ammonium transporters of plants, especially in the mitigation of ammonium toxicity. Thus, the response of the high affinity ammonium transporters of wheat to ammonium nutrition was investigated so as to understand their transient response to elevated ammonium supply.

The transcripts of both TaAMT1;1 and TaAMT1;2 increased in response to 1 mM ammonium supply after six hours (6h) (Fig. 22A, &B). This increase was sustained after a transient ammonium shock was imposed on the plants (by transferring them to a 1 mM treatment and a 10 mM treatment for a further 30 minutes (6h+30min)) (Fig. 22A, & 22B).

High affinity ammonium transporters are supposed to be responsible for plants ammonium uptake (in the net $NH4^+$ form) under conditions of little to no nitrogen and downregulated in condition of nitrogen availability (Gazzarrini et al. 1999; Shelden et al. 2001; Sohlenkamp et al. 2000). Although, there was still a slight decrease in the TaAMT1s transcripts after two hours (6h+2h), it was only to the level with the N starvation treatment (Fig. 22A, &B). This is similar to previously observed phenomenon in maize and rice, where ammonium had triggered the upregulation of OsAMT1;2 of rice and the AMT1s of Maize (Gu et al. 2013; Sonoda et al. 2003).

Meanwhile, the ammonium shock of an extremely high concentration of 50 mM was able to transiently downregulate the transcription of the TaAMT1s after 30 min (6h+30min), albeit this observed downregulation was still reversed after two hour of 50 mM ammonium exposure (Fig. 22A, &B). It was therefore inferred that the inability of the wheat seedlings to effectively downregulate the expression of their high affinity ammonium transporters (at ammonium concentration that trigger toxicity symptoms) represent a major weakness in wheat's ammonium uptake and regulation strategy.

4.5.FUNCTIONAL CHARACTERIZATION OF WHEAT TaAMT1s

Prior to proteomics investigation, the functional characterization of the high affinity ammonium transporters was carried out. TaAMT1;1 and TaAMT1;2 showed significant ammonium transporting activities in the Oocytes of *Xenopus laevis* (Fig. 23B). Both transporters also conferred ammonium uptake ability in a yeast strain lacking endogenous ammonium transporters (Fig. 23A). In oocytes however, the ammonium induced influx of positive charges indicated that NH_3 coupled with H^+ ($NH_3 + H^+$) was transported by the TaAMT1s (Fig. 23B). Like for the AMT1s of other plants (Bindel and Neuhäuser 2019; Straub et al. 2014) these currents also saturated with a high affinity in the µM range (Fig.23D), cementing their role as typical high affinity ammonium transporters. Also, the proteins displayed an affinity that was membrane potential dependent. The computed fractional electrical distance showed that ammonium ion had only passed 35% of the membrane electric field before the rate limiting binding to the protein (Fig. 23C). These characteristics were similar to previous observation in plant AMT1s and therefore suggest the existence of the known deprotonation of ammonium by a twin His motif which is conserved in most AMT1 transporters (Ganz et al. 2020).

4.6.PROTEOMICS/PHOSPHOPROTEOMIC RESPONSE OF WHEAT AMT1s TO SOLE AMMONIUM NUTRITION

The overrepresentation test showed that the supply of ammonium effectively triggered several pathways (Fig. 25). “Stress” induced pathways were triggered, showing that the plants were able to sense a potentially stressful condition. The overrepresented “transport” pathway on the other hand was indicative of the active involvement of the plant cells in the movement of molecules and ions in and out of its cell. Pathways involving “mitochondria electron transport” as well as “amino acid metabolism” showed the plants made significant effort in trying to manage the supplied ammonium N, especially via the provision of cellular energy as well as the metabolism of the supplied ammonium N (Fig. 25). Pathways involving “redox reactions” were triggered in the 10 mM treatment after 30 min (6h+30) of ammonium exposure (Fig. 26D). A change in cellular reduction–oxidation (redox) status is known as one of the earliest responses of challenged cell (Dangl and Jones 2001; Matika and Loake 2014), while enhanced cellular oxidation is known to be important for the regulation of plant growth and stress responses (Considine and Foyer 2014). Interestingly, the presence of a metabolic pathways with stronger radical formation has long been associated with ammonium fed plants (Zhu et al.

2000). Hence, it was conceivable that the plant had triggered a redox reaction pathway that is required to deal with the formation of toxic radicals.

The increase in the transcripts of wheat's high affinity ammonium transporters (Fig. 22) suggested the consideration of the protein abundance of ammonium transporters. Interestingly, the abundance of proteotypic peptides of wheat ammonium transporters increased drastically as ammonium concentration became transiently elevated (Fig. 27). While this corroborated the observed result of the qRT-PCR investigation, it also showed that the transcripts were successfully translated into proteins.

Other cations transporters also responded to ammonium supply. In fact, the protein abundance of potassium transporters was also transiently increased at elevated ammonium concentrations (Fig. 28). AKT1, a particularly important potassium channel was also only detected in the 10 mM treatment (6h+30min), suggesting a readiness of the plants to increase potassium uptake (Fig. 28). Potassium has shown the ability to mitigate the effects of ammonium toxicity (Britto and Kronzucker 2002; Guo et al. 2019; Hernández-Gómez et al. 2015). Although the mechanism (of the action of potassium in mitigating ammonium toxicity) remains unclear, it is probably via a photosynthesis-dependent pathway, as both potassium and ammonium affect the photosynthetic process of plants in significant ways (Guo et al. 2007; Jin et al. 2011). This was further buttressed by the fact that the protein abundance of Nitrogen regulatory protein P-II also increased in response to elevated ammonium concentration. PII like signal transduction proteins, GlnK has been shown to regulate the ammonium transporter (AmtB) of *E. coli*, (Arcondeguy et al. 2001; Javelle et al. 2004). In plants however, PII are chloroplast localized (Ermilova et al. 2013; Hsieh et al. 1998; Huergo et al. 2013; Sugiyama et al. 2004) thereby suggesting that their role in the regulation of plants ammonium transporters might be through a photosynthesis dependent pathway. It is also interesting that rice, a cliché ammonium specialist increased its photosynthesis rate on ammonium supply, while the supply of potassium was also able to improve the photosynthetic rate of rice, as well as the growth of wheat under ammonium nutrition (Guo et al. 2007; Guo et al. 2019). Nonetheless, it should be noted that the role of PII in plants still require enormous investigation, even though its regulatory function had been shown in bacteria.

4.7. PHOSPHOMIMIC MUTANT OF THE CONSERVED THREONINE (T453) OF TaAMT1s IMPAIRS AMMONIUM TRANSPORT FUNCTIONS

Phosphorylation plays an important role in the cellular activity of eukaryotic organisms (Garcia-Garcia et al. 2016). It facilitates the reversible modulation of the activity of several proteins and enzymes (Ardito et al. 2017; Ohta et al. 2003; Poulsen et al. 2010). Hence, the detection of proteotypic phosphopetide of the two high affinity ammonium transporters (Fig. 30A&B), which were phosphorylated at the conserved threonine residue (T453): ISAEDEMAGMDLT(ph)R (TaAMT1;1), and ISAEDEMAGMDQT(ph)R (TaAMT1;2) under ammonium treatment was fascinating (Fig. 30). Earlier experiments with phosphomimic mutants of this particular conserved threonine was able to impair ammonium transport in plants such as Arabidopsis (Lanquar and Frommer 2010; Loqué et al. 2007; Neuhäuser et al. 2007; Wu et al. 2019), Marchantia (Guo et al. 2018b) and rice (Zhu et al. 2015). Likewise, the TaAMT1s phosphomimic mutants (TaAMT1;1(T_{453}D); and TaAMT1;2(T_{453}D) showed that the mutation had caused the inactivation of the ammonium transport function of both TaAMT1 transporters in a yeast strain lacking endogenous ammonium transporters (Fig. 32). Thus, phosphorylation of the conserved threonine T453 is essential for the regulation of the activity of the high affinity ammonium transporters of wheat. Although four additional C-terminus localized phosphopeptides were detected for TaAMT1;2 (Fig. 33), their role in the regulation of ammonium uptake is unknown. However, multiple phosphorylation site in the C-terminus of the AtAMT1;3 Arabidopsis have been shown to work together in fine-tuning ammonium uptake by the transporter (Wu et al. 2019). It is conceivable that a similar scheme of regulation exist for TaAMT1;2. Thus, it is believed that the phosphorylation of the other phosphopeptide residue of TaAMT1;2 (Fig. 33) could be involved in the integration of ammonium induced signals and/or the stabilization of its trimeric complex, which is hypothesized to further fine tune the transport activities of TaAMT1;2. Nonetheless, the phosphorylation of the conserved threonine T453 was able to inactivate the transport activity of both TaAMT1;1 and TaAMT1;2.

4.8. MISCELLANEOUS PHOSPHOPETIDE RESPONSE TO ELEVATED AMMONIUM CONCENTRATION

Further analysis of the phosphoenriched samples showed that the aquaporins also responded significantly to elevated ammonium concentrations (Table S 4 – S 9). Aquaporins are channel proteins which facilitate the passive diffusion of water, ammonia, arsenite, silicic acid, boron, antimonite, hydrogen peroxide and carbon dioxide across biological membranes (Di Perez Giorgio et al. 2014; Hove and Bhave 2011; Maurel et al. 2015; Verdoucq et al. 2014). They

are localised in the plasma membrane and the tonoplast (Ludevid et al. 1992). While they can facilitate the uptake of ammonium across the plasma membrane, their ability to facilitate the compartmentalization of ammonium in the vacuoles of root cells have also been postulated as an ammonium management strategy by plants; especially since the vacuoles could contain 100 times more ammonium than the cytosol (Bittsánszky et al., 2015). Aquaporins of the TIP subfamily (Tonoplast Intrinsic Proteins) in particular have also been suggested to facilitate the efficient vacuolar sequestration of ammonium ions (Kirscht et al. 2016; Litman et al. 2009). In this work, aquaporins specific phosphopeptides which are homologous of the *Arabidopsis thaliana* plasma membrane intrinsic proteins (AT3G53420.1, AT5G60660.1, AT2G16850, AT2G39010.1, AT4G00430, AT5G37820.1) responded to elevated ammonium supply (Table S 4 – S 9).

The phosphorylation of plants aquaporins is important for the regulation of their activity in several plant tissues (Azad et al. 2004; Daniels and Yeager 2019; Johansson et al. 1998; Maurel et al. 1995; Verdoucq et al. 2014). Phosphorylation has been shown to increase the water channel activity of the bean seed TIP3 of *Phaseolus vulgaris*, plasma membrane intrinsic proteins of Tulip petals, as well as the PM28A aquaporin of the leaf of Spinach (Azad et al. 2004; Daniels and Yeager 2019; Johansson et al. 1998; Maurel et al. 1995). Other analysis have also shown that multiple phosphorylation at strategic phosphorylation sites participate in the activation of alpha-TIP aquaporin (Maurel et al. 1995). It is therefore conceivable that wheat aquaporins and its phospho-regulation might be involved in the mitigation of ammonium toxicity in wheat, especially via a pathway that include water uptake regulation, and ammonium uptake regulation. Interestingly, there was an increase in phosphorylation, as well as a decrease in phosphorylation in certain amino acid residues (majorly serine S) of the aquaporins of wheat (Table S 4 – S 9). While the function of the phosphorylation of each amino acid residue will require further elucidation, it is possible that elevated ammonium concentration had triggered the active regulation of the water flux across the plasma membrane, as well as the possible aquaporin mediated ammonium flux in a phosphorylation dependent manner.

The decrease in the phosphorylation of a putative plasma membrane ATPase in the 1 mM (6h) treatment (relative to the N starvation treatment) was also observed (Table S 4). Plasma membrane ATPase of plants are protein which drives the active transport of nutrients by H^+-transport (Haruta et al. 2015; Serrano et al. 1986). They play a crucial role in the physiological processes that are crucial for plant growth and development (Falhof et al. 2016; Haruta et al.

2015; Serrano 1989; Zhang et al. 2017). The phosphorylation of plasma membrane ATPase in specific sites is also known to increase their activity (reviewed in (Falhof et al. 2016)). Thus, the reduced phosphorylation state of putative plasma membrane ATPAse (_GLDIDTINQNYT(ph)V_) in the 1 mM (6h) (Table S 4) treatment therefore suggested a decreased proton efflux activity. Coincidentally, the previous growth experiment had shown that the wheat plants were able to manage the 1 mM of ammonium supplied (4.1 & 4.2). Therefore, there seemed to be no need for extreme plasma membrane ATPase activity, as the acquired ammonium appeared to be successfully assimilated and shoot mobilised.

Similarly, the phosphorylation state of Glucose-6-phosphate dehydrogenase (G6PDH), which is known to catalyze the rate determining step of the pentose phosphate pathway (PPP), as well as play a key role in reductive biosynthesis and antioxidant defense (Dieni and Storey 2010; Lant and Storey 2011) was decreased (Table S 8). Its differential phosphorylation (G6PDH) has been associated with the alteration of its kinetic properties, while a decreased phosphorylation state has been associated with a decreased substrate affinity (Dieni and Storey 2010). However, 6-phosphofructokinase, which is a key enzyme in the glycolytic pathway was upregulated in response to elevate ammonium supply (Fig S 1). 6-phosphofructokinase is known to catalyze the phosphorylation of fructose-6-phosphate to fructose 1,6-bisphosphate (Raben et al. 1995; Wegener and Krause 2002), thereby aiding the successful continuum of the glycolytic pathway. It is noteworthy that the ultimate function of glycolysis is to oxidizes hexoses to generate ATP, reductant and pyruvate, while also producing the necessary building blocks for anabolism (Plaxton 1996). Interestingly, ATP generation is very necessary for the mitigation of ammonium toxicity in plants, especially since much energy is consumed in the futile ammonium cycling process, as well as during the long-distance transport of assimilated ammonium N. The decreased phosphorylation state of glucose-6-phosphate 1-dehydrogenase (_(ac)AGTDSSASSRQSS(ph)FNS(ph)LAK_) at elevated ammonium concentration, and the upregulation of 6-phosphofructokinase showed that the glycolytic pathway route via the activity of 6-phosphofructokinase was favoured at elevated ammonium concentration. In fact, there was also an increase in the protein abundance of phosphoenolpyruvate carboxylase (PEPc at elevated ammonium concentration (Fig. S 1). This make sense since Fructose 1,6-bisphosphate is an important regulator of Phosphoenolpyruvate carboxylase (PEPc). Phosphoenolpyruvate carboxylase (PEPc) catalyzes the irreversible β-carboxylation of Phosphoenolpyruvate in several metabolic events; which include the assimilation of atmospheric CO_2 in Crassulacean acid metabolism (CAM) plants, the balance of pH and ionic concentrations of leaf guard cells and root cortical cells, the production of carbon skeletons for

amino acid biosynthesis in all plants, and the host cell dicarboxylic acid formation in the root nodules of nitrogen fixing plants (Chollet et al. 1996; Monson 1999; O'Leary 1982). The ability of phosphoenol pyruvate carboxylase to provide the necessary carbon skeleton for ammonium assimilation as well as its increase in response to elevated ammonium concentration show its potential role in ammonium N metabolism. This was buttressed by the fact that the protein abundance of Asparagine synthetase, an important enzyme in the nitrogen assimilation pathway also increased drastically in response to elevated ammonium concentration (Fig. S 1). Asparagine synthetase assimilate nitrogen into asparagine; which is mainly utilized in nitrogen recycling, transport, and storage (Gaufichon et al. 2010). Bearing in mind that the nitrogen concentration of the plants supplied with 10 mM of ammonium N was significantly higher in the shoot and the roots of the plants in the growth experiment (Fig. 16B), it could be proposed that the wheat plant invested significant effort in the uptake, and assimilation of the supplied ammonium N, rather than actively prevent ammonium uptake at condition of ammonium toxicity.

Meanwhile, the protein abundance of Glutamate decarboxylase, an enzyme that catalyzes the synthesis of γ-aminobutyric acid (GABA) (Astegno et al. 2015) was downregulated at elevated ammonium concentration (Fig. S1). GABA is known to act as a buffering mechanism in C and N metabolism, in the regulation of cytosolic pH, in the protection of plants against oxidative stress (Bouché et al. 2003b; Crawford et al. 1994), as well as in intracellular signaling in response to stress stimuli (Astegno et al. 2015; Bouché et al. 2003a; Palanivelu et al. 2003; Roberts 2007). While the downregulation of Glutamate decarboxylase was an unexpected strategic approach by the plants at condition of elevated ammonium concentration, the wheat plant may have only exhibited a different strategy towards mitigating the accumulation of excess ammonium N, which is no doubt worth finding out.

4.9.CANDIDATE TaCBLs REGULATE TaAMT1s OF WHEAT IN THE OOCYTE OF *Xenopus laevis*

The presence of the phosphorylated peptide that were specific to the Threonine (T) 453 of TaAMT1s and the inability of the phosphomimic mutants of those peptides to transport ammonium solidified the notion that the phosphoregulation of ammonium transporters, which have been shown in other plants (Neuhäuser et al. 2007; Straub et al. 2014; Straub et al. 2017) also exist in wheat.

Calcineurin B like proteins (CBL), and the CBL-interacting Protein Kinases (CIPK) have been shown to regulate the ammonium transporters of *Arabidopsis thaliana* via the formation of and actively regulating CBL-CIPK complex (Straub et al. 2017). Interestingly, TaCBL1, and TaCBL2, were able to independently impair the ammonium transport activity of TaMT1;1 (Fig. 46A), while TaCBL1, TaCBL2, and TaCBL6 all impaired the activity of TaAMT1;2 (Fig. 46B) in oocyte. However, the regulatory activity of TaCBL1, a close homolog of AtCBL1 was the strongest on both transporters (Fig. 46A, & B). While the AtCBL1-AtCIPK23 complex was able to impair the ammonium transport activity of AtAMT1;2 of *Arabidopsis thaliana*, AtCBL1 was unable to independently impair its transport functions (Straub et al. 2017). CBLs are calcium sensors which lack a kinase domain. Thus, their regulatory action on the TaAMT1 transporters of wheat in this work was presumed to be via the direct binding of the TaCBLs to the regulatory cytoplasmic C-terminus of the wheat's AMT trimer. Such binding was anticipated to disrupts the integrity of the trimer, and as such, impair the activity of the transporters.

A comparison of the non-conserved C-terminal part of the AMT1s of *Arabidopsis thaliana* and the TaAMT1s of wheat showed an insertion in the C- terminal sequence of the TaAMT1s (Fig. 47). These insertions were conserved on the three homeologs of the transporters. Mutants generated by deleting this particular TaAMT1s C-terminal region (TaAMT1;1C & TaAMT1;2C) were still able to transport ammonium in a yeast strain lacking endogenous ammonium transporters (Fig. 48). However, their methylammonium transport ability was further decreased (Fig. 48). In Oocytes however, TaAMT1;1 mutant (TaAMT1;1C) was inactive (Fig. 49A). The ammonium induced current of TaAMT1;2C was similar to that of the wild type transporter (Fig 49A). This highlighted the importance of the C-terminus to the function of the transporters. In fact, the lack of the C-terminus in TaAMT1;2C was able to prevent the previously observed ability of TaCBL2 and TaCBL6 to regulate the ammonium transport activity of TaAMT1;2 (Fig. 46, 49B & 49C)). This confirmed the idea that the regulatory effect of TaCBL2 and TaCBL6 on the TaAMT1;2 (and Possibly TaAMT1;1) was via the deleted C-terminus mediated interaction of the TaAMT1s with TaCBLs (TaCB2 & TaCBL6). However, TaCBL1 was still able to reduce the ammonium transport activity of TaAMT1;2 despite the deletion of the non-conserved C-terminal part (Fig. 49B&C).

Further investigation of possible protein-protein interaction (with the split YFP assay) showed no visualization of a yellow fluorescence that is indicative of a direct interaction between the candidate TaCBLs and the TaAMT1s (Fig. 55). The dimerization of CBLs after the binding of

calcium to their EF-hands (Clapham 2007; DeFalco et al. 2009) might have altered their conformation, which could have prevented the reconstitution of the subunits of the YFP proteins (thereby preventing significant fluorescence formation). Nevertheless, the loss of the ability of TaCBL2, and TaCBL6 to regulate TaAMT1;2 after a mutation that involves the deletion of its C-terminus strongly indicated that the regulation of the TaAMT1s by the TaCBLs is via a C-terminus mediated interaction, and probably via the direct interaction of the TaCBL proteins with the C-terminus of the transporters.

4.10. TaCIPKs REGULATE TaAMT1s IN A TaCBL DEPENDENT MANNER

Although none of the candidate TaCIPK proteins could regulate the TaAMT1s on their own (Fig. 50, 51 & 52), TaCBL1, TaCBL2 and TaCBL6 interacted with TaCIK9 to further impair the ammonium transport activity of TaAMT1;1 i.e., the regulatory effect of the combination of the candidate TaCBLs (TaCBL1, TaCBL2, and TaCBL6) and TaCIPK9 (TaCBL1/2/6-TaCIPK9) was stronger than the impairment caused by the single TaCBLs proteins on the TaAMT1;1 transporter (Fig. 50A&B). It was therefore interesting that while TaCBL1, TaCBL2 and TaCBL6 could independently impair the ammonium transport activity of TaAMT1;1 (Fig. 46), their regulatory activity on TaAMT1;1 could be further enhanced by the presence of TaCIPK9. Only TaCBL2 and TaCBL6 were able to interact with TaCIK9 to impair the ammonium transport activity of TaAMT1;2 in a manner that was stronger than just the effect of the individual TaCBL (TaCBL2 or TaCBL6) on the transporter (Fig. 50C&D). This was indicative of the formation of a functional TaCBL-TaCIPK9 complex. Even though the presence of TaCBL1 and TaCIPK9 (TaCBL1-TaCIPK9) did not cause a further reduction in the ammonium induced current of TaAMT1;2 than what had already been caused by TaCBL1 (Fig 50C&D), this was attributed to the fact that TaCBL1 had already independently caused a whopping 80% reduction in the transporter activity of TaAMT1;2 (Fig. 50D). It is noteworthy that CIPK9 had been implicated in the regulation of several plant processes, such as the ammonium dependent root growth of rice (Xuan et al. 2019), the regulation of seed oil in *Brassica napus* L. (Guo et al. 2018a) as well as the regulation of low potassium response in *Arabidospsis thaliana* (Pandey et al. 2007). Additionally, it has also been shown to interact with CBL2/CBL3 to facilitate the vacuolar sequestration of magnesium in *Arabidopsis thaliana* (Tang et al. 2015). Therefore, its ability to participate in the regulation of the high affinity ammonium transporter of wheat was impressive.

The presence of both TaCIPK23 and TaCBL2 (TaCBL2-TaCIPK23) reduced the ammonium induced current of TaAMT1;2 in manner that was stronger that the effect of just TaCBL2 on TaAMT1;2 (Fig. 51D). Such was the case for TaCBL6, where the presence of TaCIPK23 and TaCBL6 (TaCBL6-TaCIPK23) also reduced the ammonium induced current of TaAMT1;2, more than the reductive effect of TaCBL6 on TaAMT1;2 (Fig 51D). However, the TaCBLs-TaCIPK23 combination did not have any effect on TaAMT1;1 as there was no difference between the effects of such combination and the single effect of the candidate TaCBLs on the TaAMT1;1 transporter (Fig. 51B).

Furthermore, the combination of TaCBL2 and TaCIPK32 reduced the ammonium induced current of TaAMT1;2 in a stronger fashion than the effect of just TaCBL2 on the transporter. However, while TaCBL6 have shown the capacity to be able to independently impair the ammonium transport activity of TaAMT1;2 (Fig. 46), the presence of the combination of TaCBL6 and TaCIPK32 reversed such effect (Fig. 52D).

CBL proteins are known to activate the CIPK proteins by binding to their NAF/FISL domain, thus the enhance regulatory action of the presence of candidate TaCBLs and TaCIPKs on the TaAMT1s (which was higher than that of the individual candidate TaCBLs in several cases) was indicative of a highly functional CBL-CIPK complex, that is effectively regulating the TaAMT1s. Such were the case for TaCBL1-TaCIPK9, TaCBL2-TaCIPK9 and TaCBL6-TaCIPK9 on TaAMT1;1, as well as for the effect of TaCBL2-TaCIPK9 and TaCBL6-TaCIPK9 on TaAMT1;2. It was also the case for the TaCBL2-TaCIPK23, TaCBL6-TaCIPK23, TaCBL2-TaCIPK32, and TaCBL6-TaCIPK32 on TaAMT1;2. In fact, the observation implied that, after the candidate TaCBL proteins had independently impaired the ammonium transporters (Fig. 46), phosphorylation of the transporters by an activated candidate TaCIPK protein (via a TaCBL-TaCIPK complex formation) caused a further reduction in ammonium induced current of the transporters. This was especially the case for TaCIPK9 (Fig. 50B&D). With respect to TaCIPK23 and TaAMT1;2, it was the case for the presence TaCBL2 and TaCBL6. TaCIPK32 on the other hand only exhibited this phenomenon with TaCBL2 on TaAMT1;2 (Fig. 52D). However, the ability of TaCIPK32 to prevent the previously observed ability of TaCBL6 to impair the ammonium transport activity of TaAMT1;2 (Fig. 46, Fig. 52D) deserves further investigation.

While the candidate TaCIPKs could not independently regulate the activity of the TaAMT1;1, and TaAMT1;2; TaCIPK9 and TaCIPK23 both interacted with the TaAMT1s independently

(Fig. 54). Nevertheless, the interaction of TaCIPK9 and the TaAMT1s was disrupted by TaCBL1 and TaCBL6 (Fig. 54). Since TaCIPK9 was also unable to regulate the activities of the TaAMT1s in the absence of the candidate TaCBLs proteins in oocytes, the binding of the TaCBL1 and the TaCBL6 to the ammonium transporters is postulated to have possibly prevented the expected reconstitution of the YFP protein. Alternatively, the binding of the TaCBL1 and TaCBL2 to the NAF domain of TaCIPK9 might have also change the conformation of the kinase (TaCIPK9 protein) in a manner that prevents the reconstitution of the YFP protein.

The interaction of TaCIPK32 with the TaAMT1s on the other hand was only possible in the presence of TaCBL1 and TaCBL2 (Fig. 54). In this case, TaCBL1 and TaCBL2 appeared to activate the TaCIPK32 kinase, while also recruiting the TaCIPK32 protein to the plasma membrane, where it could be able to interact with the TaAMT1s. It is worthy to note that TaCIPK32 was only able to cause a further reduction in the ammonium induced current of TaAMT1;2 in the presence of TaCBL2 (in a manner that was stronger than the reduction already caused by TaCBL2 on the transporter). It was also fascinating that it was able to prevent the ability of TaCBL6 to impair TaAMT1;2's ammonium transport activities (Fig. 46, Fig. 52D).

5. CONCLUSION

The ability of wheat to manage ammonium in the 1 mM range was impressive. However, 10 mM of ammonium chloride was still able to trigger ammonium related toxicity symptoms in the young wheat plants. Alkaline rhizospheric pH led to an increase in the ammonium uptake rate of the wheat seedlings, which led to a situation where toxicity became more severe at elevated ammonium concentration (10 mM). Although alkaline pH had also led to an increase in root development at an ammonium concentration of 1 mM ammonium, it caused the wheat seedlings to commit to an increase in shoot development at an elevated ammonium concentration (10 mM).

The response of the candidate ammonium transporters (TaAMT1;1 and TaAMT1;2) to ammonium supply was fascinating. Even though, the upregulation of the transporters (which were proven to be high affinity ammonium transporters, which transported ammonium in the Net "NH_4^+" form) was unexpected, it was similar to previous observation in rice and in maize (Gu et al. 2013; Sonoda et al. 2003), and it highlighted the eagerness of the wheat plant for nitrogen acquisition. However, this also indicate a weak link in the ammonium regulation strategy of the wheat plant. Therefore, While the response of wheat to ammonium could be considered robust, its inability to downregulate its high affinity ammonium transporter pose as a major setback. It was therefore fascinating that the phosphoproteomics study and the corresponding phosphomimic mutant were able to show that the wheat plants also favoured the phosphorylation of its high affinity ammonium transporter, as a means of regulation.

The wheat plant was able to recruit its CBL protein in the regulation of its ammonium uptake. TaCBL1, and TaCBL2 were able to regulate TaAMT1;1 while, TaCBL1, TaCBL2, and TaCBL6 all regulated the activity of TaAMT1;2. It is therefore postulated here that the TaCBL dependent regulation mechanism of the high affinity ammonium transporters of wheat is via the C-terminus mediated interaction of the TaAMT1s with the candidate TaCBLs. While the detailed elucidation of this mechanism will require further investigation, wheat seemed to have evolved to recruit its CBL proteins (which have been previously thought to be just calcium sensors) in the regulation of its high affinity ammonium transporters. Additionally, the TaCBL-TaCIPK complex was also demonstrated to participate in the phosphorylation mediated regulation of wheat's TaAMT1s in this work. Although AtCIPK23 was able to regulate the activities of the AtAMT1;2 of *Arabidopsis thaliana* in the presence of AtCBL1 (Straub et al. 2017), TaCIPK9 appeared to perform this leading role in wheat. This was demonstrated by the

ability of TaCIPK9 to effectively regulate the activities of TaAMT1;1 in the presence of TaCBL1, TaCBL2, and TaCBL6, as well as TaAMT1;2 in the presence of TaCBL2 and TaCBL6. TaCIPK9 therefore showed itself to be a major CIPK kinase that is involved in the regulation of the high affinity ammonium transporters of wheat. Its apparent ability to form an active complex with multiple TaCBLs showed its versatility, and a potential for a multifunctional complex formation. Meanwhile, TaCIPK23 and TaCIPK32 only seemed able to regulate the activity of TaAMT1;2 in the presence of TaCBL2 and TaCBL6. It is however noteworthy that TaAMT1;2 has the lower affinity for ammonium, of the two high affinity ammonium transporters (TaAMT1;1 and TaAMT1;2). Nevertheless, the ability of TaCIPK32 to prevent the previously observed ability of TaCBL6 to impair the ammonium transport activity of TaAMT1;2 (Fig. 46, Fig. 52D) deserves further investigation. Thus, the observed TaCBL mediated regulation of the high affinity ammonium transporters of wheat is believed to be complemented by the phosphorylation mediated regulation of wheat's high affinity ammonium transporters.

Hence, the ability of the wheat plant (Bob white) to adopt strategies that are different from previously observed mechanisms in *Arabidopsis thaliana* shows that the wheat plant is exhibiting an alternative ammonium management strategy. Its response to ammonium N was shown to include the phosphoregulation of its high affinity ammonium transporters in a manner that recruits the activity of its TaCBL, as well as the combined activity of its TaCBL and TaCIPK proteins (in a functionally regulating TaCBL-TaCIPK complex). TaCBL1, and TaCBL2 showed the ability independently regulate TaAMT1;1, while TaCBL1, TaCBL2 and TaCBL6, showed the ability to regulate TaAMT1;2. Such TaCBL mediated regulatory mechanism is postulated to be compensated by the Phosphorylation activity of candidate TaCIPK (e.g. TaCIPK9), which is/are believed to be activated by the TaCBLs. On the Other hand, TaCIPK23 and TaCIPK32 were only able to regulate TaAMT1;2 by interacting with TaCBL2 and TaCBL6.

6. REFERENCES

Aksoy MA, Beghin JC (eds) (2004) Global Agricultural Trade and Developing Countries. WHEAT: THE GLOBALMARKET, POLICIES, ANDPRIORITIES. The International Bank for Reconstruction and Development / The World Bank, Washington, D.C.

Albornoz F (2016) Crop responses to nitrogen overfertilization: A review. Scientia Horticulturae 205:79–83. https://doi.org/10.1016/j.scienta.2016.04.026

Albrecht V, Ritz O, Linder S, Harter K, Kudla J (2001) The NAF domain defines a novel protein-protein interaction module conserved in Ca2+-regulated kinases. The EMBO Journal 20:1051–1063. https://doi.org/10.1093/emboj/20.5.1051

Andrade SLA, Einsle O (2007) The Amt/Mep/Rh family of ammonium transport proteins. Mol Membr Biol 24:357–365. https://doi.org/10.1080/09687680701388423

Arcondeguy T, Jack R, Merrick M (2001) PII Signal Transduction Proteins, Pivotal Players in Microbial Nitrogen Control. Microbiology and Molecular Biology Reviews 65:80–105. https://doi.org/10.1128/MMBR.65.1.80-105.2001

Ardito F, Giuliani M, Perrone D, Troiano G, Lo Muzio L (2017) The crucial role of protein phosphorylation in cell signaling and its use as targeted therapy (Review). Int J Mol Med 40:271–280. https://doi.org/10.3892/ijmm.2017.3036

Arnold MH, Austin RB (eds) (1989) Plant Breeding and Yield Stability. Variability in Grain Yields: Implications for Agricultural Research and Policy. The Johns Hopkins University Press, Baltimore and London

Astegno A, Capitani G, Dominici P (2015) Functional roles of the hexamer organization of plant glutamate decarboxylase. Biochim Biophys Acta 1854:1229–1237. https://doi.org/10.1016/j.bbapap.2015.01.001

Austin RB, Bingham J, Blackwell RD, Evans LT, Ford MA, Morgan CL, Taylor M (1980) Genetic improvements in winter wheat yields since 1900 and associated physiological changes. J. Agric. Sci. 94:675–689. https://doi.org/10.1017/S0021859600028665

Azad AK, Sawa Y, Ishikawa T, Shibata H (2004) Phosphorylation of plasma membrane aquaporin regulates temperature-dependent opening of tulip petals. Plant and Cell Physiology 45:608–617. https://doi.org/10.1093/pcp/pch069

Bao A, Liang Z, Zhao Z, Cai H (2015) Overexpressing of OsAMT1-3, a High Affinity Ammonium Transporter Gene, Modifies Rice Growth and Carbon-Nitrogen Metabolic Status. Int J Mol Sci 16:9037–9063. https://doi.org/10.3390/ijms16059037

Barreto RF, Prado RM, Leal AJF, Troleis MJB, Junior GBS, Monteiro CC, Santos LCN, Carvalho RF (2016) Mitigation of ammonium toxicity by silicon in tomato depends on the ammonium concentration. Acta Agriculturae Scandinavica, Section B — Soil & Plant Science 66:483–488. https://doi.org/10.1080/09064710.2016.1178324

Batistic O, Kudla J (2004) Integration and channeling of calcium signaling through the CBL calcium sensor/CIPK protein kinase network. Planta 219:915–924. https://doi.org/10.1007/s00425-004-1333-3

Batistic O, Kudla J (2009) Plant calcineurin B-like proteins and their interacting protein kinases. Biochim Biophys Acta 1793:985–992. https://doi.org/10.1016/j.bbamcr.2008.10.006

Batistic O, Sorek N, Schültke S, Yalovsky S, Kudla J (2008) Dual fatty acyl modification determines the localization and plasma membrane targeting of CBL/CIPK Ca2+ signaling complexes in Arabidopsis. Plant Cell 20:1346–1362. https://doi.org/10.1105/tpc.108.058123

Batistic O, Waadt R, Steinhorst L, Held K, Kudla J (2010) CBL-mediated targeting of CIPKs facilitates the decoding of calcium signals emanating from distinct cellular stores. Plant J 61:211–222. https://doi.org/10.1111/j.1365-313X.2009.04045.x

Belete F, Dechassa N, Molla A, Tana T (2018) Effect of nitrogen fertilizer rates on grain yield and nitrogen uptake and use efficiency of bread wheat (Triticum aestivum L.) varieties on the Vertisols of central highlands of Ethiopia. Agric & Food Secur 7:362. https://doi.org/10.1186/s40066-018-0231-z

Bennici A (ed) (1986a) Crops I: Durum Wheat (Triticum durum Desf.). Biotechnology in Agriculture and Forestry. Springer Berlin Heidelberg, Berlin, Heidelberg

Bennici A (1986b) Durum Wheat (Triticum durum Desf.). In: Bennici A (ed) Crops I: Durum Wheat (Triticum durum Desf.), vol 2. Springer Berlin Heidelberg, Berlin, Heidelberg, pp 89–104

Bindel N, Neuhäuser B (2019) Electrophysiological characterization of AtAMT1;4, an extraordinarily high affinity ammonium transporter from Arabidopsis thaliana Biorxiv: the preprint server for biology. https://doi.org/10.1101/820712

Bittsánszky A, Pilinszky K, Gyulai G, Komives T (2015) Overcoming ammonium toxicity. Plant Sci 231:184–190. https://doi.org/10.1016/j.plantsci.2014.12.005

Bloom AJ, Sukrapanna SS, Warner RL (1992) Root respiration associated with ammonium and nitrate absorption and assimilation by barley. Plant Physiol 99:1294–1301. https://doi.org/10.1104/pp.99.4.1294

Boeckstaens M, André B, Marini AM (2008) Distinct transport mechanisms in yeast ammonium transport/sensor proteins of the Mep/Amt/Rh family and impact on filamentation. J Biol Chem 283:21362–21370. https://doi.org/10.1074/jbc.M801467200

Boeckstaens M, Llinares E, van Vooren P, Marini AM (2014) The TORC1 effector kinase Npr1 fine tunes the inherent activity of the Mep2 ammonium transport protein. Nat Commun 5:3101. https://doi.org/10.1038/ncomms4101

Bouché N, Lacombe B, Fromm H (2003a) GABA signaling: a conserved and ubiquitous mechanism. Trends Cell Biol 13:607–610. https://doi.org/10.1016/j.tcb.2003.10.001

Bouché N, Fait A, Bouchez D, Møller SG, Fromm H (2003b) Mitochondrial succinic-semialdehyde dehydrogenase of the gamma-aminobutyrate shunt is required to restrict levels of reactive oxygen intermediates in plants. Proc Natl Acad Sci U S A 100:6843–6848. https://doi.org/10.1073/pnas.1037532100

Boudsocq S, Niboyet A, Lata JC, Raynaud X, Loeuille N, Mathieu J, Blouin M, Abbadie L, Barot S (2012) Plant preference for ammonium versus nitrate: A neglected determinant of ecosystem functioning? The American Naturalist 180:60–69. https://doi.org/10.1086/665997

Brady NC, Weil RC (2001) The nature and properties of soils, 13th edn. Prentice-Hall, Upper Saddle River, NJ

Brian Gordon Forde, and David T. Clarkson (ed) (1999) Nitrate and Ammonium Nutrition of Plants: Physiological and Molecular Perspectives. Advances in Botanical Research, vol 30. Elsevier

Britto DT, Siddiqi MY, Glass ADM, Kronzucker HJ (2001) Futile transmembrane NH4+ cycling: A cellular hypothesis to explain ammonium toxicity in plants. Proc Natl Acad Sci U S A 98:4255–4258. https://doi.org/10.1073/pnas.061034698

Britto DT, Kronzucker HJ (2002) NH4+ toxicity in higher plants: a critical review. J Plant Physiol 159:567–584. https://doi.org/10.1078/0176-1617-0774

Britto DT, Kronzucker HJ (2005) Nitrogen acquisition, PEP carboxylase, and cellular pH homeostasis: New views on old paradigms. Plant Cell Environ 28:1396–1409. https://doi.org/10.1111/j.1365-3040.2005.01372.x

Britto DT, Kronzucker HJ (2013) Ecological significance and complexity of N-source preference in plants. Annals of Botany 112:957–963. https://doi.org/10.1093/aob/mct157

Canales J, Moyano TC, Villarroel E, Gutiérrez RA (2014) Systems analysis of transcriptome data provides new hypotheses about Arabidopsis root response to nitrate treatments. Front Plant Sci 5:22. https://doi.org/10.3389/fpls.2014.00022

Carpenter SR (2005) Eutrophication of aquatic ecosystems: Bistability and soil phosphorus. Proc Natl Acad Sci U S A 102:10002–10005. https://doi.org/10.1073/pnas.0503959102

Chaillou S, Morot-Gaudry J-F, Lesaint C, Salsac L, Jolivet E (1986) Nitrate or ammonium nutrition in french bean. Plant Soil 91:363–365. https://doi.org/10.1007/BF02198124

Chaves-Sanjuan A, Sanchez-Barrena MJ, Gonzalez-Rubio JM, Moreno M, Ragel P, Jimenez M, Pardo JM, Martinez-Ripoll M, Quintero FJ, Albert A (2014) Structural basis of the regulatory mechanism of the plant CIPK family of protein kinases controlling ion homeostasis and abiotic stress. Proc Natl Acad Sci U S A 111:E4532-41. https://doi.org/10.1073/pnas.1407610111

Chen G, Guo S, Kronzucker HJ, Shi W (2013) Nitrogen use efficiency (NUE) in rice links to NH4 + toxicity and futile NH4 + cycling in roots. Plant Soil 369:351–363. https://doi.org/10.1007/s11104-012-1575-y

Cheong YH, Kim K-N, Pandey GK, Gupta R, Grant JJ, Luan S (2003) CBL1, a calcium sensor that differentially regulates salt, drought, and cold responses in Arabidopsis. Plant Cell 15:1833–1845. https://doi.org/10.1105/tpc.012393

Cheong YH, Pandey GK, Grant JJ, Batistic O, Li L, Kim B-G, Lee S-C, Kudla J, Luan S (2007) Two calcineurin B-like calcium sensors, interacting with protein kinase CIPK23, regulate leaf transpiration and root potassium uptake in Arabidopsis. Plant J 52:223–239. https://doi.org/10.1111/j.1365-313X.2007.03236.x

Cho JH, Lee JH, Park YK, Choi MN, Kim K-N (2016) Calcineurin B-like Protein CBL10 Directly Interacts with TOC34 (Translocon of the Outer Membrane of the Chloroplasts) and Decreases Its GTPase Activity in Arabidopsis. Front Plant Sci 7:1911. https://doi.org/10.3389/fpls.2016.01911

Chollet R, Vidal J, O'Leary MH (1996) PHOSPHOENOLPYRUVATE CARBOXYLASE: A Ubiquitous, Highly Regulated Enzyme in Plants. Annu Rev Plant Physiol Plant Mol Biol 47:273–298. https://doi.org/10.1146/annurev.arplant.47.1.273

Clapham DE (2007) Calcium signaling. Cell 131:1047–1058. https://doi.org/10.1016/j.cell.2007.11.028

Coleto I, Vega-Mas I, Glauser G, González-Moro MB, Marino D, Ariz I (2019) New Insights on Arabidopsis thaliana Root Adaption to Ammonium Nutrition by the Use of a Quantitative Proteomic Approach. Int J Mol Sci 20. https://doi.org/10.3390/ijms20040814

Conley DJ, Paerl HW, Howarth RW, Boesch DF, Seitzinger SP, Havens KE, Lancelot C, Likens GE (2009) Ecology. Controlling eutrophication: Nitrogen and phosphorus. Science 323:1014–1015. https://doi.org/10.1126/science.1167755.

Conroy MJ, Durand A, Lupo D, Li X-D, Bullough PA, Winkler FK, Merrick M (2007) The crystal structure of the Escherichia coli AmtB-GlnK complex reveals how GlnK regulates the ammonia channel. Proc Natl Acad Sci U S A 104:1213–1218. https://doi.org/10.1073/pnas.0610348104

Considine MJ, Foyer CH (2014) Redox regulation of plant development. Antioxid Redox Signal 21:1305–1326. https://doi.org/10.1089/ars.2013.5665

Couturier J, Montanini B, Martin F, Brun A, Blaudez D, Chalot M (2007) The expanded family of ammonium transporters in the perennial poplar plant. New Phytol 174:137–150. https://doi.org/10.1111/j.1469-8137.2007.01992.x

Crawford LA, Bown AW, Breitkreuz KE, Guinel FC (1994) The Synthesis of gamma-Aminobutyric Acid in Response to Treatments Reducing Cytosolic pH. Plant Physiol 104:865–871. https://doi.org/10.1104/pp.104.3.865

Curtis BC, Rajaram S., Macpherson (Ed.) HG (eds) (2002) BREAD WHEAT. Improvement and Production. FAO Plant Production and Protection Series, vol 30, Rome

Dalrymple DG (1974) Development and Spread of High-Yielding Varieties of Wheat and Rice in the Less Developed Nations, Washington, D.C.

Dangl JL, Jones JD (2001) Plant pathogens and integrated defence responses to infection. Nature 411:826–833. https://doi.org/10.1038/35081161

Daniels MJ, Yeager M (2019) Phosphorylation of TIP3 Aquaporins during Phaseolus vulgaris Embryo Development. Cells 8. https://doi.org/10.3390/cells8111362

D'Apuzzo E, Rogato A, Simon-Rosin U, El Alaoui H, Barbulova A, Betti M, Dimou M, Katinakis P, Marquez A, Marini A-M, Udvardi MK, Chiurazzi M (2004) Characterization of three functional high-affinity ammonium transporters in Lotus japonicus with differential transcriptional regulation and spatial expression. Plant Physiol 134:1763–1774. https://doi.org/10.1104/pp.103.034322

DeFalco TA, Bender KW, Snedden WA (2009) Breaking the code: Ca2+ sensors in plant signalling. Biochem J 425:27–40. https://doi.org/10.1042/BJ20091147

Di Perez Giorgio J, Soto G, Alleva K, Jozefkowicz C, Amodeo G, Muschietti JP, Ayub ND (2014) Prediction of aquaporin function by integrating evolutionary and functional analyses. J Membr Biol 247:107–125. https://doi.org/10.1007/s00232-013-9618-8

Dieni CA, Storey KB (2010) Regulation of glucose-6-phosphate dehydrogenase by reversible phosphorylation in liver of a freeze tolerant frog. J Comp Physiol B, Biochem Syst Environ Physiol 180:1133–1142. https://doi.org/10.1007/s00360-010-0487-5

Dixon R, Kahn D (2004) Genetic regulation of biological nitrogen fixation. Nat Rev Microbiol 2:621–631. https://doi.org/10.1038/nrmicro954

Dubcovsky J, Dvorak J (2007) Genome plasticity a key factor in the success of polyploid wheat under domestication. Science 316:1862–1866. https://doi.org/10.1126/science.1143986

Dubcovsky J, Loukoianov A, Bonafede MD (2007) Regulation of Flowering Time in Wheat. In: Buck HT, Nisi JE, Salomón N (eds) Wheat Production in Stressed Environments, vol 12. Springer Netherlands, Dordrecht, pp 659–665

Dvorak J, McGuire PE, Cassidy B (1988) Apparent sources of the A genomes of wheats inferred from polymorphism in abundance and restriction fragment length of repeated nucleotide sequences. Genome 30:680–689. https://doi.org/10.1139/g88-115

Dyhr-Jensen K, Brix H (1996) Effects of pH on ammonium uptake by Typha latifolia L. Plant Cell Environ 19:1431–1436. https://doi.org/10.1111/j.1365-3040.1996.tb00022.x

Eckardt NA (2001) Move it on out with MATEs. Plant Cell 13:1477–1480. https://doi.org/10.1105/tpc.13.7.1477

Engelsberger WR, Schulze WX (2012) Nitrate and ammonium lead to distinct global dynamic phosphorylation patterns when resupplied to nitrogen-starved Arabidopsis seedlings. Plant J 69:978–995. https://doi.org/10.1111/j.1365-313X.2011.04848.x

Ermilova E, Lapina T, Zalutskaya Z, Minaeva E, Fokina O, Forchhammer K (2013) PII signal transduction protein in Chlamydomonas reinhardtii: Localization and expression pattern. Protist 164:49–59. https://doi.org/10.1016/j.protis.2012.04.002

Esteban R, Ariz I, Cruz C, Moran JF (2016) Review: Mechanisms of ammonium toxicity and the quest for tolerance. Plant Sci 248:92–101. https://doi.org/10.1016/j.plantsci.2016.04.008

Falhof J, Pedersen JT, Fuglsang AT, Palmgren M (2016) Plasma Membrane H(+)-ATPase Regulation in the Center of Plant Physiology. Mol Plant 9:323–337. https://doi.org/10.1016/j.molp.2015.11.002

FAO (2014) Wheat - the largest primary commodity. http://www.fao.org/resources/infographics/infographics-details/en/c/240943/. Accessed 27 October 2020

FAO (2019) WHEAT. http://www.fao.org/faostat/en/#data/QC/visualize

Findenegg GR (1987) A comparative study of ammonium toxicity at different constatn pH of the nutrient solution. Plant and Soil 103:239–243. https://doi.org/10.1007/BF02370395

Fischer T, Byerlee D, Edmeades G (2014) Crop yields and global food security: Will yield increase continue to feed the world? ACIAR Monograph, vol 158. Australian Centre for International Agricultural Research (ACIAR), Canberra

Fischer RA, Maurer R (1978) Drought resistance in spring wheat cultivars. I. Grain yield responses. Aust. J. Agric. Res. 29:897. https://doi.org/10.1071/AR9780897

Fredeen AL, Field CB (1992) Ammonium and nitrate uptake in gap, generalist and understory species of the genus Piper. Oecologia 92:207–214. https://doi.org/10.1007/BF00317366

Fuertes-Mendizábal T, González-Torralba J, Arregui LM, González-Murua C, González-Moro MB, Estavillo JM (2013) Ammonium as sole N source improves grain quality in wheat. J Sci Food Agric 93:2162–2171. https://doi.org/10.1002/jsfa.6022

Ganz P, Ijato T, Porras-Murillo R, Stührwohldt N, Ludewig U, Neuhäuser B (2020) A twin histidine motif is the core structure for high-affinity substrate selection in plant ammonium transporters. J Biol Chem. https://doi.org/10.1074/jbc.RA119.010891

Garcia-Garcia T, Poncet S, Derouiche A, Shi L, Mijakovic I, Noirot-Gros M-F (2016) Role of Protein Phosphorylation in the Regulation of Cell Cycle and DNA-Related Processes in Bacteria. Front Microbiol 7:184. https://doi.org/10.3389/fmicb.2016.00184

Gaufichon L, Reisdorf-Cren M, Rothstein SJ, Chardon F, Suzuki A (2010) Biological functions of asparagine synthetase in plants. Plant Science 179:141–153. https://doi.org/10.1016/j.plantsci.2010.04.010

Gazzarrini S, Lejay L, Gojon A, Ninnemann O, Frommer WB, Wirén N von (1999) Three functional transporters for constitutive, diurnally regulated, and starvation-induced uptake of ammonium into Arabidopsis roots. Plant Cell 11:937–948. https://doi.org/10.1105/tpc.11.5.937

Gentili R, Ambrosini R, Montagnani C, Caronni S, Citterio S (2018) Effect of Soil pH on the Growth, Reproductive Investment and Pollen Allergenicity of Ambrosia artemisiifolia L. Front Plant Sci 9:1335. https://doi.org/10.3389/fpls.2018.01335

Gietz RD, Schiestl RH, Willems AR, Woods RA (1995) Studies on the transformation of intact yeast cells by the LiAc/SS-DNA/PEG procedure. Yeast 11:355–360. https://doi.org/10.1002/yea.320110408

Gifford JL, Walsh MP, Vogel HJ (2007) Structures and metal-ion-binding properties of the Ca2+-binding helix-loop-helix EF-hand motifs. Biochem J 405:199–221. https://doi.org/10.1042/BJ20070255

Glass ADM, Britto DT, Kaiser BN, Kinghorn JR, Kronzucker HJ, Kumar A, Okamoto M, Rawat S, Siddiqi MY, Unkles SE, Vidmar JJ (2002) The regulation of nitrate and ammonium transport systems in plants. J Exp Bot 53:855–864. https://doi.org/10.1093/jexbot/53.370.855

Gong D, Guo Y, Schumaker KS, Zhu J-K (2004) The SOS3 family of calcium sensors and SOS2 family of protein kinases in Arabidopsis. Plant Physiol 134:919–926. https://doi.org/10.1104/pp.103.037440

Gu R, Duan F, An X, Zhang F, Wirén N von, Yuan L (2013) Characterization of AMT-mediated high-affinity ammonium uptake in roots of maize (Zea mays L.). Plant Cell Physiol 54:1515–1524. https://doi.org/10.1093/pcp/pct099

Guether M, Neuhäuser B, Balestrini R, Dynowski M, Ludewig U, Bonfante P (2009) A mycorrhizal-specific ammonium transporter from Lotus japonicus acquires nitrogen released by arbuscular mycorrhizal fungi. Plant Physiol 150:73–83. https://doi.org/10.1104/pp.109.136390

Guo Y, Halfter U, Ishitani M, Zhu JK (2001) Molecular characterization of functional domains in the protein kinase SOS2 that is required for plant salt tolerance. Plant Cell 13:1383–1400. https://doi.org/10.1105/tpc.13.6.1383

Guo S, Chen G, Zhou Y, Shen Q (2007) Ammonium nutrition increases photosynthesis rate under water stress at early development stage of rice (Oryza sativa L.). Plant Soil 296:115–124. https://doi.org/10.1007/s11104-007-9302-9

Guo Y, Huang Y, Gao J, Pu Y, Wang N, Shen W, Wen J, Yi B, Ma C, Tu J, Fu T, Zou J, Shen J (2018a) CIPK9 is involved in seed oil regulation in Brassica napus L. and Arabidopsis thaliana (L.) Heynh. Biotechnol Biofuels 11:124. https://doi.org/10.1186/s13068-018-1122-z

Guo H, Wang N, McDonald TR, Reinders A, Ward JM (2018b) MpAMT1;2 from Marchantia polymorpha is a High-Affinity, Plasma Membrane Ammonium Transporter. Plant Cell Physiol 59:997–1005. https://doi.org/10.1093/pcp/pcy038

Guo J, Jia Y, Chen H, Zhang L, Yang J, Zhang J, Hu X, Ye X, Li Y, Zhou Y (2019) Growth, photosynthesis, and nutrient uptake in wheat are affected by differences in nitrogen levels and forms and potassium supply. Sci Rep 9:1248. https://doi.org/10.1038/s41598-018-37838-3

Hachiya T, Watanabe CK, Fujimoto M, Ishikawa T, Takahara K, Kawai-Yamada M, Uchimiya H, Uesono Y, Terashima I, Noguchi K (2012) Nitrate addition alleviates ammonium

toxicity without lessening ammonium accumulation, organic acid depletion and inorganic cation depletion in Arabidopsis thaliana shoots. Plant Cell Physiol 53:577–591. https://doi.org/10.1093/pcp/pcs012

Haruta M, Gray WM, Sussman MR (2015) Regulation of the plasma membrane proton pump (H(+)-ATPase) by phosphorylation. Current Opinion in Plant Biology 28:68–75. https://doi.org/10.1016/j.pbi.2015.09.005

Hawkesford MJ (2017) Genetic variation in traits for nitrogen use efficiency in wheat. J Exp Bot 68:2627–2632. https://doi.org/10.1093/jxb/erx079

Hendricks GS, Shukla S, Roka FM, Sishodia RP, Obreza TA, Hochmuth GJ, Colee J (2019) Economic and environmental consequences of overfertilization under extreme weather conditions. Journal of Soil and Water Conservation 74:160–171. https://doi.org/10.2489/jswc.74.2.160

Hernández-Gómez E, Valdez-Aguilar LA, Cartmill DL, Cartmill AD, Alia-Tajacal I (2015) Supplementary calcium ameliorates ammonium toxicity by improving water status in agriculturally important species. AoB Plants 7. https://doi.org/10.1093/aobpla/plv105

Hinzman L, Bauer M, and Daughtry C (1986) Effects of nitrogen fertilization on growth and reflectance characteristics of winter wheat☆. Remote Sensing of Environment 19:47–61. https://doi.org/10.1016/0034-4257(86)90040-4

Ho C-H, Lin S-H, Hu H-C, Tsay Y-F (2009) CHL1 functions as a nitrate sensor in plants. Cell 138:1184–1194. https://doi.org/10.1016/j.cell.2009.07.004

Holm LM, Jahn TP, Møller ALB, Schjoerring JK, Ferri D, Klaerke DA, Zeuthen T (2005) NH3 and NH4+ permeability in aquaporin-expressing Xenopus oocytes. Pflugers Arch 450:415–428. https://doi.org/10.1007/s00424-005-1399-1

Hove RM, Bhave M (2011) Plant aquaporins with non-aqua functions: deciphering the signature sequences. Plant Mol Biol 75:413–430. https://doi.org/10.1007/s11103-011-9737-5

Howarth RW, Marino R (2006) Nitrogen as the limiting nutrient for eutrophication in coastal marine ecosystems: Evolving views over three decades. Limnol. Oceanogr. 51:364–376. https://doi.org/10.4319/lo.2006.51.1_part_2.0364

Howitt SM, Udvardi MK (2000) Structure, function and regulation of ammonium transporters in plants. Biochimica et Biophysica Acta (BBA) - Biomembranes 1465:152–170. https://doi.org/10.1016/S0005-2736(00)00136-X

Hrabak EM, Chan CWM, Gribskov M, Harper JF, Choi JH, Halford N, Kudla J, Luan S, Nimmo HG, Sussman MR, Thomas M, Walker-Simmons K, Zhu J-K, Harmon AC (2003) The Arabidopsis CDPK-SnRK superfamily of protein kinases. Plant Physiol 132:666–680

Hsieh MH, Lam HM, van de Loo FJ, Coruzzi G (1998) A PII-like protein in Arabidopsis: Putative role in nitrogen sensing. Proc Natl Acad Sci U S A 95:13965–13970. https://doi.org/10.1073/pnas.95.23.13965

Hu H-C, Wang Y-Y, Tsay Y-F (2009) AtCIPK8, a CBL-interacting protein kinase, regulates the low-affinity phase of the primary nitrate response. Plant J 57:264–278. https://doi.org/10.1111/j.1365-313X.2008.03685.x

Huang H, Ullah F, Zhou D-X, Yi M, Zhao Y (2019) Mechanisms of ROS Regulation of Plant Development and Stress Responses. Front Plant Sci 10:800. https://doi.org/10.3389/fpls.2019.00800

Huergo LF, Chandra G, Merrick M (2013) P(II) signal transduction proteins: Nitrogen regulation and beyond. FEMS Microbiol Rev 37:251–283. https://doi.org/10.1111/j.1574-6976.2012.00351.x

Ishikita H, Knapp E-W (2007) Protonation states of ammonia/ammonium in the hydrophobic pore of ammonia transporter protein AmtB. J Am Chem Soc 129:1210–1215. https://doi.org/10.1021/ja066208n

Ishitani M, Liu J, Halfter U, Kim CS, Shi W, Zhu JK (2000) SOS3 function in plant salt tolerance requires N-myristoylation and calcium binding. Plant Cell 12:1667–1678. https://doi.org/10.1105/tpc.12.9.1667

Ismailov II, Benos DJ (1995) Effects of phosphorylation on ion channel function. Kidney Int 48:1167–1179. https://doi.org/10.1038/ki.1995.400

Javelle A, Severi E, Thornton J, Merrick M (2004) Ammonium sensing in Escherichia coli. Role of the ammonium transporter AmtB and AmtB-GlnK complex formation. J Biol Chem 279:8530–8538. https://doi.org/10.1074/jbc.M312399200

Jin SH, Huang JQ, Li XQ, Zheng BS, Wu JS, Wang ZJ, Liu GH, Chen M (2011) Effects of potassium supply on limitations of photosynthesis by mesophyll diffusion conductance in Carya cathayensis. Tree Physiol 31:1142–1151. https://doi.org/10.1093/treephys/tpr095

Johansson I, Karlsson M, Shukla VK, Chrispeels MJ, Larsson C, Kjellbom P (1998) Water transport activity of the plasma membrane aquaporin PM28A is regulated by phosphorylation. Plant Cell 10:451–459. https://doi.org/10.1105/tpc.10.3.451

Jurczyk B, Pociecha E, Janeczko A, Paczyński R, Rapacz M (2014) Assessment of candidate reference genes for the expression studies with brassinosteroids in Lolium perenne and Triticum aestivum. J Plant Physiol 171:1541–1544. https://doi.org/10.1016/j.jplph.2014.07.008

Khademi S, O'Connell J, Remis J, Robles-Colmenares Y, Miercke LJW, Stroud RM (2004) Mechanism of ammonia transport by Amt/MEP/Rh: Structure of AmtB at 1.35 A. Science 305:1587–1594. https://doi.org/10.1126/science.1101952

Khalil JK, Sawaya WN, Hamdallah G, Devi Prasad J (1987) Effect of nitrogen fertilization on the nutritional quality of wheat variety, Yecora Rojo. Plant Food Hum Nutr 36:279–293. https://doi.org/10.1007/BF01892350

Kim KN, Cheong YH, Gupta R, Luan S (2000) Interaction specificity of Arabidopsis calcineurin B-like calcium sensors and their target kinases. Plant Physiol 124:1844–1853. https://doi.org/10.1104/pp.124.4.1844

Kirscht A, Kaptan SS, Bienert GP, Chaumont F, Nissen P, Groot BL de, Kjellbom P, Gourdon P, Johanson U (2016) Crystal Structure of an Ammonia-Permeable Aquaporin. PLoS Biol 14:e1002411. https://doi.org/10.1371/journal.pbio.1002411

Kolukisaoglu U, Weinl S, Blazevic D, Batistic O, Kudla J (2004) Calcium sensors and their interacting protein kinases: Genomics of the Arabidopsis and rice CBL-CIPK signaling networks. Plant Physiol 134:43–58. https://doi.org/10.1104/pp.103.033068

Kong L, Sun M, Wang F, Liu J, Feng B, Si J, Zhang B, Li S, Li H (2014) Effects of high NH(+) 4 on K(+) uptake, culm mechanical strength and grain filling in wheat. Front Plant Sci 5:703. https://doi.org/10.3389/fpls.2014.00703

Kronzucker HJ, Siddiqi MY, Glass ADM (1995) Compartmentation and flux characteristics of ammonium in spruce. Planta 196:691–698

Kronzucker HJ, Siddiqi MY, Glass ADM (1996) Kinetics of NH4+ Influx in Spruce. Plant Physiol 110:773–779

Kronzucker HJ, Schjoerring JK, Erner Y, Kirk GJD, Yaeesh Siddiqi M, Glass ADM (1998) Dynamic Interactions between Root NH4+ Influx and Long-Distance N Translocation in Rice: Insights into Feedback Processes. Plant and Cell Physiology 39:1287–1293. https://doi.org/10.1093/oxfordjournals.pcp.a029332

Kudla J, Xu Q, Harter K, Gruissem W, Luan S (1999) Genes for calcineurin B-like proteins in Arabidopsis are differentially regulated by stress signals. Proc Natl Acad Sci U S A 96:4718–4723. https://doi.org/10.1073/pnas.96.8.4718

Kudla J, Batistic O, Hashimoto K (2010) Calcium signals: The lead currency of plant information processing. Plant Cell 22:541–563

Kurimoto K, Day DA, Lambers H, Noguchi K (2004) Effect of respiratory homeostasis on plant growth in cultivars of wheat and rice. Plant Cell Environ 27:853–862. https://doi.org/10.1111/j.1365-3040.2004.01191.x

Laidig F, Piepho H-P, Drobek T, Meyer U (2014) Genetic and non-genetic long-term trends of 12 different crops in German official variety performance trials and on-farm yield trends. Theor Appl Genet 127:2599–2617. https://doi.org/10.1007/s00122-014-2402-z

Lan W-Z, Lee S-C, Che Y-F, Jiang Y-Q, Luan S (2011) Mechanistic analysis of AKT1 regulation by the CBL-CIPK-PP2CA interactions. Mol Plant 4:527–536. https://doi.org/10.1093/mp/ssr031

Lanquar V, Frommer WB (2010) Adjusting ammonium uptake via phosphorylation. Plant Signal Behav 5:736–738. https://doi.org/10.4161/psb.5.6.11696

Lanquar V, Loqué D, Hörmann F, Yuan L, Bohner A, Engelsberger WR, Lalonde S, Schulze WX, Wirén N von, Frommer WB (2009) Feedback inhibition of ammonium uptake by a phospho-dependent allosteric mechanism in Arabidopsis. Plant Cell 21:3610–3622. https://doi.org/10.1105/tpc.109.068593

Lant B, Storey KB (2011) Glucose-6-Phosphate Dehydrogenase Regulation in Anoxia Tolerance of the Freshwater Crayfish Orconectes virilis. Enzyme Res 2011:524906. https://doi.org/10.4061/2011/524906

Lassaletta L, Billen G, Grizzetti B, Anglade J, Garnier J (2014) 50 year trends in nitrogen use efficiency of world cropping systems: The relationship between yield and nitrogen input to cropland. Environ. Res. Lett. 9:105011. https://doi.org/10.1088/1748-9326/9/10/105011

Lee RB, Rudge KA (1986) Effects of Nitrogen Deficiency on the Absorption of Nitrate and Ammonium by Barley Plants. Annals of Botany 57:471–486. https://doi.org/10.1093/oxfordjournals.aob.a087129

Lee SC, Lan W-Z, Kim B-G, Li L, Cheong YH, Pandey GK, Lu G, Buchanan BB, Luan S (2007) A protein phosphorylation/dephosphorylation network regulates a plant potassium channel. Proc Natl Acad Sci U S A 104:15959–15964. https://doi.org/10.1073/pnas.0707912104

Lejay L, Gansel X, Cerezo M, Tillard P, Müller C, Krapp A, Wirén N von, Daniel-Vedele F, Gojon A (2003) Regulation of root ion transporters by photosynthesis: Functional importance and relation with hexokinase. Plant Cell 15:2218–2232

Lewis WM, Wurtsbaugh WA, Paerl HW (2011) Rationale for control of anthropogenic nitrogen and phosphorus to reduce eutrophication of inland waters. Environ Sci Technol 45:10300–10305. https://doi.org/10.1021/es202401p.

Li X-D, Lupo D, Zheng L, Winkler F (2006) Structural and functional insights into the AmtB/Mep/Rh protein family. Transfus Clin Biol 13:65–69. https://doi.org/10.1016/j.tracli.2006.02.014

Li X, Jayachandran S, Nguyen H-HT, Chan MK (2007) Structure of the Nitrosomonas europaea Rh protein. Proc Natl Acad Sci U S A 104:19279–19284. https://doi.org/10.1073/pnas.0709710104

Li Y, Gao Y, Ding L, Shen Q, Guo S (2009a) Ammonium enhances the tolerance of rice seedlings (Oryza sativa L.) to drought condition. Agricultural Water Management 96:1746–1750. https://doi.org/10.1016/j.agwat.2009.07.008

Li R, Zhang J, Wei J, Wang H, Wang Y, Ma R (2009b) Functions and mechanisms of the CBL–CIPK signaling system in plant response to abiotic stress. Progress in Natural Science 19:667–676. https://doi.org/10.1016/j.pnsc.2008.06.030

Li B, Li G, Kronzucker HJ, Baluška F, Shi W (2014) Ammonium stress in Arabidopsis: Signaling, genetic loci, and physiological targets. Trends Plant Sci 19:107–114. https://doi.org/10.1016/j.tplants.2013.09.004

Li T, Liao K, Xu X, Gao Y, Wang Z, Zhu X, Jia B, Xuan Y (2017) Wheat Ammonium Transporter (AMT) Gene Family: Diversity and Possible Role in Host-Pathogen Interaction with Stem Rust. Front Plant Sci 8:1637. https://doi.org/10.3389/fpls.2017.01637

LI B-Z, Merrick M, LI S-M, LI H-y, ZHU S-w, SHI W-M, SU Y-h (2009) Molecular Basis and Regulation of Ammonium Transporter in Rice. Rice Science 16:314–322. https://doi.org/10.1016/S1672-6308(08)60096-7

LI S-M, LI B-Z, SHI W-M (2012) Expression Patterns of Nine Ammonium Transporters in Rice in Response to N Status. Pedosphere 22:860–869. https://doi.org/10.1016/S1002-0160(12)60072-1

Litke L, Gaile Z, Ruža A (2018) Effect of nitrogen fertilization on winter wheat yield and yield quality. 332.2Kb. https://doi.org/10.15159/AR.18.064

Litman T, Søgaard R, Zeuthen T (2009) Ammonia and urea permeability of mammalian aquaporins. Handb Exp Pharmacol:327–358. https://doi.org/10.1007/978-3-540-79885-9_17

Liu J, Zhu JK (1998) A calcium sensor homolog required for plant salt tolerance. Science 280:1943–1945. https://doi.org/10.1126/science.280.5371.1943

Liu Y, Wirén N von (2017) Ammonium as a signal for physiological and morphological responses in plants. J Exp Bot 68:2581–2592. https://doi.org/10.1093/jxb/erx086

Liu Y, Lai N, Gao K, Chen F, Yuan L, Mi G (2013) Ammonium inhibits primary root growth by reducing the length of meristem and elongation zone and decreasing elemental expansion rate in the root apex in Arabidopsis thaliana. PLoS ONE 8:e61031. https://doi.org/10.1371/journal.pone.0061031

Lobell DB, Schlenker W, Costa-Roberts J (2011) Climate trends and global crop production since 1980. Science 333:616–620. https://doi.org/10.1126/science.1204531

Loqué D, Wirén N von (2004) Regulatory levels for the transport of ammonium in plant roots. J Exp Bot 55:1293–1305. https://doi.org/10.1093/jxb/erh147

Loqué D, Ludewig U, Yuan L, Wirén N von (2005) Tonoplast intrinsic proteins AtTIP2;1 and AtTIP2;3 facilitate NH3 transport into the vacuole. Plant Physiol 137:671–680. https://doi.org/10.1104/pp.104.051268

Loqué D, Yuan L, Kojima S, Gojon A, Wirth J, Gazzarrini S, Ishiyama K, Takahashi H, Wirén N von (2006) Additive contribution of AMT1;1 and AMT1;3 to high-affinity ammonium uptake across the plasma membrane of nitrogen-deficient Arabidopsis roots. Plant J 48:522–534

Loqué D, Lalonde S, Looger LL, Wirén N von, Frommer WB (2007) A cytosolic trans-activation domain essential for ammonium uptake. Nature 446:195–198. https://doi.org/10.1038/nature05579

Loqué D, Mora SI, Andrade SLA, Pantoja O, Frommer WB (2009) Pore mutations in ammonium transporter AMT1 with increased electrogenic ammonium transport activity. J Biol Chem 284:24988–24995. https://doi.org/10.1074/jbc.M109.020842

Luan S, Kudla J, Rodriguez-Concepcion M, Yalovsky S, Gruissem W (2002) Calmodulins and calcineurin B-like proteins: Calcium sensors for specific signal response coupling in plants. Plant Cell 14 Suppl:S389-400

Ludevid D, Höfte H, Himelblau E, Chrispeels MJ (1992) The Expression Pattern of the Tonoplast Intrinsic Protein gamma-TIP in Arabidopsis thaliana Is Correlated with Cell Enlargement. Plant Physiol 100:1633–1639. https://doi.org/10.1104/pp.100.4.1633

Ludewig U, Wirén N von, Rentsch D, Frommer WB (2001) Rhesus factors and ammonium: A function in efflux? Genome Biol 2:REVIEWS1010. https://doi.org/10.1186/gb-2001-2-3-reviews1010

Ludewig U, Wirén N von, Frommer WB (2002) Uniport of NH4+ by the root hair plasma membrane ammonium transporter LeAMT1;1. J Biol Chem 277:13548–13555. https://doi.org/10.1074/jbc.M200739200

Ludewig U, Wilken S, Wu B, Jost W, Obrdlik P, El Bakkoury M, Marini A-M, André B, Hamacher T, Boles E, Wirén N von, Frommer WB (2003) Homo- and hetero-oligomerization of ammonium transporter-1 NH4 uniporters. J Biol Chem 278:45603–45610. https://doi.org/10.1074/jbc.M307424200

Ludewig U, Neuhäuser B, Dynowski M (2007) Molecular mechanisms of ammonium transport and accumulation in plants. FEBS Lett 581:2301–2308. https://doi.org/10.1016/j.febslet.2007.03.034

Maathuis FJM (2009) Physiological functions of mineral macronutrients. Current Opinion in Plant Biology 12:250–258. https://doi.org/10.1016/j.pbi.2009.04.003

Mackay I, Horwell A, Garner J, White J, McKee J, Philpott H (2011) Reanalyses of the historical series of UK variety trials to quantify the contributions of genetic and environmental factors to trends and variability in yield over time. Theor Appl Genet 122:225–238. https://doi.org/10.1007/s00122-010-1438-y

Magalhães JR, Huber DM (1989) Ammonium assimilation in different plant species as affected by nitrogen form and pH control in solution culture. Fertilizer Research 21:1–6. https://doi.org/10.1007/BF01054728

Majumdar D (2003) The Blue Baby Syndrome. Reson 8:20–30. https://doi.org/10.1007/BF02840703

Malagoli M, Dal Canal A, Quaggiotti S, Pegoraro P, Bottacin A (2000) Differences in nitrate and ammonium uptake between Scots pine and European larch. Plant and Soil 221:1–3. https://doi.org/10.1023/A:1004720002898

Marini AM, Vissers S, Urrestarazu A, André B (1994) Cloning and expression of the MEP1 gene encoding an ammonium transporter in Saccharomyces cerevisiae. The EMBO Journal 13:3456–3463. https://doi.org/10.1002/j.1460-2075.1994.tb06651.x

Marini AM, Soussi-Boudekou S, Vissers S, Andre B (1997) A family of ammonium transporters in Saccharomyces cerevisiae. Mol Cell Biol 17:4282–4293. https://doi.org/10.1128/mcb.17.8.4282

Marini AM, Springael JY, Frommer WB, André B (2000) Cross-talk between ammonium transporters in yeast and interference by the soybean SAT1 protein. Mol Microbiol 35:378–385. https://doi.org/10.1046/j.1365-2958.2000.01704.x

Marino D, Moran JF (2019) Can Ammonium Stress Be Positive for Plant Performance? Front Plant Sci 10:1103. https://doi.org/10.3389/fpls.2019.01103

Marschner H2 (2008) Mineral nutrition of higher plants, 2nd edn. Academic Press, London

Matika DEF, Loake GJ (2014) Redox regulation in plant immune function. Antioxid Redox Signal 21:1373–1388. https://doi.org/10.1089/ars.2013.5679

Matsumoto H, Wakiuchi N (1974) Changes in ATP in cucumber leaves during ammonium toxicity. Zeitschrift für Pflanzenphysiologie 73:82–85. https://doi.org/10.1016/S0044-328X(74)80147-9

Maurel C, Kado RT, Guern J, Chrispeels MJ (1995) Phosphorylation regulates the water channel activity of the seed-specific aquaporin alpha-TIP. The EMBO Journal 14:3028–3035

Maurel C, Boursiac Y, Luu D-T, Santoni V, Shahzad Z, Verdoucq L (2015) Aquaporins in Plants. Physiol Rev 95:1321–1358. https://doi.org/10.1152/physrev.00008.2015.

McFadden ES, Sears ER (1946) The origin of Triticum spelta and its free-threshing hexaploid relatives. J Hered 37:81 107. https://doi.org/10.1093/oxfordjournals.jhered.a105590

McGuire AM, Bryant DC, Denison RF (1998) Wheat Yields, Nitrogen Uptake, and Soil Moisture Following Winter Legume Cover Crop vs. Fallow. Agronomy Journal 90:404. https://doi.org/10.2134/agronj1998.00021962009000030015x

Meeks JC, Wolk CP, Lockau W, Schilling N, Shaffer PW, Chien WS (1978) Pathways of assimilation of 13NN2 and 13NH4+ by cyanobacteria with and without heterocysts. J Bacteriol 134:125–130

Melinda Smale (ed) (1996) Understanding Global Trends in the Use of Wheat Diversity and International Flows of Wheat Genetic Resources. E C O N O M I C S, Working Paper 96-02

Mohanta TK, Mohanta N, Mohanta YK, Parida P, Bae H (2015) Genome-wide identification of Calcineurin B-Like (CBL) gene family of plants reveals novel conserved motifs and evolutionary aspects in calcium signaling events. BMC Plant Biol 15:189. https://doi.org/10.1186/s12870-015-0543-0

Monahan BJ, Fraser JA, Hynes MJ, Davis MA (2002) Isolation and characterization of two ammonium permease genes, meaA and mepA, from Aspergillus nidulans. Eukaryotic Cell 1:85–94. https://doi.org/10.1128/EC.1.1.85-94.2002

Monson RK (1999) The Origins of C4 Genes and Evolutionary Pattern in the C4 Metabolic Phenotype. In: C4 Plant Biology. Elsevier, pp 377–410

Mpanga IK, Nkebiwe PM, Kuhlmann M, Cozzolino V, Piccolo A, Geistlinger J, Berger N, Ludewig U, Neumann G (2019) The Form of N Supply Determines Plant Growth Promotion by P-Solubilizing Microorganisms in Maize. Microorganisms 7. https://doi.org/10.3390/microorganisms7020038

Nakhoul NL, Hering-Smith KS, Abdulnour-Nakhoul SM, Hamm LL (2001) Transport of NH(3)/NH in oocytes expressing aquaporin-1. Am J Physiol Renal Physiol 281:F255-63. https://doi.org/10.1152/ajprenal.2001.281.2.F255

Neuhäuser B, Dynowski M, Mayer M, Ludewig U (2007) Regulation of NH4+ transport by essential cross talk between AMT monomers through the carboxyl tails. Plant Physiol 143:1651–1659. https://doi.org/10.1104/pp.106.094243

Neuhäuser B, Dynowski M, Ludewig U (2009) Channel-like NH3 flux by ammonium transporter AtAMT2. FEBS Lett 583:2833–2838. https://doi.org/10.1016/j.febslet.2009.07.039

Nühse TS, Stensballe A, Jensen ON, Peck SC (2004) Phosphoproteomics of the Arabidopsis plasma membrane and a new phosphorylation site database. Plant Cell 16:2394–2405. https://doi.org/10.1105/tpc.104.023150

Ohta M, Guo Y, Halfter U, Zhu J-K (2003) A novel domain in the protein kinase SOS2 mediates interaction with the protein phosphatase 2C ABI2. Proc Natl Acad Sci U S A 100:11771–11776. https://doi.org/10.1073/pnas.2034853100

Okonechnikov, Golosova, Fursov, the UGENE team (2012) Unipro UGENE: a unified bioinformatics toolkit. Bioinformatics:1166–1167

O'Leary MH (1982) Phosphoenolpyruvate Carboxylase: An Enzymologist's View. Annu. Rev. Plant. Physiol. 33:297–315. https://doi.org/10.1146/annurev.pp.33.060182.001501

Ortiz-Monasterio RJI, Sayre KD, Rajaram S, McMahon M (1997) Genetic Progress in Wheat Yield and Nitrogen Use Efficiency under Four Nitrogen Rates. Crop Science 37:898. https://doi.org/10.2135/cropsci1997.0011183X003700030033x

Ortiz-Ramirez C, Mora SI, Trejo J, Pantoja O (2011) PvAMT1;1, a highly selective ammonium transporter that functions as H+/NH4(+) symporter. J Biol Chem 286:31113–31122. https://doi.org/10.1074/jbc.M111.261693

Palanivelu R, Brass L, Edlund AF, Preuss D (2003) Pollen Tube Growth and Guidance Is Regulated by POP2, an Arabidopsis Gene that Controls GABA Levels. Cell 114:47–59. https://doi.org/10.1016/S0092-8674(03)00479-3

Pan WL, Madsen IJ, Bolton RP, Graves L, Sistrunk T (2016) Ammonia/Ammonium Toxicity Root Symptoms Induced by Inorganic and Organic Fertilizers and Placement. Agronomy Journal 108:2485. https://doi.org/10.2134/agronj2016.02.0122

Pandey GK, Cheong YH, Kim B-G, Grant JJ, Li L, Luan S (2007) CIPK9: a calcium sensor-interacting protein kinase required for low-potassium tolerance in Arabidopsis. Cell Res 17:411–421. https://doi.org/10.1038/cr.2007.39

Pantoja O (2012) High affinity ammonium transporters: Molecular mechanism of action. Front Plant Sci 3:34. https://doi.org/10.3389/fpls.2012.00034

Peng JH, Sun D, Nevo E (2011) Domestication evolution, genetics and genomics in wheat. Mol Breeding 28:281–301. https://doi.org/10.1007/s11032-011-9608-4

Plaxton WC (1996) The organization and regulation of plant glycolysis. Annu Rev Plant Physiol Plant Mol Biol 47:185–214. https://doi.org/10.1146/annurev.arplant.47.1.185

Poulsen H, Morth P, Egebjerg J, Nissen P (2010) Phosphorylation of the Na+,K+-ATPase and the H+,K+-ATPase. FEBS Lett 584:2589–2595. https://doi.org/10.1016/j.febslet.2010.04.035

Provart N, Zhu T (2003) A Browser-based Functional Classification SuperViewer for Arabidopsis Genomics. Currents in Computational Molecular Biology 2003:271–272

Raben N, Exelbert R, Spiegel R, Sherman JB, Nakajima H, Plotz P, Heinisch J (1995) Functional expression of human mutant phosphofructokinase in yeast: genetic defects in French Canadian and Swiss patients with phosphofructokinase deficiency. Am J Hum Genet 56:131–141

Rappsilber J, Ishihama Y, Mann M (2003) Stop and go extraction tips for matrix-assisted laser desorption/ionization, nanoelectrospray, and LC/MS sample pretreatment in proteomics. Anal Chem 75:663–670. https://doi.org/10.1021/ac026117i

Rawat SR, Silim SN, Kronzucker HJ, Siddiqi MY, Glass AD (1999) AtAMT1 gene expression and NH4+ uptake in roots of Arabidopsis thaliana: Evidence for regulation by root glutamine levels. Plant J 19:143–152. https://doi.org/10.1046/j.1365-313X.1999.00505.x

Reisenauer HM (ed) (1978) Absorption and utilization of ammonium nitrogen by plants. Nitrogen in the environment. Academic Press, New York

Rekaby SA, M. A. Eissa, S. A. Hegab and H. M. Ragheb (2016) Effect of Nitrogen Fertilization Rates on Wheat Grown under DripIrrigation System. Assiut J. Agric. Sci. 47:104–119

Roberts MR (2007) Does GABA Act as a Signal in Plants?: Hints from Molecular Studies. Plant Signal Behav 2:408–409. https://doi.org/10.4161/psb.2.5.4335

Rogato A, D'Apuzzo E, Barbulova A, Omrane S, Parlati A, Carfagna S, Costa A, Lo Schiavo F, Esposito S, Chiurazzi M (2010) Characterization of a developmental root response caused by external ammonium supply in Lotus japonicus. Plant Physiol 154:784–795. https://doi.org/10.1104/pp.110.160309

Ronald F. Follett (ed) (2001) Nitrogen in the Environment: Sources, Problems and Management. Nitrogen in the Environment: Sources, Problems and Management. Elsevier

Roosta HR, Schjoerring JK (2007) Effects of Ammonium Toxicity on Nitrogen Metabolism and Elemental Profile of Cucumber Plants. Journal of Plant Nutrition 30:1933–1951. https://doi.org/10.1080/01904160701629211

Roosta HR, Schjoerring JK (2008) Root Carbon Enrichment Alleviates Ammonium Toxicity in Cucumber Plants. Journal of Plant Nutrition 31:941–958. https://doi.org/10.1080/01904160802043270

Sánchez-Barrena MJ, Martínez-Ripoll M, Zhu J-K, Albert A (2005) The structure of the Arabidopsis thaliana SOS3: Molecular mechanism of sensing calcium for salt stress response. J Mol Biol 345:1253–1264. https://doi.org/10.1016/j.jmb.2004.11.025

Sánchez-Barrena MJ, Fujii H, Angulo I, Martínez-Ripoll M, Zhu J-K, Albert A (2007) The structure of the C-terminal domain of the protein kinase AtSOS2 bound to the calcium sensor AtSOS3. Mol Cell 26:427–435. https://doi.org/10.1016/j.molcel.2007.04.013

Sanders, Brownlee, Harper (1999) Communicating with calcium. Plant Cell 11:691–706. https://doi.org/10.1105/tpc.11.4.691

Sanders D, Pelloux J, Brownlee C, Harper JF (2002) Calcium at the crossroads of signaling. Plant Cell 14 Suppl:S401-17. https://doi.org/10.1105/tpc.002899

Sanyal SK, Pandey A, Pandey GK (2015) The CBL-CIPK signaling module in plants: A mechanistic perspective. Physiol Plant 155:89–108. https://doi.org/10.1111/ppl.12344

Sanz-Cobena A, Lassaletta L, Aguilera E, Prado Ad, Garnier J, Billen G, Iglesias A, Sánchez B, Guardia G, Abalos D, Plaza-Bonilla D, Puigdueta-Bartolomé I, Moral R, Galán E, Arriaga H, Merino P, Infante-Amate J, Meijide A, Pardo G, Álvaro-Fuentes J, Gilsanz C, Báez D, Doltra J, González-Ubierna S, Cayuela ML, Menéndez S, Díaz-Pinés E, Le-Noë J, Quemada M, Estellés F, Calvet S, van Grinsven HJM, Westhoek H, Sanz MJ, Gimeno BS, Vallejo A, Smith P (2017) Strategies for greenhouse gas emissions mitigation in Mediterranean agriculture: A review. Agriculture, Ecosystems & Environment 238:5–24. https://doi.org/10.1016/j.agee.2016.09.038

Sarasketa A, González-Moro MB, González-Murua C, Marino D (2016) Nitrogen Source and External Medium pH Interaction Differentially Affects Root and Shoot Metabolism in Arabidopsis. Front Plant Sci 7:29. https://doi.org/10.3389/fpls.2016.00029

Schachtman DP, Schroeder JI, Lucas WJ, Anderson JA, Gaber RF (1992) Expression of an inward-rectifying potassium channel by the Arabidopsis KAT1 cDNA. Science 258:1654–1658. https://doi.org/10.1126/science.8966547

Schortemeyer M (1997) Ammonium Tolerance and Carbohydrate Status in Maize Cultivars. Annals of Botany 79:25–30. https://doi.org/10.1006/anbo.1996.0298

Serrano R (1989) Structure and Function of Plasma Membrane ATPase. Annu Rev Plant Physiol Plant Mol Biol 40:61–94. https://doi.org/10.1146/annurev.pp.40.060189.000425

Serrano R, Kielland-Brandt MC, Fink GR (1986) Yeast plasma membrane ATPase is essential for growth and has homology with (Na+ + K+), K+- and Ca2+-ATPases. Nature 319:689–693. https://doi.org/10.1038/319689a0

Shelden MC, Dong B, Bruxelles GL de, Trevaskis B, Whelan J, Ryan PR, Howitt SM, Udvardi MK (2001) Arabidopsis ammonium transporters, AtAMT1;1 and AtAMT1;2, have different biochemical properties and functional roles. Plant and Soil 231:151–160. https://doi.org/10.1023/A:1010303813181

Shewry PR (2009) Wheat. J Exp Bot 60:1537–1553. https://doi.org/10.1093/jxb/erp058

Shewry PR, Hey SJ (2015) The contribution of wheat to human diet and health. Food Energy Secur 4:178–202. https://doi.org/10.1002/fes3.64

Shi J, Kim KN, Ritz O, Albrecht V, Gupta R, Harter K, Luan S, Kudla J (1999) Novel protein kinases associated with calcineurin B-like calcium sensors in Arabidopsis. Plant Cell 11:2393–2405. https://doi.org/10.1105/tpc.11.12.2393

Shi X, Ling H-Q (2018) Current advances in genome sequencing of common wheat and its ancestral species. The Crop Journal 6:15–21. https://doi.org/10.1016/j.cj.2017.11.001

Sohlenkamp C, Shelden M, Howitt S, Udvardi M (2000) Characterization of Arabidopsis AtAMT2, a novel ammonium transporter in plants. FEBS Lett 467:273–278. https://doi.org/10.1016/S0014-5793(00)01153-4

Sohlenkamp C, Wood CC, Roeb GW, Udvardi MK (2002) Characterization of Arabidopsis AtAMT2, a high-affinity ammonium transporter of the plasma membrane. Plant Physiol 130:1788–1796. https://doi.org/10.1104/pp.008599

Sonoda Y, Ikeda A, Saiki S, Wirén N von, Yamaya T, Yamaguchi J (2003) Distinct expression and function of three ammonium transporter genes (OsAMT1;1-1;3) in rice. Plant and Cell Physiology 44:726–734. https://doi.org/10.1093/pcp/pcg083

Stewart GR, Mann AF, Fentem PA (1980) Enzymes of glutamate formation: glutamate dehydrogenase, glutamine synthetase and glutamate syntase. In: Stumpf K, Conn EE (eds) The Biology of Plants 5:217–237

Straub D, Ludewig U, Neuhäuser B (2014) A nitrogen-dependent switch in the high affinity ammonium transport in Medicago truncatula. Plant Mol Biol 86:485–494. https://doi.org/10.1007/s11103-014-0243-4

Straub T, Ludewig U, Neuhäuser B (2017) The Kinase CIPK23 Inhibits Ammonium Transport in Arabidopsis thaliana. Plant Cell 29:409–422. https://doi.org/10.1105/tpc.16.00806

Sugiyama K, Hayakawa T, Kudo T, Ito T, Yamaya T (2004) Interaction of N-acetylglutamate kinase with a PII-like protein in rice. Plant and Cell Physiology 45:1768–1778. https://doi.org/10.1093/pcp/pch199

Sun T, Wang Y, Wang M, Li T, Zhou Y, Wang X, Wei S, He G, Yang G (2015) Identification and comprehensive analyses of the CBL and CIPK gene families in wheat (Triticum aestivum L.). BMC Plant Biol 15:269. https://doi.org/10.1186/s12870-015-0657-4

Sun C-H, Yu J-Q, Hu D-G (2017) Nitrate: A Crucial Signal during Lateral Roots Development. Front Plant Sci 8:485. https://doi.org/10.3389/fpls.2017.00485

Susan W. Gay and Katharine F. Knowlton (2009) Ammonia Emissions and Animal Agriculture

Svihus B (ed) (2014) Wheat and Rice in Disease Prevention and Health: Nutritive and Digestive Effects of Starch and Fiber in Whole Wheat. Elsevier

Szczerba MW, Britto DT, Ali SA, Balkos KD, Kronzucker HJ (2008) NH4+-stimulated and -inhibited components of K+ transport in rice (Oryza sativa L.). J Exp Bot 59:3415–3423. https://doi.org/10.1093/jxb/ern190

Tang R-J, Zhao F-G, Garcia VJ, Kleist TJ, Yang L, Zhang H-X, Luan S (2015) Tonoplast CBL-CIPK calcium signaling network regulates magnesium homeostasis in Arabidopsis. Proc Natl Acad Sci U S A 112:3134–3139. https://doi.org/10.1073/pnas.1420944112.

Thevelein JM, Geladé R, Holsbeeks I, Lagatie O, Popova Y, Rolland F, Stolz F, van de Velde S, van Dijck P, Vandormael P, van Nuland A, van Roey K, van Zeebroeck G, Yan B (2005) Nutrient sensing systems for rapid activation of the protein kinase A pathway in yeast. Biochem Soc Trans 33:253–256. https://doi.org/10.1042/BST0330253

Towler DA, Gordon JI, Adams SP, Glaser L (1988) The biology and enzymology of eukaryotic protein acylation. Annu Rev Biochem 57:69–99. https://doi.org/10.1146/annurev.bi.57.070188.000441

USGS (2019) Nitrogen and Water: Nutrients, such as nitrogen and phosphorus, are essential for plant and animal growth and nourishment, but the overabundance of certain nutrients in water can cause several adverse health and ecological effects. https://www.usgs.gov/special-topic/water-science-school/science/nitrogen-and-water?qt-science_center_objects=0#qt-science_center_objects. Accessed 31 October 2019

Vaarst M, Escudero AG, Chappell MJ, Brinkley C, Nijbroek R, Arraes NAM, Andreasen L, Gattinger A, Almeida GF de, Bossio D, Halberg N (2017) Exploring the concept of agroecological food systems in a city-region context. Agroecology and Sustainable Food Systems 42:686–711. https://doi.org/10.1080/21683565.2017.1365321

van der Eerden LJM (1982) Toxicity of ammonia to plants. Agriculture and Environment 7:223–235. https://doi.org/10.1016/0304-1131(82)90015-7

van Grinsven HJM, Berge HFM ten, Dalgaard T, Fraters B, Durand P, Hart A, Hofman G, Jacobsen BH, Lalor STJ, Lesschen JP, Osterburg B, Richards KG, Techen A-K, Vertès F, Webb J, Willems WJ (2012) Management, regulation and environmental impacts of nitrogen fertilization in northwestern Europe under the Nitrates Directive; a benchmark study. Biogeosciences 9:5143–5160. https://doi.org/10.5194/bg-9-5143-2012

Verdoucq L, Rodrigues O, Martinière A, Luu DT, Maurel C (2014) Plant aquaporins on the move: reversible phosphorylation, lateral motion and cycling. Current Opinion in Plant Biology 22:101–107. https://doi.org/10.1016/j.pbi.2014.09.011

Wang MY, Siddiqi MY, Ruth TJ, Glass A (1993) Ammonium Uptake by Rice Roots (II. Kinetics of 13NH4+ Influx across the Plasmalemma). Plant Physiol 103:1259–1267. https://doi.org/10.1104/pp.103.4.1259

Wang MY, Glass A, Shaff JE, Kochian LV (1994) Ammonium Uptake by Rice Roots (III. Electrophysiology). Plant Physiol 104:899–906. https://doi.org/10.1104/pp.104.3.899

Wegener G, Krause U (2002) Different modes of activating phosphofructokinase, a key regulatory enzyme of glycolysis, in working vertebrate muscle. Biochem Soc Trans 30:264–270

Weinl S, Kudla J (2009) The CBL-CIPK Ca(2+)-decoding signaling network: Function and perspectives. New Phytol 184:517–528. https://doi.org/10.1111/j.1469-8137.2009.02938.x

Wirén N von, Gazzarrini S, Gojon A, Frommer WB (2000) The molecular physiology of ammonium uptake and retrieval. Current Opinion in Plant Biology 3:254–261. https://doi.org/10.1016/S1369-5266(00)80074-6

Wirén N., and Merrick M. (ed) (2004) Regulation and function of ammonium carriers in bacteria, fungi, and plants, Molecular Mechanisms Controlling Transmembrane Transport. Topics in current genetics, vol 9. Springer, Berlin, Heidelberg

Wood CC, Porée F, Dreyer I, Koehler GJ, Udvardi MK (2006) Mechanisms of ammonium transport, accumulation, and retention in ooyctes and yeast cells expressing Arabidopsis AtAMT1;1. FEBS Lett 580:3931–3936. https://doi.org/10.1016/j.febslet.2006.06.026

Wu X, Liu T, Zhang Y, Duan F, Neuhäuser B, Ludewig U, Schulze WX, Yuan L (2019) Ammonium and nitrate regulate NH4+ uptake activity of Arabidopsis ammonium transporter AtAMT1;3 via phosphorylation at multiple C-terminal sites. J Exp Bot. https://doi.org/10.1093/jxb/erz230

Wu XN, Xi L, Pertl-Obermeyer H, Li Z, Chu L-C, Schulze WX (2017) Highly Efficient Single-Step Enrichment of Low Abundance Phosphopeptides from Plant Membrane Preparations. Front Plant Sci 8:1673. https://doi.org/10.3389/fpls.2017.01673

Xu J, Li H-D, Chen L-Q, Wang Y, Liu L-L, He L, Wu W-H (2006) A protein kinase, interacting with two calcineurin B-like proteins, regulates K+ transporter AKT1 in Arabidopsis. Cell 125:1347–1360. https://doi.org/10.1016/j.cell.2006.06.011

Xuan YH, Kumar V, Han X, Kim SH, Jeong JH, Kim CM, Gao Y, Han C-D (2019) CBL-INTERACTING PROTEIN KINASE 9 regulates ammonium-dependent root growth downstream of IDD10 in rice (Oryza sativa). Annals of Botany 124:947–960. https://doi.org/10.1093/aob/mcy242

Yan P, Peng H, Yan L, Zhang S, Chen A, Lin K (2019) Spatial variability in soil pH and land use as the main influential factor in the red beds of the Nanxiong Basin, China. PeerJ 7:e6342. https://doi.org/10.7717/peerj.6342

Yang X-e, Wu X, Hao H-l, He Z-l (2008) Mechanisms and assessment of water eutrophication. J Zhejiang Univ Sci B 9:197–209. https://doi.org/10.1631/jzus.B0710626

Yasuda S, Aoyama S, Hasegawa Y, Sato T, Yamaguchi J (2017) Arabidopsis CBL-Interacting Protein Kinases Regulate Carbon/Nitrogen-Nutrient Response by Phosphorylating Ubiquitin Ligase ATL31. Mol Plant 10:605–618. https://doi.org/10.1016/j.molp.2017.01.005

Yuan L, Loqué D, Kojima S, Rauch S, Ishiyama K, Inoue E, Takahashi H, Wirén N von (2007) The organization of high-affinity ammonium uptake in Arabidopsis roots depends on the spatial arrangement and biochemical properties of AMT1-type transporters. Plant Cell 19:2636–2652. https://doi.org/10.1105/tpc.107.052134

Yuan L, Gu R, Xuan Y, Smith-Valle E, Loqué D, Frommer WB, Wirén N von (2013) Allosteric regulation of transport activity by heterotrimerization of Arabidopsis ammonium transporter complexes in vivo. Plant Cell 25:974–984. https://doi.org/10.1105/tpc.112.108027

Zhang H, Yang B, Liu W-Z, Li H, Wang L, Wang B, Deng M, Liang W, Deyholos MK, Jiang Y-Q (2014) Identification and characterization of CBL and CIPK gene families in canola (Brassica napus L.). BMC Plant Biol 14:8. https://doi.org/10.1186/1471-2229-14-8

Zhang J, Wei J, Li D, Kong X, Rengel Z, Chen L, Yang Y, Cui X, Chen Q (2017) The Role of the Plasma Membrane H+-ATPase in Plant Responses to Aluminum Toxicity. Front Plant Sci 8:1757. https://doi.org/10.3389/fpls.2017.01757

Zhang K, Wu Y, Hang H (2019a) Differential contributions of NO3-/NH4+ to nitrogen use in response to a variable inorganic nitrogen supply in plantlets of two Brassicaceae species in vitro. Plant Methods 15:86. https://doi.org/10.1186/s13007-019-0473-1

Zhang Y-Y, Wu W, Liu H (2019b) Factors affecting variations of soil pH in different horizons in hilly regions. PLoS ONE 14:e0218563. https://doi.org/10.1371/journal.pone.0218563

Zhao S, Liu J-J, Banerjee S, Zhou N, Zhao Z-Y, Zhang K, Tian C-Y (2018) Soil pH is equally important as salinity in shaping bacterial communities in saline soils under halophytic vegetation. Sci Rep 8:4550. https://doi.org/10.1038/s41598-018-22788-7

Zheleznova EE, Markham P, Edgar R, Bibi E, Neyfakh AA, Brennan RG (2000) A structure-based mechanism for drug binding by multidrug transporters. Trends in Biochemical Sciences 25:39–43. https://doi.org/10.1016/s0968-0004(99)01514-5

Zheng T, Qi P-F, Cao Y-L, Han Y-N, Ma H-L, Guo Z-R, Wang Y, Qiao Y-Y, Hua S-Y, Yu H-Y, Wang J-P, Zhu J, Zhou C-Y, Zhang Y-Z, Chen Q, Kong L, Wang J-R, Jiang Q-T, Yan Z-H, Lan X-J, Fan G-Q, Wei Y-M, Zheng Y-L (2018) Mechanisms of wheat (Triticum aestivum) grain storage proteins in response to nitrogen application and its impacts on processing quality. Sci Rep 8:11928. https://doi.org/10.1038/s41598-018-30451-4

Zhong Y, Yan W, Chen J, Shangguan Z (2014) Net ammonium and nitrate fluxes in wheat roots under different environmental conditions as assessed by scanning ion-selective electrode technique. Sci Rep 4:7223. https://doi.org/10.1038/srep07223

Zhu Z, Gerendás J, Bendixen R, Schinner K, Tabrizi H, Sattelmacher B, Hansen U-P (2000) Different Tolerance to Light Stress in NO3−- and NH4+-Grown Phaseolus vulgaris L. Plant Biology 2:558–570. https://doi.org/10.1055/s-2000-7498

Zhu XF, Cai WH, Jung JH, Xuan YH (2015) NH4+-mediated Protein Phosphorylation in Rice Roots. Acta Biologica Cracoviensia s. Botanica 57:38–48. https://doi.org/10.1515/abcsb-2015-0022

Zi Y, Ding J, Song J, Humphreys G, Peng Y, Li C, Zhu X, Guo W (2018) Grain Yield, Starch Content and Activities of Key Enzymes of Waxy and Non-waxy Wheat (Triticum aestivum L.). Sci Rep 8:4548. https://doi.org/10.1038/s41598-018-22587-0

Zörb C, Ludewig U, Hawkesford MJ (2018) Perspective on Wheat Yield and Quality with Reduced Nitrogen Supply. Trends Plant Sci 23:1029–1037. https://doi.org/10.1016/j.tplants.2018.08.012

7. APPENDIX

Table S 1. Gene ID, Database location, and the Ammonium transporters of *Triticum aestivum, Oryza sativa, Arabidopsis thaliana, Medicago truncatula,* and *Saccharomyces cerevisiae*

	Database & Dene ID		
Gene	Plant.ensemble.org	Arabidopis.org	yeastgenome.org
AtAMT1;1	-	AT4G13510.1	-
AtAMT1;2	-	AT1G64780.1	-
AtAMT1;3	-	AT3G24300.1	-
AtAMT1;4	-	AT4G28700	-
AtAMT1;5	-	AT3G24290	-
AtAMT2;1	-	AT2G38290.1	-
ScMEP1	-	-	SGD:S000003353
ScMEP2	-	-	SGD:S000005086
ScMEP3		-	SGD:S000006342
MtAMT1;1	MTR_1g045550	-	-
MtAMT1;2	MTR_7g113340	-	-
MtAMT1;3	MTR_7g098930	-	-
MtAMT1;4	MTR_1g079760	-	-
MtAMT2;1	MTR_7g069640	-	-
MtAMT2;2	MTR_8g095040	-	-
MtAMT2;3	MTR_8g074750	-	-
MtAMT2;4	MTR_7g115050	-	-
MtAMT2;5	MTR_1g036410	-	-
MtAMT2;6	MTR_4g017820	-	-
OsAMT1;1	Os04t0509600-01	-	-
OsAMT1;2	Os02t0620600-01	-	-
OsAMT1;3	Os02t0620500-00	-	-
OsAMt2;1	Os05t0468700-01	-	-
OsAMT2;2	Os01t0831900-01	-	-
OsAMT2;3	Os01t0831300-01	-	-
OsAMT3;1	Os01t0870300-02	-	-
OsAMT3;2	Os03t0838400-01	-	-
OsAMT4;1	Os03t0749000-00	-	-
TaAMT1;1	TraesCS2A02G365000.1	-	-
TaAMT1;1	TraesCS2B02G383600.1	-	-
TaAMT1;1	TraesCS2D02G362900.1	-	-
TaAMT1;2	TraesCS6A02G226800.1	-	-
TaAMT1;2	TraesCS6B02G254800.1	-	-
TaAMT1;2	TraesCS6D02G208200.1	-	-
TaAMT2;1	TraesCS4A02G352900.1	-	-
TaAMT2;1	TraesCS5B02G520200.1	-	-
TaAMT2;1	TraesCS5D02G519400.1	-	-
TaAMT2;2	TraesCS5A02G388100.1	-	-
TaAMT2;2	TraesCS5B02G393200.1	-	-
TaAMT2;2	TraesCS5D02G398200.1	-	-
TaAMT2;3	TraesCS3A02G381600.1	-	-

TaAMT2;3	TraesCS3B02G414300.1	-	-
TaAMT2;3	TraesCS3D02G374800.1	-	-
TaAMT2;4	TraesCS1D02G296600.1	-	-
TaAMT2;4	TraesCS1A02G295300.1	-	-
TaAMT2;5	TraesCS3A02G350800.1	-	-
TaAMT2;5	TraesCS3B02G383400.1	-	-
TaAMT2;5	TraesCS3D02G344800.1	-	-
TaAMT2;6	TraesCS3A02G381700.1	-	-

Table S 2. Gene ID of the CBL proteins of *Triticum aestivum* (including homologs), *and the* AtCBL1 of *Arabidopsis thaliana*

	Gene name	Gene ID
	AtCBL1	AT4G17615
1	TaCBL1	TraesCS1B02G229300.1
2	TaCBL1	TraesCS1A02G215800.1
3	TaCBL1	TraesCSU02G178500.1
4	TaCBL2	TraesCS5A02G060600.1
5	TaCBL2	TraesCS5B02G071500.1
6	TaCBL2	TraesCS5D02G072100.1
7	TaCBL3	TraesCS4A02G245500.1
8	TaCBL3	TraesCS4B02G069900.1
9	TaCBL3	TraesCS4D02G068700.1
10	TaCBL4	TraesCS1D02G358400.1
11	TaCBL4	TraesCS1B02G370900.1
12	TaCBL12	TraesCS1D02G358200.1
13	TaCBL6	TraesCS5B02G124300.1
14	TaCBL6	TraesCS5D02G132500.1
15	TaCBL6	TraesCS5A02G124700.1
16	TaCBL7	TraesCS1D02G261200.1
17	TaCBL7	TraesCS1A02G261200.1
18	TaCBL7	TraesCS1B02G272000.1
19	TaCBL9	TraesCS3A02G053300.1
20	TaCBL9	TraesCS3B02G064500.1
21	TaCBL10	TraesCS3A02G208300.1
22	TaCBL10	TraesCS3D02G211300.1
23	TaCBL10	TraesCS3B02G235500.1
24	TaCBL12	TraesCS1B02G370500.1
25	TaCBL12	TraesCS1A02G352200.1
26	TaCBL4	TraesCS1B02G370800.1
27	TaCBL14	TraesCS1D02G346500.1
28	TaCBL14	TraesCS1D02G346400.1
29	TaCBL14	TraesCS1B02G357200.1
30	TaCBL15	TraesCS3D02G328300.1
31	TaCBL15	TraesCS3A02G335000.1
32	TaCBL15	TraesCS3B02G365900.1

33	TaCBL13	TraesCS1B02G370600.1
34	TaCBL5	TraesCS5A02G545500.1
35	TaCBL5	TraesCSU02G129500.1
36	TaCBL5	TraesCS4B02G379200.1
37	TaCBL11	TraesCS4D02G162400.1
38	TaCBL16	TraesCS5B02G269200.1
39	TaCBL16	TraesCS5D02G277000.1
40	TaCBL16	TraesCS5A02G269000.1
41	TaCBL17	TraesCS6A02G368000.1
42	TaCBL17	TraesCS6D02G350800.1

Table S 3. Gene ID of the CIPK proteins of *Triticum aestivum* (including homeologs), *and the* AtCIPK23 of *Arabidopsis thaliana*

	Gene name	Gene ID
	AtCIPK23	AT1G30270
1	TaCIPK2	TraesCS2D02G106800.1
2	TaCIPK2	TraesCS2B02G123900.1
3	TaCIPK3	TraesCS2D02G097700.1
4	TaCIPK3	TraesCS2B02G114000.1
5	TaCIPK3	TraesCS2A02G098300.1
6	TaCIPK5	TraesCS3D02G151500.1
7	TaCIPK5	TraesCS3B02G169300.1
8	TaCIPK5	TraesCS3A02G135500.1
9	TaCIPK7	TraesCS5A02G377900.1
10	TaCIPK7	TraesCS5D02G387900.1
11	TaCIPK7	TraesCS5B02G381500.1
12	TaCIPK6	TraesCS4D02G113100.1
13	TaCIPK6	TraesCS4B02G115400.1
14	TaCIPK6	TraesCS4A02G200000.1
15	TaCIPK8	TraesCS3A02G200900.1
16	TaCIPK8	TraesCS3D02G203000.1
17	TaCIPK8	TraesCS3B02G225800.1
18	TaCIPK9	TraesCS4B02G319900.1
19	TaCIPK9	TraesCS5A02G492000.1
20	TaCIPK9	TraesCS4D02G316500.1
21	TaCIPK10	TraesCS4D02G170700.1
22	TaCIPK10	TraesCS4A02G136500.1
23	TaCIPK11	TraesCS3B02G377800.1
24	TaCIPK11	TraesCS3D02G339800.1
25	TaCIPK11	TraesCS3A02G346100.1
26	TaCIPK13	TraesCS3D02G136700.1
27	TaCIPK13	TraesCS3B02G153800.1
28	TaCIPK13	TraesCS3A02G135700.1
29	TaCIPK14	TraesCS4B02G120400.1
30	TaCIPK14	TraesCS4D02G118500.1

31	TaCIPK14	TraesCS4A02G194800.1
32	TaCIPK15	TraesCS5D02G144800.1
33	TaCIPK15	TraesCS5A02G148000.1
34	TaCIPK15	TraesCS5B02G146500.1
35	TaCIPK16	TraesCS5B02G223900.1
36	TaCIPK16	TraesCS5D02G232600.1
37	TaCIPK16	TraesCS5A02G225300.1
38	TaCIPK17	TraesCS1A02G080600.1
39	TaCIPK17	TraesCS1D02G082500.1
40	TaCIPK17	TraesCS1B02G098600.1
41	TaCIPK18	TraesCS1A02G080700.1
42	TaCIPK18	TraesCS1D02G082600.1
43	TaCIPK17	TraesCS1A02G080500.1
44	TaCIPK19	TraesCS3A02G305900.1
45	TaCIPK19	TraesCS3B02G330600.1
46	TaCIPK20	TraesCS1B02G347100.1
47	TaCIPK20	TraesCS1A02G333800.1
48	TaCIPK21	TraesCS2A02G150600.1
49	TaCIPK21	TraesCS2D02G155700.1
50	TaCIPK21	TraesCS2B02G175800.1
51	TaCIPK22	TraesCS2D02G537400.1
52	TaCIPK22	TraesCS2A02G536100.1
53	TaCIPK22	TraesCS2B02G566800.1
54	TaCIPK23	TraesCS2A02G251800.1
55	TaCIPK23	TraesCS2B02G271700.1
56	TaCIPK23	TraesCS2D02G252600.1
57	TaCIPK24	TraesCS7B02G279300.1
58	TaCIPK24	TraesCS7D02G374400.1
59	TaCIPK24	TraesCS7A02G377600.1
60	TaCIPK25	TraesCS7B02G275800.1
61	TaCIPK25	TraesCS7A02G352200.1
62	TaCIPK26	TraesCS6D02G124200.1
63	TaCIPK26	TraesCS6A02G135100.1
64	TaCIPK26	TraesCS6B02G163100.1
65	TaCIPK27	TraesCS5B02G223800.1
66	TaCIPK27	TraesCS5A02G225200.1
67	TaCIPK27	TraesCS5D02G232500.1
68	TaCIPK28	TraesCS1A02G299600.1
69	TaCIPK28	TraesCS1D02G298500.1
70	TaCIPK28	TraesCS1B02G309400.1
71	TaCIPK29	TraesCS2D02G107100.1
72	TaCIPK29	TraesCS2B02G124100.1
73	TaCIPK29	TraesCS2A02G106500.1
74	TaCIPK30	TraesCS3A02G306000.1
75	TaCIPK30	TraesCS3D02G295900.1
76	TaCIPK30	TraesCS3B02G330500.1
77	TaCIPK31	TraesCS4B02G178100.1
78	TaCIPK31	TraesCS4D02G179700.1

79	TaCIPK31	TraesCS4A02G126800.1
80	TaCIPK32	TraesCS4D02G126200.1
81	TaCIPK32	TraesCS4A02G187300.1
82	TaCIPK32	TraesCS4B02G131000.1
83	TaCIPK22	TraesCS2B02G567900.1
84	TaCIPK22	TraesCS2D02G537600.1

Table S 4. A table showing the fold change of the 1mM (6h) treatment relative to the Nitrogen starvation (-N) treatment. Log2FC was computed using the normalized ion intensity of the listed proteotypic peptide. Data presented was filtered using the log2FC cutoff score of Log2FC ≥ 1.5 or Log2FC ≤ -1.5.

Leading protein	AGI	Fasta	Peptide	Log2FC
Traes_7AS_28D654039.1	AT5G59540.1	1-aminocyclopropane-1-carboxylate oxidase homolog 4, putative, expressed	_(ac)MMARPS(ph)EEEK_	-2.3
Traes_2DS_D09901183.1	AT5G10360.1	40S ribosomal protein S6, putative, expressed	_S(ph)KLS(ph)AATKAPAASA_	-1.8
Traes_2DS_D09901183.1	AT5G10360.1	40S ribosomal protein S6, putative, expressed	_SKLSAAT(ph)KAPAASA_	-2.4
Traes_2AL_DD284DEA9.1	AT3G53420.1	aquaporin protein, putative, expressed	_FGSS(ph)ASFGSR_	2.8
Traes_2AL_DD284DEA9.1	AT3G53420.1	aquaporin protein, putative, expressed	_FGSSAS(ph)FGS(ph)R_	-2.2
Traes_2AL_DD284DEA9.1	AT3G53420.1	aquaporin protein, putative, expressed	_FGSSAS(ph)FGSR_	-5.8
Traes_2BL_D274D68D2.5	AT5G60660.1	aquaporin protein, putative, expressed	_LGSS(ph)ASFGRS_	6.5
Traes_2DL_039832D76.1	AT5G60660.1	aquaporin protein, putative, expressed	_LGS(ph)SASFGRN_	1.7
Traes_7DL_98EC3AE06.9	AT5G02560.1	Core histone H2A/H2B/H3/H4 domain containing protein, putative, expressed	_(ac)MDAS(ph)ATGAGAK_	-1.6
Traes_2DL_2924C6399.1	AT5G49890.1	expressed protein	_TSGS(ph)FVLRR_	2.3
Traes_2DL_489652871.3	AT1G78880.1	expressed protein	_SS(ph)GPQS(ph)GGVTPMAR_	-2.0
Traes_4BL_09186DE10.1	AT5G24530.1	flavonol synthase/flavanone 3-hydroxylase, putative, expressed	_LSTS(ph)FNVR_	3.0
Traes_4BL_09186DE10.1	AT5G24530.1	flavonol synthase/flavanone 3-hydroxylase, putative, expressed	_LSTS(ph)FNVRK_	-1.6

Traes_2AL_6C0963A18.1	AT3G43660.1	integral membrane protein, putative, expressed	_GGGGGIDS(ph)DSDVDFAGR_	2.3
Traes_4AS_E609B22C1.2	AT1G74910.2	mannose-1-phosphate guanyltransferase, putative, expressed	_RVS(ph)SFEALQSATK_	2.0
Traes_4BL_7091749BF.1	AT1G04120.1	multidrug resistance-associated protein, putative, expressed	_LTPSVS(ph)NIDNLK_	-1.8
Traes_1DL_69D4A3E8B.2	AT3G51800.3	peptidase, M24 family protein, putative, expressed	_(ac)S(ph)S(ph)DEEVREEK_	-2.2
Traes_1DL_69D4A3E8B.2	AT3G51800.3	peptidase, M24 family protein, putative, expressed	_(ac)S(ph)SDEEVREEK_	4.0
Traes_1DL_69D4A3E8B.2	AT3G51800.3	peptidase, M24 family protein, putative, expressed	_(ac)S(ph)SDEEVREEKELDLSSNEVVTK_	2.1
Traes_1DL_69D4A3E8B.2	AT3G51800.3	peptidase, M24 family protein, putative, expressed	_(ac)SS(ph)DEEVREEKELDLSSNEVVTK_	2.2
Traes_6DS_3B0856CD9.7	AT3G63400.3	peptidyl-prolyl cis-trans isomerase, putative, expressed	_LSIDS(ph)S(ph)EDEGNEEK_	-3.1
Traes_2AL_2C50DEE4C.1	AT4G30190.1	plasma membrane ATPase, putative, expressed	_GLDIDTINQNYT(ph)V_	-1.5
Traes_2AL_47B1A5BF2.1	AT3G61260.1	remorin, putative, expressed	_VES(ph)EKRNSLIK_	-1.6
Traes_6AS_62FDBBB97.2	AT5G64270.1	splicing factor 3B subunit 1, putative, expressed	_LPGGLVT(ph)PT(ph)PK_	1.8
Traes_3B_3D1F3FBC5.4	AT3G53500.2	splicing factor, arginine/serine-rich, putative, expressed	_ARS(ph)PT(ph)PPGS(ph)RS(ph)PAPR_	-3.5

Traes_1DS_474BD1144.1	AT1G32400.3	tetraspanin family protein, putative, expressed	_AM(ox)NKPAEYDS(ph)DDEIIGTAR_	2.4
Traes_1AL_FA799A213.1	AT1G19450.1	transporter family protein, putative, expressed	_LGS(ph)SAYGLR_	1.9
Traes_5DL_A3084808F.2	AT3G29185.1	WRKY4, expressed	_LAASAVPHPRS(ph)S(ph)RR_	-2.5

Table S 5. A table showing the fold change of the 1mM (6h + 30min) treatment relative to the Nitrogen starvation (-N) treatment. Log2FC was computed using the normalized ion intensity of the listed proteotypic peptide. Data presented was filtered using the log2FC cutoff score of Log2FC ≥ 1.5 or Log2FC ≤ -1.5.

Leading protein	AGI	Fasta	Peptide	Log2FC
Traes_7AS_28D654039.1	AT5G59540.1	1-aminocyclopropane-1-carboxylate oxidase homolog 4, putative, expressed	_(ac)MMARPS(ph)EEEK_	-5.5
Traes_2DS_D09901183.1	AT5G10360.1	40S ribosomal protein S6, putative, expressed	_S(ph)KLS(ph)AATKAPAASA_	-1.8
Traes_2BS_50BE66985.1	AT3G50690.1	acidic leucine-rich nuclear phosphoprotein 32-related protein 1, putative, expressed	_AVEAALHTAGEGSSS(ph)PAR_	2.6
Traes_2DL_955B1070C.1	AT5G57330.1	aldose 1-epimerase, putative, expressed	_(ac)AGASS(ph)PPPT(ph)PKSPK_	-1.9
Traes_2BL_F1A254464.1	AT4G13510.1	ammonium transporter protein, putative, expressed	_ISAEDEM(ox)AGM(ox)DLT(ph)R_	1.7

Traes_6DL_3286E5385.1	AT4G13510.1	ammonium transporter protein, putative, expressed	_SAQTSQVAADATS(ph)PSS(ph)SV_	-1.8
Traes_2AL_DD284DEA9.1	AT3G53420.1	aquaporin protein, putative, expressed	_FGS(ph)SASFGSR_	-1.8
Traes_2AL_DD284DEA9.1	AT3G53420.1	aquaporin protein, putative, expressed	_FGSS(ph)ASFGSR_	3.5
Traes_2AL_DD284DEA9.1	AT3G53420.1	aquaporin protein, putative, expressed	_FGSSAS(ph)FGS(ph)R_	-2.4
Traes_2AL_DD284DEA9.1	AT3G53420.1	aquaporin protein, putative, expressed	_FGSSAS(ph)FGSR_	-6.2
Traes_2BS_D8EC76A3B.2	AT2G16850.1	aquaporin protein, putative, expressed	_ALGS(ph)FRSS(ph)RS(ph)N_	-2.2
Traes_5BL_E1F6D3732.2	AT5G66560.1	BTBN9 - Bric-a-Brac, Tramtrack, Broad Complex BTB domain with non-phototropic hypocotyl 3 NPH3 and coiled-coil domains, expressed	_AITGTLLAS(ph)TASPR_	-2.4
Traes_5BL_B8C3AE4A5.1	AT5G33280.1	chloride channel protein, putative, expressed	_S(ph)ATNNIS(ph)QVAMVGSK_	-2.3
Traes_7DL_98EC3AE06.9	AT5G02560.1	Core histone H2A/H2B/H3/H4 domain containing protein, putative, expressed	_(ac)MDAS(ph)ATGAGAK_	-1.9
Traes_7BL_D90A3700B.1	AT5G55310.1	DNA topoisomerase 1, putative, expressed	_IVQSNDDS(ph)EDEKPLASR_	-1.9
Traes_1BL_9DA22ABF9.1	AT5G20100.1	expressed protein	_VSPALDPPS(ph)PR_	1.9
Traes_2DL_2924C6399.1	AT5G49890.1	expressed protein	_TSGS(ph)FVLRR_	2.3
Traes_2DL_99A21BFBF.1	AT4G20410.1	gamma-soluble NSF attachment protein, putative, expressed	_DVGGDDGDS(ph)LDEDDLT_	-2.0
Traes_3B_386880998.1	AT5G49760.1	leucine-rich repeat family protein, putative, expressed	_SQS(ph)FAS(ph)LDMK_	-2.8

Traes_2BL_B09F6D195.1	AT5G63190.1	MA3 domain containing protein, expressed	_(ac)AAEDGARS(ph)PTR_	-1.9
Traes_4AS_E609B22C1.2	AT1G74910.2	mannose-1-phosphate guanyltransferase, putative, expressed	_RVSS(ph)FEALQSATK_	-1.8
Traes_4BL_7091749BF.1	AT1G04120.1	multidrug resistance-associated protein, putative, expressed	_LTPSVS(ph)NIDNLK_	-2.0
Traes_1DL_69D4A3E8B.2	AT3G51800.3	peptidase, M24 family protein, putative, expressed	_(ac)S(ph)S(ph)DEEVREEK_	-3.8
Traes_1DL_69D4A3E8B.2	AT3G51800.3	peptidase, M24 family protein, putative, expressed	_(ac)S(ph)SDEEVREEKELDLSSNEVVTK_	1.6
Traes_5AL_33E5EE51F.5	AT1G79570.1	protein kinase domain containing protein, expressed	_S(ph)VGTGIINPQIR_	-1.6
Traes_7DL_C206F8511.2	AT4G35785.2	RNA recognition motif containing protein, expressed	_GYS(ph)PHRS(ph)PPPYGGR_	-2.0
Traes_1BL_38FE8B094.11	AT5G42820.2	splicing factor U2AF, putative, expressed	_YGGS(ph)PPRR_	2.2
Traes_1BS_15F9D276D.3	AT3G28730.1	SSRP1-like FACT complex subunit, putative, expressed	_GAGAAPVDVDS(ph)ADGS(ph)SD_	-2.4
Traes_1BS_15F9D276D.3	AT3G28730.1	SSRP1-like FACT complex subunit, putative, expressed	_GAGAAPVDVDSADGS(ph)SD_	-3.9
Traes_1DS_474BD1144.1	AT1G32400.3	tetraspanin family protein, putative, expressed	_AM(ox)NKPAEYDS(ph)DDEIIGTAR_	2.8
Traes_1AL_0B9EA6007.4	AT2G17200.1	ubiquitin family protein, putative, expressed	_GGAGDGEGAGSES(ph)PPSGAR_	-2.4

Table S 6. A table showing the fold change of the 10 mM (6h + 30min) treatment relative to the Nitrogen starvation (-N) treatment. Log2FC was computed using the normalized ion intensity of the listed proteotypic peptide. Data presented was filtered using the log2FC cutoff score of Log2FC ≥ 1.5 or Log2FC ≤ -1.5.

Leading protein	AGI	Fasta	Peptide	Log2FC
Traes_7AS_28D654039.1	AT5G59540.1	1-aminocyclopropane-1-carboxylate oxidase homolog 4, putative, expressed	_(ac)MMARPS(ph)EEEK_	-5.8
Traes_2AL_DD284DEA9.1	AT3G53420.1	aquaporin protein, putative, expressed	_ASATKFGS(ph)SAS(ph)FGSR_	1.6
Traes_2AL_DD284DEA9.1	AT3G53420.1	aquaporin protein, putative, expressed	_ASATKFGS(ph)SASFGSR_	1.8
Traes_2AL_DD284DEA9.1	AT3G53420.1	aquaporin protein, putative, expressed	_FGSS(ph)ASFGSR_	2.4
Traes_2AL_DD284DEA9.1	AT3G53420.1	aquaporin protein, putative, expressed	_FGSSAS(ph)FGS(ph)R_	-1.8
Traes_2BL_D274D68D2.5	AT5G60660.1	aquaporin protein, putative, expressed	_LGSS(ph)ASFGRS_	5.2
Traes_2BL_D274D68D2.5	AT5G60660.1	aquaporin protein, putative, expressed	_LGSSAS(ph)FGR_	-1.5
Traes_2BS_D8EC76A3B.2	AT2G16850.1	aquaporin protein, putative, expressed	_ALGS(ph)FRS(ph)SR_	-2.5
Traes_2DL_039832D76.1	AT5G60660.1	aquaporin protein, putative, expressed	_LGSSAS(ph)FGRN_	-1.5
Traes_5DS_643ED07F6.3	AT2G39010.1	aquaporin protein, putative, expressed	_GYGS(ph)FRS(ph)NA_	1.7
Traes_2AL_F5AF1DBC9.1	AT4G31880.1	AT hook motif family protein, expressed	_VAES(ph)SDEEEEEEEPVSAK_	-1.5
Traes_5BL_57CBDD724.1	AT1G09020.1	CBS domain containing membrane protein, putative, expressed	_MGS(ph)LSDGALQEGSPR_	-2.7
Traes_5BL_B8C3AE4A5.1	AT5G33280.1	chloride channel protein, putative, expressed	_S(ph)ATNNIS(ph)QVAMVGSK_	-1.7
Traes_5DL_9D2643A18.2	AT1G31970.1	DEAD-box ATP-dependent RNA helicase, putative, expressed	_ITFGDS(ph)DEE_	-2.6
Traes_2BL_F855555E8.2	AT1G25530.1	expressed protein	_(ac)GS(ph)PSVVLPK_	-2.2

Traes_2DL_2924C6399.1	AT5G49890.1	expressed protein	_TSGS(ph)FVLRR_	2.6
Traes_2DL_489652871.3	AT1G78880.1	expressed protein	_SS(ph)GPQS(ph)GGVTPMAR_	-2.6
Traes_4AL_DD344FC87.5	AT5G60720.1	expressed protein	_GFS(ph)SS(ph)T(ph)LLTK_	-1.7
Traes_2AL_3C99F42A5.1	AT1G19870.1	IQ calmodulin-binding motif family protein, putative, expressed	_SNS(ph)SSFLDAPSK_	-1.9
Traes_2DL_B2963E457.2	AT1G19870.1	IQ calmodulin-binding motif family protein, putative, expressed	_SNS(ph)SSFLDVPSK_	-1.5
Traes_3AL_31EAD29CE.2	AT1G74690.1	IQ calmodulin-binding motif family protein, putative, expressed	_VGS(ph)DTQISPEK_	-3.6
Traes_2DL_3D83B32F9.1	AT5G05850.1	leucine rich repeat containing protein, expressed	_SMAAAAAES(ph)PQAS(ph)TPK_	1.5
Traes_3B_386880998.1	AT5G49760.1	leucine-rich repeat family protein, putative, expressed	_SQS(ph)FASLDMK_	-1.7
Traes_4AS_E609B22C1.2	AT1G74910.2	mannose-1-phosphate guanyltransferase, putative, expressed	_VSS(ph)FEALQSATK_	-1.6
Traes_3B_4E8E69A20.5	AT5G20490.2	myosin, putative, expressed	_QQAVAIS(ph)PTAK_	-2.6
Traes_1DL_69D4A3E8B.2	AT3G51800.3	peptidase, M24 family protein, putative, expressed	_(ac)S(ph)S(ph)DEEVREEK_	-1.8
Traes_1DL_69D4A3E8B.2	AT3G51800.3	peptidase, M24 family protein, putative, expressed	_(ac)S(ph)SDEEVREEK_	3.9
Traes_1DL_69D4A3E8B.2	AT3G51800.3	peptidase, M24 family protein, putative, expressed	_(ac)S(ph)SDEEVREEKELDLSSNEVVTK_	2.9

Traes_1DL_69D4A3E8B.2	AT3G51800.3	peptidase, M24 family protein, putative, expressed	_(ac)SS(ph)DEEVREEKELDLSSNEVVTK_	3.3
Traes_4DS_717A43204.1	AT2G48010.1	protein kinase domain containing protein, expressed	_AAAAALAADS(ph)R_	-1.5
Traes_4DS_BCEF8A384.2	AT5G60460.1	protein transport protein Sec61 subunit beta, putative, expressed	_T(ph)SSSASGGGGFSGGGGNNM(ox)LR_	-1.5
Traes_4DS_BCEF8A384.2	AT5G60460.1	protein transport protein Sec61 subunit beta, putative, expressed	_TSSS(ph)ASGGGGFSGGGGNNMLR_	-4.2
Traes_2AL_58214CDDF.4	AT4G11790.1	ranBP1 domain containing protein, expressed	_AAEASADADEDAEAEQPSS(ph)PSVK_	-1.7
Traes_2AL_A9D66A1CD.3	AT2G19130.1	serine/threonine-protein kinase receptor precursor, putative, expressed	_LLNAITAGVGS(ph)PTSDT_	-1.7
Traes_3B_3D1F3FBC5.4	AT3G53500.2	splicing factor, arginine/serine-rich, putative, expressed	_ARS(ph)PT(ph)PPGS(ph)RS(ph)PAPR_	-2.6
Traes_1BS_15F9D276D.3	AT3G28730.1	SSRP1-like FACT complex subunit, putative, expressed	_GAGAAPVDVDS(ph)ADGS(ph)SD_	-2.7
Traes_1DS_474BD1144.1	AT1G32400.3	tetraspanin family protein, putative, expressed	_AM(ox)NKPAEYDS(ph)DDEIIGTAR_	4.4
Traes_4AS_125EAE3ED.1	AT3G19770.1	vacuolar sorting protein, putative, expressed	_ASGNS(ph)DVNLPLK_	-1.6
Traes_6DL_3FBA5B70E.1	AT3G13300.2	WD domain, G-beta repeat domain containing protein, expressed	_IQDDSIS(ph)SPR_	-2.1

Table S 7. A table showing the fold change of the 1 mM (6h + 30min) treatment relative to the 1mM (6h) treatment. Log2FC was computed using the normalized ion intensity of the listed proteotypic peptide. Data presented was filtered using the log2FC cutoff score of Log2FC ≥ 1.5 or Log2FC ≤ -1.5.

Leading protein	AGI	Fasta	Peptide	Log2FC
Traes_7AS_28D654039.1	AT5G59540.1	1-aminocyclopropane-1-carboxylate oxidase homolog 4, putative, expressed	_(ac)MMARPS(ph)EEEK_	-3.2
Traes_7DL_695A3E829.1	AT3G16340.1	ABC-2 type transporter, putative, expressed	_VMS(ph)VGS(ph)NEAAPR_	-1.8
Traes_2DL_955B1070C.1	AT5G57330.1	aldose 1-epimerase, putative, expressed	_(ac)AGASS(ph)PPPT(ph)PKSPK_	-1.6
Traes_6DL_3286E5385.1	AT4G13510.1	ammonium transporter protein, putative, expressed	_SAQTSQVAADAT(ph)SPSSSV_	-1.8
Traes_6DL_3286E5385.1	AT4G13510.1	ammonium transporter protein, putative, expressed	_SAQTSQVAADATS(ph)PSS(ph)SV_	-2.6
Traes_2AL_DD284DEA9.1	AT3G53420.1	aquaporin protein, putative, expressed	_FGS(ph)SASFGSR_	-2.2
Traes_2BL_D274D68D2.5	AT5G60660.1	aquaporin protein, putative, expressed	_LGSS(ph)ASFGRS_	-7.0
Traes_6AL_00EDAC7DB.3	AT4G00430.1	aquaporin protein, putative, expressed	_LGANRYS(ph)ERQPIGTAAQGGGADEK_	1.8
Traes_2DL_CA10E09CD.2	AT4G31880.1	AT hook motif family protein, expressed	_IVREDS(ph)PVSSAK_	-2.0
Traes_5BL_E1F6D3732.2	AT5G66560.1	BTBN9 - Bric-a-Brac, Tramtrack, Broad Complex BTB domain with non-phototropic hypocotyl 3 NPH3 and coiled-coil domains, expressed	_AITGTLLAS(ph)TASPR_	-2.0
Traes_6DS_85BB674BE.3	AT3G52870.1	calmodulin-binding protein, putative, expressed	_TLS(ph)GGLQSPR_	-1.5

Traes_2DL_B7F8FFEB9.2	AT1G26630.1	eukaryotic translation initiation factor 5A, putative, expressed	_(ac)SDT(ph)DEHHFESK_	-1.8
Traes_2DL_99A21BFBF.1	AT4G20410.1	gamma-soluble NSF attachment protein, putative, expressed	_DVGGDDGDS(ph)LDEDDLT_	-1.5
Traes_2AL_6C0963A18.1	AT3G43660.1	integral membrane protein, putative, expressed	_GGGGGIDS(ph)DSDVDFAGR_	-1.7
Traes_2DL_3D83B32F9.1	AT5G05850.1	leucine rich repeat containing protein, expressed	_SMAAAAAES(ph)PQAS(ph)TPK_	-1.7
Traes_3B_386880998.1	AT5G49760.1	leucine-rich repeat family protein, putative, expressed	_SQS(ph)FAS(ph)LDMK_	-1.9
Traes_4AS_E609B22C1.2	AT1G74910.2	mannose-1-phosphate guanyltransferase, putative, expressed	_RVS(ph)SFEALQSATK_	-1.7
Traes_4AS_E609B22C1.2	AT1G74910.2	mannose-1-phosphate guanyltransferase, putative, expressed	_RVSS(ph)FEALQSATK_	-2.7
Traes_1DL_69D4A3E8B.2	AT3G51800.3	peptidase, M24 family protein, putative, expressed	_(ac)S(ph)S(ph)DEEVREEK_	-1.6
Traes_2AL_120E7CB68.1	AT4G32720.2	RNA binding protein, putative, expressed	_ANKVQKLDSS(ph)P_	-1.8
Traes_1BS_15F9D276D.3	AT3G28730.1	SSRP1-like FACT complex subunit, putative, expressed	_GAGAAPVDVDS(ph)ADGS(ph)SD_	-1.6
Traes_5DL_FAD9C2941.2	AT5G43830.1	stem-specific protein TSJT1, putative, expressed	_VGS(ph)AADWSNHF_	-1.6
Traes_5AS_7914936EA.4	AT4G37190.2	tubulin, putative, expressed	_AFHPDGGLT(ph)S(ph)DSD_	-1.7

Traes_1AL_0B9EA6007.4	AT2G17200.1	ubiquitin family protein, putative, expressed	_GGAGDGEGAGSES(ph)PPSGAR_	-1.8
Traes_4BS_D5227ED8B.2	AT3G42170.1	WRKY105, expressed	_LAITIGT(ph)DNDGDGTVER_	2.2
Traes_5DL_A3084808F.2	AT3G29185.1	WRKY4, expressed	_LAASAVPHPRS(ph)S(ph)RR_	2.1

Table S 8. A table showing the fold change of the 10 mM (6h + 30min) treatment relative to the 1mM (6h) treatment. Log2FC was computed using the normalized ion intensity of the listed proteotypic peptide. Data presented was filtered using the log2FC cutoff score of Log2FC ≥ 1.5 or Log2FC ≤ -1.5.

Leading protein	AGI	Fasta	Peptide	Log2FC
Traes_7AS_28D654039.1	AT5G59540.1	1-aminocyclopropane-1-carboxylate oxidase homolog 4, putative, expressed	_(ac)MMARPS(ph)EEEK_	-3.5
Traes_6DL_3286E5385.1	AT4G13510.1	ammonium transporter protein, putative, expressed	_SAQTSQVAADAT(ph)SPSSSV_	-1.6
Traes_2AL_DD284DEA9.1	AT3G53420.1	aquaporin protein, putative, expressed	_ASATKFGS(ph)S(ph)ASFGSR_	2.3
Traes_2AL_DD284DEA9.1	AT3G53420.1	aquaporin protein, putative, expressed	_ASATKFGS(ph)SAS(ph)FGSR_	1.9
Traes_2AL_DD284DEA9.1	AT3G53420.1	aquaporin protein, putative, expressed	_FGSSAS(ph)FGSR_	5.5
Traes_2BL_D274D68D2.5	AT5G60660.1	aquaporin protein, putative, expressed	_LGSSAS(ph)FGR_	-1.6
Traes_2BS_D8EC76A3B.2	AT2G16850.1	aquaporin protein, putative, expressed	_ALGS(ph)FRS(ph)SR_	-3.3
Traes_2BS_D8EC76A3B.2	AT2G16850.1	aquaporin protein, putative, expressed	_ALGS(ph)FRS(ph)SRSN_	-4.1
Traes_2DL_039832D76.1	AT5G60660.1	aquaporin protein, putative, expressed	_LGSSAS(ph)FGRN_	-1.6
Traes_6DL_481276D28.1	AT5G37820.1	aquaporin protein, putative, expressed	_LQS(ph)QSVAADDDELDHIPV_	2.6

Traes_5BL_57CBDD724.1	AT1G09020.1	CBS domain containing membrane protein, putative, expressed	_MGS(ph)LSDGALQEGSPR_	-2.3
Traes_5DL_9D2643A18.2	AT1G31970.1	DEAD-box ATP-dependent RNA helicase, putative, expressed	_ITFGDS(ph)DEE_	-1.8
Traes_2BL_F855555E8.2	AT1G25530.1	expressed protein	_(ac)GS(ph)PSVVLPK_	-2.0
Traes_2DL_489652871.3	AT1G78880.1	expressed protein	_S(ph)SGPQSGGVTPMAR_	-1.6
Traes_4AL_DD344FC87.5	AT5G60720.1	expressed protein	_GFS(ph)SS(ph)T(ph)LLTK_	-1.9
Traes_2AL_7F64A38C7.2	AT5G40760.1	glucose-6-phosphate 1-dehydrogenase, cytoplasmic isoform, putative, expressed	_(ac)AGTDSSASSRQSS(ph)FNS(ph)LAK_	-2.9
Traes_2AL_3C99F42A5.1	AT1G19870.1	IQ calmodulin-binding motif family protein, putative, expressed	_SNS(ph)SSFLDAPSK_	-2.4
Traes_3AL_31EAD29CE.2	AT1G74690.1	IQ calmodulin-binding motif family protein, putative, expressed	_VGS(ph)DTQISPEK_	-2.3
Traes_4AS_E609B22C1.2	AT1G74910.2	mannose-1-phosphate guanyltransferase, putative, expressed	_VSS(ph)FEALQSATK_	-2.4
Traes_3B_4E8E69A20.5	AT5G20490.2	myosin, putative, expressed	_QQAVAIS(ph)PTAK_	-1.5
Traes_7DS_3F91E7A16.5	AT2G25620.1	protein phosphatase 2C, putative, expressed	_SIS(ph)ADGLNSLR_	-3.3
Traes_2AL_58214CDDF.4	AT4G11790.1	ranBP1 domain containing protein, expressed	_AAEASADADEDAEAEQPSS(ph)PSVK_	-1.5
Traes_2AL_47B1A5BF2.1	AT3G61260.1	remorin, putative, expressed	_VES(ph)EKRNSLIK_	2.2
Traes_1BS_15F9D276D.3	AT3G28730.1	SSRP1-like FACT complex subunit, putative, expressed	_GAGAAPVDVDS(ph)ADGS(ph)SD_	-1.8

Traes_1DS_474BD1144.1	AT1G32400.3	tetraspanin family protein, putative, expressed	_AM(ox)NKPAEYDS(ph)DDEIIGTAR_	2.0
Traes_6DL_64573D0A6.1	AT2G06210.1	tetratricopeptide repeat domain containing protein, expressed	_SVQPTS(ph)PGPNDLS(ph)E_	-1.8
Traes_4BS_D5227ED8B.2	AT3G42170.1	WRKY105, expressed	_LAITIGT(ph)DNDGDGTVER_	3.0
Traes_4BS_D5227ED8B.2	AT3G42170.1	WRKY105, expressed	_LAITIGT(ph)DNDGDGTVERR_	2.7
Traes_5DL_A3084808F.2	AT3G29185.1	WRKY4, expressed	_LAASAVPHPRS(ph)S(ph)RR_	2.9

Table S 9. A table showing the fold change of the 10 mM (6h + 30min) treatment relative to the 1mM (6h + 30min) treatment. Log2FC was computed using the normalized ion intensity of the listed proteotypic peptide. Data presented was filtered using the log2FC cutoff score of Log2FC ≥ 1.5 or Log2FC ≤ -1.5.

Leading protein	AGI	Fasta	Peptide	Log2FC
Traes_2BS_50BE66985.1	AT3G50690.1	acidic leucine-rich nuclear phosphoprotein 32-related protein 1, putative, expressed	_AVEAALHTAGEGSS(ph)SPAR_	1.8
Traes_2DL_955B1070C.1	AT5G57330.1	aldose 1-epimerase, putative, expressed	_(ac)AGASS(ph)PPPTPKS(ph)PK_	1.8
Traes_2AL_DD284DEA9.1	AT3G53420.1	aquaporin protein, putative, expressed	_ASATKFGS(ph)S(ph)ASFGSR_	1.7
Traes_2AL_DD284DEA9.1	AT3G53420.1	aquaporin protein, putative, expressed	_ASATKFGS(ph)SAS(ph)FGSR_	2.0
Traes_2AL_DD284DEA9.1	AT3G53420.1	aquaporin protein, putative, expressed	_FGS(ph)SASFGSR_	2.0
Traes_2AL_DD284DEA9.1	AT3G53420.1	aquaporin protein, putative, expressed	_FGSSAS(ph)FGSR_	5.8
Traes_2BL_D274D68D2.5	AT5G60660.1	aquaporin protein, putative, expressed	_LGSS(ph)ASFGRS_	5.7

Traes_2BS_D8EC76A3B.2	AT2G16850.1	aquaporin protein, putative, expressed	_ALGS(ph)FRS(ph)SR_	-2.9
Traes_2BS_D8EC76A3B.2	AT2G16850.1	aquaporin protein, putative, expressed	_ALGS(ph)FRS(ph)SRSN_	-4.3
Traes_2DL_039832D76.1	AT5G60660.1	aquaporin protein, putative, expressed	_LGSSAS(ph)FGRN_	-2.3
Traes_5DS_643ED07F6.3	AT2G39010.1	aquaporin protein, putative, expressed	_GYGS(ph)FRS(ph)NA_	1.7
Traes_2AL_FCACEE2AC.4	AT5G55980.1	expressed protein	_HPAS(ph)PSSSSGIVATQ_	-2.0
Traes_2BL_F855555E8.2	AT1G25530.1	expressed protein	_(ac)GS(ph)PSVVLPK_	-1.9
Traes_4AL_DD344FC87.5	AT5G60720.1	expressed protein	_GFS(ph)SS(ph)T(ph)LLTK_	-2.1
Traes_2DL_99A21BFBF.1	AT4G20410.1	gamma-soluble NSF attachment protein, putative, expressed	_DVGGDDGDS(ph)LDEDDLT_	1.6
Traes_2AL_3C99F42A5.1	AT1G19870.1	IQ calmodulin-binding motif family protein, putative, expressed	_SNS(ph)SSFLDAPSK_	-1.8
Traes_3AL_31EAD29CE.2	AT1G74690.1	IQ calmodulin-binding motif family protein, putative, expressed	_VGS(ph)DTQISPEK_	-2.2
Traes_2DL_3D83B32F9.1	AT5G05850.1	leucine rich repeat containing protein, expressed	_SMAAAAAES(ph)PQAS(ph)TPK_	2.1
Traes_3B_386880998.1	AT5G49760.1	leucine-rich repeat family protein, putative, expressed	_SQS(ph)FAS(ph)LDMK_	2.2
Traes_3B_4E8E69A20.5	AT5G20490.2	myosin, putative, expressed	_QQAVAIS(ph)PTAK_	-1.9
Traes_1DL_69D4A3E8B.2	AT3G51800.3	peptidase, M24 family protein, putative, expressed	_(ac)S(ph)S(ph)DEEVREEK_	2.0
Traes_1DL_69D4A3E8B.2	AT3G51800.3	peptidase, M24 family protein, putative, expressed	_(ac)SS(ph)DEEVREEKELDLSSNEVVTK_	2.4

Traes_7DS_3F91E7A16.5	AT2G25620.1	protein phosphatase 2C, putative, expressed	_SIS(ph)ADGLNSLR_	-3.5
Traes_4DS_BCEF8A384.2	AT5G60460.1	protein transport protein Sec61 subunit beta, putative, expressed	_T(ph)SSSASGGGGFSGGGGNNM(ox)LR_	-1.7
Traes_2AL_47B1A5BF2.1	AT3G61260.1	remorin, putative, expressed	_VES(ph)EKRNSLIK_	2.1
Traes_2AL_A9D66A1CD.3	AT2G19130.1	serine/threonine-protein kinase receptor precursor, putative, expressed	_LLNAITAGVGS(ph)PTSDT_	-1.6
Traes_1BS_15F9D276D.3	AT3G28730.1	SSRP1-like FACT complex subunit, putative, expressed	_GAGAAPVDVDSADGS(ph)SD_	3.2
Traes_5DL_FAD9C2941.2	AT5G43830.1	stem-specific protein TSJT1, putative, expressed	_VGS(ph)AADWSNHF_	2.0
Traes_1DS_474BD1144.1	AT1G32400.3	tetraspanin family protein, putative, expressed	_AM(ox)NKPAEYDS(ph)DDEIIGTAR_	1.6
Traes_1BL_66D2E2865.3	AT4G35300.1	transporter family protein, putative, expressed	_GGGQSALGSALGLM(ox)S(ph)R_	2.8
Traes_1AL_0B9EA6007.4	AT2G17200.1	ubiquitin family protein, putative, expressed	_GGAGDGEGAGSES(ph)PPSGAR_	2.5
Traes_4BS_D5227ED8B.2	AT3G42170.1	WRKY105, expressed	_LAITIGT(ph)DNDGDGTVERR_	3.1

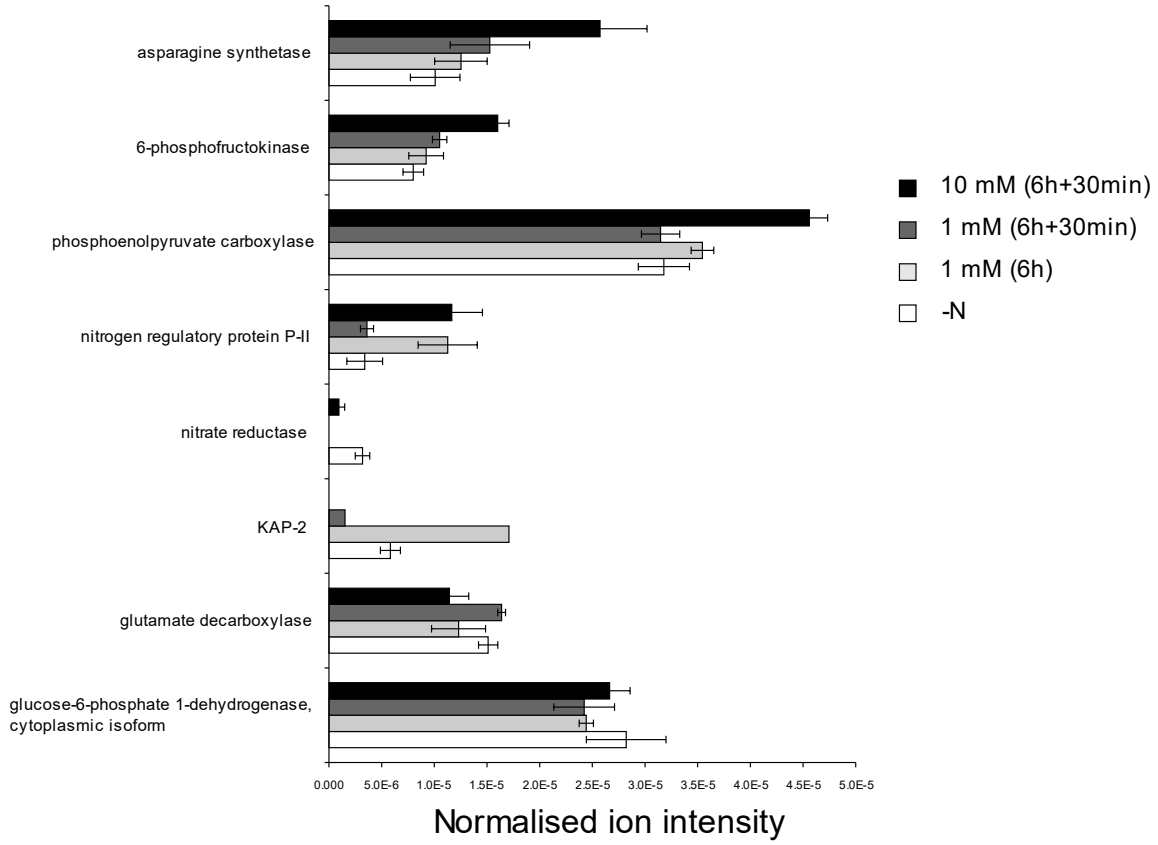

Figure S 1. Graphical representation of the response of selected proteins to ammonium supply. Normalised ion intensity ("fraction of total intensity" computed as "peptide ion intensity/total sum of sample's ion intensities"). Analysis performed with the non-phosphoenriched sample's dataset. Error bars show standard error of the mean.

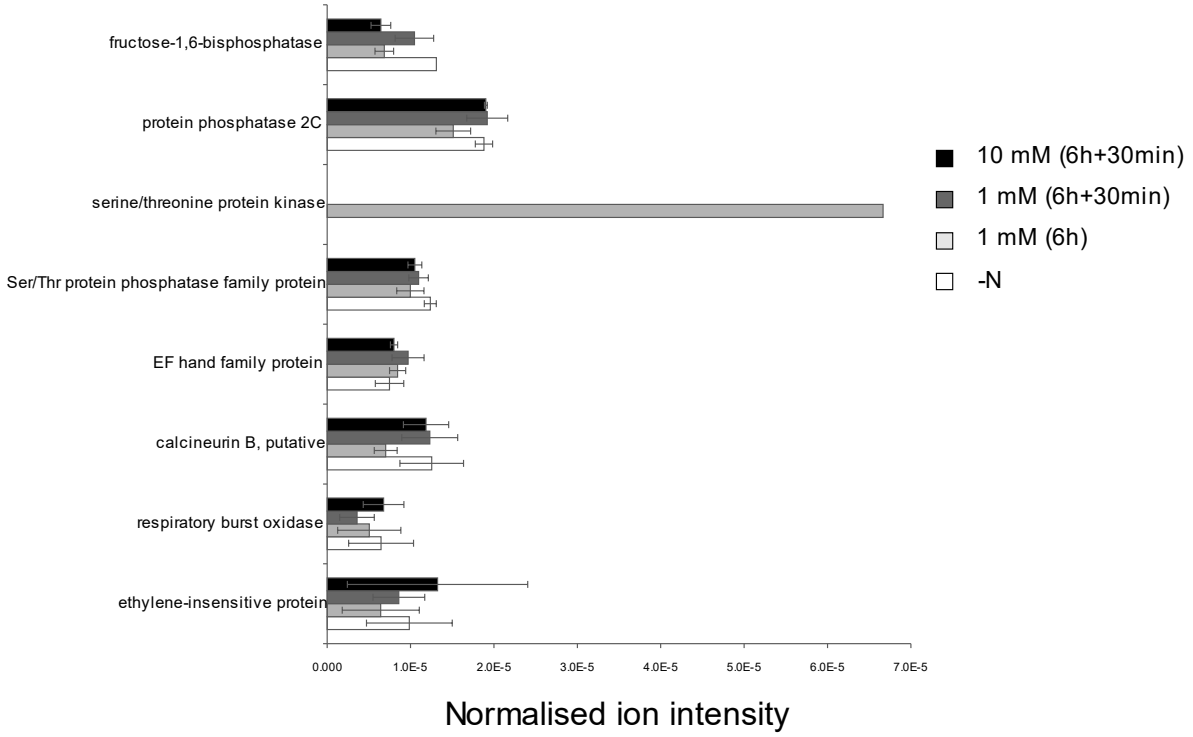

Figure S 2. Graphical representation of the response of selected proteins to ammonium supply. Normalised ion intensity ("fraction of total intensity" computed as "peptide ion intensity/total sum of sample's ion intensities"). Analysis performed with the non-phosphoenriched sample's dataset. Error bars show standard error of the mean.

8. ACKNOWLEDGEMENT

I would like to thank the almighty God for his grace, his blessings, and the fortitude he gave my soul to embark on this journey. To him be all glory!

My special thanks go to the faculty of Agricultural sciences of the University of Hohenheim who deemed me fit for the scholarship with which this work was started. It is my belief that the success of this work was greatly ensured by the immense financial support that this scholarship provided, for this, I am eternally grateful.

Words would not suffice to express my sincere appreciation to my supervisor Prof. Dr. Uwe Ludewig for offering me this immense opportunity to study under his learned tutelage. I wish to state that I have immensely benefitted from your altruistic mentorship, fatherly guidance, intelligent leadership, and scientific insight. I am incredibly grateful. A special “thank you” erupts always from the depths of my heart to Dr. Benjamin Neuhaeuser. I appreciate your guidance, supervision, and patience throughout the years, and through the course of this work. Sir I am greatly honoured to have grown under your scientific tutelage; thank you sir. Also, I wish to thank Prof. Dr. Waltraud Schulze and the entire Department of Plant Systems Biology of the University of Hohenheim (Stuttgart, Germany) for their immense support in making this work a success.

I thank my wife (Latricia Ijato) and my son (Isaiah Ijato) for their support and inspiration throughout this journey. I sincerely appreciate my parents (Margaret and Abel, Ijato) and my siblings (Oluwaseun, Oluwadamilola, Olayide, and Oluwanifemi; Ijato) for their support since the very beginning. Abayomi Ebitaope, you are highly appreciated.

Finally, my special thanks go to all my colleagues, and the entire staff at the Institute of Nutritional Crop Physiology ((340h) of the University of Hohenheim (Stuttgart, Germany) (most especially Yapping, Xuelian, Mellisa, Pascal, Philip, Emil, Andreas, and Romano) for their immense support. I appreciate you guys for the memories of the times we had together. It is my wish that the future ahead of us is blessed with the best success.

9. CURRICULUM VITAE

TOYOSI B. IJATO

560 McGuire street, Colorado Springs, 80916, Colorado, United States of America.

Telephone: +12055184949; **Email**: toyosi.ijato@uni-hohenheim.de, babtoy1@gmail.com.

Education

Year	Degree	Institution	Grade/Max.	USA Equivalence	
				Degree	Grade
On-going	Ph.D in **Agricultural sciences**	Univ. of Hohenheim, Stuttgart, Germany			
2017	Master of Science in **Environmental Protection and Agricultural Food Production**	Univ. of Hohenheim, Stuttgart Germany.	1.7/1	Master of Science	3.85/4
2011	Bachelor of Science in **Botany**	Univ. of Benin, Benin-city, Edo State, Nigeria	4.02/5	Bachelor of Science	3.21/4
				Evaluation by UCREDO: an endorsed member of *the Association of International Credential Evaluators (AICE)*	

Scientific Publication(s):

1. Ijato T, Porras-Murillo R, Ganz P, Ludewig U, Neuhäuser B (2020). "Concentration Dependent Physiological and Transcriptional Adaptations of Wheat Seedlings to Ammonium." Physiologia Plantarum. https://doi.org/10.1111/ppl.13113
2. Ganz P, Ijato T, Porras-Murillo R, Stührwohldt N, Ludewig U, Neuhäuser B (2020). "A Twin Histidine Motif is the Core Structure for High- affinity Substrate Selection in Plant Ammonium Transporters." Journal of Biological Chemistry. https://doi.org/10.1074/jbc.RA119.010891
3. Ganz P, Mink R, Ijato T, Porras-Murillo R, Ludewig U, Neuhäuser B (2019). "A Pore-occluding Phenylalanine Gate Prevents Ion Slippage through Plant Ammonium Transporters." Scientific Report - Nature 9:16765. https://doi.org/10.1038/s41598-019-53333-9

Work Experience

Research Assistant / Doctoral studies Apr 2017 - Present

Institute of Nutritional Crop Physiology, University of Hohenheim – Stuttgart, Germany

- Experimental design
- Conduction of plant growth experiments in green houses and in climate chambers
- Gene amplification (PCR) / Gene cloning
- Electrophysiological studies with the two-electrode voltage clamp
- Preparation of tissue culture from the immature embryo of wheat
- Stable *Agarobacteria* mediated transformation of plants and Callus
- Protein-protein interaction assay systems
- Bi-molecular fluorescence complementation assays

Teaching experiences:

1. Biology Teacher Feb 2013 - Sep 2013
Model Secondary School – Akure, Ondo State, Nigeria

2. Biology Teacher Nov 2011 - Oct 2012
Government Day Secondary School – Zamfara State, Nigeria (NYSC)

3. Biology/Agricultural science Teacher Feb 2011 - Oct 2011
Heritage Classic College – Oba-Akoko, Ondo state, Nigeria

- Ability to manage a classroom of youths
- Design of lesson plan
- Preparation of examination questions and grading of students' examination answer sheets
- Preparation of a detailed monthly report for the National Youth Service Corps (NYSC) local government coordinator
- Ability to manage a classroom of youths[2]
- Exposure of students to agriculture[3]
- Preparation of students for the West African Senior Secondary Certificate Examination WASSCE)[2,3]

Intern Feb 2010 - Apr 2010
Ondo State Ministry of Agriculture – Akure, Ondo State, Nigeria

- Extension works to rural communities
- Education of local farmers on the implementation of modern agricultural technologies
- Education of farmers on optimal fertilization strategies

Conference Appearances:

- **11th RegioPlantScience Meeting**; Stuttgart-Tübingen-Ulm, Uni. of Hohenheim, Stutgart, Germany, **2019.**
  - ❖ **Poster Presentation:** *Mutation Mimicking Phosphorylation Suggests the Existence of a Phospho-regulatory Mechanism for Wheat AMT1's*

- **10th RegioPlantScience Meeting**; Stuttgart-Tübingen-Ulm; ZMBP Tübingen Germany, **2018.**
  - ❖ **Poster Presentation:** *CIPK/CBL Regulation of Ammonium transporters in Triticum Aestivum*

Academic Projects:

- **Master of Science Thesis –** Characterization of regulators of plant ammonium transport, (with a focus on the phosphatase PP2C, CIPK23 Kinase, and the AMT1 transporters of *Arabidopsis thaliana*)*;* submitted January 2017
- **Bachelor of Science Thesis –** Cytotoxicity and getotoxicity screening of the extract of *Ganorderma lucidum* using the *Allium cepa* assay; Submitted January 2011

Coloradao Springs, Co, USA/15th-Apr-2021

(Place, date)

(Toyosi B., IJATO: Signature)

10. AFFIDAVIT

Pursuant to Sec. 8(2) of the University of Hohenheim's doctoral degree regulations for Dr.sc.agr.

1. I hereby declare that I independently completed the doctoral thesis submitted on the topic:

Understanding the role of the Calcineurin B-like (CBL) proteins and the CBL-Interacting Protein Kinases (CIPK) of wheat (*Triticum aestivum*) in the regulation of its high affinity ammonium transporters.

2. I only used the sources and aids documented and only made use of permissible assistance by third parties. In particular, I properly documented any contents which I used - either by directly quoting or paraphasing - from other works.
3. I did not accept any assistance from a commercial doctoral agency or consulting firm.
4. I am aware of the meaning of this affidavit and the criminal penalties of an incorrect or incomplete affidavit.

I hereby confirm the correctness of the above declaration. I hereby affirm in lieu of oath that I have, to the best of my knowledge, declared nothing but the truth and have not omitted any information.

Coloradao Springs, Co, USA/15th-Apr-2021 

…….....

(Place, date) (Signature)

AFFIDAVIT
INFORMATION

The University of Hohenheim requires an affidavit declaring that the academic work was done independently in order to credibly claim that the doctoral candidate independently completed the academic work.

Because the legislative authorities place particular importance on affidavits, and because affidavits can have serious consequences, the legislative authorities have placed criminal penalties on the issuance of a false affidavit. In the case of wilful (that is, with the knowledge of the person issuing the affidavit) issuance of a false affidavit, the criminal penalty includes a term of imprisonment for up to three years or a fine.

A negligent issuance (that is, an issuance although you should have known that the affidavit was false) is punishable by a term of imprisonment for up to one year or a fine.

The respective regulations can be found in Sec. 156 StGB (Criminal Code) (false affidavit) and in Sec. 161 StGB (negligent false oath, negligent false affidavit).

Sec. 156 StGB: False Affidavit

Issuing a false affidavit to an authority body responsible for accepting affidavits or perjury under reference to such an affidavit shall be punishable with a term of imprisonment up to three years or with a fine.

Sec. 161 StGB: Negligent False Oath, Negligent False Affidavit:

Subsection 1: If one of the actions described in Secs. 154 and 156 is done negligently, the action shall be punishable by a term of imprisonment of up to one year or a fine. Subsection 2: Impunity shall apply if the perpetrator corrects the false information in a timely manner. The regulations in Sec. 158 (2) and (3) apply mutatis mutandis.

The German original version of this affidavit is solely valid; all other versions are merely informative.

I have taken note of the information on the affidavit.

Coloradao Springs, Co, USA/15th-Apr-2021 

…….....

(Place, date) (Signature)

This thesis was accepted as a doctoral thesis (Dissertation) in fulfillment of the regulations to acquire the doctoral degree "Doktor der Agrarwissenschaften by the Faculty of Agricultural Sciences at University of Hohenheim on …….....

Date of the oral examination: 29th of March, 2021

Examination Committee

Chairperson of the oral examination	Prof. Dr. Jörn Bennewitz
Supervisor and Reviewer	Prof. Dr. Uwe Ludewig
Co-Reviewer	Prof. Dr. Waltraud Schulze
Additional examiner	Prof. Dr. Christian Zörb
Dean Faculty of Agriculture	Prof. Dr. Ralf T. Vögele